PROCEEDINGS OF I-IDEA

INTERNATIONAL SCIENCES, TECHNOLOGY & ENGINEERING CONFERENCE (ISTEC)

ADVANCED GEOSPATIAL AND SURVEYING (AGeoS) 2020

October, 7th 2020 | Virtual Conference

"EMPOWERING GEOSPATIAL SURVEYING TOWARDS THE 5TH INDUSTRIAL REVOLUTION"

EXTENDED ABSTRACT

ORGANIZED BY
RESEARCH, INDUSTRY, COMMUNITY & ALUMNI NETWORK (RICAN)
UNIVERSITI TEKNOLOGI MARA PERLIS BRANCH

Available online: http://ageos.i-idea.org/conference-info/e-proceedings-extended-abstract

Proceedings of International Sciences, Technology and Engineering Conference (ISTEC): Advance Geospatial and Surveying (AGeoS) 2020 Extended Abstract

Editors

Dr. Rohayu Haron Narashid

Siti Aminah Anshah

Nursyahani Nasron

Email : ageos.istec2020.iidea@gmail.com

Publication Date: 12 November 2020

Perpustakaan Negara Malaysia

Published by

Universiti Teknologi MARA Perlis Branch
Arau Campus, 02600 Arau,
Perlis, Malaysia.

PREFACE

It is a great privilege for us to present one of the special satellite events which brought to you by the 5th International Innovation, Design and Articulation (i-IDeA 2020). The event named, ISTEC: Advanced Geospatial and Surveying (AGeoS) Conference 2020 specially organized by the Research, Industry, Community and Alumni Network (RICAN) of Universiti Teknologi MARA, Perlis Branch with the theme of *"Empowering Geospatial Surveying Towards the 5th Industrial Revolution"*.

The main objective of AGeoS2020 is to provide a platform for researchers, academicians, practitioners, consultants, students as well as industrial professionals from all over the world to present their findings and share their innovative and valuable experience from different backgrounds and experiences. AGeoS 2020 bring the entire field that synchronized with geospatial and surveying.

AGeoS 2020 is divided into two (2) categories; full paper and extended abstract which presented in virtual and digital mode. The event is held on October 7th 2020 for a virtual conference. At the same time, the video of the poster takes place digitally. Optionally the authors need to prepare the extended abstract. The judging process started from September, 28th to October 2nd 2020.

These proceedings contain 21 extended abstracts and 3 full papers in field of Surveying and Geomatics, GPS and GNSS, UAV, GIS, Remote Sensing, and Sustainable Environment. We want to express our gratitudeto everyone involvedin AGeoS2020 including authors, reviewera, invited speakers, program committee, judges, local organization, and others.

We hope you enjoy reading the proceedings.

Publication Committee

Dr. Nazirah Md Tarmizi
Noorzalianee Ghazali
Noorazwani Mohd Razi
Nurhafiza Md Saad
Noorfatekah Talib

Editors

Dr. Rohayu Haron Narashid
Siti Aminah Anshah
Nursyahani Nasron

Table of Contents

AGeoS2020: Extended Abstract

Perpustakaan Negara Malaysia eISBN 987-967-17889-6-7

AGeoS2020: Full Paper

Perpustakaan Negara Malaysia eISBN 987-967-17889-6-7

Improvement of Power Transmission Line Location at Tropical Forest Area in Avoiding Endangered Tree Species

Sofiya Zulaikha Ruslan[1], Nurul Ain Mohd Zaki[1], Zulkiflee Abdul Latif[2], Mohd Nazip Suratman[3], Hamdan Omar[4], Mohd Zainee Zainal[1], Sharifah Norashikin Bohari[1]

[1]Environment and Climate Change Research Group, Centre for Surveying Science and Geomatics Studies, Faculty of Architecture, Planning and Surveying, Universiti Teknologi MARA, 02600, Arau,Perlis, Malaysia
[2]Applied Remote Sensing & Geospatial Research Group, Centre for Surveying Science and Geomatics Studies, Faculty of Architecture, Planning and Surveying, Universiti Teknologi MARA, 40000, Shah Alam, Selangor, Malaysia
[3]Centre for Biodiversity and Sustainable Development, Universiti Teknologi MARA, 40000, Shah Alam, Selangor, Malaysia
[4]Forest Research Institute Malaysia (FRIM), 52109, Kepong, Selangor Darul Ehsan, Malaysia

e-mail : fiyaruslan@gmail.com

Abstract

In order to meet the demand for power supply, site exploration for a suitable transmission Right-Of-Way (ROW) using automated technology is in dire need. Unfortunately, suitable sites do at the time involved tropical forest area and cause forest degradation that could become a threat to endangered tree species.Therefore, this research conducted with Geographic Information System (GIS) technologies in optimizes Least-Cost Path (LCP) siting by considering multicriteria decision related which are feature classes, endangered tree species, slope, average wind speed, and human mask. Before, finding the best route for transmission siting required expert advice and opinion in investigated site location and drawn manually on the paper. With the innovation of GIS work as powerful tools in optimize power transmission line siting at tropical forest area. Reclassify algorithm used to weight the multi-criteria related to optimize power transmission line siting. The data processing procedure carried out on a model builder platform that customizes design in optimizing transmission line siting. The transmission line siting optimization has been conducted using the Reclassify algorithm and LCP tools that carried out processing on the Model Builder platform. Forest degradation and extinction of endangered tree species could be prevented in tropical forest areas for future development in utility industries.

Keywords: Optimize route, Least-Cost Path (LCP), Reclassify algorithm, GIS

Introduction

The power lines industry is increasing the national economy through construction and maintenance development that has a massive result in power energy transmission corridors and loops around cities (Xu et al., 2016). There have several parameters that need to be considered whenever a new development of power transmissions carried out, such as slope, urbanization growth, average wind speed, and distance. All the parameters have different risks and costs involved. The focus of the power transmission industry is to build the power transmission line sitting with a short distance and less cost involved with minimal environmental impact (Zipf et al., 2019).

The meteorological condition was one of the parameters in siting transmission lines that important factor in siting line operation and determine the operation limitation (Mo et al., 2017). According to Xu et al., (2016), Hubei Province in China has several natural accidents caused by a high voltage power line that caused wildfires and icing that lead to outage and tripping accidents. Those tragedy involving power transmission line causes a major loss from the economic and human life aspect. In 2013 about 30

Perpustakaan Negara Malaysia eISBN 987-967-17889-6-7

tripping accidents caused by wildfires and economic loss about more than 1.5 million US dollars happened at Hubei Province in China (Xu et al., 2016).

Transmission line siting was one of the forest development activity that causes this endangered tree species issues. Any trees blocking the transmission line sitting path need to be removed. (Devices, 2013). Repeated such activities without replantation activities mean possible for the trees to become extinct. The impact of the power transmission line also leads to the threat of the trees. Some of the tree species unable to survive under high voltage of power electrical that near the transmission line. Some tree faces diseases and leads to death (Devices, 2013). Transmission line development has a degree of impact to environmental in temporarily and permanently.

Developing geospatial data in optimizing power transmission line siting was an intensive way. All the parameter data was required for analysis and processing. The Digital Elevation Model (DEM) used to analyze slope surface area, while the meteorology data provided temperature and weather data to analyze wind speed and rain quantity on the area. The study was carried out at Pahang, Malaysia, that consists of most of the tropical forests. Through data processing, the best location for power transmission line siting could be a map and identify. The output gives an advantage to the utility survey department. They could use to analyze the best routing for power transmission line siting with fulfilling the specification and parameters.

Malaysia forestry department was also able to refer this study to protect endangered tree species that available in the study area. In Malaysia, the utility company referred to rules and regulations from the City Planning and Development Department as transmission line development guidelines. The rules and regulations prepared in minimizing impact and potential risks to human and living things especially development in the forest area. This thesis carried out a pilot study at the Forest Research Institute Malaysia (FRIM) forest area in investigated route suitability. Improvement of transmission line location in tropical forest areas could be performed as initiative ways in protecting endangered tree species from extinction due to uncontrollable forest cleaning.

The research studies carried out for future references in the improvement of power transmission line location in tropical forest areas in avoiding endangered tree species. The model builder was a processing platform to optimize the line route for future research with similar characteristics with the type of forest, geospatial data, and size of the study area. With a multicriteria decision as weight, the reclassify algorithm application is assigned the weighted values for each criterion decision. The transmission line location determined for the LCP route from the start point to the endpoint using GIS technology tools which able to be used for future analysis and error detection. The improvement in determining transmission line locations in tropical forest areas could give a minimal degree of impact on the environment.

Problem statement

The power transmission line has a potential impact on the environment in both temporary and long-term impacts (Devices, 2013). Loss of woodlands such as forest, land use restriction, and the aesthetic impact was the example of environmental impact from transmission line construction activities (Devices, 2013). The most popular natural disaster that occurs because of power transmission line maintenance is wildfires and icing lead to outages and tripping accidents that has been happened in Hubei Province, China in 2013 (Xu et al., 2016).

The tropical forest became the target area because of area suitability as mention above, while an endangered tree species occurs due to power transmission line siting 18 development. Reported in an article written by Li & Lin, (2019), forest fragmentation and degree impact on vegetation since 2014 in state grid of China caused by transmission line construction activities of cleared the forest area along transmission line within Right-of-Way (ROW) width with buffer zone about 50 to 100 meters for every two or three years.

The major environmental impact causes from the High Voltage Transmission Line (HVTL) is the land used land cover (Li & Lin, 2019). The ROW result shows a permanent impact on the land cover as the trees cut for the cleaning process for avoided any direct contact between trees and HVTL tower may cause disaster as stated by (Xu et al., 2016) above. Moreover, Devices, (2013), explicated how the transmission line development affected temporarily large-scale areas surrounding the actual ROW line area that permanently affected until it causes loss to the land benefits. The wildlife's habitat at tropical forest could temporarily be destroyed due to construction required a long duration to rebuild the habitats and shelter back into normal condition.

The tropical forest was an area that keeps major carbon stock in above-ground living biomass of high density of trees (Mohd Zaki & Abd Latif, 2017). Forest degradation caused by power transmission line development also makes a loss in carbon stock and

Perpustakaan Negara Malaysia eISBN 987-967-17889-6-7

above-ground forest biomass occur. Previously in Mohd Zaki et al., (2018) research proved Southeast Asia at the higher ranking for deforestation activity such as forest clearing increasing for the past decade especially happen in tropical forest areas. Development of power transmission line siting at tropical forest areas could be part of causes lead to an issue regarding forests such as deforestation, forest degradation, and forest fragmentation increasing till occur loss in carbon stock.

Solution to the problem

Further studies carried out to determine the solution for forest fragmentation issues in tropical forest areas by reduces the impact on wildlife and endangered tree species (Li & Lin, 2019). Through both incidents, it shows power transmission transfers electric power in high voltage required well management and maintenance as prevention actions.

Project was carried out began with identifying the parameters need to establish power transmission line routing optimization in the tropical forest area. The procedure required to determine the correlation between the parameters for power transmission line routing optimization in the tropical forest area. Complete the task by create a map with proposed the power transmission line routing optimization in the tropical forest area by avoiding endangered tree species.

Planning structure

Figure 1 below shows the research methodology workflow design customize accordingly to propose the research aim and objectives to be achieved. The methodology divided into four (4) stages which begin with planning, continue with data acquisition, carried out data processing, and the final stage involved with the result or output for this research. The stages design in this methodology has its own goals to be achieved in the short term for a purpose to achieve a long-term output for this research.

The waterfall methodology type was selected for this research due to study conditions, data, and output to be produced. This methodology ensures each stage needs to be complete and achieve the goal desired before carried out the future stages. The monitoring, controlling, and evaluation of processing procedure much easier with this waterfall methodology type compared to other types such spiral that involved with experiment and trial procedures. The research methodology design through well planning and discussion between expert advice and previous references.

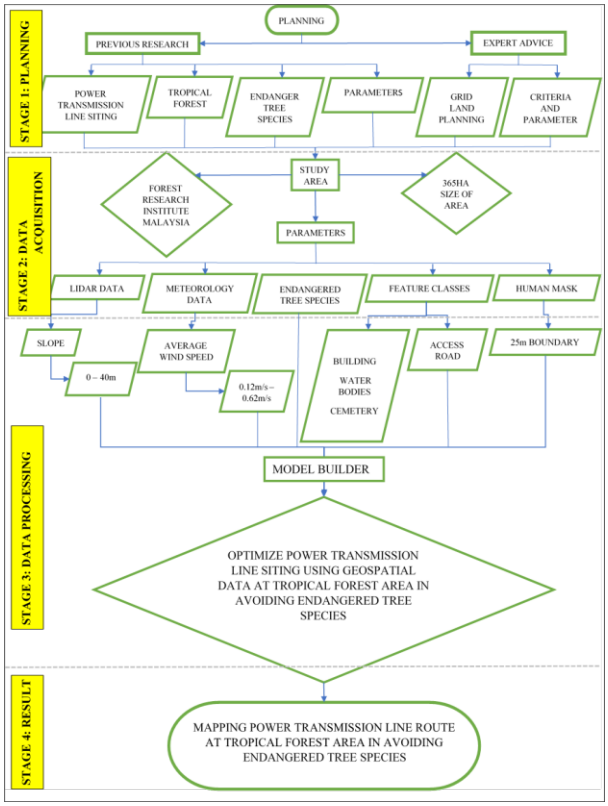

Figure 1: Research Methodology

Knowledge impact

New experiences working with different software and data processing enhance more knowledge that could give advantage to skill and knowledge for future work. Working with four (4) different dataset with different format required different software and applications for data acquisition and data collection. The flexibles and critical thinking skills was developed through processing with a purpose to solve any problems introduced.

Contribution to the society and country

The output will be a guideline and work as references for Utility Company for further transmission line siting development at tropical forest area with concern about parameters required. The environmental impact due to transmission line development could be control and minimize for both temporal and long-term. Improvement in transmission line development could be achieved by referring to this research.

Perpustakaan Negara Malaysia eISBN 987-967-17889-6-7

Minimizing environmental impact to forest and trees could save and protect endangered and critically endangered species goes extinction. This research prepared to ensure the country development and living things could keep together growth without threatening the ecosystem of nature. The benefits of nature and innovation of high technologies could be felt without any negative impacts.

Cost impact

Cost for this project requires data purchase for unavailable data such as Meteorology data for Average Windspeed and labour fees for Tree Inventory field survey at FRIM forest for 4 days involving 13 persons. The survey equipment rental from UiTM facilities and transportation also rental from UiTM transportation.
The cost impact involved for Tree Inventory field survey and Meteorology data. While the other data such as LiDAR, Orthophoto and WorldView-2 satellite image from existing sources. Due to the availabilities of data from previous sources, the cost impact was minimal.

Commercialization potential

The commercialization potential of this research occurred various positive impact could lead to an improvement in transmission line developments. There are three (3) main commercial potential as follows:

1. To analyze the best routing for power transmission line siting
2. To protect endangered tree species that available in the study area.
3. Minimize impact on the environment

REFERENCES

Aien, A., Kalantari, M., Rajabifard, A., Williamson, I. Chua, L. S. L., Suhaida, M., Hamidah, M., & Saw, L. G. (2008). Malaysia plant red list. *Peninsular Malaysian dipterocarpaceae. Research Pamphlet No. 29*, 230. https://doi.org/ISBN 978-967-5221-34-7

Devices, I. M. (2013). Measuring and Identifying Environmental Impacts Quantifying Potential Impacts Identifying the Duration of Potential Impacts. *Public Service Commission of Wisconsin*, 1–32. Retrieved from https://psc.wi.gov/Documents/Brochures/Environmental Impacts TL.pdf

Latif, A. (2017). A publication covering 74 IUCN RED List Tree Species of Malaysia prepared by Sime Darby Property in collaboration with specialist organisations. 54.

Leica Geosystem AG. (2006). Leica ALS50-II Airborne Laser Scanner Leica ALS50-II Product Specifications. Leica ALS50-II Airborne Laser Scanner, 1–12.

Li, X., & Lin, Y. (2019). Do high-voltage power transmission lines affect forest landscape and vegetation growth: *Evidence from a case for southeastern of China*. Forests, 10(2), 1–13. https://doi.org/10.3390/f10020162

Matikainen, L., Lehtomäki, M., Ahokas, E., Hyyppä, J., Karjalainen, M., Jaakkola, A., … Heinonen, T. (2016). Remote Sensing Methods for Power Line Corridor Surveys. *ISPRS Journal of Photogrammetry and Remote Sensing*, 119, 10– 31. https://doi.org/10.1016/j.isprsjprs.2016.04.011

Mo, Y., Zhou, X., Wang, Y., & Liang, L. (2017). Study on operating status of overhead transmission lines based on wind speed variation. Progress In Electromagnetics Research M, 60(September), 111–120. https://doi.org/10.2528/PIERM17072605

Mohd R, M., T, S. A., K. A, H., A, M. N., & Tariq M, H. (2011). Potential use of geospatial technologies in assessing tropical forest environmental depletions – A case study in Berkelah Forest Reserve, Pahang. Geoinformation Programme Division of Forestry & Environment Forest Research Institute Malaysia (FRIM), (November), 1–3.

Mohd Zaki, N. A., & Abd Latif, Z. (2017). Carbon sinks and tropical forest biomass estimation: a review on role of remote sensing in aboveground-biomass modelling. *Geocarto International*, 32(7), 701–716. https://doi.org/10.1080/10106049.2016.1178814

Perpustakaan Negara Malaysia eISBN 987-967-17889-6-7

Mohd Zaki, N. A., Latif, Z. A., & Suratman, M. N. (2018). Modelling above-ground live trees biomass and carbon stock estimation of tropical lowland Dipterocarp forest: integration of field-based and remotely sensed estimates. *International Journal of Remote Sensing*, 39(8), 2312–2340. https://doi.org/10.1080/01431161.2017.1421793

Tuck, S. L., O'Brien, M. J., Philipson, C. D., Saner, P.,
Tanadini, M., Dzulkifli, D., … Hector, A. (2016). The value of biodiversity for the functioning of tropical forests: Insurance effects during the first decade of the Sabah biodiversity experiment. Proceedings of the Royal Society B: Biological Sciences, 283(1844). https://doi.org/10.1098/rspb.2016.1451

Xu, K., Zhang, X., Chen, Z., Wu, W., & Li, T. (2016). Risk assessment for wildfire occurrence in high-voltage power line corridors by using remote sensing techniques: a case study in Hubei Province, China. *International Journal of Remote Sensing*, 37(20), 4818–4837. https://doi.org/10.1080/01431161.2016.1220032

Zipf, M., Kumar, S., Scharf, H., Zöphel, C., Dierstein, C., & Möst, D. (2019). Multi-Criteria High-Voltage Power Line Routing—An Open Source GIS-Based Approach. *ISPRS International Journal of Geo-Information*, 8(8), 316. https://doi.org/10.3390/ijgi8080316

Perpustakaan Negara Malaysia eISBN 987-967-17889-6-7

Determination of Possible Route for Invaders at Kota Putra, Padang Terap Using UAV Image

Ismail Ma'arof[1] and Mohamad Arham Mahasan[1]

[1] Faculty of Architecture, Planning & Surveying, Universiti Teknologi MARA, Perlis Branch, Arau Campus, 02600 Arau, Perlis, Malaysia

e-mail: ismailmaarof@uitm.edu.my

Abstract

Protecting the country's boundaries from enemy encroachment is the sovereign state responsibility. The Lahad Datu attack by a foreign country has sent a massive shock to Malaysia. The question arises in questioning the fragility of the country's defence structure and the failure of the Malaysian Maritime Enforcement Agency (APMM) for delays in detecting the entry of the armed forces to enable them to capture Kampung Tanduo and Felda Sahabat 17 in Sabah. Therefore, this study was established through "Persatuan Sejarah Malaysia Cawangan Kedah Darul Aman" to discuss the direction and sovereignty of the Kedah State borders from being infringed. The study was started by conducting a literature view of area Padang Terap history and followed by the land surface study of the area. The lowest altitude found in the area is at "Genting Pahat" area of 155meter. Application of confidential data has been applied to JUPEM in obtaining topographical data on the area and found there are two routes; a creek lane and rubber tappers route that has potential to be the gateway for intruders to enter the country legally. Currently, the use of UAV in topographic mapping is still new in Malaysia and with a potential to determine this kind of routes.

The UAV method was chosen because it has better accuracy as well as cost-efficient compared to the conventional method. The comparison between the data taken using the UAV with the topographic data applied did not show a significant difference between the two data and the use of UAVs in the subject of this study is coincide and meets the desired requirements.

Keywords: Country boundaries, border invaders, potential route, topographical characteristic, UAV, confidential data

Introduction

Our country delineation needs utmost attention; therefore, a study to detect the point of threat at the country borders are needed to safeguard the country sovereignty. The title for this study is to test the capabilities of the UAV in delivering the best results for topographic mapping in tracking the paths that are potential to be transmitted by intruders.

This study begins with a study of limited topographic data from JUPEM. Furthermore, data retrieval is made using UAV and made a comparison in terms of accuracy and desired requirements. Thus, with the creation of this potential path, it facilitates the authorities in carrying out their duties in safeguarding national sovereignty.

Aim and Objective

This module aims to study the capability of UAV system in mapping the potential area of border invasion.

The objectives of this project are:

i. To produce orthophoto mosaics, digital elevation model, contours and topographic mapping for potential area.
ii. To determine which path is potentially used by an intruder.
iii. To compare topographical profile characteristic of the specific area between JUPEM and Drone Imagery.

Methodology

There were five phases of methodology in this study (Fig.1):

Perpustakaan Negara Malaysia eISBN 987-967-17889-6-7

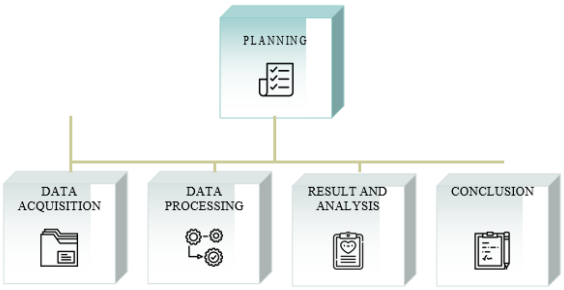

Figure 1: Methodology Phases

Planning: Phase (1)

Take first place in any study to do. Planning should cover from the beginning of the study to the results of the study. For this study, planning is made in terms of data collection, data collection methods, data sources, planning for selection of UAV types and subsequently cost-based planning during data acquisition. Block division was also made to standardize the study to be done. For this study, block A2 has been selected as the study area for this project.

Data Acquisition: Phase (2)

Data acquisition act as a second phase which is about data needed to complete the results of this study. The first data is the topographic data requested from JUPEM. This data is categorized as confidential data as it covers the topography of the earth for parts of Thailand. Next, the establishment of control points. The ground control point (GCP) is set up using GPS tools. A total of 8 control points were observed for 30 minutes according to the static observation method for each point. All these control points cover the area of the study conducted. The next data is via UAV mapping. The selection of Quadcopter type UAV model Dji Phantom 3Pro was chosen as the medium for data acquisition for this study. The flight is made with a height of 200 meters and covers an area of 0.569 km².

Data Processing: Phase (3)

In conjunction with this research, three (3) datasets need to be processed to get the desired result. The first data processed is JUPEM topographic data. The data obtained is a vector data which has been processed through ArcGis software. Through this software, the first objective of this study was achieved is to produce topographic maps, DEM, maps of potential routes and topographical profiles for this area. Next is the processing of GPS data. The observation data of the control points performed is processed using the TopconTools software. According to absolute positioning method. This GPS observation will be adjusted from Cors Station (Arau, UUM) to obtain the true point value for the control point observation. The third is data mapping using UAV. The result of this UAV aerial photo is processed using Agisoft Photoscan. In this processing, aerial photographs are taken through processing to produce DEM and orthophoto data.

Result and Analysis: Phase (4)

Evaluation and analyzing the result measured based on data acquisition made in the third phase and also as evidence to indicate each of the objectives stated successfully achieved. There are three results obtained according to the objective of the study—first, topography maps, Digital Elevation Models (DEM), digital maps and contours. Second, analyzing and evaluating the products produced on the first objective. Third, the difference between JUPEM data and UAV data.

Result and Discussion

Objective 1: To produce orthophoto mosaics, digital elevation model, contours and topographic mapping for potential area. The production of this first objective is divided into two parts. The first part is from JUPEM data and the second part is from UAV data. Before mapping generated (Fig.3). The block division for the study area was conducted to standardize the research to be done. The diagram (Fig.2) below shows a block division for the study area.

Objective 2: From research and study to the area. There are two potential routes to use as a route for intruders. First of the creeks and second the route of rubber tappers. The diagram (Fig.4) below shows both the path.

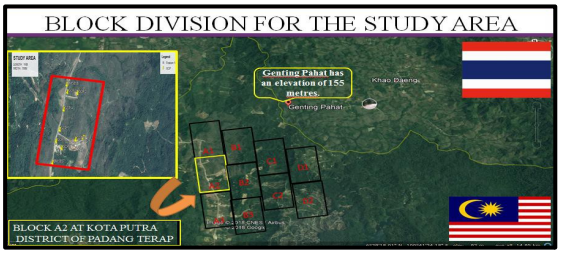

Figure 2: Block division of study area

Perpustakaan Negara Malaysia eISBN 987-967-17889-6-7

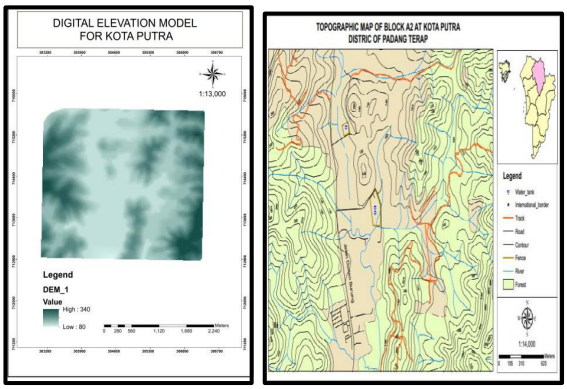

Figure 3: The production of DEM maps and topographic maps above is based on JUPEM data. This Vector data is processed using ArcGIS software. The scale of the topographic map is 1: 8000. The interval between the contours is 20 meters. For DEM, the lowest altitude for the study area is 80 meters, and the highest altitude is 340 meters

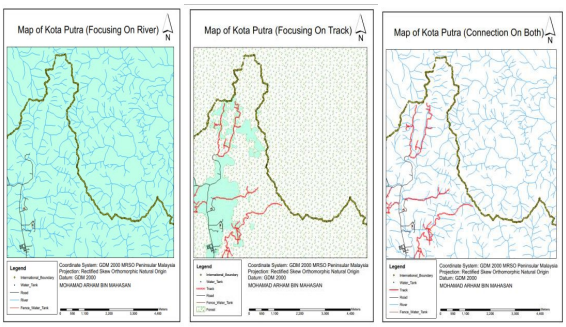

Figure 4: For a map that focuses on the above rivers, we can see roughly the tributary connection for the area that is connected to the tributaries of southern Thailand. Another factor for determining this potential route is the weather factor and rainfall for the area. Rainfall of 50mm per month and the effects of the dry season that last for four months a year make this route as a potential route for use by intruders. Therefore for block A2, there is a creek path that is connected to another block.

Figure.5: Shows the creek route for the study area.

Aerial photos in the figure above are taken using the UAV. The flight height is 200 meters. The route for this creek is seen connected with other blocks. Creek route is the last route of the intruder before meeting the existing road. Figure 6. below shows the conditions for this creek route.

Figure 6: Condition for creek route.

Figure 7: The situation of the rubber tapper

Figure 7 focusing on the rubber tapper route. The route is close to the boundaries of the country and ends with the existing road. It is also seen according to the tributaries. From the mapping above, intruders can use either a creek route or rubber tappers or both before they reach the existing road.

Rubber trees along this route surround the rubber trowel path. Clear roads and steep slopes allow for vehicles to use this route. As a result, these two routes are potential to be used as a route by intruders. Figure 8 below shows DEM data and orthophoto maps for Block A2 obtained from UAV mapping.

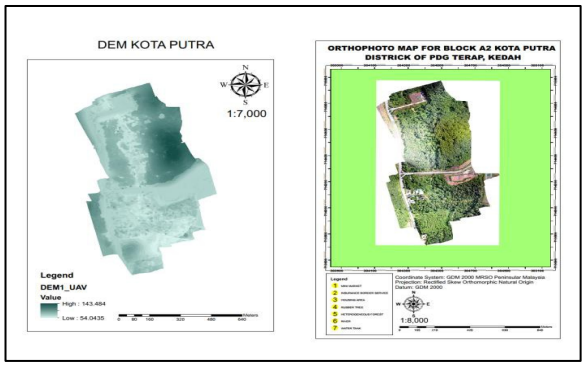

Figure 8: DEM data and orthophoto maps for Block A2 obtained from UAV mapping

Perpustakaan Negara Malaysia eISBN 987-967-17889-6-7

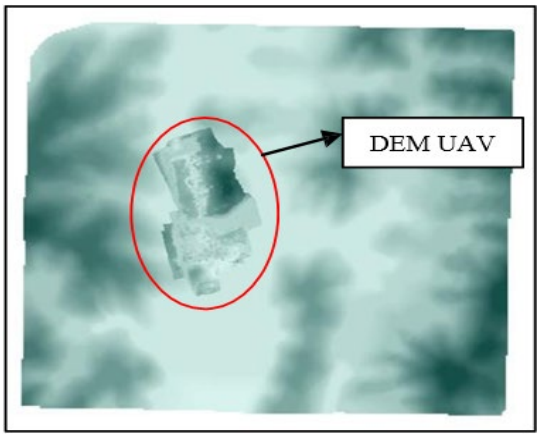

Figure 9: The position of DEM UAV when combined with DEM JUPEM in ArcGIS.

For DEM data, the lowest altitude recorded is 54 meters, and the highest altitude for the area is 143 meters. The scale for the orthophoto map is 1: 8000, as shown in the figure above. Figure 9, shows the position of DEM UAV when combined with DEM JUPEM in ArcGis software

The purpose of this combination is to ensure the accuracy of the position of the DEM UAV value with the DEM value of JUPEM. From the figure, it is found that DEM UAV is in DEM JUPEM, showing the location of both DEM is accurate.

Objective 3: To compare the topographical profile characteristic of the focus area between data JUPEM and UAV imagery

CHAINAGE	UAV	JUPEM
00	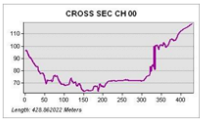	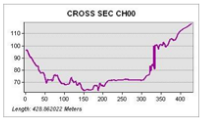
200	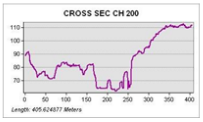	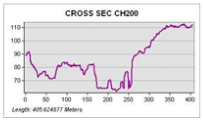
400	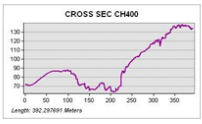	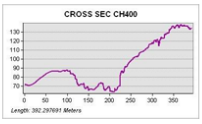
600	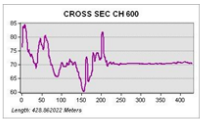	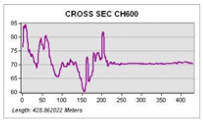
800	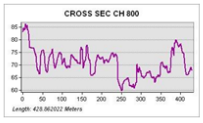	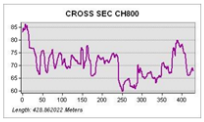

The figure above shows there is no difference for both profiles. It shows that data obtained from UAV aerial photography is capable of providing high accuracy data and comply with or meets the requirements to be obtained. With the existence of aerial photo technology from the UAV, it is seen capable of rivalling Lidar technology. In terms of cost of data acquisition it may be seen more for the cost of mapping using the UAV, but in terms of time and quality of data, it saves more time and the quality of data obtained is also very good. Thus, the use of the UAV system in aerial photo mapping is seen as a brilliant transformation for aerial photography techniques.

Conclusion

This general, this article presents each final result obtained based on the processing performed in the field of study methodology. The final result is divided into two results from aerial photo mapping using UAV and the result of vector data processing from JUPEM. In order to ensure that the main objectives of the study are achieved, each outcome for both case studies needs to undergo an analysis process to investigate the quality and accuracy of the results obtained. It is found that photogrammetry products obtained from UAV mapping such as orthophoto, DEM and contour lines are accurate and can be used as reference for earth topographic studies. In conclusion, UAV's method or system is seen to be able to handle the task of aerial mapping that has been held by Lidar and Remote Sensing technology.

REFERENCES

Ahmad, A. (2011). Digital mapping using low altitude UAV. Pertanika Journal of Science and Technology,19(SPEC. ISSUE), 51–58.

Bristeau, P. J., Callou, F., Vissière, D., & Petit, N. (2011). The Navigation and Control technology inside the AR.Drone micro UAV. IFAC Proceedings Volumes (IFAC-PapersOnline) (Vol. 18). IFAC. https://doi.org/10.3182/20110828-6-IT-1002.02327

D'Oleire-Oltmanns, S., Marzolff, I., Peter, K. D., & Ries, J. B. (2012). Unmanned aerial vehicle (UAV) for monitoring soil erosion in Morocco. Remote Sensing, 4(11), 3390–3416. https://doi.org/10.3390/rs4113390

Perpustakaan Negara Malaysia eISBN 987-967-17889-6-7

Everaerts, J. . (2008). The use of unmanned aerial vehicles (uavs) for remote sensing and mapping. The International Archives of the Photogrammetry, Remote Sensing and Spatial Information Sciences, XXXVII(Part B1), 1187–1192. Retrieved from http://www.isprs.org/proceedings/XXXVII/congress/1_pdf/203.pdf [Accessed 23 October 2015]

Fang, P., Lu, J., Tian, Y., & Miao, Z. (2011). An improved object tracking method in UAV videos. Procedia Engineering, 15, 634–638. https://doi.org/10.1016/j.proeng.2011.08.118

Perpustakaan Negara Malaysia eISBN 987-967-17889-6-7

Analysis of Ground Movements on the Steep Hillside Using the Geological Approach Method Study Case: Inhabited Resident of Bukit Kencana Jaya, Meteseh, Semarang, Central Java

Kartika Luthfia Ariwibowo[1], Miftahul Jannah[2], Adelia Gading Wanazizah[3], Kurnia Fadhli[4] and Muhammad Nanda Nurhaqqy5

[1]Geological Engineering, Diponegoro University, Semarang, Indonesia

e-mail: kartikabasymeleh@gmail.com

Abstract

Ground movement is a movement of the mass of a material perpendicularly, obliquely, or horizontally that is influenced by the presence of gravity and other factors. One of the areas that experienced ground movement is Bukit Kencana Jaya Housing which is located in the Meteseh, Tembalang, Semarang. It is a failed marketing housing that has broken cracks before it is inhabited even before construction is completed and the housing was built on the steep hillside. This research aims to study the causes of land movements that occur in Bukit Kencana Jaya Housing. The research method used is geological engineering investigations and direct investigation of surface data and to conduct slope stability analysis using Rocscince Slide software. The results are Meteseh have geomorphological conditions in the form of sloping hills; geological conditions where the lithology is in the form of soil, sandstone, and claystone; controlled by Left Thrust Slip Fault in the direction of N284ºE/32º; as well as a fairly steep slope with a safety factor of 1.019 which means it is classified as frequent ground motion. So, the geological engineer can recommend to build with construction techniques like soil nailing and show the area is safe.

Keywords: Ground movement, geological condition, slope stability, Bukit Kencana Jaya Housing

Introduction

Soil movement is a movement down the slope by the mass of the soil or rocks making up the slope due to disruption of soil or rock stability on the slope (Skempton and Hutchinson, 1969). The Meteseh area, Tembalang is located in the city of Semarang; it is one of the areas prone to ground movements or landslides. (Figure 1). Based on local geological conditions, Meteseh is in the Kendeng Zone, including the Damar Formation which is composed of the lithology of sandstones, breccias, conglomerates, and at the bottom is a clay layer which has slippery characteristics. Meteseh is an area that has a fairly rapid level of development, such as many residential facilities (Figure 1). There is housing that experiences problems during the finishing period with a crack in the wall before house completion. It is safe to assume that there might be some errors during the planning and the methods used to resolve this. Geomorphological conditions, geological conditions, and fairly steep slopes in the study area could be the reason for this problem to occur. To find out the cause to make conclusions about the solutions that can be offered is to conduct several investigations using a geological engineering approach and direct investigation of surface data.

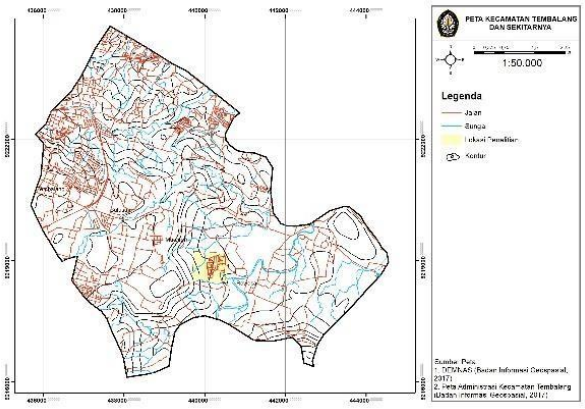

Figure 1: Map of Research Area

Perpustakaan Negara Malaysia eISBN 987-967-17889-6-7

Problem statement

Bukit Kencana Housing Tembalang is a residential area where there are problematic housing development projects that have not yet been inhabited. The housing stands on steep land with slopes between 30º to 40º and the housing construction follows the sloping slope. (Figure 2). There are damaged in almost every wall after two years of construction completed. Soil conditions in the area are local soils which have fine-grain properties, composed of clay material so that the soil is sticky and very elastic. Also, a poor drainage system conditions that create accumulated water puddles and humid conditions that are controlled by high rainfall cause the land to tend to expand based on the characteristics of clay soils in the area of Kencana Jaya Housing. (Figure 3). These soil characteristics are not good for a building foundation. From geological condition, the area is having many ground movements such as landslides on the cliff to the north of the building. For lithology, the soft rock is easy to experience weathering.

Figure 2: Housing is built on sloping land with damaged house walls

Figure 3: water accumulation due to poor drainage system

Research methodology

The research methods used in this research are observation and analysis methods. Observation methods include data collection and direct sampling in the area of Meteseh, Tembalang District, Semarang City, Central Java. Data collection in the field includes geomorphology, lithology, geological structure, slope, and ground movement data. And the analysis method used to process the data obtained from the observation method is the preparation of research location maps and geological maps using ArcGIS 10.5 software, geological structure analysis using Dips 6.0 software, as well as making slope sections and calculating the value of slope safety factors using Rocscince Slide software. (Figure 4).

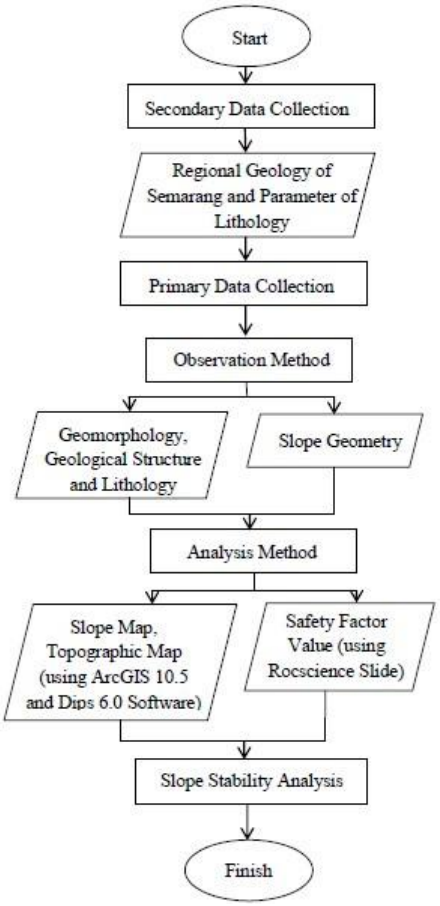

Figure 4: Research Flowchart

Result and Discuss

Geomorphology

The Bukit Kencana Jaya Housing research area, Kelurahan Meteseh, Tembalang District, Semarang City has a denuded structural form. (Brahmatyo, 1999). It can be seen from the appearance found in the field where the sloping hills that have undergone an intensive exogenous process. The research area is at the highest point of 100 meters

Perpustakaan Negara Malaysia eISBN 987-967-17889-6-7

above sea level and the lowest point at the elevation of 92 meters above sea level. The sloping hills in this study area are composed by claystone lithology. Based on the slope map made based on DEM (digital elevation model) data. (Figure 5) It is known that this area has a steep slope where all mass movements, creepings, erosion and landslides are known. The geomorphological conditions that make the ground movement in this area occur intensively. (Figure 6). The slope of more than 30 degrees causes the mass movement of soil and rocks to be faster down the slope, causing soil erosion on the surface to cause landslides. Also, the lithological conditions are the soil and clay, which become the slip plane which makes the soil move faster. Apart from geomorphological and lithological conditions, house structure weight also accelerates the occurrence of ground movements and landslides.

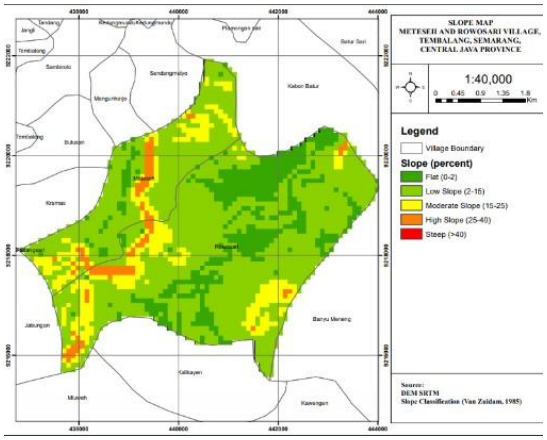

Figure 5: slope map of the area of Meteseh and surrounding areas

Figure 6: Ground movement (landslides) in the study area

Stratigraphy and Geological Structure

From the results of direct research activities in the field and secondary data in the form of regional geology, the lithology of the study area is compiled, there is lithology in the form of Claystone and Sandstone. Lithology which dominates the research area is Batulempung. Because the research area is dominated by Batulempung, this research area belongs to Kalibeng formation.

Satuan Batulempung

Claystone is a rock that has a very fine and dense grain size. This rock has good sorting, composed of uniform size of rock granules, composed of clay minerals which have a massive structure. The layer of claystone is quite thick. There are clay soils, and there are 3 - 15 cm breccias.

Satuan Batupasir

Sandstones are formed from rock grains which undergo cementation processes into mineral crystal fragments or original rock fragments. This lithology unit is described based on its physical appearance in a megascopic way. Based on the results of fieldwork in the study area, the Sandstone lithology unit has a very fine grain size. Around this, sandstone also found clay material.

The research area is in the Kendeng Basin boundary with the North Serayu Basin, that is undergoing formation in the tertiary era, and the process is still ongoing until now. Meteseh is located in the highland area of Semarang which is located at the north of the southern mountain range. This area has undergone several deformations. Structural forming activities at Tinggi Semarang are controlled by its closest fault, the Muria-Kebumen Fault. (Romario, 2016). Based on field data, geological structures were found that cut lithology layers of thick claystone with very fine sandstones that had layers of N212ºE / 58º, a layer that had a dip showed that the area had experienced tectonism so that lithology was deformed. A fault was found on a small river near the construction of a Metro Jaya housing complex and in the Bukit Kencana housing area with direction N284ºE / 32º. (Figure 8). After an analysis using Dips 6.0 software, the main direction of N18ºE / 64º is generated, the fault is a left thrust slip fault (Rickard, 1972). (Figure 7).

The fault was formed after lithology in the Kalibeng formation which was deposited on late Miocene until the early Pliocene was formed. So based on the deformation on the island of Java interpreted the fault experienced formation in the Plio tectonic period. With the direction of the main stress N-S fault was the fault result of re-activation of the meratus pattern. Young deformation in the central part of Java is controlled by intensive subduction again, in the Pliocene-Pleistocene with the direction of the N-S affirmation it forms an oblique wrench fault (Natalia, 2009) so from the results of the analysis according to the classification of Rickard (1972), the fault was a rising fault which at the same time experienced a shift to the left. These faults control the movement of the soil at the study site so that the location of fault discoveries is often found in landslide movements that occur on the river wall.

Perpustakaan Negara Malaysia eISBN 987-967-17889-6-7

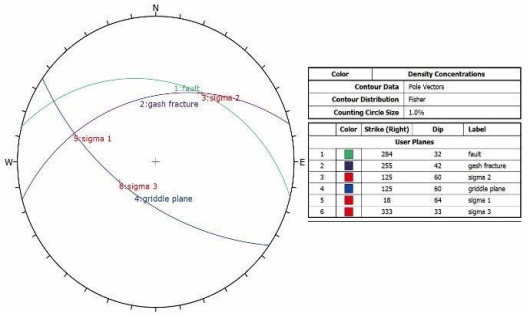

Figure 7: Fault Analysis using Dips 6.0 software

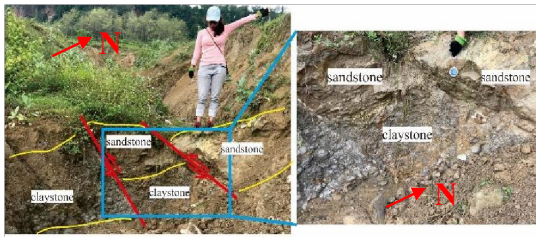

Figure 8: Kenampakan Sesar di Lapangan

Slope Stability Analysis with Slide Software

In the study area, slope stability analysis is carried out. The slope stability analysis aims to determine the level of safety of the slope against the loading given to the slope. The slope stability analysis is carried out using the Rocscience Slide application, which aims to determine the value of the safety factor of a slope. Modeling is made by describing the geometrical shape of the slope and entering the value of lithology parameters. The parameters used in this slope stability analysis are obtained from secondary data contained in the following table.

Table 1: Lithology parameter values (Arafat, 2018)

Lithology	Specific gravity (kN/m3)	Inside Sliding Angle	Cohesion (kPa)
Soil	30	29.12	2.2
Claystone	29.1	14.67	24.1

Slope modelling is done using the fellenius method with a slope of 30 degrees. From the analysis carried out obtained modelling as follows.

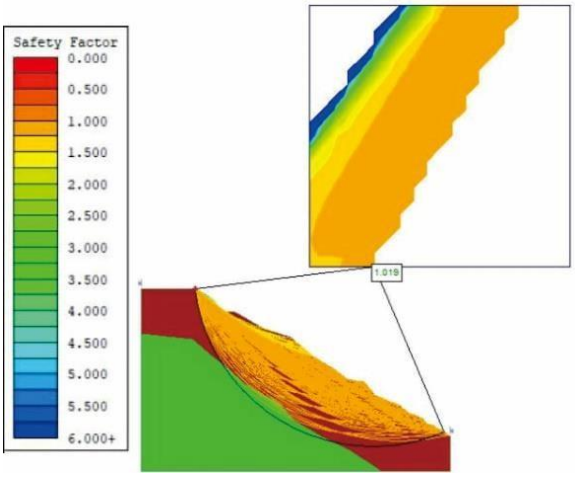

Figure 9: Results of slope stability analysis with Rocscince Slide software

The value of the safety factor based on this analysis is 1,019. (Figure 9). This value indicates that the slope has a very unbalanced condition and often occurs ground movement. (Bowles, 1991).

Counselling Program and Recommendation

From the results of activities in the field and the results of determining the distribution of soil movements, it shows that the research area has an area prone to soil movements. The results of this study indicate the need for vigilance from surrounding residents to the potential for ground movements that occur and landslides are quite high. From the results of the spread of the ground movement and also the events that occurred significantly in the study area were cracked and unsuitable housing, recommendations were given to local citizen so that before carrying out housing construction activities to present a geologist who aims to carry out geological engineering activities through observational activities related to structure, rock type, geomorphology, and topography to know the geological conditions of the study area whether or not it is proper to carry out development activities. Besides this, it is also recommended for the residents to do building construction techniques such as Soil Nailing. Soil Nailing is a sloping ground drilling technique, then in the slope is inserted concrete iron which is then mixed with cement. Soil Nailing is useful for holding buildings that are in sloping areas or prone to landslides. In addition to Soil Nailing, another method that can be used is the Concrete Sheet Pile method that is useful for holding a permanent load after building construction.

Perpustakaan Negara Malaysia eISBN 987-967-17889-6-7

Conclusion

The results of the analysis and identification of the causes of the movement that occurred in Bukit Kencana Jaya Housing, Meteseh, Tembalang District, Semarang City, Central Java, are the Geomorphological Conditions in the study area in the form of denuded structural landforms with sloping hill morphology (Van Zuidam, 1985) with a slope of about 30 ˚-40˚. The lithology (stratigraphy) of the research area is in the form of soil, claystone and sandstone—geological structure in the form of a fault with a type of Left Thrust Slip Fault. A slope safety factor value of 1.019 means that ground movement is frequent, and the soil is very unbalanced. The results of this study indicate the need for vigilance of residents around the potential for land movements that occur. It is better before housing construction is carried out, presenting a geologist to find out whether the study area is feasible for housing construction or not.

REFERENCES

Arafat, W. (2018). Analisis Pergerakan Tanah di Perumahan Bukit Kencana Jaya, Meteseh, Tembalang, Semarang, Jawa Tengah. Fakultas Tenik Departemen Teknik Geologi, Semarang.

Bowles, Joseph, E., Johan, K., Helnim. (1991). *Sifat-sifat Fisis dan Geoteknis Tanah (Mekanika Tanah*). P.T Erlangga, Jakarta.

Karnawati, D. (2005). *Bencana Alam Gerakan Massa Tanah di Indonesia dan Upaya Penanggulanggannya*. Teknik Geologi Universitas Gajah Mada, Yogyakarta.

Natalia, P. (2009). *Geologi Pulau Jawa*. Departemen Departemen Pendidikan Nasional Universitas Jenderal Soedirman Fakultas Sains Dan Teknik Program Studi Teknik Geologi, Purbalingga.

PSBA. (2007). *Sosialisasi Mitigasi Bencana Gempabumi Dan Tsunami Di Pesisir Pantai Selatan Pulau Jaw*a. Laporan Akhir Kerjasama Antara Psba Ugm Dengan Departemen Sosial Ri, Yogyakarta.

Rickard. (1972). *Classification Of Translational Fault Slip: Geological Socieaty Of America.*

Romario, I., Suprapto, R., Pambudi, D., Chandra, R., Pratama, I., Fauzan, M., Pratama, R., Rachman, R. (2016). Studi Paleogeografi Neogen Batas Cekungan Kendeng-Serayu Utara: Tantangan Dan Implikasi Pada Konsep Eksplorasi Minyak Dan Gas Bumi Di Tinggian Semarang Regional Jawa Tengah Bagian Utara. *Proceeding Seminar Nasional Kebumian Ke-9, Gadjah Mada University, Special Region Of Yogyakarta, Indonesia, (6-7 October 2016), 115-126.*

Skempton, Aw., Hutchinson, J. (1969). *Stability Of Natural Slopes And Embankment Foundations In : Soil Mechanics Amd Foundation Engineering Conference Proceeding Mexico*. Bershire, Trid, Pp: 291-340.

Van Zuidam. (1983). *Aspects Of The Applied Geomorphology Map Of Republic Of Indonesia*. Itc Faculty Of Geo-Information Science And Earth Observation, Netherlands.

Perpustakaan Negara Malaysia eISBN 987-967-17889-6-7

A Case Study of Sentinel-2 Utilization for Harvest Activity Detection in a Sugarcane Industry Thailand

Soravis Supavetch[1], Chayanut Kerenart[2], Teerawat Panchangchaiyasit[3]

[1]Affliation: Department of Civil Engineering, Faculty of Engineering, Kasetsart University, Thailand

e-mail:fengsvsu@ku.ac.th

Abstract

Sugarcane is an important economic crop of Thailand in which the sugarcane sector and the sugar industry have been highly regulated by the government since the approval of the Cane and Sugar Act in 1984. That aims to maintain the economic stability of the country and safeguard the interests of sugarcane farmers in the production and distribution of sugarcane. Thailand has 54 cane sugar production factories which produce 55 - 60 million tons in 2016 - 2017 export to the global market (13%) (a third of the world producer). In Thailand, most of the sourcing of sugarcane mills comes from contracted sugarcane growers in which sugarcane mills support the contracted farmers in terms of cane varieties and fertilizers. These contracted farms (thousands of farms) require a precise and timely technology to monitor, manage and help the growers to have good productivity. This study demonstrates the utility of the Sentinel-2 dataset in which used to monitor harvest activities and discriminate the factors relevant quality and productivity at a farm level in a large area monitoring. This proposed and demonstrated techniques are a crucial framework in a supply chain of the sugarcane industry for supporting cause analysis for planting for good production and help growers take care of their farm, then building better policies for good governance and balancing sustainability.

Keywords: Sentinel-2, Harvest Activity Detection, Sugarcane Industry.

Introduction

Sugarcane is one of the most important crops in Thailand. The government policy, such as Cane and Sugar Act in 1984, was issued in the supported industry and helped to stabilize the sector, enabling sugarcane mills to maintain their profitability even during times of depressed sugar prices in the world market. Responding to highly competitive both domestically and in the world market, the quota system (contract farming) was designed and used to guarantees the availability of sugar domestic consumption and export to the world market. The value chain of Thai sugar processing includes sugarcane plantation, harvesting, transportation, and sugar processing (Phengkhouane and Emmanuelle, 2017) all these chains require technology-enabled solutions for efficient and sustainable sugarcane. The supply of cane is said one of the three critical challenges for sugarcane mills (i.e., High variation in output, Supply of cane, and Environmental/climate change) which supports the improvement of the productivity by using incentivized and trained in better production practices from mill toward farmers. In practical, these practices implementation receive investment, and the mill currently provides financial support through the quota system.

To monitor a thousand farmers in a quota system is not simple. Also, the information for making a decision to encourage the right farmer (who need supports) requires technology to overcome the time of information gathering. Copernicus Sentinel-2 satellite data is proved that timely and accurate for harvest detection (Supavetch, 2019). Moreover, in this paper, the harvest activity, including time of harvest imply more meaning to policymakers as follows.

- Farmland faced the effect of climate change (low productivity) and needs irrigation, fertilizer for the next crop season.
- Remaining capacity in the vicinity area

Finally, all demonstrations in this paper mainly focus on showing the case study that underlines the causal relationship between the use of Copernicus Sentinel-2 satellite data and benefits resulting from their application to the Thai sugarcane industry.

Perpustakaan Negara Malaysia eISBN 987-967-17889-6-7

Problem statement

A challenge during the harvest period of the factory sector is the monitoring of cane resources, which closed to the vicinity of the mill. When it supplies are gone, the mill will request the far resources (out of a quota system) with extra cost to keep going on a sugarcane processing until the deadline. Cane resources monitor by the mill during the harvest period with a time-consuming process, such as sending their labour to visit a quota farmland every week and then gathering data to evaluate the remain resources for making a decision.

The solution to the problem

Sentinel-2 based satellite data is a high resolution (10 x 10 meters) with a frequently revisit interval of five days. That opens the opportunity to monitor the timely changing in farmland (harvesting in our case) with an ability to shift from sample inspections to largescale monitoring. The examples showing the efficiency of Sentinel-2 data explain in the following examples.

Urška et al. (2018) reports the use of the Sentinel2 based analysis system supports the EU's Common Agricultural Policy monitoring through the target of the CwRS (Control With Remote Sensing) procedure. Reports the use of the Sentinel-2 based analysis system supports the EU's Common Agricultural Policy monitoring through the target of the CwRS (Control With Remote Sensing) procedure. In this case, the time-series data is used to detect the agricultural land use anomalies supporting subsidy operation, which responding to government policy.

Another example in implementation at a farm level, ESA was setting up a Sentinels Benefits Study (SeBS) with a case study in Poland to demonstrate a concrete case and the benefits of operational use of Sentinel data. The Sentinel-2 data is analyzed to measure plant properties across a given field and in connection to the applied farming practices (e.g., fertilization) that allow farmers to make informed decisions on what needed where and when (Lefteris et al. 2019).

In this paper, the successful case by using SAVI (Soil Adjusted Vegetation Index) for a harvest detection in the previous research (Supavetch, 2019), caused this implementation framework is designed in interoperability between Remote Sensing and GIS technique to identify and report the remaining resources (canes). The context of the framework is explained in detail as follows.

Study Area

Office of Cane and Sugar Board (OCSB) reports 38% of sugarcane mills located in the North-eastern region (Figure 1). That means the part contains many growers in which already collected and registered in a quota system. This area is appropriate for demonstrating the power and utility of high-resolution satellite data (Sentinel-2) processing toward the agricultural industry, Thailand.

Figure 1: North-eastern region of Thailand

Harvest Monitoring Framework

An application of Sentinel-2 satellite data to a process of sugarcane supply chain during the crushing season contains three processing steps (Figure 2). (1) pre-check sugarcane farmland by using the NDVI anomaly. (2) harvest monitoring by using SAVI and the threshold value. (3) cane resources assessment by comparison with the data from a quota system (purchases).

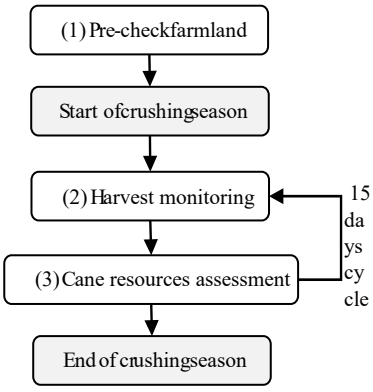

Figure 2: A crushing season process sequence

(1) Pre-check farmland

In 2019, Thailand was facing a worth drought in at least a decade. This severe drought damage mainly causes the low productivity of sugarcane crops. We found that some area in the study region has irrigation support, but others rely on rainfall for the grand growth period. An affected area investigates

Perpustakaan Negara Malaysia eISBN 987-967-17889-6-7

the production yield by using the NDVI threshold. NDVI mean value lower than 0.5 identifies canes irregular growth. These farmlands mainly used to estimate the effect on the total product. An example of the comparison of NDVI value and field check from this process demonstrated in Figure 3.

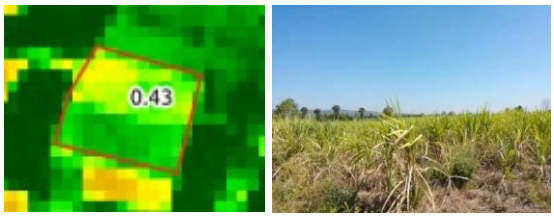

(a)

(b)

Figure 3: (a) drought effected farmland (NDVI=0.43) (b) normal yield farmland (NDVI=0.63)

The result from the processing found that 6% of total farmlands majorly affected drought (NDVI less than 0.5). Thus, additional agricultural information, such as irrigation, cultivation, and treatment, is collected. These collected data aim to analyst and define a factor for improving a plantation in the next crop.

(2) Harvest monitoring

In Thailand, the majority of farms are small and medium farms, 52% and 31%, respectively causes that sugarcane usually harvested by hand more than mechanical (Phengkhouane and Emmanuelle, 2017). The 15 days detection cycle set up for at least four satellite imageries has sensed at the study region (S2A and S2B) then using minimum value composite for preparing a dataset for harvest detection. This satellite imageries cover 110,000 square kilometres and overlap between map grid UTM zone 47 and 48. The workflow of this harvest monitoring is demonstrated in Figure 3.

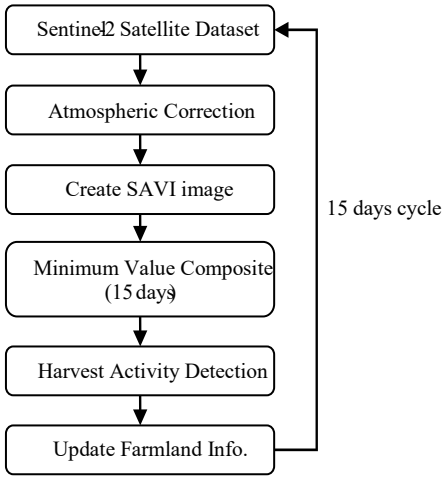

Figure 3: Harvest Monitoring workflow

(2.1) Dataset Automatic Download

Copernicus Open Access Hub provides free and open access to REST API for a user registered on SciHub access to Sentinel data through a programming language (Copernicus Open Access Hub, 2014). In this Harvest Monitoring process, every five days, a python script is executed to query and sending a request to download the lastest Sentinel-2 Level-1C (L2C) Top of Atmosphere (TOA) dataset. It was set up five days due to its synchronous to the re-visit interval of the satellite.

(2.2) Atmospheric Correction

The main propose of using Sen2Cor for atmospheric correction due to it produces a classification map that crucial for cloud masking used in the multi-temporal images composition process.

Sen2Cor command-line program is executed to perform a pre-processing of L1C product to Level-2A (L2A) Bottom of Atmosphere (BOA) product, and that also applied scene classification. Sen2Cor corrects the effects of atmospheric, cirrus clouds, and terrain then converts the result into an ortho-image product. Scene Class (SC) module produces a useful classification map consist of clouds (including cirrus), shadows, vegetation, soils, and water. This SC image used to eliminate cloud cover in the composition process. Finally, Sentinel-2 L1C resolution 10 x 10 square meters are resampled to 20 x 20 square meters L2A product (Mueller-Wilm, Devignot and Pessiot, 2019).

Perpustakaan Negara Malaysia eISBN 987-967-17889-6-7

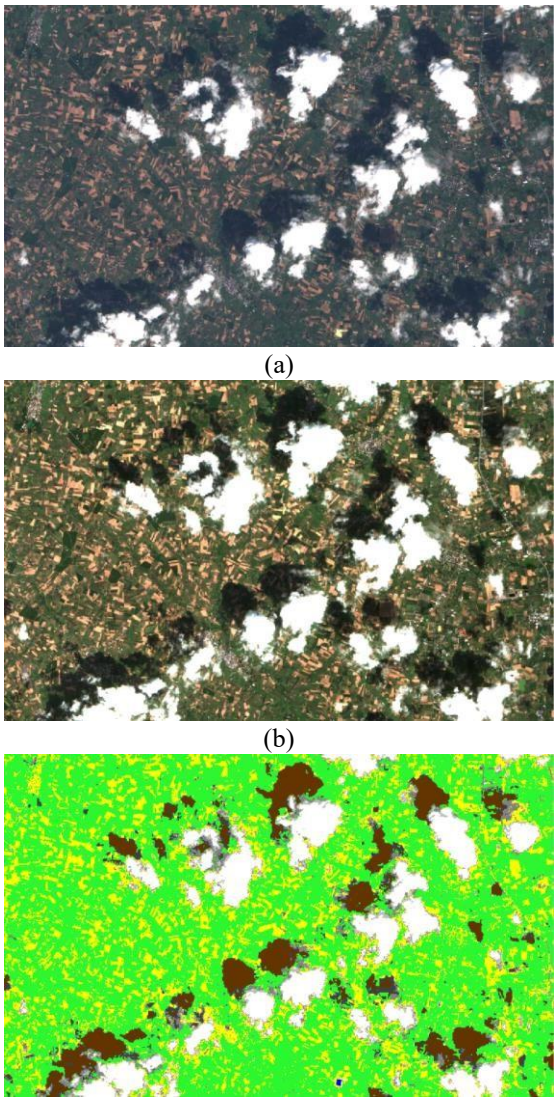

Figure 4: (a) Level-1C (TOA) product, (b) Level-2A (BOA) product, (c) Classification map from SC module

In Figure 4 (b), product L2A in visible bands seems to be more clearly then L1C (a) due to atmospheric effects is ready corrected. Supavetch (2019) evaluated the difference between none correct and correct atmospheric effect by Sen2Cor; the result has shown that difference is symmetrically shape and might not a significant difference in terms of the ratio of the bands indexed (SAVI). In Figure 4 (c), display a classification map, clouds classed as white, shadows classed as brown, vegetations classed as green, and soils classed as yellow.

(2.3) Create SAVI image

Red and NIR bands used to process a soil adjusted vegetation index from equation (1). Soravis (2019) reports the selection of SAVI for the harvest detection process caused it reduces the effect of the soil, especially in the harvest period that vicinity usually has a lows plant density. Precisely, the soil effect is a crucial contribution through the reflectance. In conform to that report, the canopy background adjustment factor in the equation uses L=0.48, as recommend by Sentinel Hub.

$$SAVI = (1+L)*(NIR-Red)/(NIR+Red+L) \quad (1)$$

(2.4) Minimum Value Composition

Every 15 days, which starts from 1st Nov 2019 to 30th Apr 2020, Sentinel-2 data collected into a prepared data stack. These data composed into a single dataset by using a minimum value composite algorithm. In contrast to vegetation health monitoring, plant in a harvest detection monitors when it disappears rather than how they grow. Additionally, during the process, cloud, cirrus, shadow, and water identified and removed by a classification map from the SC module, then the result will be a cloud-free.

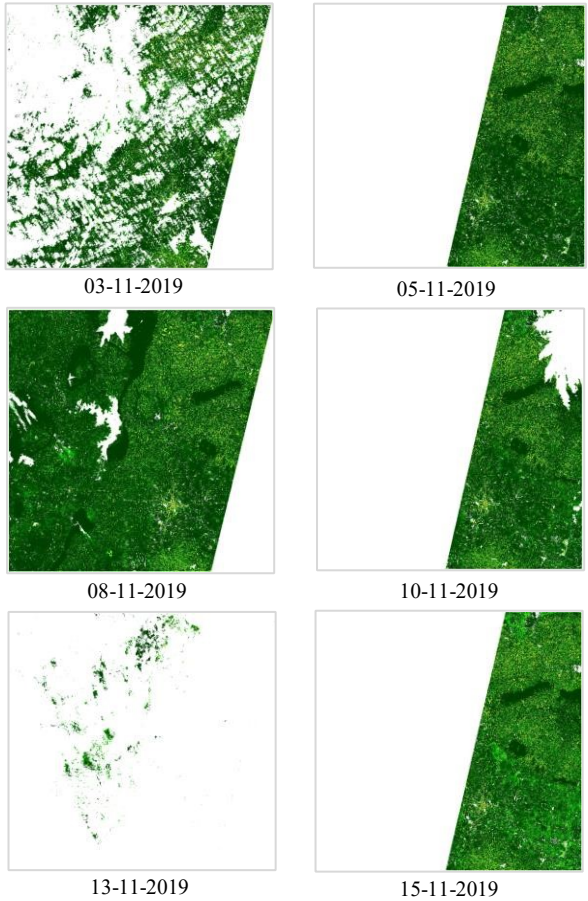

(a)

Perpustakaan Negara Malaysia eISBN 987-967-17889-6-7

(b)

Figure 5: (a) SAVI imageries between 01st Nov 2019 to 15th Nov 2019, (b) SAVI Composite image for pre-check farmland (or using NDVI).

(2.5) Harvest Activity Detection

The harvest activity detection process uses calculating zonal statistics in farmland and determines the mean value lower than 0.4 as finish a harvest. The cause of using this value due to it examined in the previous research (Supavetch, 2019). Besides, It also used in the case study of Urška, Nataša, and Tatjana (2018) in an assessment of the suitability of Sentinel-2 data for monitoring fragmented and small-size agricultural land in Slovenia in the preparation to support the European Common Agricultural Policy (CAP) post-2020 reform.

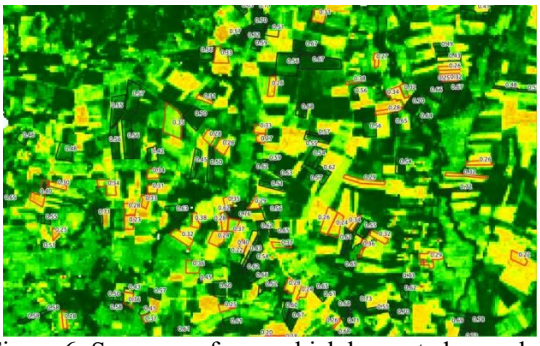

Figure 6: Sugarcane farms which harvested remark as a red polygon.

Figure 6 displays the result of harvest activity detection in the North-eastern region of Thailand. The study of the result found that since the start of the crushing season on 1st Dec 2019 until 31st Dec 2019 sugarcane farmlands harvested 34% including the 6% drought-affected. This progress rate shows that the harvest of farmlands in the quota system will end on Feb 2020.

(2.6) Update Farmland Information

Information on the detected farmlands is integrated into the GIS system. Scientific information, i.e., mean, median, min, max, and standard deviation (with a timestamp) can describe the quality and quantity of sugarcane. This data critical for future research such as the study of the effect of climate change by study the plant phenotype, modelling the sugarcane yield, and so on.

(3) Cane resources assessment

Sugarcane productivity of 30 sample farmlands that having high SAVI (more than 0.7) detected the finish of harvest are used to analyze a productivity anomaly. The result shows the high correlation between the value of the farmland area and total productivity (0.94). The R-square of the linear model of the estimation equation is 0.82. We found that the production line (red line in Figure 7) can use as an anomaly detection of farmland, which means it occurs from an unnormal activity. For example, the farm which overcapacity is a quota head or low over average productivity is a drought-effect.

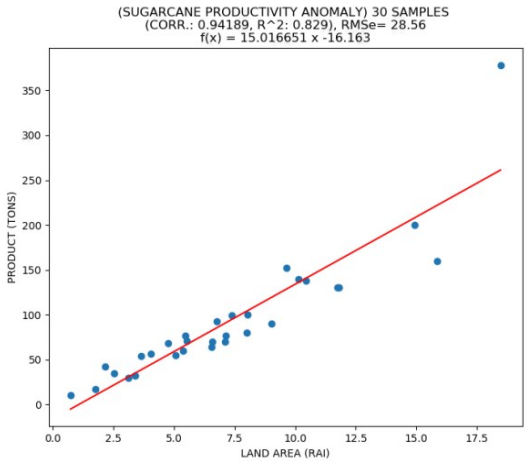

Figure 7: The sugarcane productivity anomaly

Conclusion

This study demonstrates the use of the free and open opportunity Copernicus Sentinel satellite data in implementation to monitoring a farm level on a large scale. It proofs that it can make benefits to the Thai agricultural industry and initiate a starting point to it further research and development.

Knowledge impact

This harvest detection case study, a part of the supply chain in the sugarcane industry, demonstrated the utilization steps of high-resolution imagery from

Perpustakaan Negara Malaysia eISBN 987-967-17889-6-7

Copernicus Sentinel-2 satellite data in monitoring at the farm level. The ability of this agricultural activity detection by mean of follow-up on vegetation change is a novel and useful method from free and open access to Sentinel data. That has special characteristics such as the multispectral image, high-resolution, and high frequently re-visit (5 days) since it launched the operation in 2016.

The analysis of the result of this high-resolution data processing on coverage of a large scale area, display the fluctuation of satellite data due to it influenced from more precise factors such as type of cultivation (mixed-crop), patterns of a plantation, various kind of irrigation, fertilizer, weeding, and so on. For a farm-level analysis using high-resolution satellite data, we recommend integrating a natural factor such as temperature, soil moisture, and evapotranspiration that can retrieves more from another Sentinel-1 and 3 for building more precision model.

Contribution to society and country

This research has the main aim to understand and demonstrate the value which is generated using Sentinel-2 for supporting the operation of the political affairs in the agricultural country such as Thailand, especially for crucial agriculture crops and critical to its economy. The decision-makers can use this concrete case as an example for pushing the research and development of more benefits for the country.

REFERENCES

Copernicus Open Access Hub. Accessed 12 1, 2019. https://scihub.copernicus.eu/userguide/OpenSear chAPI.

Lefteris, Manmais, Milosavlevic Igor, Khabarov Nikolay, and Tassa alessandra. 2019. A Case Study Farm Management Support in Poland. European Association of Remote Sensing Companies.

Mueller-Wilm, U., O. Devignot, and L. Pessiot. 2019. "S2 MPC Sen2Cor Configuration and User Manual." European Space Agency, 02 05.

Phengkhouane, Manivong, and Bourgois Emmanuelle. 2017. White Paper Thai Sugarcane Sector & Sustianability. FairAgora Asia Co. Ltd.

Pornpimol, Kamloi, and Chaiprasert Pawinee. 2014. "Application of value chain to analyze harvesting method and milling efficiency in sugarcane processing." The 26th Annual Meeting of the Thai Society for Biotechnology and International Conference. Chiang Rai Province.

Supavetch, Soravis. 2019. "Sentinel-2 based Remote Evaluation System for a Harvest Monitoring of Sugarcane Area in the Northeast Thailand Contract Farming." The 5th International Conference on Geographical Information Systems Theory, Applications and Management. Crete, Greece. 234-241.

Urška, Kanjir, Đurić Nataša, and Veljanovski Tatjana. 2018. "Sentinel-2 Based Temporal Detection of Agricultural Land Use Anomalies in Support of Common Agricultural Policy Monitoring." Geo-Information.

Perpustakaan Negara Malaysia eISBN 987-967-17889-6-7

School Mapping System Using GIS in Kulim Bandar Baharu District

Norina Omar[1], Nur Hani Nasihah Hedzir[2], Nor Hidayah Hamdan[3]

[123]Politeknik Tuanku Sultanah Bahiyah, Department of Civil Engineering, Kulim Hi tech Park, 090 00 Kulim, Kedah Darul Aman.

e-mail: omar.norina@gmail.com

Abstract

This paper presents the use of the Geographic Information System (GIS) system in the management of geospatial school location data. This geographical mapping of schools plays an important role, especially when the country is facing a crisis such as environmental pollution. The difficulty of obtaining school information around the study area and not having a centralized school database complicates the planning and decision-making processes. The objective of this study was to develop a geospatial information system for school locations through WebGIS and Mobile Apps. This research study utilized Erdas Imagine 2014, ArcGIS 10.2 and ArcGIS Online software. The school attribute data were gathered from Kulim Bandar Baru District Education. The findings of this research benefit the public, stakeholders and the Ministry in improving the quality of education and school management, as well as planning for future strategic development and advancement. This study can help to identify schools' locations near disaster areas for emergency response plans. It is also important for parents or guardians as a guide in selecting the best schools for children by taking into account their needs and priorities. Besides, it helps the Ministry of Education to determine the location of new schools by mapping the existing school locations.

Keywords: GIS, school, mapping, geospatial

Introduction

The rapid development of information technology has now enabled public society to obtain information easily and quickly. Various explorations of information can be obtained without access limit and boundaries. The continuous exploration of information in education is something that should be encouraged and in line with the concept of lifelong learning that is emphasized in the development of the country by the government.

School mapping is also known as a process to identify the location where the facilities are provided in the map. It consists of the formation of a geospatial database of educational, demographic and socioeconomic data for educational institutions (Sabir, 2013). The database contains data such as school geography, number of schools at different levels in public and private sectors as well as the number of teachers and number of students.

Geographic Information System (GIS) is one of the computer-based information systems used to receive, store, process, analyze and display spatial and nonspatial data (Setiawan, 2015). It is capable of helping to process geographic data to produce information and mapping digitally as well as analyze something that exists on the surface of the earth. GIS can provide geographical data or geospatial data needed by today's society. Internet technology can be used as a medium to obtain GIS data developed through media or based on digital or web mapping known as webGIS.

The GIS system is usually used in various fields, including in the education field, such as school mapping. It may help the school administration to decide an appropriate site of locating new school buildings efficiently and rationally (Agrawal & Gupta, 2016). Sudhir P. Khobragade (2016) used GIS to identify bus routes plan to school locations and facilitate the selection of schools close to home. Utomo, Saputra, Rahmawati, & Nisa (2020) utilized the GIS for mapping educational facilities in the city of Palu. They admitted that the GIS method enables getting results quickly, accurately and efficiently.

Based on the capability of GIS technology, this study applied it potential to build a database system for schools in Kulim Bandar Baharu District. This complete school mapping system shows the location school distribution around the study area together with other geospatial layers such as administrative boundaries, land use and slope. The system can be

Perpustakaan Negara Malaysia eISBN 987-967-17889-6-7

accessed accurately and effectively anywhere and anytime through WebGIS or Mobile Apps.

Methodology

This study is divided into several main phases, literature review phase and study area, data collection, database development and the production of school location distribution map through WebGIS display and Mobile Apps, as shown in Figure 1.

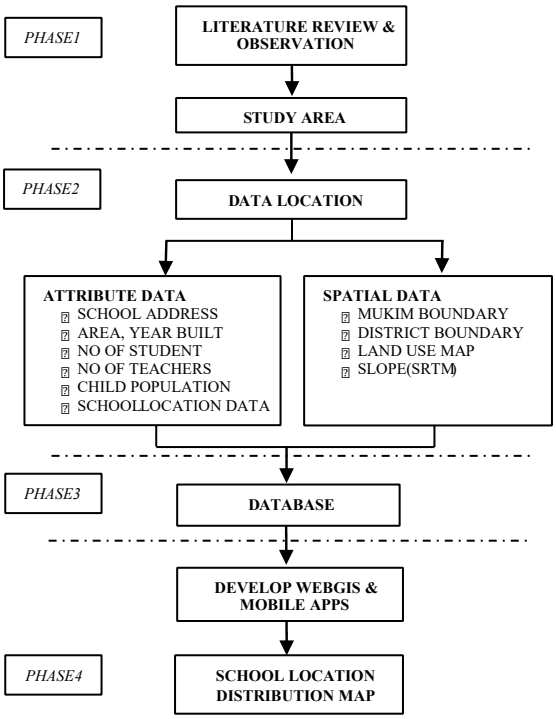

Figure 1: Flow chart of research methodology

In the first phase, a preliminary discussion on the selection of topics, the main objectives of the study as well as the survey study was conducted. This phase is important where the researcher has searched for the necessary information through the internet to find out more about mapping the location of the school. An interview session with the District Education Office (PPD) was also conducted to review the existing system and identify the needs of the PPD.

The next phase involved the data collection, which is divided into attribute data and spatial data. The attribute data were obtained from the Kulim Bandar Baharu PPD that includes the name of the school, school address, area and year of the school built, type of school, number of teachers, number of students and school location. Meanwhile, the population data is retrieved from the Department of Statistics Malaysia.

Spatial data such as administrative boundaries, land use maps, school locations, as well as slope maps, were also generated. These data processing were done using ArcGIS 10.2 and Erdas Imagine 2014 software. A hardcopy map for Kulim Bandar Baharu area was obtained from the Department of Survey and Mapping (JUPEM) Kulim Branch, Kedah. The mukim and district boundary was produced through the digitizing process. Landsat 8 image was downloaded from the United State Geological Survey (USGS) to create land use maps for the study area.

The slope map was retrieved from Shuttle Radar Topography Mission (SRTM). Besides, the school location spatial data was generated from the location details. Next, the population distribution map was produced based on the attribute information of the total population aged from 7-19 years. All these data layers were joined into one complete and organized database. Finally, WebGIS and Mobile App were developed by using ArcGIS online to portray the school's location distribution map.

Result and Analysis

1. Geospatial Database of School Locations

Figure 2 shows a view of the database system that has been developed. All these geospatial layers are grouped in one centralized system. This is to make it easier for data to be updated, organized, managed and maintained. Systems developed through GIS can facilitate the storage of information as it includes spatial data and attributes.

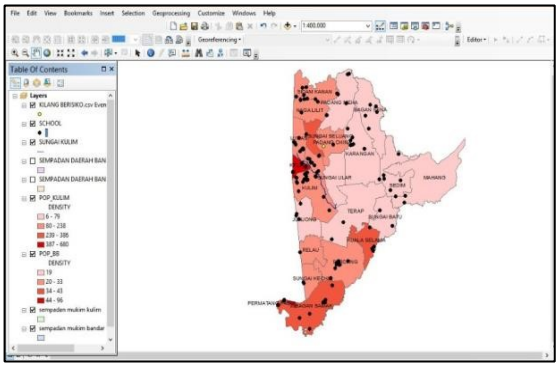

Figure 2: GIS database system

2. School location distribution (WebGIS & Mobile Apps).

This GIS application can be browsed through WebGIS or Mobile Apps. Figure 3 shows the distribution of the school location. The geographical distribution of schools around the study area is divided into seven different categories namely national school, secondary school, Chinese national type school (SJKC), Tamil national type school

Perpustakaan Negara Malaysia eISBN 987-967-17889-6-7

(SJKT), religious school, form 6 college and vocational college. These types of schools have been divided according to different classification colors to facilitate the search for information. In total, the schools in the study area have 119 schools.

Various other geospatial data such as population density, land use map, slope map and administrative boundary are also placed together to facilitate users to perform ad hoc analysis.

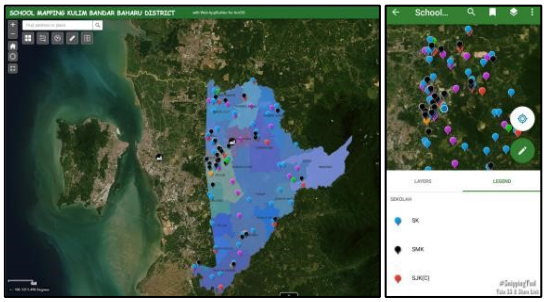

Figure 3: School location distribution map through WebGIS & Mobile Apps.

A quick analysis has been made based on assumptions in the event of a disaster faced in the school environment. The assumption that risky factory areas and polluted rivers close to schools are tested through a system that has been developed to see its potential in obtaining information.

Figure 4 shows the area of the buffer zone that has been generated through the system developed against the geographical position of the contaminated factories location with an assumed distance of 5 km. The results show that there are approximately two high-risk factories with a distance from a nearby school is 3 meters distance. Through this buffer zone analysis, schools near the distressed location or school-related problems can be identified quickly and easily, supported by Yogesh Sharma (2018).

Similarly, if the stakeholders want to know which schools need to be closed in the event of a toxic spill disaster in the river area such as pollution cases that occur in the Kim Kim River. The researchers have estimated 5 km buffer distance to identify schools affected by toxic waste dumped in the river. Figure 5 shows all the selected school from the hotspot area. The creation of the buffer zone directly from the system may help the stakeholders to identify the troubled school quickly as an emergency response plan.

The capability of this system by using ArcGIS online can make it easier for users to see the location and geographical information contained in it.

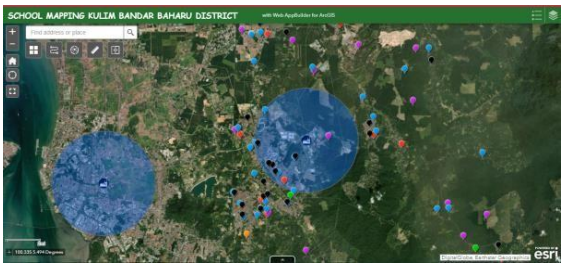

Figure 4: School Distribution and buffer zone from high risk factories

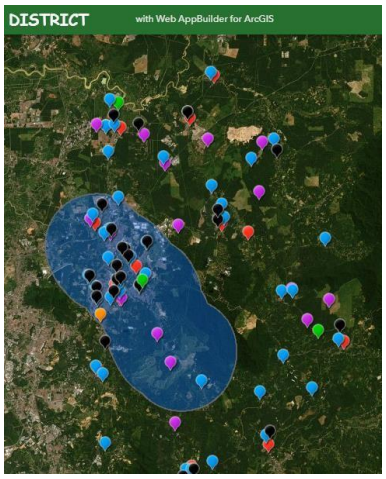

Figure 5: School distribution and buffer zone from polluted river areas.

Figure 6 shows a density distribution map, generated through density analysis. It can reveal the spatial distribution of school, whether they are clustered or randomly. Different colours are used to indicate the density of the school for an area. Dark colours indicate a dense school density compared to light colours. Density mapping is useful for modelling or understanding school data statistics in a given region.

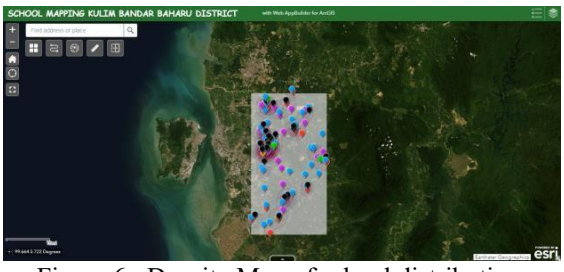

Figure 6 : Density Map of school distribution.

Conclusion and Recommendation

The use of GIS applications in school location mapping can give benefits to the public and stakeholders, especially to the ministry of education in improving the quality of education and school management and for future strategic development planning. Based on the findings in this study, a web-

Perpustakaan Negara Malaysia eISBN 987-967-17889-6-7

based and Mobile App was developed for PPD Kulim Bandar Baharu. GIS can assist with processing and analyze the school-related data faster and efficiently.

The administrators of education can see a big picture of the school-related problem through maps. Whenever data are to be viewed, they can easily visualize it. Another advantage is that they can easy compare the data with others. These

WebGIS Mobile Apps should be applied to all schools in Malaysia. The use of ArcGIS Online is an effective way to make a simple and ad hoc analysis and its display more attractive, easy to understand and interactive. The accuracy of geospatial data such as slope and land use map is better if it's generated from high-resolution images.

ACKNOWLEDGMENTS

The authors acknowledge the data provided from Pejabat Pendidikan Daerah (PPD) Kulim Bandar Baharu.

REFERENCES

Agrawal, S., & Gupta, R. D. (2016). School mapping and geospatial analysis of the schools in jasra development block of India. International Archives of the Photogrammetry, Remote Sensing and Spatial Information Sciences - ISPRS Archives, XLI-B2, 145–150. https://doi.org/10.5194/isprsarchives-XLI-B2-1452016

Sabir, M.M. (2013). School Mapping in the Light of Education Reforms in Pakistan. American Journal of Educational Research, 1, 279-282.

Setiawan, I. (2015). PERAN SISTEM INFORMASI GEOGRAFIS (SIG) DALAM MENINGKATKAN KEMAMPUAN BERPIKIR SPASIAL (SPATIAL THINKING). Jurnal Pendidikan Geografi, 15, 63–89.

Sudhir P. Khobragade, K. V. K. (2016). School Mapping System Using GIS for Aurangabad City. International Journal of Innovative Research in Computer and Communication Engineering, 4(10), 17110. https://doi.org/DOI: 10.15680/IJIRCCE.2016. 0410002

Utomo, L. P., Saputra, I. A., Rahmawati, & Nisa, Z. (2020). Mapping education facilities based on geographic information system. *IOP Conference Series: Earth and Environmental Science*, 485(1). https://doi.org/10.1088/1755-1315/485/1/012104

Yogesh Sharma. (2018). Application Of Geographic Information System (GIS) in Education. Journal of Technical Science and Technologies, 2(1), 53– 58.

Perpustakaan Negara Malaysia eISBN 987-967-17889-6-7

Plumb Bob 2.0

Norina Binti Omar[1], Bavithira A/P Ganesa[2], Maniarasiy A/P Revindran[3]

[1,2,3]Department of Civil Engineering, Polytechnic Tuanku Sultanah Bahiyah 09000 Bandar Kulim Hi-Tech, Kedah Darul Aman, Malaysia

e-mail: omar.norina@gmail.com

Abstract

A plumb bob or sometimes called plumb line and plummet have been used since ancient age. Even now, the plumb bob is still the most accurate and effective tools for determining a vertical reference line or plumb line. However, the problem that has been in a typical type of plumb bob is it took a long time to set up and do not have a proper place to store the plumb bob. The plumb bob will become dirty if frequently use in site to do the measurement. If it as excessive dirt or debris on a plumb bob and a chipped or dented by a day's work may make it unbalance and less accurate. Therefore, Plumb Bob 2.0 is created particularly for surveyors and masons' purposes. This innovative product has reel built-in to the body of the plumb bob for ease of use. The objective of this Plumb Bob 2.0 is to provide a plumb line for engineering measurement and to provide a proper way to store the plumb bob. A protective case may avoid the plumb bob from rust while keeping in a bag. A set of questionnaire forms were distributed to Geomatic and Civil Engineering student to study the effectiveness of Plumb Bob 2.0. Based on findings, this product can help surveyor and masons on-site to get a vertical datum line easily and at low cost.

Keywords: Plumb Bob 2.0, vertical line, plumb line

Introduction

The plumb bob or plummet is a bob of lead or heavyweight material to make the weight of a vertical reference line or plumb line (Shin & Alexander Y., 2018). It was generally hanging from a string to find a vertical datum and it also a precursor to the spirit level to establish a horizontal datum. The plumb bob has been used since the dawn of civilization, and it was used by Babylonians, Egyptians, Greeks and Romans to find the accurate vertical line. In ancient time, the shape that uses by ancient people called 'turnip, apple and egg'. It is a natural shape created by ancient people.

The special about the conventional plumb bob is has been used to build a pyramid in ancient time, and it was still used until the modern age especially for surveying and construction (masons to general contractors) field (Baker et al., 2010). This an ancient tool is used by carpenters, architects, bridge builders, surveyors and engineer. Plumb bob helps to mark a vertical point above and below another point such as to transfer points from a floor layout plan to a ceiling joist or suspended an interior door. The surveyor still using this tool to find accurate vertical lines in the sites. They use a plumb bob to create the nadir with respect to the gravity of a point in space as coordinate transfer devices (Kahmen, Heribert, and Wolfgang Faig, 2012).

The tool was used by a variety of instruments such as total station and steel tape to fix the instrument over the marker or position. With the advantages of extensive prowess, the plumb bob is demanded widely by a variety of users. Therefore, various shapes, features and design are created for its use nowadays to facilitate the user works—the shape made of geometric shapes which named as 'cylinder, pencil, bullet and sphere.

Electronic versions of laser plumb bob are also available that give quick and perfect readings (Schorr, Christian, and Frank Schroeder, 2018). The advantage of this toolkits is that it settles quickly once it is turned on. It generates point shapes or line shape laser beams for performing levelling or marking work in exterior or interior construction (Steffen, R., & Haefele, C., 2014). However, the price for laser plumb bob is very expensive in the market and not worth it for its function, which only to get vertical and horizontal datum. The plumb bob storage to keep this tool out there is still not proper. This may cause the plumb bob quickly damage, and the effect is not able to give an accurate reading.

Perpustakaan Negara Malaysia eISBN 987-967-17889-6-7

Hence, the Plumb Bob 2.0 is created to get a perfect vertical line for engineers and surveyor in measurement and to provide a proper way to store the plumb bob. This innovative tool has reel built-in to the body of the plumb bob for ease of use. Meanwhile, a protective case may avoid the plumb bob from rust while keeping in a bag—Plumb Bob 2.0 relatively inexpensive and straightforward in use.

Methodology

This innovation has been created to ease the students, surveyors and engineers in their works that related to the determination of plumb reference line. Figure 1.0 shows the research methodology for this innovative product, Plumb Bob 2.0. There are divided into four main phases. It is started in phase 1 is to identify the problems faced by Geomatic and civil student in using the plumb bob. Then the idea has been generated to recreate the new features of plumb bob, which can use more easily by Geomatic and civil students.

In phase 2, the Plumb Bob 2.0 have been designed with various features to assist the measurement on site. This innovative product has been sketched in AutoCAD software. Figure 2.0 and Figure 3.0 shows the front view and side view of the product, respectively. Figure 4.0 indicates front view plumb bob storage bag. The product has been assessed on-site together with other survey equipment such as total station, prism and tripod to test its centre gravity. The questionnaire was distributed to the Geomatic students, semester 1 and 5 and civil semester 1 to get their comment about the product. Then, improved the product based on the feedback received. Finally, the final product was produced according to the user's requirement.

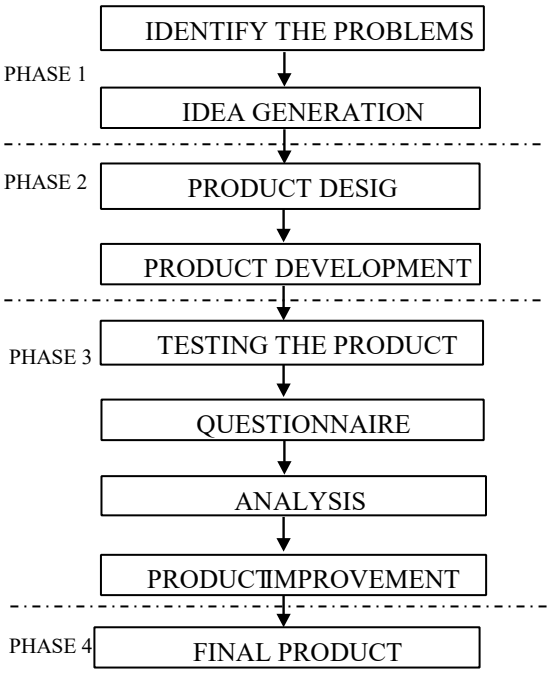

Figure 1.0: Research Methodology

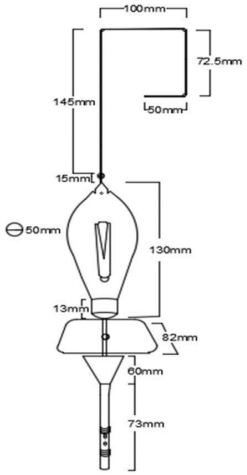

Figure 2.0: Product Front view

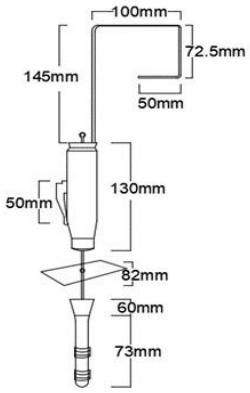

Figure 3.0: Product Side view.

Perpustakaan Negara Malaysia eISBN 987-967-17889-6-7

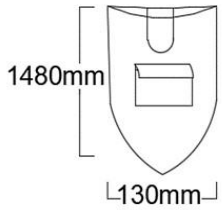

Figure 4.0: Storage bag of plumb bob

Product Cost

Table 1.0 specify the cost of the product that has been used for one (1) unit, with the total cost is RM40.20. The plumb bob 2.0 consist of a laser, plumb bob, nylon thread, plate, canvas, body part, hook, tailoring fee and hanging steel, as shown in Table 1.0.

Table 1.0: Cost of the product.

No	Material/ Item	Function	Unit	Cost (RM)
1.	Laser	To display laser light	1	3.20
2.	Plumb bob	To get vertical line	1	3.00
3.	Nylon thread	To long lasting the plumb bob	1	1.00
4.	Plate	To stable the string	1	2.50
5.	Canvas	To cover the tool	1	6.00
6.	Body part	To fixed the equipment of tool	1	3.50
7.	Hook	To hold the equipment	1	1.00
8.	Tailoring fee	To sewing the bag	1	18.00
9.	Hanging Steel (optional)	To fix or attach with concrete and build	1	10.00
TOTAL				40.20

The use of canvas for plumb bob bag is due to its capability such as sturdy, heavy-duty and durable. By combining cotton with synthetic fibres, the canvas can become water-resistant or waterproof, make it a great outdoor fabric.

Result and Analysis

Figure 5.0 shows the final product Plumb Bob 2.0. This product can help surveyor and masons on-site to get a vertical datum line easily and at low cost. Table 2.0 shows the mean score interpretation.

Figure 5.0: Plumb Bob 2.0

Table 2.0: The mean score interpretation

Mean score	Interpretation/ Level
1.00-2.33	Low
2.34-3.67	Neutral
3.68-5.00	High

Source: Landell (1997) & Mohd Najib (1994)

Results from the questionnaire as shown in Table 3.0, Table 4.0, Table 5.0 and Table 6.0. Each table indicates the respondent's feedback about the innovative product which consist of product usefulness item, friendly product item, cost of product item and product design material item respectively. Based on the results, it generally shows that the mean score for each item is high with range from 3.60 and 4.40.

Perpustakaan Negara Malaysia eISBN 987-967-17889-6-7

Table 3.0: Respondent's feedback on product usefulness.

No	Item	Mean	Level	Std. Dev
1.	Plumb bob 2.0 which helps Geomatic and civil student to get prefect vertical line easily.	4.2	High	1.08
2.	Laser plumb bob will take less time to set up.	3.7	High	1.11
3.	Plumb bob 2.0 is more productive compared to standard plumb bob.	3.7	High	1.11
4.	This product will help complete the work easier.	4.6	High	1.5
5.	Plumb bob 2.0 is helping to be effective in producing the plumb line.	4.2	High	1.09

Table 4.0: Respondent's feedback on friendly product (easy to use).

No	Item	Mean	Level	Std. Dev
1.	Plumb bob 2.0 is easy to use in construction and survey sites.	3.6	Neutral	1.2
2.	Plumb bob 2.0 is simple to use.	3.6	Neutral	1.2
3.	This product can be used without any instruction.	3.5	Neutral	1.05
4.	Plumb bob 2.0 is flexible because laser light and plate is not easy broken equipment.	3.6	Neutral	1.23
5.	This plumb bob 2.0 is effortless.	3.9	High	1.8

Table 5.0: Respondent's feedback on the cost of the product.

No	Item	Mean	Level	Std. Dev
1.	Plumb bob 2.0 is cheap with a lot of function.	3.4	Neutral	1.3
2.	This equipment is affordable to do measurements	3.8	High	1.2
3.	The price of this tool is low	3.7	High	1.12
4.	Plumb bob 2.0 is inexpensive if compare to product at the market.	3.1	High	1.3

Table 6.0: Respondent's feedback on product design and material.

No	Item	Mean	Level	Std. Dev
1.	The string which carries the plumb bob and the hold of a string is avoided from stuck.	4.1	High	1.07
2.	The hook in circle to fix on the tripod.	4.2	High	1.09
3.	This laser light in the straight line help to get the vertical line	4.2	High	1.09
4.	The plate is to stabilize more easily and faster.	4	High	1.00
5.	The bag made in the canvas is for avoiding tools from rust and dirt.	4.4	High	1.9
6.	The body parts which can carry the overall weight of plumb bob 2.0	4.3	High	1.7

Conclusion

This product is mainly created for surveying and construction works. The product may save the surveyor and engineer time in the site. The plumb

Perpustakaan Negara Malaysia eISBN 987-967-17889-6-7

bob 2.0 was also equipped with a bag that has a strong quality of canvas material. It can keep the product in the proper place, more safety and long-lasting which avoided rust and broke. This tool may help those people who need to establish vertical datum more easily at a reasonable price.

Commercialization potential

The plumb bob 2.0 obviously will save cost in term of doing the measurement. Besides, able to use other related to an engineering company for engineering measurement and surveying works. Finally, this product fulfils the user requirement.

REFERENCES

Baker, J. D., Baker, R. W., & Gregory, M. J. (2015). U.S. Patent No. 9,121,700. Washington, DC: U.S. Patent and Trademark Office.

Kahmen, H., & Faig, W. (2012). Surveying. Walter de Gruyter.

Schorr, C., & Schroeder, F. (2018). U.S. Patent No. 10,054,441. Washington, DC: U.S. Patent and Trademark Office.

Shin, A. Y. (2018). The Plumb Line and Hand Surgery.

Steffen, R., & Haefele, C. (2014). U.S. Patent No. 8,668,182. Washington, DC: U.S. Patent and Trademark Office.

Perpustakaan Negara Malaysia eISBN 987-967-17889-6-7

Towards a 3D Cadastre Augmented Reality in Malaysia

Farah Ilyana Hairuddin, Abdul Rauf Abdul Rasam, and Mohamad Hezri Razali

[1] *Faculty of Architecture, Planning and Surveying, Universiti Teknologi MARA, 40450 Shah Alam, Selangor Darul Ehsan, MALAYSIA*

e-mel: farahilyanawork@gmail.com, rauf@uitm.edu.my.hezrirazali@uitm.edu.my

Abstract

This paper discusses the capabilities of augmented reality (AR) and 3D visualization in enhancing the geovisibility and geoinformation of the stratified property to the current strata plan towards the implementation of Malaysia 3D cadastre AR. Though there has been an initiative on the development of stratified properties' 3D model in the current strata system by encoding the 3D parcel in the format of .xml, the 3D visualization and AR availability are limited in the context of desktop-based approach. With the integration of AR and 3D visualization, the documentation of stratified properties in a strata plan is potential to be enhanced from 2D planimetric to 3D representation due to the technological advancement of augmented reality that overlays virtual object onto the real world and in the context of this paper, which is overlaying 3D model of the stratified property and standard strata information virtually on the present strata plan to create an enhanced reality which brings the information to be viewed by more stakeholders with less restriction by using a smartphone device.

Keywords: Augmented Reality, 3D Cadastre Visualization, Strata Management, 3D Modelling.

Introduction

Augmented reality (AR) is a technology that overlays virtual object onto the real world with the conceptual basis of require using computer graphic technique on an object that contains necessary information and present it into the real environment, making it an enhanced reality. Application of AR is seen to be a potential problem solver in tackling limited space of a paper to show more information with its capability in retrieving more information together with the implementation of a smartphone application (Yuchen, 2017).

By enhancing strata plan visualization, information on stratified properties hold on the surface of the land is seen capable of being delivered effectively with the application of AR technology. The mechanism that allows AR to overlay virtual objects onto the real world is due to its tracking technologies which consist of three types which are sensor-based, vision-based, and hybrid-based (Qiao et al., 2019). With enhancement using AR technology, usage of a physical version of the strata plan can still be preserved. At the same time, new information is being added virtually by using a vision-based technique where it works by aligning the virtual content with real-world object based on the information from the pose estimation of the feature correspond. The digital strata plan will be registered as object recognition. As the smartphone device's camera detects and tracks the physical version of the strata plan, the information will be augmented on the hardcopy of strata plan virtually on the screen of smartphone device. Hence, the type of vision-based method suggested is marker-based.

The idea behind this study was inspired by research regarding the attempt in implementing 3D Cadastre in Malaysia. Due to the fasten development and urbanization, there are many infrastructures above and below the land surfaces that involved different ownership on the same column of land surfaces and the situation is no longer able to be portrayed on the 2D flat surface (Chai, 2006; Hassan et al., 2008). Ever since 2006, the community is aware of the advantages of 3D representation in cadastral mapping.

It has been discussed in previous research that the opting 3D database can obtain good and efficient land management in Malaysia in the cadastral system and 3D cadastral can be made realizable with the development in 3D GIS (Nizar Hashim et al., 2018). Utilizing 3D model into 3D GIS and application of the web-based system will bring benefit to the land administration system as it enabled managing the strata rights in 3D and enhanced the information to be

Perpustakaan Negara Malaysia eISBN 987-967-17889-6-7

visualized in 3D as conducted by previous research such as Jamil et al., (2017) and Hashim et al., (2019).

However, with the application of AR, the 3D visualization enhancement can be extended into legal documentation such as certified plan and certified strata plan by utilizing 3D model into AR environment which enables producing 3D legal documentation due to the integration of augmented reality and 3D visualization. The integration enables viewing the stratified property in 3D on the 2D plan surface of the current format of the strata plan. This could bring benefits to many stakeholders of the legal documentation as more information can be retrieved in digital and virtually augmented on the physical documentation.

The initial step requires preparing digital content to be used with AR technology where 3D models of the stratified property have been developed, and its strata information has been prepared in Autodesk Revit 2019. The schedule of the parcel was used as a reference on the horizontal and vertical dimensions of the stratified property during 3D model development. Two types of 3D models have been developed, which is a 3D model by floor and 3D model for the whole stratified property. The generated 3D models were then exported into the format of.FBX (Filmbox) and converted its material in Autodesk 3Ds Max to enable being used in the game- engine software where in this study, Unity game-engine software was used. Next, the development of AR was conducted in Unity by importing the AR environment, which is the Vuforia System Development Kit (SDK) onto the game-engine.

The expected product in the study is to enable viewing the enhanced visualization of Strata plan in AR mode that will bring benefits to government, private sectors by maximizing the information retrieved in aspect providing 3D information being displayed on the 2D plan surface of the current strata plan. This study will be beneficial to surveying or geomatics field, especially in a cadastral or land information management system.

Methodology

There were five stages involved in allowing the integration of augmented reality and 3D visualization, as shown in Figure 1. The designation of the flow chart was inspired by the four phases required to develop complete AR application developed by Chi et al., (2013) which has also been applied by Williams et al., (2014) and suggested as the workflow in developing AR application by Usmani (2018).

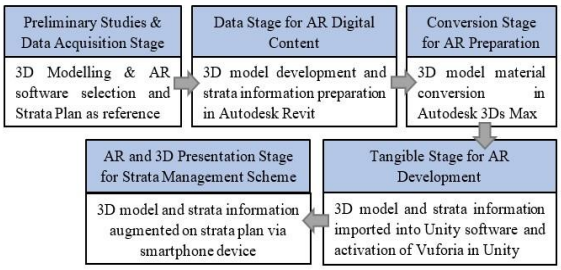

Figure 1: Framework of Integrating AR with 3D model

Towards A 3D Cadastre AR: Practical Stages

Preliminary Studies & Data Acquisition Stage

During this stage, the tasks conducted consist of acquiring data to develop the 3D model of the stratified property and selecting compatible 3D model development and augmented reality software, as shown in Figure 2.

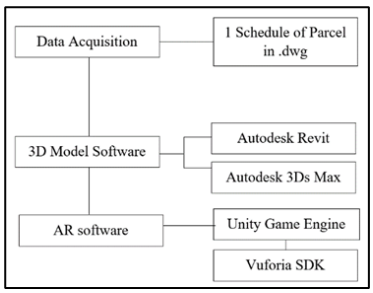

Figure 2: Framework of the preliminary stage

To generate a 3D building model, the building's schedule of parcels (JP) was acquired as a secondary data source. The horizontal dimension value in JP acted as the building footprint. In contrast, the vertical section value acted to extrude the building to enable the stratified property able to be visualized in 3D.

As for 3D Model development, the software used as Autodesk Revit, next, Autodesk 3Ds Max was used to convert the material format of the 3D model to allow compatibility to be used in the game engine.

For AR development process, the game engine software used was Unity software. The AR environment activation in Unity was conducted with the installation of Vuforia software development kit (SDK) into Unity. Besides that, to allow building the AR application into an Android smartphone device, Android Build Support was installed in Unity. Brief explanations for components used together with Unity software are as below.

Perpustakaan Negara Malaysia eISBN 987-967-17889-6-7

(a) Unity 2017.2

Majorly utilized as 2D and 3D game engine developed by Unity Technologies engine and it specializes in supporting 3D content creation, VFX, and filmmaking (Crossplatform Augmented Reality with Unity | Viget, n.d.). With its cross-platform features, many AR software development kit (SDK) is Unity-support such as Vuforia, ARCore, ARKit, and AR Foundation. Unity is not opensource software. It offers individual and enterprise plans. The free version of Unity can be obtained by subscribing to a student or personal plan under the individual category. For this study, the personal plan of Unity was acquired, and the features sufficiently
complement the study's need

(b) Vuforia

Vuforia is a software development kit used for the development of AR apps and it is installed in Unity game engine and have the capabilities in robust tracking and able to be performed with a variety of hardware such as mobile devices, a head-mounted display and Microsoft Hololens (Unity - Manual: Vuforia, n.d.). There are several targets that Vuforia capable of working with to enable the digital content to be augmented onto the selected target which consists of model targets, image targets, multi targets, cylinder targets, object targets, and VuMarks (Vuforia | AR Features, n.d.). In this study, image target was used as the type of target since within one schedule parcel consists of two-floor plans and a vertical section that acted as the targets.

(c) Android Build Support

Since the application will be built in Android device, Android Build Support platform module allows building and running the AR application in Android as it is responsible for switching Unity project to Android Project before the AR development process started. The required dependencies for Android Build Support consists of Android SDK & NDK tools, and OpenJDK.

Data Stage for AR Digital Content

Data digitally presented in AR application were prepared in this stage using Autodesk Revit 2019. The two types of data being prepared consist of geometry information which is the 3D model of the stratified property and non-geometry information which is the parcel's textual information.

Figure 3 shows the framework of this stage, where there were two main tasks involved in this stage. The first task was 3D modelling, where three 3D models of Block A Low-Cost Apartment Mawar were developed. Next is object attribute where each parcel in Floor 1 and 2 was assigned with a set of strata information attribute.

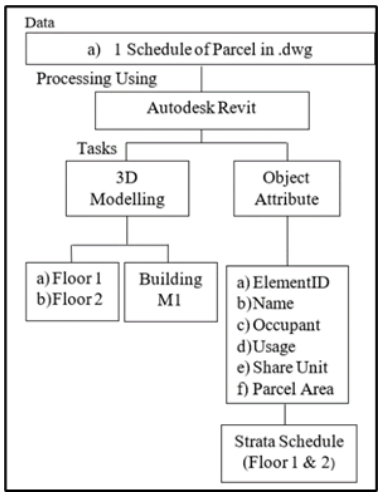

Figure 3: Framework of data stage for AR digital content

The 3D modelling was developed using an architectural template. The building's elevation was referred to the vertical section in JP and developed in the elevation view of Autodesk Revit using the level tool. The horizontal dimension of the building was defined using Wall function. To ensure the dimensions drawn were following the JP, modify tools and measurement tools were used as checking tools.

To delineate the parcel from the centre of the wall in the 3D model requires using Space Separator tool where the parcel's walls were separated to its centerline as shown in Figure 4. Next, the space tool was used to define the area of the parcel from the wall's centerline. Both of these functions can be found under the analyze tab.

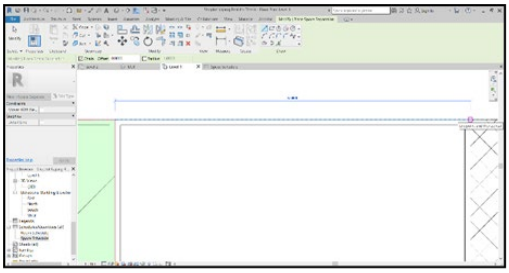

Figure 4: Delineating parcel boundary from the centre of the wall using space separator tool

Perpustakaan Negara Malaysia eISBN 987-967-17889-6-7

At the end of this stage, three 3D models as shown in Figure 5 were exported in. FBX format and the strata schedule as shown in Figure 6 was exported in.TXT format to be used as AR digital content.

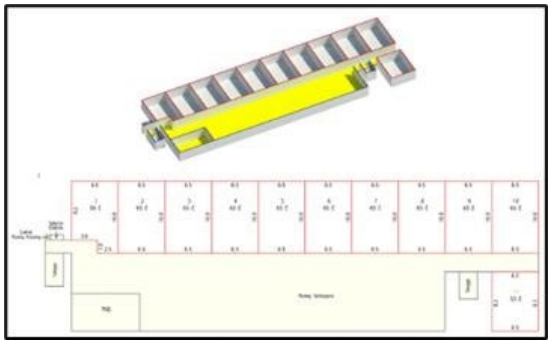

Figure 5: 3D Model and 2D drawing of Floor 1

<Strata Schedule>

A	B	C	D	E	F	G
ParcelID	Name	Number	Occupancy	Area	Purpose	Unit Share
452240	Parcel	1	Rafi	59 m²	Business	50
453165	Parcel	2	Shahira	65 m²	Business	55
453356	Parcel	3	Ihsan	65 m²	Business	55
453657	Parcel	4	Atikah	65 m²	Business	55
453939	Parcel	5	Hizam	65 m²	Business	55
454194	Parcel	6	Sakinah	65 m²	Business	55
454456	Parcel	7	Faez	65 m²	Business	55
454702	Parcel	8	Syazwani	65 m²	Business	55
454954	Parcel	9	Alif	65 m²	Business	55
455260	Parcel	10	Nadhirah	65 m²	Business	55
455878	Parcel	11	Zalina	53 m²	Business	45
456208	Common Property			10 m²	Stairs	
457119	Common Property			49 m²	TNB	
458182	Common Property			11 m²	Stairs	
458523	Common Property			1 m²	Void	
458723	Common Property			1 m²	Electric Flow	
459649	Common Property			559 m²	Multipurpose Spac	

Figure 6: Strata Schedule of Floor 1 in Autodesk Revit

Conversion Stage for AR Preparation

The 3D models prepared in Autodesk Revit in the format FBX was imported into Autodesk 3Ds Max to allow the 3D models material compatible to be used in Unity during AR development process. In this stage, standard material was applied to all the 3D models' component to allow the material to stay intact on the 3D models when it is being imported into Unity. The 3D models were then exported in the format of.FBX to be used in Unity. Figure 7 shows the framework of this stage.

Assigning material to the wall that has been conducted in Autodesk Revit was for the purpose to retain the element of 2D documentation format to the 3D model where the parcel boundary, common property, and accessory parcel were recognized by colour, which is red, yellow and blue.

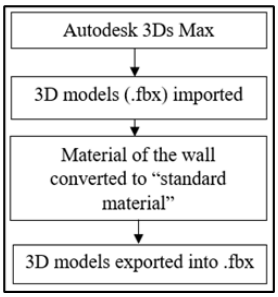

Figure 7: Framework of the conversion stage

Tangible Stage for AR Development

Tangible Stage for AR development consists of selecting suitable AR software for preparing a 3D model into the AR environment and selecting the appropriate device to run the AR experience. For this study, Unity has been chosen as the game engine software for AR development process, and smartphone device was selected as the tangible tool to display the output. The software selection was based on the mention and usage of it from previous studies on AR studies such as Carrion-Ruiz (2019) in the recreation of the Queen Victoria sculpture for AR apps and Vincenzo Barille (2019) in developing cultural heritage AR apps.

Three 3D models were imported into Unity and activating Vuforia in Unity has allowed the activation of the 3D models into AR environment, and the digital schedule of the parcel was registered as the marker by Vuforia system for the 3D model to be augmented on top of the hardcopy of the schedule of the parcel.

In this stage based on Greene (2018), the operations involved setting up Unity game engine for augmented reality development, converting images to trackable data sets which in this study was the schedule of parcel's (JP) digital image, adding overlays which is the 3D model of the stratified property to trigger images of JP upon detection by the smartphone device's camera to allow augmenting the 3D model virtually and lastly is building standalone augmented reality application to Android device.

(a) Setting up Unity game engine for AR development

In this initial stage, the Android SDK was connected to Unity. To enable the Unity game engine to be in augmented reality environment, Vuforia was activated in the Unity as it consists of AR Camera function that shall activate AR functionality which is an image function for the registration of Image Target that acted as the marker to the scene.

Perpustakaan Negara Malaysia eISBN 987-967-17889-6-7

(b) Converting the image target to a dataset

The image that l act as the marker need to be easily distinguished in reality and consists of complex shapes to enable easy detection due to the uniqueness. For this study, the schedule of the parcel in .jpg and .png was uploaded to Vuforia system to code the image with tracking information. Upon obtaining the augmentability rating, the image database was downloaded, and the image was imported into Unity to register as the target/marker.

(c) Adding overlays to trigger images

In Unity, the 3D models were located under 'Image Target'. The 3D models were positioned on top of the schedule of parcel .jpg after imported into Unity, as shown in Figure 8. This allows the 3D models to overlay onto the physical version of JP when the AR camera function tracks the physical version of the plan.

Next, Three C# language scripting was developed and attached to the 3D models in Unity to allow strata information retrieval from each parcel of augmented Floor 1 and Floor 2 3D model during running the AR application in a smartphone device. The three scripting consists of Strata Schedule Parser, Parcel's Metadata, and Parcel's Information Retrieval. Brief explanations on the scripts are as below.

a. Strata Schedule Parser Script

Responsible in reading the .txt file of Room Schedule and add the parcel information onto the 3D model by identifying the element in the .txt file and match it with the element of the 3D model.

b. Parcel's Metadata Script

Responsible in attaching parcel information to its 3D model.

c. Parcel's Information Retrieval Script

Display information of the parcel when the 3D model is being touched on the smartphone device's screen.

(d) Building the AR application into an Android device

The Augmented Reality application was prepared and built in the format of Android Package Kit (.APK). The Build and Run options in Unity has built the.APK AR application file to the smartphone device through USB debugging by enabling developer mode in the smartphone device.

Figure 8: 3D models utilized into AR environment into Unity software

AR and 3D Presentation Stage

The presentation stage involved visualization of Floor 1, Floor 2 & Block A of LCA Mawar's 3D model, and each parcel's strata information as the digital content of the JP through the AR application built into the smartphone device. The presentation stage involved using the smartphone device as the tangible tool and the sensor built in the smartphone device has allowed visualizing the digital content in reality.

The augmentation onto the physical JP occurred due to the four basic operations conducted by the smartphone device camera upon tracking JP as the marker. The basic operation is as shown in Figure 9.

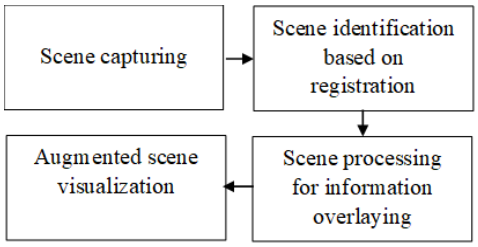

Figure 9: Framework of the presentation stage (Khan et al., 2015)

During the visualization on the physical version of the schedule of parcel, the 3D model of the floor one and floor two were augmented on the floor plan while the 3D model of M1 augmented on the vertical section. Strata information for each of the parcels were able to be retrieved when touching the parcel in the floor 3D model from the screen of the smartphone device. Figure 10 shows the framework of the visualization during the execution of the AR application in the smartphone device while Figure 11 shows the proposed enhancement towards the strata plans upon applying the AR technology.

Perpustakaan Negara Malaysia eISBN 987-967-17889-6-7

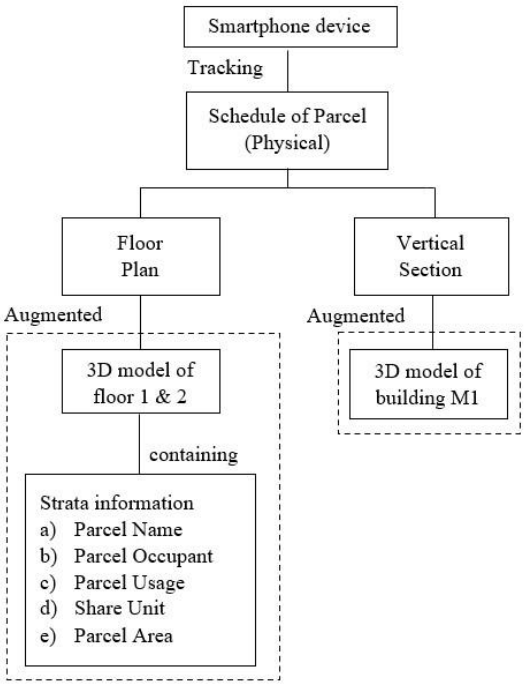

Figure 10: Framework of the enhanced strata plan visualization

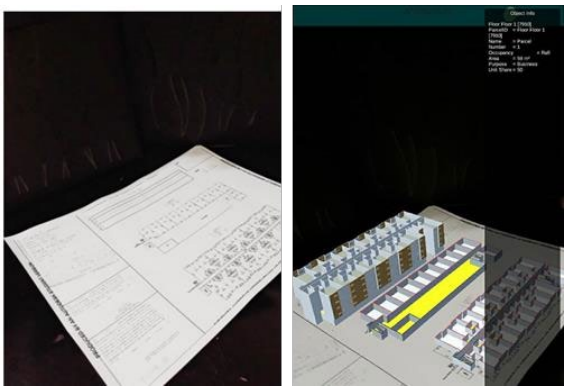

Figure 11: Strata Plan enhancement upon applying AR technology

Conclusion

Integration of augmented reality (AR) and 3D modelling can enrich the presentation and contents of cadastral information system in Malaysia. AR technology is capable of creating an enhanced reality by overlaying virtual components onto reality, and AR can be experienced through its medium devices such as mobile devices, head-mounted display, and Microsoft Hololens. The emergence of partially immersive visualization experience of AR is seen capable of redefining the way user interact, communicate and work together with the information retrieve making it to own its place in varieties of sectors such as in medical, military, tourism, navigation, education, disaster response, and games. If looking at the geomatics field and its state-of-the-art technology, there has been increasing interest in using Terrestrial Laser Scanner as a tool to measure the building due to its capabilities in providing more accurate parcel dimension measurement and three-dimensional stratified properties. 3D data collection can be obtained with ease with today's advanced technology. Geomatics field must be prepared on the technique to visualize the 3D data being collected and venturing into integrating augmented reality and 3D visualization seems like a promising possibility to maximize information deliverance to the stakeholders

Acknowledgement

The authors would like to express appreciation to the Department of Survey and Mapping Malaysia (JUPEM) for providing cadastral inputs in this research paper. The authors would also like to sincerely thank Universiti Teknologi MARA Selangor for providing LESTARI Research Fund (600-IRMI5/3/LESTARI (005/2018).

REFERENCES

Barrile, V., Fotia, A., Bilotta, G., & De Carlo, D. (2019). Integration of geomatics methodologies and the creation of a cultural heritage app using augmented reality. Virtual Archaeology Review, 10(20), 40–51.

Carrión-Ruiz, B., Blanco-Pons, S., Duong, M., Chartrand, J., Li, M., Prochnau, K., … Lerma, J. L. (2019). Augmented Experience to Disseminate Cultural Heritage: House of Commons Windows, Parliament Hill National Historic Site (Canada). ISPRS Annals of the Photogrammetry, Remote Sensing and Spatial Information Sciences, 42(2/W9), 243–247.

Chi, H. L., Kang, S. C., & Wang, X. (2013). Research trends and opportunities of augmented reality applications in architecture, engineering, and construction. Automation in Construction, 33, 116–122.

Chong, S. C. (2006). Towards a 3D Cadastre in Malaysia - An Implementation Evaluation (Issue September).

Cross-platform Augmented Reality with Unity | Viget. (n.d.). Retrieved December 5, 2019, from https://www.viget.com/articles/cross-platform-arwith-unity/

Perpustakaan Negara Malaysia eISBN 987-967-17889-6-7

Hashim, M. N., Hassan, M. I., & Rahman, A. A. (2018). 3D modelling towards strata registration. International Archives of the Photogrammetry, Remote Sensing and Spatial Information Sciences - ISPRS Archives, 42(4/W9), 23–26

Hashim, M. N., Hassan, M. I., & Abdul Rahman, A. (2019). Mobile Indoor Laser Scanning For 3d Strata Registration Purposes Based On IndoorGML. International Archives of the Photogrammetry, Remote Sensing and Spatial Information Sciences - ISPRS Archives, 42(4/W16), 241–245.

Hassan, M. I., Ahmad-Nasruddin, M. H., Yaakop, I. A., & Abdul-Rahman, A. (2008). An Integrated 3D Cadastre-Malaysia As An Example.

Jacob.W.Greene. (2018). Creating Mobile Augmented Reality Experiences in Unity | Programming Historian. Retrieved December 5, 2019, from https://programminghistorian.org/en/lessons/creat ing-mobile-augmented-reality-experiences-in-unity

Jamil, H., Noor ISA, M., Teng, C., CHAN, K. L., ABDUL RAHMAN, A., Amri MUSLIMAN, I., Ujang, U., Hassan, I., Siew, B., Karim, H., Amalina Zulkifli, N., Azri, S., & Van Oosterom, P. (2017). Converting The Strata Building to LADM (8920). FIG Working Week 2017Surveying the World of Tomorrow-From Digitalization to Augmented Reality.

Khan, A., Azhar, R., Kusro, S., & Mahfooz, S. (2015). (PDF) Rebirth of Augmented Reality – Enhancing Reality via Smartphones | Shah Khusro - Academia.edu. Bahria University Journal of Information & Communication Technologies, 8(1), 110.

Qiao, X., Ren, P., Dustdar, S., Liu, L., Ma, H., & Chen, J. (2019). Web AR: A Promising Future for Mobile Augmented Reality-State of the Art, Challenges, and Insights. Proceedings of the IEEE, 107(4), 651–666.

Unity - Manual: Vuforia. (n.d.). Retrieved December 5, 2019, from https://docs.unity3d.com/Manual/vuforia-sdkoverview.html

Usmani, A. R. A. (2018). Integration Of As-Built Building Information Modelling and Augmented Reality in Construction Industry: A Case Study Of The (UTM) Eco-Home.

Vuforia | AR Features. (n.d.). Retrieved December 5, 2019, from https://engine.vuforia.com/features

Williams, G., Gheisari, M., Chen, P. J., & Irizarry, J. (2014). BIM2MAR: An efficient BIM translation to mobile augmented reality applications. Journal of Management in Engineering, 31(1).

Yuchen, L. (2017). Augmented Reality Visualization of Building Information Model.

Perpustakaan Negara Malaysia eISBN 987-967-17889-6-7

BASIC SURV COMP TOOL

Norul Huda binti Shamsudin[1], Azilawati Binti Harun, I'zzatul Fadzilah Binti Adam, Norhayati Binti Yusof

[1]Politeknik Tuanku Sultanah Bahiyah: Kulim Hitech Park, 09000 Kulim, Kedah Darul Aman.

e-mail: norul@ptsb.edu.my[1]

Abstract

The basic concepts of angles and bearings are important because they are fundamental to the field of Geomatics. Understanding the basic angles and bearing with the help of Teaching Aids, (TA) called Basic SurvComp Tool is able to increase the knowledge of students, especially students in semester 1 of the Diploma Geomatics (DGU) Polytechnic Tuanku Sultanah Bahiyah (PTSB) program. This is because students have difficulty in distinguishing the angles and bearings and the mathematical operations behind its. The use of the tool in Teaching and Learning (T&L) process help students better understand the concept of angles and bearing that has been learned at the school level and early studies in this Geomatics program through the sense of touch and sight. The performance shown before and after the use of the tool through Pre and Post Tests has a very positive impact. Analysis of the study from the data obtained found that the increase in the percentage of students getting full marks is 38%, namely Pre-Test 25% and Post Test 63%. While low marks for Pre Test 58% and Post Test 4% only. There was an increase of 54% of students able to renew Pre and Post-test marks after using the TA.

Keywords: Fundamental of Geomatics, Bearing and Angle & Teachings Aid

Introduction

There are various basic field to Geomatics or Land Surveying namely Engineering Surveying, Cadastral Surveying, Photogrammetry, Land Development Law, Cartography, Remote Sensing, Geographic Information System (GIS), Global Positioning System (GPS) and most recently the measurement for mapping using the drone, i.e. Unmanned Aerial Vehicle (UAV) from the advancement of photogrammetric technology. All of these fields involve calculations where the basis of calculations in Geomatics is one of which is angular and bearing.

According to (Noorizal Bin Mohamed, 2005) in the field of education in Malaysia, Mathematics education is one of the fastest-growing subjects, and it is a huge challenge to make the teaching and learning of Mathematics more meaningful for students. Same as Geomatics program, this angle and bearing calculation is included in the calculation course, which starts with the basic knowledge of angle and direction, i.e. bearing. Angle and bearing teaching is generally taught in the first semester of study sessions in almost every Institution of Higher Education, (Institut Pengajian Tinggi, IPT) in Malaysia which offers Geomatic Engineering Program either government or private.

The basis of angle and bearing calculation is very important, especially in the Cadastral Survey field, which involves the measurement of land titles involving land boundaries. The boundary of the land so-called the land lot must measure it must be through the measurement of the cross-section which is the control measure that surrounds the lot to determine the boundary mark or need to plant a new boundary mark for the case of the new land lot to be measured. This control measurement involves a network of nonuniform polygon-shaped lines. Measurement and calculation are angular and bearing concepts.

This Basic SurvComp Tool is an innovation of TA creation in helping students determine mathematical operations for angle and bearing calculations. For an introduction, students will first learn the basic concepts of angles and bearings in theory, and then the students will be shown with this tool in the solution of angle and bearing calculations. This tool will make it easier for students to understand basic concepts better. Thus, these tools would help to increase the comprehension and understanding in the classroom. According to (Hayazi bin Mohd Yasin, 2008) as such, technical teachers

Perpustakaan Negara Malaysia eISBN 987-967-17889-6-7

should always be responsive to current developments about teaching techniques and their impact on the student learning process. Technical teachers also need to strive towards positive impact teaching on his students constantly. This will not only improve the quality of teaching and learning in schools; it also helps to produce students who can contribute energy to the development of the country.

Problem statement

This TA is a burst of ideas from the lecturers' observations while in the classroom being implemented. Some students are still unable to determine mathematical operations to calculate angles and to make things worse, and they are unable to calculate the number and vice versa. This confusion will slow down the T & L process implemented to focus on these students.

Figure 1 below shows an example of the calculation of the bearing B to C if given the bearing B to A and the angle. Some of these students are unable to determine the mathematical operations of either add or subtract. Some still do not know how to identify the bearing .geomatics bearing reading is from two points. Where those two points can be started, for example, in the diagram below, the reading of the bearing must be from point B because the given angle is at point B. To calculate the bearing B to C, then the bearing B to A must be subtracted by the angle □. Bearing or angle calculation cannot be performed if bearing reading is incorrect.

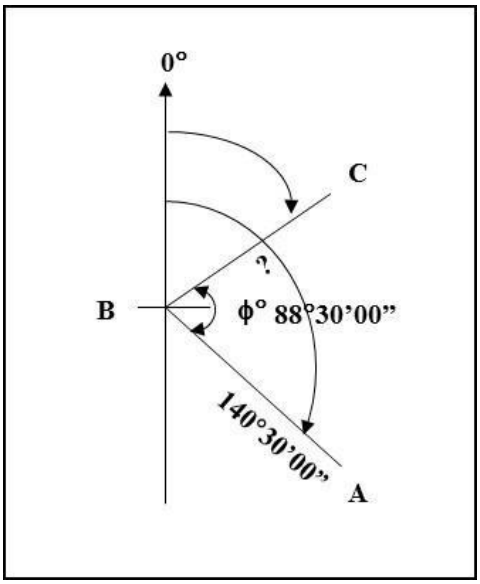

Figure 1: Diagram of counting B to C if bearing B to A and angle are given

Therefore, the knowledge base related to the basics of angles and bearing is a basic thing that Geomatics students need to know that is contained in the course DCG1012 Surveying Computation 1. From the statistics of continuous assessment and final assessment of students, it is found that students do not achieve good results.

Table 1: Comparison of grade turnover for June and December 2018 Sessions

Gred / Sesi	A+	A	A-	B+	B	B-	C+	C	C-	D+	D	E	E-	F	Jumlah
Jun 2018	0	4.7	11.8	12.9	9.4	11.8	9.4	3.5	4.7	8.2	10.6	10.6	1.2	1.2	100
Dis 2018	5.6	0	5.6	5.6	22.2	11.1	22.2	22.2	0	5.6	0	0	0	0	100

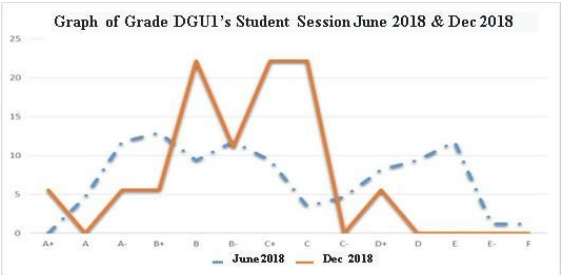

Figure 2: Comparison graph of student achievement Session June and December 2018

Based on Figure 2 found a comparison of student grades for two sessions, namely June 2018 Session and December 2018 for DCG1012 Surveying Computation course 1. From the data obtained, there are students in the June 2018 session failed for this course. While for the December 2018 session, no students failed, but there are still students who get a D + grade.

Therefore, a TA needs to be designed to overcome the problem of lack of understanding of the basics of angles and bearing because angles and bearing are important foundations to learn calculation knowledge and apply measurements in cadastral measurements to solve the problem of bearing data and distances recorded during surveying observations, to calculate the area of the lot, determination of new boundaries for subdivision and land boundaries and measuring distances that cannot be measured directly if there are obstacles in the field.

The solution to the problem

Theoretical teaching in TA is a very good method for students. Several aspects will be broken down to be studied as follows:

Teaching methods

The usual teaching methods we practice are by referring to notebooks, pens and whiteboards. Various methods need to be adapted to the current circulation according to time and technology. Hence the use of appropriate teaching materials and interesting in teaching basic reading in class recovery

Perpustakaan Negara Malaysia eISBN 987-967-17889-6-7

is important because it can improve the learning success, even more so for the teaching of English. Learning strategies using teaching aids (BBM) can improve reading knowledge and comprehension. (Mohd Hanafi, Hasnah & Mohd Mokhtar, 2007)

Student Understanding

The understanding of the concept of Mathematics differs from one individual to another and at the same time produces different achievements among them. (Mohamad Nurizwan Bin Jumiran, 2014). Thus the performance of each individual will be different from each other. More worrying if there is a group of students who did not pass for the course taken. Therefore, lecturers need to think of a new method to increase the percentage of graduates for students.

Teaching Aid (TA)

The development of education has been rapid in this country. Various efforts and methods have been applied to improve the quality of learning for students. Therefore, teaching aids have been among the rational use of teaching aids in this teaching and learning process is to highlight the concept. This means that students can witness for themselves the demonstrations and teaching aids used by teachers while delivering lessons in the classroom (Noor Azlan bin Ahmad Zanzali & Nurdalina Binti Daud, 2010). According to (Hamdan Said & Surizan Mohamad A'zmi, 2009), the TA designed can increase and accelerate again the process of understanding the concept and mastery of the topic of incarnation as students can apply yourself by using existing materials to be realized in incarnation topic skills especially rotational subtopics.

Learning Atmosphere

According to (Tay Meng Guat, 2015), fun learning is also related to the use of teaching aids. The use of interesting teaching aids will create a pleasant learning environment. This opinion is also supported by (Yahya and Dayang Raini, 2011) where the results of the study show that there is a significant difference for the mean of reading comprehension performance between middle-achieving students who follow reading comprehension teaching using computer applications interactively with middle-achieving students who follow the teaching using traditional methods in the post-test. In conclusion, fun learning should involve the creativity of teachers that can affect learning in the classroom.

Planning structure

TA Implementation Method based on Design Thinking

This method of TA implementation is to follow the Design Thinking guide to measure the needs of TA innovation that will be produced later. Next, the methodology flow chart can be drawn up through observations obtained during T & L conducted in the classroom.

Empathise

From the observations and results of students show that students are weak in the knowledge of bearing and angles which students still cannot distinguish between angles and bearing.

Define

Therefore, a TA tool needs to be created apart from relying on notes in the form of writing and diagrams only. Based on an opinion by (Firhan Bin Salian, Fauzul Azhan Bin Abdul Aziz, Mohamed Yusup Bin Mohamad Yackup, 2014) teaching and learning process has changed a lot and experienced its evolution. If previously used oral and written become a habit in teaching, now technology has changed with the use of more sophisticated tools such as a computer, video, and various uses other equipment that incorporates elements visual, audio and text. Furthermore, TA can help students better understand how to calculate angles and bears where students can hold the tool and then students can distinguish between the meanings of angles and bearing.

Ideate

A TA tool named Basic SurvComp Tool was created to meet the needs of students in helping to understand angular and bearing calculations. This statement supported by (Mohd Suhaidy Bin Rohani, 2008) a teacher should use teaching methods which aids in teaching aids or teaching media optimally can make the teaching and learning process (T&L) more effective and attract.

Prototype (Prototype)

The Basic SurvComp Tool is designed using plastic hard paper before being made on a hard and durable prospect.

Perpustakaan Negara Malaysia eISBN 987-967-17889-6-7

Test

The Basic SurvComp Tool is tested by explaining its use first along with the manual instructions on the tool. After that, students are given a Post Test question where a Pre question has been given before the Basic SurvComp Tool is given to the student.

Next the methodology flow chart is designed to produce the Basic SurvComp Tool. The methodology chart is as follows:

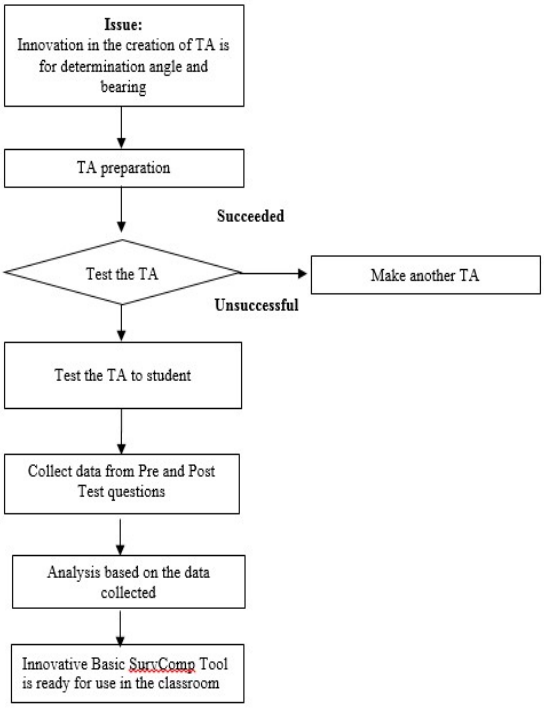

Figure 3: Flow Chart Methodology of Basic SurvComp Tool creation

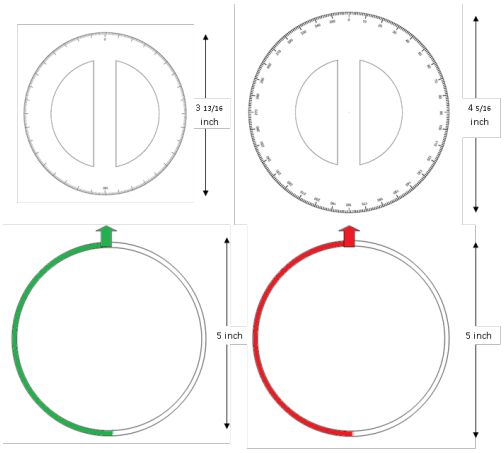

Figure 4: Dimension of Basic SurvComp Tool Figure

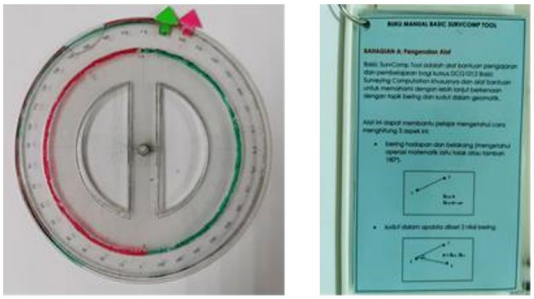

Figure 5: Basic SurvComp Tool

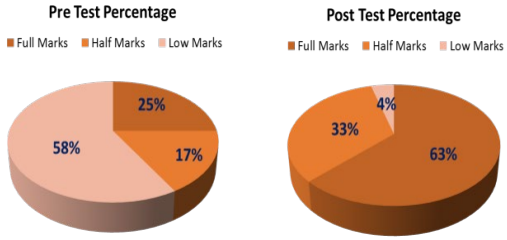

Figure 6: Percentage of Pre & Post Test Achievement

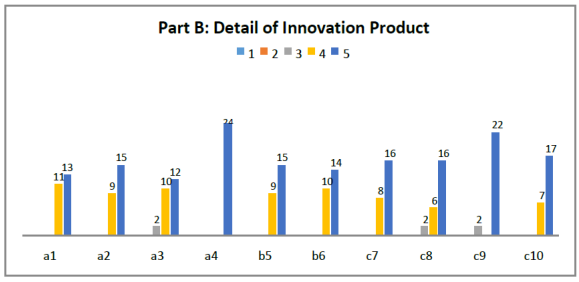

Figure 7: Graph of Detail of Innovation Product

In conclusion, in part B of question a4, tools and manual cards are easy to carry elsewhere get a high mean score of 5.0. This is because the size of the tool is suitable for holding and storing. Question c9 the appropriate tool size answers to a4 question, which is the appropriate size to hold and carry anywhere whose score is 4.8.

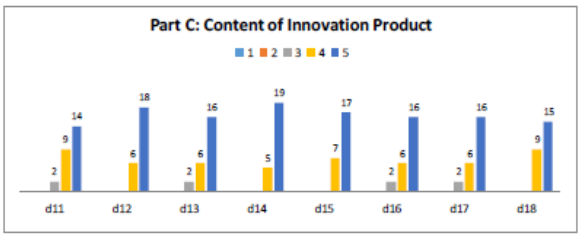

Figure 8: Graph of Content of Innovation Product

In part C, in conclusion, question d12, tool works well, and question d14 facilitates the calculation of angles in getting the highest mean score of 4.8. This shows that students agree that the tool can operate well and perfectly; that is, achieve the objective of tool creation. Also, this tool can help students in calculating the internal angle correctly.

Perpustakaan Negara Malaysia eISBN 987-967-17889-6-7

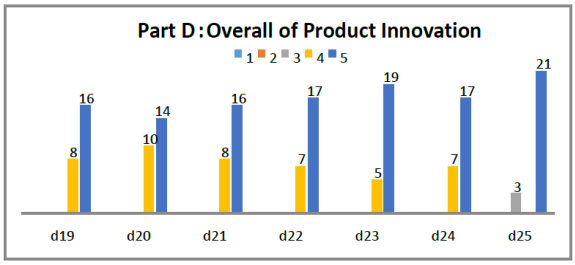

Figure 9: Overall of Product Innovation

In part D, in conclusion, question d23 students agree this tool is used by students in polytechnics and questions d25 this tool is very user-friendly got the highest mean score of 4.8 where students agreed that this tool is used to other educational institutions especially in other polytechnics. Also, this tool is user-friendly, which is very suitable for use by students to practice in the classroom and outside of class time.

Knowledge Impact

This tool is helping students sketch bearing and provide reading guidance of bearing. Also, help to know the use of mathematical operations either add or subtract to get angles or bearing. Besides, helps students calculate internal angles and determine bearing values.

Contribution to the Society and Country

In part D of the overall product, Innovation student agrees on this product use for another polytechnic. Besides, this tool has already received feedback from the Assistant Director of Survey, Strata/ Stratum/ Marin Section, Survey and Mapping Malaysia, Kedah Darul Aman, Sr. Nor Azri Juhari bin Ahmad. He agreed that this tool is widely used in other institutions, especially in other polytechnics, because a huge potential will be obtained for students.

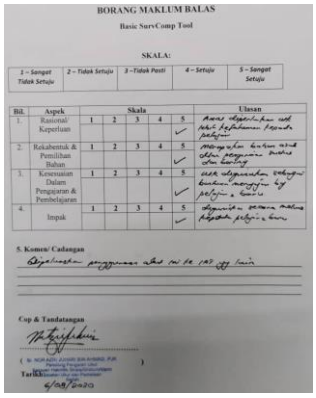
BORANG MAKLUM BALAS

Basic SurvComp Tool

SKALA:

Figure 10: Feedback of Innovation Product

Cost Impact

The cost involved in developing the innovation of the project is in table 2 below:

Table 2: Cost of Basic SurvComp Tool

Num.	Material	Cost (RM)	Total
1	Prospect 2 mm	RM55/8 pcs RM6.90 per pcs 1 set tool=4 pcs prospect	RM27.60
2	Nail 1 inch	RM1	RM0.10
3	Colour Paper	RM1	RM1.00
4	Laminate Plastic	RM2	RM2.00
Total per unit for 1 set of Basic SurComp Tool			RM30.70

REFERENCES

Tay Meng Guat, 2015, Pembelajaran Menyeronokkan Dalam Pengajaran Dan Pembelajaran Bahasa Melayu.

Firhan Bin Salian, Fauzul Azhan Bin Abdul Aziz, Mohamed Yusup Bin Mohamad Yackup, 2014, Pembangunan Perisian Modul Interaktif Hitungan 2 Berasaskan Macromedia Authorware 7

Mohamad Nurizwan Bin Jumiran, 2014, Kesan Teknik "Huntto Square" Terhadap Pencapaian Pelajar Bagi Mata Pelajaran Matematik Di Sekolah Rendah.

Yahya dan Dayang Raini, 2011, Pelaksanaan Pembelajaran Menyeronokkan Dalam Pengajaran Dan Pembelajaran Bahasa Melayu.

Noor Azlan bin Ahmad Zanzali & Nurdalina binti Daud, 2010, Penggunaan Bahan Bantu Mengajar Di Kalangan Guru Pelatih Utm Yang Mengajar Matapelajaran Matematik.

Hamdan Said & Surizan Mohamad A'zmi, 2009, Penilaian Kesesuaian Bahan Bantu Mengajar Jangka Sudut Khas Bagi Mata Pelajaran Matematik.

Perpustakaan Negara Malaysia eISBN 987-967-17889-6-7

Mohd Suhaidy Bin Rohani, 2008, Kesan Penggunaan Kit Pengajaran Bermodul (KPB) Bagi Mata Pelajaran Matematik (Sudut Dongak Dan Sudut Tunduk) Tingkatan 4 Di Dua Buah Sekolah Menegah Kebangsaan Di Daerah Pontian, Johor.

Hayazi Bin Mohd Yasin, 2008, Penggunaan Alat Bantu Mengajar (Abm) Di Kalangan Guru-guru Teknikal Di Sekolah Menengah Teknik Daerah Johor Bahru, Johor.

Mohd Hanafi, Hasnah & Mohd Mokhtar, 2007, Penggunaan Bahan Bantu mengajar Dalam Pengajaran Murid-murid Pemulihan Khas.

Noorizal Bin Mohamed, 2005, Membangunkan Perisian Modul Bahan Bantu Mengajar (BBM) Bertajuk "Solid Geometry II" Bagi Mata Pelajaran Matematik Tingkatan Dua.

Perpustakaan Negara Malaysia eISBN 987-967-17889-6-7

Dominant Tree Species Classification Using Remote Sensing Data and Object-Based Image Analysis (OBIA)

Juhaida Jamal[1], Nurul Ain Mohd Zaki[2], Mohd Nazip Suratman[3], Zulkiflee Abd Latif[4], Hamdan Omar[5], Mohd Zainee Zainal[6], Sharifah Norashikin[7]

[1] Faculty of Architecture, Planning & Surveying, Universiti Teknologi MARA, Perlis Branch, Arau Campus, 02600 Arau, Perlis, Malaysia
[2]Environment and Climate Change Research Group, Center for Surveying Science & Geomatics Studies, Faculty of Architecture, Planning & Surveying Universiti Teknologi MARA, 02600, Arau, Perlis, Malaysia
[3]Institute for Biodiversity and Sustainable Development, Universiti Teknologi MARA, 40450 Shah Alam, Selangor, Malaysia
[4]Geoinformation Programme, Division of Forestry & Environment, Forest Research Institute Malaysia (FRIM), 52109 Kepong Selangor, Malaysia

[1]juhaida0421@gmail.com, [2]nurulainzaki@gmail.com

Abstract

Forests have been the victims of over logging and deforestation. Uncontrolled of this activity gave an impact to the tree species to be endangered. Inventory of tree species is needed for forest planning. Many techniques had been done to identify tree species. Nowadays, remote sensing technique was widely used to study the distribution of tree species. In this study, an object-based image analysis (OBIA) with a combination of high-resolution multispectral satellite imagery (WV-2) and airborne laser scanning (LiDAR) data was tested for the classification of tree species at Forest Research Institute Malaysia (FRIM) forest, Selangor. LiDAR data was taken using fixed-wing aircraft with 0.15m horizontal and 0.25m vertical resolution while WV-2 was captured with a 0.5m spatial resolution. In this study, hyperspectral data with 0.3 resolution was used to extract the spectral reflectance of tree species. Study area with total area 3.5 hectare was grid into 35 rectangular subplots which each subplot has 500m^2 area. Segmentation of the image was performed using multi-resolution segmentation in eCognition software. Segmentation validation was done by measuring the 'goodness fit' between the training object and segmentation output. The overall accuracy of the segmentation was 86%. For species classification, the accuracy assessment was performed using the error matrix confusion technique, and the result had shown the overall classification accuracy was 64%.

Keywords: LiDAR, OBIA, Remote Sensing, Tree Species Classification, Multi-resolution segmentation

Introduction

Forest is one of the important natural resources for all living things. Undeniably, that forest gives a positive impact on each individual and community in social, cultural, and economic contexts. Forest released a large amount of oxygen (O_2) resulted from their photosynthesis process. The uptake of carbon dioxide (CO_2) during photosynthesis, has caused a cooling impact on the global climate. Besides providing habitats for animals and livelihoods for humans, forests and trees were the main sources in enhancing rainfall, recharging groundwater, and preventing erosion and flooding (Sanderson, Santini, Valentini, and Pope, 2012). Malaysia, which is one of the most diverse flora and fauna regions in the world, has nearly 15,000 native plant species. Eight thousand two hundred species (about 250 families) are found in Peninsular Malaysia, and 12,000 species are found in Sabah and Sarawak. (L.S.L.Chua, M.Suhaida, and B.Aslina, 2008). Due to overexploitation, the forest had to face a great threat. Uncontrolled deforestation had contributed to the negative effect on tree species diversity which resulted in the loss of valuable economic and medicinal trees (Abiola, Samuel, and Medugu, 2016). In Peninsular Malaysia, almost ninety-two taxa of dipterocarps species were in the

Perpustakaan Negara Malaysia eISBN 987-967-17889-6-7

endangered categories (L.S.L.Chua et al., 2008). This would lead to the extinction of this species if no action were taken to protect the remaining species.

In protecting the diversity of trees species, endangered tree species need to be protected. Nowadays, the use of remote sensing techniques has become a common method in forest management and tree species classification. Remote sensing improved the traditional field surveys for doing forest tree inventory, especially in obtaining species information as this method can be applied within large and inaccessible areas (Shang and Chisholm, 2014). The capability of the multispectral sensor in remote sensing technology to record spectral reflectance of the object had capable them to classify the tree species (Nordin, 2017). In classifying the tree species for large forest areas, high spectral resolution data such as satellite World View (WV-2) image is needed and helpful. This is because the WV-2 image can provide a high-resolution image with a multispectral sensor. Beside time-efficient and user-friendly, WV-2 image can provide high accuracy results for the classification of major forest tree species. Apart from that, the use of advanced remote sensing technology such as LiDAR had been introduced to be used in the study of the forest inventory as it can improve the segmentation and classification process (Hycza, Stere, and Balazy, 2019).

Problem statement

In protecting the diversity of trees species, endangered tree species need to be protected. Nowadays, the use of remote sensing techniques has become a common method in forest management and tree species classification. Remote sensing improved the traditional field surveys for doing forest tree inventory, especially in obtaining species information as this method can be applied within large and inaccessible areas (Shang & Chisholm, 2014). Conventional methods in maintaining and updating tree inventory may be challenging in terms of time, money, and effort. This is because a lot of time needs to measure the tree manually. In the large area and inaccessible area, the process may take a lot of time and energy. A large cost is required to finance employees, instruments, and transportation. In classify the tree species manually, species expert was needed. The number of species experts may not be enough or possible to classify individual tree species manually.

The capability of the multispectral sensor in remote sensing technology to record spectral reflectance of the object had capable them to classify the tree species (Nordin, 2017). In classify the tree species for large forest areas, high spectral resolution data such as satellite World View (WV-2) image is needed and helpful. This is because the WV-2 image can provide a high-resolution image with a multispectral sensor. Beside time-efficient and userfriendly, WV-2 image can provide high accuracy results for the classification of major forest tree species. However, there are difficulties in classifying the tree species using the WV-2 image. This is because there are some issues in determining the tree segmentation for the classification process if only WV-2 is used. Multispectral imagery does not have enough spatial detail to delineate the crown of the tree (Verlic et al., 2014). Apart from that, the use of advanced remote sensing technology such as LiDAR had been introduced to be used in the study of the forest inventory as it can improve the segmentation and classification process (Hycza et al., 2019).

Significant of Study

For this study, authorities and related organizations can use this information for better forest planning and management. The spectral reflectance and tree inventory results of tree species can improve forest management in identifying the position and location of the endangered tree species. This also can help in maintain the process to monitor the tree species diversity. The area that contains valuable and endangered species can be avoided from forest activity to maintain the sustainability of the species for the future generation. For the economy, this study is significant to provide a safe guideline for logging the selected tree based on species value. Hence the economy production can be increased.

Study Area

The study area for this research took place at Forest Research Institute Malaysia (FRIM) forest located at Kepong, Selangor Darul Ehsan with coordinate (3.235339, 101.634269). FRIM forest was about 80m above sea level and was categorized as lowland dipterocarp forests managed by the FRIM. FRIM forest comprises more than 2500 tree species that dominant by the family tree from *Dipterocarpacaea*. Some of the species available in this study area are listed as Endangered (EN) for example *Neobalanocarpus heimii* (Chengal), *Hopea helferi* (Giam Lintah Bukit) and, *Dipterocarpus hasseltii* (Keruing Ropol), Figure 1 show the location of the study area.

Perpustakaan Negara Malaysia eISBN 987-967-17889-6-7

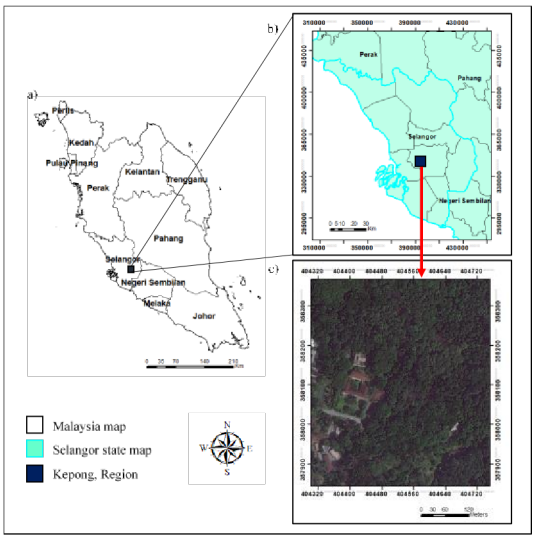

Figure 1: Location of the study area

Materials

Multispectral WorldView-2 image was used to carry out this study. The image was acquired on 23rd January 2010 covering FRIM forest at Kepong, located in the northwest of Kuala Lumpur. The image has a spatial resolution of approximately 0.5 m. The 0.5 m spatial resolution of the WorldView-2 image is one of its advantages in modern forestry. The level of detail enables the forest parameter to be analyzed at the individual crown level. Besides that, LiDAR and hyperspectral data are also used to support this study. LiDAR data was used to generated CHM while hyperspectral used to extract spectral reflectance for tree species. LiDAR and Hyperspectral data were acquired on 9 April 2013 with both have a spatial resolution of 0.15m and 0.3m respectively.

Methodology

However, remotely sensed data alone could not work efficiently without ground-based truth information, especially for this type of study. Field data collection activities were therefore carried out to support the analysis. Some survey instruments have been used in the field, such as Global Positioning System (GPS) device, total station, and tape diameter. These were used to determine location, measure tree's diameter, and height. Overall, this study consists of 4 phases. Figure 2 indicates the flowchart of methodology, represents the overall processes involved in this study.

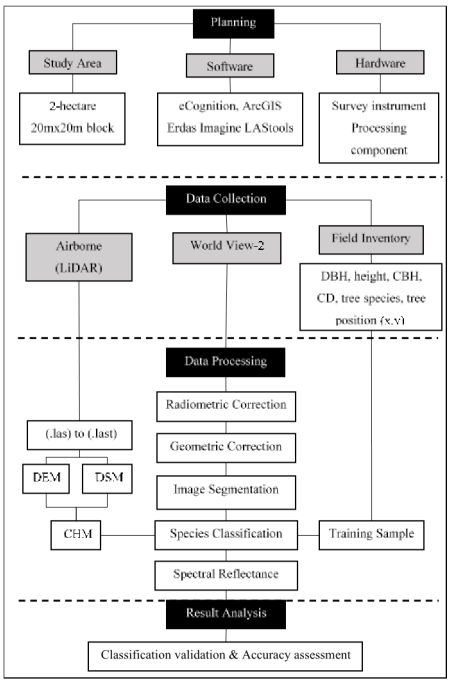

Figure 2: Flow of the methodology

Ground truth observation of the study area was carried out on 3 March 2020. The study area with a total of 3.5 hectares was grid into 35 rectangular subplots with each subplot have 500m2.area each. Three hundred twenty-seven trees were recorded during the field observation. Twenty-five species from 11 families were measured in the sampling plot. Diameter at Breast Height (DBH), height, crown diameter, tree species, and tree position (x,y) was the tree inventory parameter that was measured as the forest inventory. Figure 3 shows some process involved in the inventory.

Figure 3: Process involves during field inventory; (a) show thesub plot; (b) ID tree tagging; (c) position of tree survey; (d) DBH measurement; (e) Tree height measurement and (f) Tree species identification

Perpustakaan Negara Malaysia eISBN 987-967-17889-6-7

The image was georeferenced according to the reference coordinate. The coordinate used is Kertau GDM 2000. WV-2 image was enhanced to improve the image quality and was converted to the reflectance value for the classification purpose.

LiDAR data was then was filtered to generated DTM and DSM using ArcGIS software. Both were the main output used to generate the CHM. Canopy height model can be derived from subtracting DSM into DTM, (Abd Latif.Z, Aman.S.N.A, & Ghazali.R, 2011).In this study, CHM was derived by subtracting the DSM into DEM using the minus tools in ArcMap software. During DSM generation all classified point cloud and all return were selected while for DEM only ground returns were included.

Before the segmentation process, the convolution filter was applied to WV-2 image. A 3x3 convolution filter was applied to NIR and Red band to remove noise and increase the distinction of the features. In this study, classification was done on the object created by multi-resolution segmentation using parameter 23 for scale parameter, 0.8 for shape creation, and 0.5 for the compactness criterion. According to (Chen, et al 2015), multiresolution segmentation is often used as a segmentation algorithm in high-resolution remote sensing data. This is because image objects can be generated with greater geographical significance and good adaptability (Hay et al, 2003). Specific segmentation settings were created. The Image layer weights were adjusted for the best differentiation of forested areas, with the emphasis being put mainly on the NIR band. Before runs, the classification, the minimum and maximum NDVI value of tree were determined to classify between vegetation and nonvegetation segmented area. Non-vegetated areas were then classified into two further which is shadow and building using assign class algorithm. The features classification was done using the assign class algorithm. Table 1 show the threshold condition used to classify the features in the study.

Table 1: Features assign class threshold condition

	Classification	Threshold condition
Vegetation	Vegetation area	NDVI >= -0.01
	Tree	Vegetation with brightness > 312 & < 299.44
	Grass land	Vegetation with brightness >= 299.44 & <= 312.00
Non-Vegetation	Non-Vegetation area	NDVI <= -0.01
	Shadow	Non-vegetation with brightness <= 221
	Building	Non-vegetation with brightness > 221

There are large segments region produced from the segmentation process. This is because there is a cluster of trees in one segmented region. Since individual trees segment needs in this study, the cluster of trees is separated into individual trees using a watershed transformation algorithm. According to (Beucher, 2014) a watershed transformation image was considered as a topographic surface that defines watershed lines and a catchment basin by flooding process. Watershed transformation process had resulted in the shapeless tree segments. Tree segments are normally expected to be circular. All the tree segments were then reshaped to give them a more rounded shape. eCognition morphology algorithm was applied. The processing of morphological images includes two fundamental operations which are erosion and dilation. Dilation and erosion, respectively, are operations that thicken and thin the object in the photograph (Yahya, Tan, & Hu, 2013).

In this study, accuracy assessment of segmentation was done by using a method by (Clinton, Holt, Scarborough, Yan, & Gong, 2010) which validated the segmentation output by measuring the 'goodness of fit' (Distance index). The nearest the D value of the segmented validation result to 0 the ideal the match between xi and yj while the nearest the result to 1, this means the segmentation has the minimum value mismatch. The Distance index was measured by calculating the over and under segmentation which involves the area training sample (xi), segmentation output (yj), and the intersect area between the training and segmentation area. In this study, the training sample was done by manually digitizing the tree crown. There are 72 sample crowns that were digitized manually and been intersect with the segmentation output result. Formula (1)-(3) describe the equation to calculate the

Perpustakaan Negara Malaysia eISBN 987-967-17889-6-7

over and under segmentation and D value. The intersection process was done using ArcGIS software (3D analyst tools).

$$Over\ segmentation = 1 - \frac{area\ (xi \cap yj)}{area\ (yj)} \quad ....(1)$$

$$Under\ segmentation = 1 - \frac{area\ (xi \cap yj)}{area\ (xi)} \quad ...(2)$$

Where, xi is the training sample and yj is segmentation output.

$$Dij = \frac{Oversegmentation^2 + Undersegmentation^2}{2} \quad ..(3)$$

Each species was assigned with one to two species samples to train the software the characteristics of each tree species. Before the training sample was selected, classes of trees that had been identified during the field observation were inserted in the class hierarchy in the eCognition software. About 20 species of tree was classes into 10 family class. Vegetation class has been reclassified into forests and non-forests, including the field and garden. To archive, the second objective of this study a supervised Nearest Neighbour (NN) classification was then used for a detailed classification of the forest area. Standard NN features space was edited using the arithmetic features (equation) that had been created and test by (Machala & Zejdova 2014).This equation used 5 image layers which are R,G,B,NIR, and CHM. This approach was to resolve the problem inequality in brightness since the study area contains not uniform tree height that results in inequality of brightness distribution. After the standard NN was finally set, the classification algorithm was run to classify the individual tree into their species. The classification was divided into two which is classified by a family group and classify by the tree species group. A new export rule was created to export the image vector layer result for the future used in other software.

Accuracy assessment for species classification was done by using error confusion matrix. Error confusion matrix is a table that is often used to describe the performance of a classification model on a set of test data for which the true values are known. This method is done by analysis of the result based on the training sample. For this study, the accuracy assessment was done to species from *Dipterocarpace* family, which is *Dryobalanops aromatica, Dipterocarpus baudii, Shorea macroptera, Shorea bracteolate,* and *Shorea leprosula*. While another 3 species are *Scorodocarpus borneensis* and *Ochanostachys amentacea* from *Olacaceae* family, and *Elateriospermum Tapos* from *Euphorbiaceae* family. This is because the sample for this species is more compare then other species. Some species have only one sample and this was used as a sample classify the tree species. The using of testing sample from classification sample for accuracy assessment will affect the accuracy result. Apart from that, 5 species from *Dipterocarpaceae, Olacaceae* and *Euphorbiaceae* which is *Elateriospermum tapos* was used as the validation sample to check the accuracy of the tree classification result. The total testing sample was 17 samples.

Segmentations and tree species classification vector result was used to extract the spectral reflectance of the tree species. The exported vector layer results were overlay with the WV2 image as the indicator to create the sample polygon of the tree species. This is to make sure the created polygon was within the crown area of the tree species and not included the border of the other species crown. ArcGIS software was used to extract the spectrum value of the tree species. Using the 'tree sample manager' from classification tools in ArcGIS, the distribution of tree sample was drawn using the polygon. The value was then export to Microsoft Excel to plot the spectral reflectance graph. Spectral reflectance result was separated into two categories which is dominant and endangered tree species group. Dominant tree species refer to the highest number of tree species in the study area. There are about 10 endangered tree species and 8 dominant tree species.

Result and Analysis

This study consists of endangered and dominant tree species map and spectral reflectance as the final result. Only the tree recognized in the image during the fieldwork was used for the analysis. Statistical analysis was done to analyze the tree inventory data using SPSS software. Table 2 show the summary of statistical analysis for 100 selected trees collected from the field.

Table 2: Table of descriptive

Variable	No of tree	Min	Max	Mean	SD
Height [m]	100	14.00	27.00	21.00	2.84
CBH [m]	100	0.00	27.00	14.44	5.61
DBH [m]	100	19.00	117.00	51.68	21.21
CD [m]	100	0.00	24.00	5.03	4.91

Table 3 shows the highest and the lowest CHM, DEM and, DSM value of the study area. Figure 4 shows the CHM map of the study area.

Perpustakaan Negara Malaysia eISBN 987-967-17889-6-7

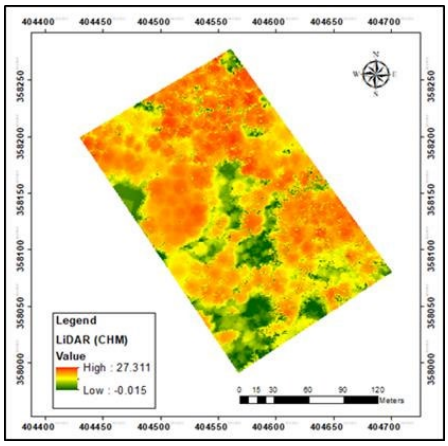

Figure 4: CHM map of the study area

Table 3: DSM, DEM and CHM result

Model	Highest [m]	Lowest [m]
DSM [m]	80.02	37.86
DEM [m]	59.97	37.36
CHM [m]	27.31	-0.02

The CHM value was validated by applying regression statistical analysis as shown in graph provided in figure 4. Based on the result its is shown that the R square equal to 0.670 and adjusted R square equal to 0.666. This result showed that LiDAR-derived height was best predicted at 67%. This shows that there are no significant changes between the tree height measure from the field and extract from CHM. Figure 5 show the regression graph between CHM and field measurement.

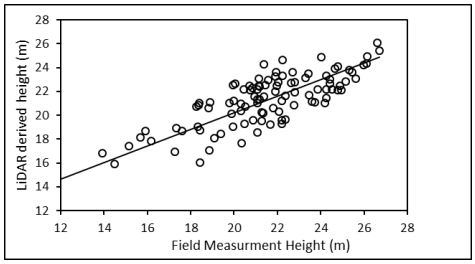

Figure 5: Regression graph of CHM vs tree height

Figure 6 shows the result of the segmentation using a parameter of 0.8 Shape criterion, 0.5 Compactness criterion and 23 Scale Parameter. The segmentation process had undergone several sub-processes such as object classification, water transformation, and morphology. Figure 7 show the result form the segmentation process; (a)multi-resolution segmentation, (b) classification of vegetation and non-vegetation, (c) object classification, (d) object merge, (e) watershed transformation, (f) segmentation result.

Figure 6: Segmentation of WV-2 imagery

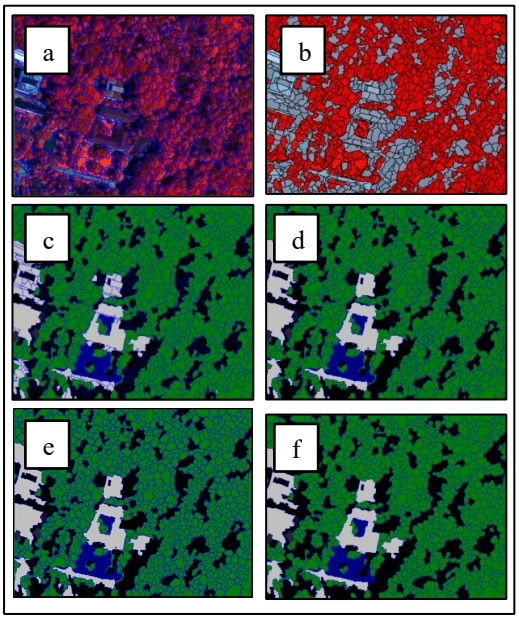

Figure 7: Result of (a) multi-resolution segmentation (b) classification of vegetation and non-vegetation, (c) object classification, (d) object merge, (e) watershed transformation, (f) segmentation.

After done with the segmentation process, tree segmentation result was validated first. concept of under and over-segmentation to evaluate the multiresolution segmentation result. Figure 8 shows the example of the individual tree crown resulted from the OBIA method and manually digitized in different cases. Manually digitized tree crown was indicated by the red color while segmented tree crown output in yellow color.

Perpustakaan Negara Malaysia eISBN 987-967-17889-6-7

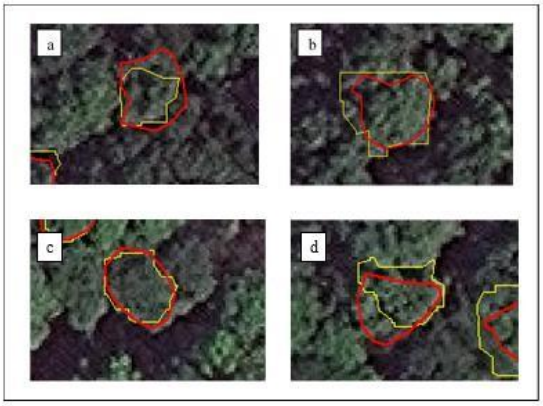

Figure 8: Manually segmented tree crown (in the red line) and segmented output (in the yellow line). (a) shows over, (b) under, (c) perfect match, and (d) mismatch segmentation.

D value was measured as 86% segmentation accuracy with 16% error. The overall accuracy of multi-resolution segmentation resulted in 86% in 1:1 match. From the results can be analysed that the segmented result was between 1 and 0 which is valid to be used for species classification. Table 4 shows the segmentation validation result.

Table 4: Segmentation Validation result

Table Head	Accuracy Segmentation				
1:1	Total Reflectance Polygon	Total 1:1 match	Over Seg	Under Seg	D
Goodness of fit	72	62	0.41	0.39	0.16
Total accuracy		86%			84%

The segmentation result used to classify the tree species in the study area. There are almost 26 types of tree species from 11 families. The result shows the distribution of *Dipterocarpace* family, dominant the study area. This is in line with the characteristic of FRIM forest which is dominated by the *Dipterocarpace*. Figure 9 shows the species distribution at study area.

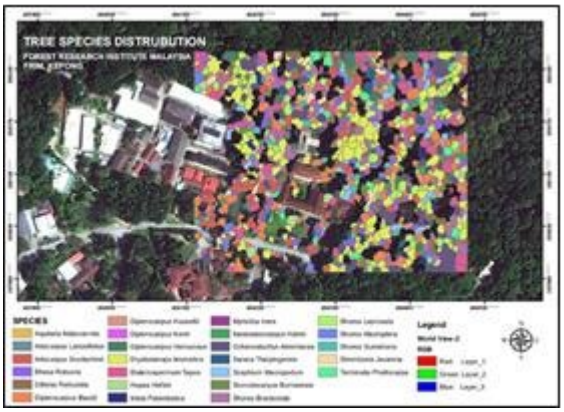

Figure 9: Tree species distribution at study area

Figure 10 show the distribution of dominant tree tree species at study area. *Dipterocarpus baudii* (keruing bulu), *Shorea macroptera* (Meranti Melantai), *Shorea bracteolata* (Meranti Pa'ang), *Dryobalanops aromatica* (Kapur), and *Shorea leprosula* (Meranti Tembaga) was the species from *Dipterocarpace* that dominant the FRIM forest. Besides that, *Olacaceaea* family show a large number of endangered trees after *Dipterocarpace* family.

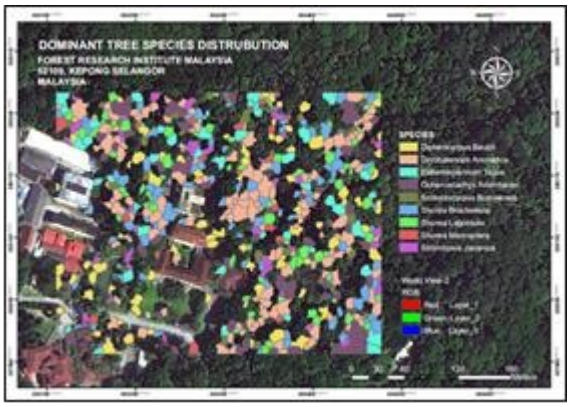

Figure 10: Dominant tree species distribution map

This study had found one critically endangered species which is Aquilaria *malaccensis* (gaharu) from *Thymelaeaceae* family. Even *Dipterocarpaceae* family dominant the FRIM forest, there are several species from this species listed as the endangered species. The result shows *Neobalanocarpus heimii* (Chengal), *Hopea helferi* (Giam Lintah Bukit), *Dipterocarpus hasseltii* (Keruing Ropol), *Shorea sumatrana* (Balau sengkawang air) and *Dipterocarpus kerrii* (Keruing gondol) from *Dipterocarpaceae* family listed as endangered species by IUCN. Figure 11 shows the endangered species map at FRIM forest. From the map, there is only 5 *Aquilaria malaccensis* (Gaharu) tree in the study area. showing that these species is critically endangered.

Perpustakaan Negara Malaysia eISBN 987-967-17889-6-7

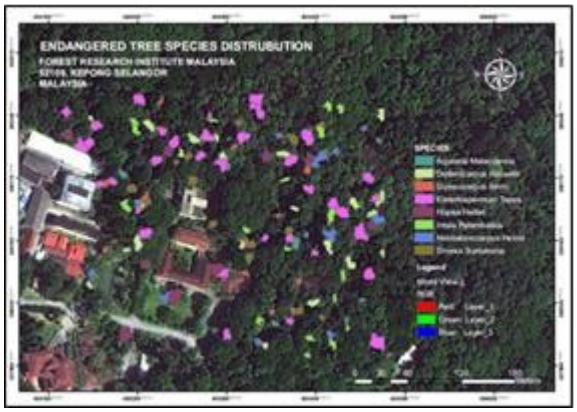

Figure 11: Endangered tree species distribution map

Classification accuracy assessment was done for 8 classes. Overall accuracy was 62% with kappa coefficient 0.57. The lowest accuracy is *Shorea macroptera* with 30% and highest accuracy *Scorodocarpus borneensis* with 63%.

Spectral reflectance of endangered and dominant species is excreted after the classification result is accepted. Figure 12 and 13 show the result of spectral reflectance of the dominant and endangered species extract from the WV-2 image. As shown in figure 11 the reflectance value was high in band 3 and band 4 while low in band 1 and band 2. This is because Band 3 carries the red band while band 4 carries the NIR band. Chlorophyll absorbs visible light very effectively but absorbs red and NIR wavelengths more strongly than blue and green producing a small reflectance peak within the green wavelength range (Kume, 2017).

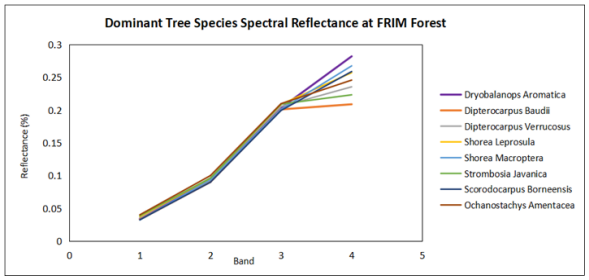

Figure 12: Spectral reflectance of dominant tree species using WV-2

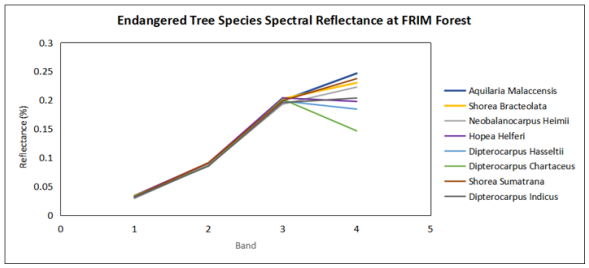

Figure 13: Spectral reflectance of endangered tree species using WV-2

Figures 14 and 15 show the spectral reflectance of dominant and endangered tree species extract from hyperspectral data. The hyperspectral used represent red and NIR band in the wavelength range 700 to 1000. This is the reason why the reflectance value is high at that range. If compared to spectral reflectance result extract by using WV-2 it is challenging to recognize individual spectral reflectance for each species because the pattern of spectral reflectance was the same and may also have the same reflectance value for a certain band. This had been shown in figure 12 as there is an obvious difference between the spectral reflectance produce from WV-2 imagery and hyperspectral data. This is because the WV-2 image has a limited spectral band that makes their spectral band difficult to be differentiated by one other. The hyperspectral image that consists of more than 100 spectral bands makes it easy to produce accurate spectral reflectance. The pattern of spectral reflectance of each species also can be differentiated easily

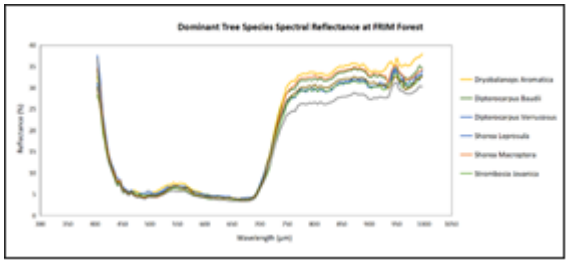

Figure 14: Spectral reflectance of dominant tree species using hyperspectral

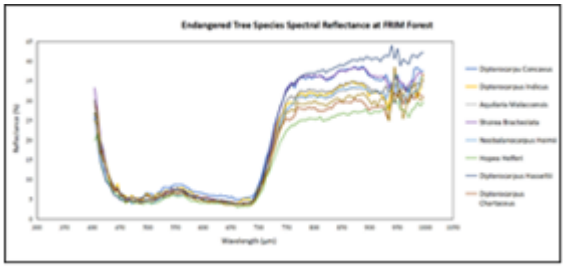

Figure 15: Spectral reflectance of endangered tree species using hyperspectral

Conclusion

In conclusion, all objectives of this study had been achieved. This study had produced three types of map which is tree species map, dominant tree species map, and also endangered map. The field inventory data had been successfully recorded and the data show that most of the trees at the study area have a height range from 21m until 24m. The result also shows that most of the dominant trees have a DBH measurement of more than 50cm. The most dominant tree was an emergent tree with a large area of the crown. Image segmentation has produced a

Perpustakaan Negara Malaysia eISBN 987-967-17889-6-7

good result for this study which is individual tree crown delineation. Most of the tree crown was segmented fitly and was accepted when validated by calculated the over and under segmentation area between reference polygon and segmented object. The overall accuracy which is 86% had shown that the multi-resolution segmentation was valid to be used to segment the crown of a tropical tree.

The classification of tree species using the Nearest Neighbour supervised classification had produced 62 % of accuracy assessment result when being test by using a testing sample. The species classification result had shown that FRIM forest was dominated by *Dipterocarpaceae* family. This also been supported by the research by (Omar, 2016) which had mentioned that FRIM forest was dominated by *Dipterocarpaceae.* This shows that the classification by eCognition software was valid to be to classify the tree species using WV-2 data. But to be concluded, it is difficult to classify the tree species in tropical forest as it consists of many species of trees whose position is scattered even in a small area. For example, the total area for this study was 3.5 hectare, but the tree species in the study area was more than 25 species. In addition, FRIM forest is a planted forest, it may be that natural forests have more tree species than in the FRIM. A deep study can be done to get the best classification method for tropical tree species.

REFERENCES

Abd Latif, Z., Aman, S. N. A., & Ghazali, R. (2011). Delineation Of Tree Crown and Canopy Height Using Airborne LiDAR and Aerial Photo. Proceedings - 2011 *IEEE 7th International Colloquium on Signal Processing and Its Applications*, CSPA 2011, (2), 354–358.

Abiola, K. A., Samuel, A., & Medugu, N. I. (2016). The Effect of Deforestation on Tree Species in IGALAMELA Local Government Area of KOGI State , Nigeria. Environmental Science, Toxicology and Food Technology, 10(7), 90–94.

Beucher, S. (2014). The Watershed Transformation Applied To Image Segmentation. (July 2000).

Chen, B., Qiu, F., Wu, B., & Du, H. (2015). Image Segmentation Based on Constrained Spectral Variance Difference And Edge Penalty. Remote Sensing, 7(5), 5980–6004.

Clinton, N., Holt, A., Scarborough, J., Yan, L. I., & Gong, P. (2010). Accuracy Assessment Measures for Object-Based Image Segmentation Goodness. Photogrammetric Engineering and Remote Sensing, 76(3), 289–299.

Hay, G. J., Blaschke, T., Marceau, D. J., & Bouchard, A. (2003). A Comparison Of Three Image-Object Methods for the Multiscale Analysis of Landscape Structure. ISPRS Journal of Photogrammetry and Remote Sensing, 57(5–6), 327–345.

Hycza, T., Stere, K., & Balazy, R. (2019). Potential Use of Hyperspectral Data to Classify Forest Tree Species. 9(2018).

L.S.L.Chua, M.Suhaida, & B.Aslina. (2008). Species Dipterokarpa Terancam di Semenanjung Malaysia.

Machala, M., & Zejdová, L. (2014). Forest Mapping through Object-Based Image Analysis of Multispectral And Lidar Aerial Data. European Journal of Remote Sensing, 47(1), 117–131.

Nordin, S. N. A. (2017). Tree Crown Segmentation of Gonystylus Bancanus in Tropical Peat Swap Forest Using Hyperspectral Imange. University Teknologi Mara.

Sanderson, M., Santini, M., Valentini, R., & Pope, E. (2012). Relationships between Forests and Weather. (January).

Shang, X., & Chisholm, L. A. (2014). Classification Of Australian Native Forest Species using Hyperspectral Remote Sensing and MachineLearning Classification Algorithms. IEEE Journal of Selected Topics in Applied Earth Observations and Remote Sensing, 7(6), 2481–2489.

Verlic, A., Duric, N., Kokalj, Z., Marsetic, A., Simoncic, P., & Ostir, K. (2014). Tree Species Classification using Worldview-2 Satellite Images and Laser Scanning Data In A Natural Urban Forest. Sumarski List, 138(9–10), 477–488.

Yahya, A. A., Tan, J., & Hu, M. (2013). A Novel Model of Image Segmentation Based on Watershed Algorithm. Advances in Multimedia, 2013.

Perpustakaan Negara Malaysia eISBN 987-967-17889-6-7

Reliability Study of Solar Observation as Constraints in Cadastral Network Adjustment

M F M Zaim[a,1], M A Abbas[a], and N M Hashim[a]

[a] Faculty of Architecture, Planning & Surveying, Universiti Teknologi MARA, Perlis Branch, Arau Campus, 02600 Arau, Perlis, Malaysia

[1]e-mail: muhd.faizzaim@gmail.com

Abstract

The demand for positional accuracy and multi-dimensional data have demonstrated drastic changing in geomatics data adjustment approach. Furthermore, the capability of modern sensors to provide high accuracy data (i.e. global navigation satellite system) have caused the crucial requirement for rigorous adjustment, which able to process data from multi-sensors. To adapt with current demand, geomatics practitioners have gradually transformed the adjustment procedure to the most rigorous approach (i.e. parametric linear regression). However, legacy datasets that utilising independent lines constraints in traditional adjustment approach have caused significant uncertainties in parametric linear regression (LR) adjustment. The solution, this research has robust design experiments using both closed traverse types: i) Single line constraint; ii) Multi-lines constraints, and iii) Subnetwork line constraint. Through errors trend analysis, the outcomes have visually and numerically verified the insignificant of independent lines constraints in parametric LR. However, the establishment of control points at either initial of end of lines could solve the limitation of abovementioned issue. In the analysis, control points at initial lines have demonstrated the best solution for constrained adjustment.

Keywords: Parametric linear regression, line Constraints, positional Accuracy, uncertainties

Introduction

With the unconditional fundamental principle that every acquired data could be augmented with errors; thus, adjustment procedure has become a crucial approach to arithmetically resolve these uncertainties by taking into account the geometric condition. Due to the limitation of previous technology, Bowditch and Transit adjustments are the most appropriate option to distribute random errors in spatial data. Conversely, with state-of-the-art processor technology in these few decades, computer performance has made complex, and sophisticated computation requires less exertion. Geomatics practitioners have gradually taken wise steps by revising the adjustment procedure to the most rigorous approach [1], linear regression (LR) or least square estimation (LSE). For instance, with determination to embark an efficient land delivery system, several countries have exploited the advancement of Information and Communications Technology (ICT) by introducing electronic-based cadastral system (Haanen et al., 2002) (Hope et al., 2008) (Yusoff et al., 2013) (Čeh et al., 2019). One of the enhancement element in this system is a conversion of the conventional adjustment method (e.g. Bowditch) into more advanced technique (i.e. linear regression) which manage to provide the best and most reliable cadastral network adjustment.

As stated in Ghilani and Wolf (2015), linear regression is applicable after all outliers, and systematic errors have been confiscated from the measured data. Embracing the condition of mathematical probability, LR yields the most probable values by minimising the sum of the squares of the random errors concerning the assigned weights. To perform the adjustment, datum definition in LR can be based on the minimum trace, minimum constraints or partial minimum trace (Halim, 1995). Some circumstance requires free network adjustment (minimum trace datum) where all stations are assumed to be unstable. There is a situation that necessitates partial minimum trace, whereas part of control points are considered as stable. In a common implementation, minimum constraint datum is favoured due to its simplicity. This datum definition considers that control points are stable by setting the coordinates correction vectors as zero. In the modern cadastral implementation which utilise multi-sensors such as total station and global navigation satellite

Perpustakaan Negara Malaysia eISBN 987-967-17889-6-7

system (GNSS), the partial minimum trace is the most favourable alternative. Errors propagation suffered from traversing data (i.e. bearings and distances) should be considered by control points established through GNSS measurement, which is more favourable to positional accuracy (Woodgate et al., 2017). To ensure that the adjustment procedure manages to successfully converge, it is inevitable to allow the control points to adjust following their expected levels of accuracy.

Other than abovementioned datum definition occurrences, it is sometimes essential to fix the measurement to an unambiguous value. Ghilani (2017) has discussed in detail regarding this issue which is also known as constraint equations. For example, a set of less accurate control points are held fixed in trilateration adjustment. Thus, the measurement will be forced to converge the erroneous control. In this condition, the reliable azimuth of baseline could be assigned as adjustment constraints. According to Ghilani (2017), holding the direction of line as datum can be carried out using: 1. Elimination of constraints; or 2. Helmert's method. Concerning this concern, inherited previous cadastral data (legacy datasets) that utilised line-based adjustment (i.e. Bowditch method) by fixing directions of lines (i.e. from previous observation or azimuth from solar observation) might be solved by LR adjustment. However, inherit data with multi-classes of accuracy, limitation of traditional measurement, and adjustment technique have relatively depleted the positional accuracy of cadastral legacy datasets (Hashim et al., 2019). It is also found that direct conversion from Bowditch to LR adjustments require a stringent study. As depicted in Figure 1, constraint equations only concern on held fixed the direction of the line during adjustment procedure without taking into account the position of points that form the line. In this example, black lines represent an adjusted network of open traverse which consisted with errors propagation, on the other hand, red lines are adjusted network where the end line (line 45) was constrained. Surprisingly, adjusted data for points 2, 3 and 4 remain similar except for the last point that affected by constraint equation. In contrast, the cadastral implementation that exploited GNSS measurement to constraints the network adjustment more interested in positional accuracy rather than direction (Felus, 2007). Thus, adopting line constraint in cadastral network adjustment is remain questionable, and the worst situation, it could jeopardise the land information record. To scrutinise this argument, this study has carried out rigorous experiments to evaluate the significance of line (azimuth) constraint in parametric linear regression. Both types of closed traverse (i.e. link and polygon) with multi constraints configurations were used to concretely verify the outcomes of this research.

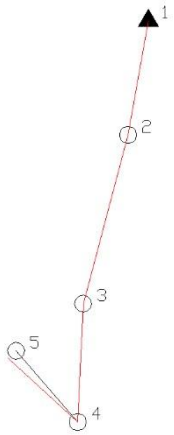

Figure 1: Before (black line) and after (red line) adjustment using the constraint equation (Ghilani and Wolf, 2015).

Lines Constraints Algorithm

To avoid a weak solution of parametric linear regression adjustment caused by less accurate control points, Ghilani (2017) has discussed constraint equations that enable trustworthy observation to be fixed. Two approaches have been presented to performed constraint equations, whether using the elimination of constraints approach or Helmert's method.

Elimination of Constraints

First-line constraint approach is executed by eliminating unknown parameters of one point, the other point that form line remains unadjusted (or fixed). With the aid of Figure 2, the constraint equation was design by considering that point A is held fixed, and the position of point B is constrained to adjust along the AB direction during LR procedure linearly. The movement of point B between prior and post adjustment (B') can be described using this formula [9]:

$$dxB = dyB \tan(\theta) \quad (1)$$

This constraint equation (1) then is arithmetically substituted into the parametric equations to eliminate the unknown parameters in the design matrix. As illustrated in Figure 2, a polygon traverse is acquired from four (4) series of lines consisted of points A, B, C and D. Point A is known point (held fixed), while the direction of line AB is to be constrained and other points are unknown parameters.

Perpustakaan Negara Malaysia eISBN 987-967-17889-6-7

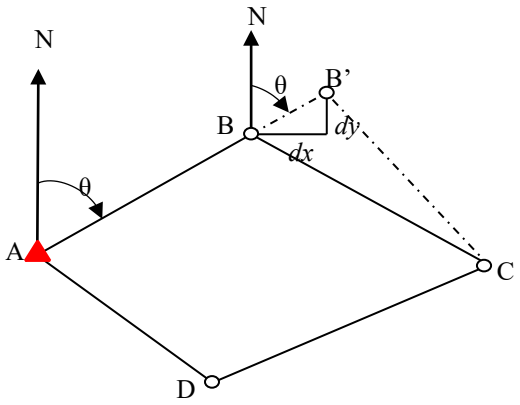

Figure 2: Constraint elimination in polygon traverse.

Parametric equations for line AB, which consist of distance (l_d) and bearing (l_b) measurement can be expressed as follow:

$$l_d + v_{ld} = \frac{x_{B_0} - x_A}{AB_0} dx_B + \frac{y_{B_0} - y_A}{AB_0} dy_B \qquad (2)$$

$$l_b + v_{lb} = \frac{y_{B_0} - y_A}{AB_0^2} dx_B + \frac{x_A - x_{B_0}}{AB_0^2} dy_B$$

Substituting equation (1) into equation (2) and after factorising dy_B, the constrained parametric equations are:

$$l_d + v_{ld} = \frac{(x_{B_0} - x_A).\tan(\theta) + (y_{B_0} - y_A)}{AB_0} dy_B \qquad (3)$$

$$l_b + v_{lb} = \frac{(y_{B_0} - y_A).\tan(\theta) + (x_A - x_{B_0})}{AB_0^2} dy_B$$

Adopting line constraints in parametric equations, there are slight amendments for design (A) and vectors (X) matrices after removing parameter X_B and dx_B, respectively.

$$X' = [dy \;\; x_C \;\; dy_C \;\; dx_D \;\; dy_D]$$

Helmert's Method

This constrained method was introduced by F. R. Helmert in 1872. As formulated in equation (4), Helmert's method is performed by augmenting constraint equations as the border of the normal matrix ($ATWA$), where A and W are design and weight matrices.

$$\begin{bmatrix} A^TWA & \vdots & C^T \\ \cdots & \cdots & \cdots \\ C & \vdots & 0 \end{bmatrix} \begin{bmatrix} X_1 \\ \cdots \\ X_2 \end{bmatrix} = \begin{bmatrix} A^TWL_1 \\ \cdots \\ L_2 \end{bmatrix} \qquad (4)$$

Where, $L_{1/2}$ = L_b (actual observation) – L_0 (approximate observation). Equation (4) demonstrates that line constraints have been encompassed in parametric equations with the addition of rows (C) and columns (C^T), X_2 and, L_2 into normal, vectors and, constant matrices, respectively. To resolve the parameter vectors (X), the matrices in equation (4) is organised as equation (5). However, X_2 is not employed in the later procedure to derive unknown parameters.

$$\begin{matrix} X_1 \\ \cdots \\ X_2 \end{matrix} = \begin{bmatrix} A^TWA & \vdots & C^T \\ \cdots & \cdots & \cdots \\ C & \vdots & 0 \end{bmatrix}^{-1} \begin{bmatrix} A^TWL_1 \\ \cdots \\ L_2 \end{bmatrix} \qquad (5)$$

Based on the example in Figure 2, the linearized equation for the bordering matrix, C (the direction of line AB) is as follows.

$$\left[\frac{y_{B_0} - y_A}{AB_0^2} \;\; \frac{x_A - x_{B_0}}{AB_0^2} \;\; 0 \;\; 0 \;\; 0 \;\; 0 \vdots 0\right] \times \begin{bmatrix} dx_B \\ dy_B \\ dx_C \\ dy_C \\ dx_D \\ dy_D \\ \cdots \\ dx_2 \end{bmatrix} = [L_2] \qquad (6)$$

Experiments

Determination of this study is to verify that lines constraints implementation in parametric linear regression without the aid of known points is insignificant for positional accuracy perseverance. Robust experiments have been designed to visually and mathematically validate the arguments. Furthermore, it is expected that the findings manage to advise constraints adjustment practitioner on appropriate employment in exploiting line constraints. Three circumstances for both polygon and link traverses network were utilised in this study:

i. Traverse with single line constraint;
ii. Traverse with multi-lines constraints;
iii. Traverse with sub-network line constraint;

For each experiment, there is a benchmark network that has been established or constrained using known points. To lessen the bias, azimuth employed for a line or lines constraints are derived from those known points as illustrated in Figure 3.

Perpustakaan Negara Malaysia eISBN 987-967-17889-6-7

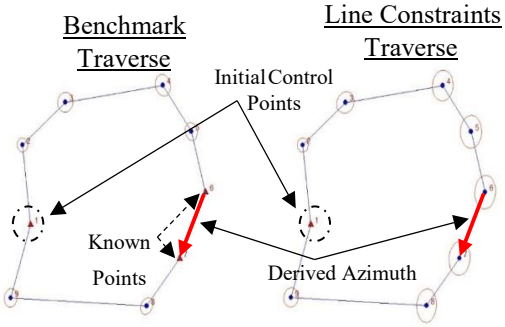

Figure 3: Azimuth derived from known points.

Adjusted data of each traverse network circumstances obtained from parametric linear regression are used to compute two-dimensional vectors with respect to benchmark traverse. These vectors are a substantial instrument to demonstrate the positional accuracy of the evaluated traverse network. Eventually, the reliability of independent line constraints can be analysed, together with the investigation of the suitable implementation of constraint adjustment.

To concretely verify the findings, three dimensional (3D) conformal coordinate transformation is employed to measure the network deterioration of other configurations with respect to benchmark network. According to Ghilani (2017), the 3D form-fitting between two coordinates system can be described as follows:

$$Xi = T + S \cdot r \cdot xi \qquad (7)$$

where,
Xi = 3D coordinates of points in the first system.
S = Scale vector between two (2) systems.
T = Translation.
r = Rotation matrix.
xi = 3D coordinates of points in the second system.

Root mean square error (RMSE) derived from the 3D conformal coordinate transformation computation will indicate the level of network form closeness between evaluated traverse configurations with the benchmark network.

Single Line Constraint

For a single fixed line experiment, the main intention is to scrutinise the effect of single line constraint in the polygon (Figure 4) and link (Figure 5) traverses. The idea is to demonstrate the limitation of fixing azimuth without the assistance of other known point or points. Disregard initial control point for both traverses; there are five types of constraints were employed for this experiment (as depicted in Figure 4 and Figure 5 for polygon and links traverses, respectively):

i. No line constraint (Figure 4a and Figure 5a)
ii. Independent line constraint using azimuth at line 6-7 (Figure 4b) and 24-25 (Figure 5b);
iii. Constraints using line and initial point (Figure 4c and Figure 5c);
iv. Constraints using line and endpoint (Figure 4d and Figure 5d); and
v. Constraints using points (benchmark as illustrated in Figure 4e and Figure 5e).

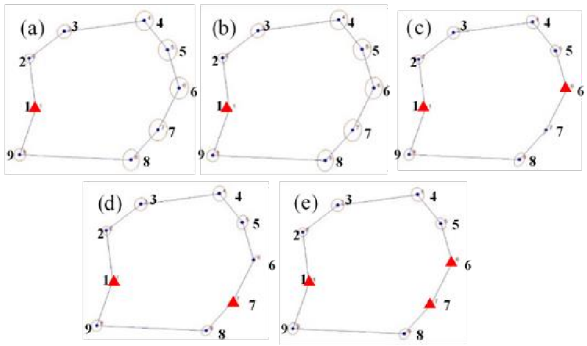

Figure 4: Multi constraints configurations used for polygon traverse with a single fixed line experiment.

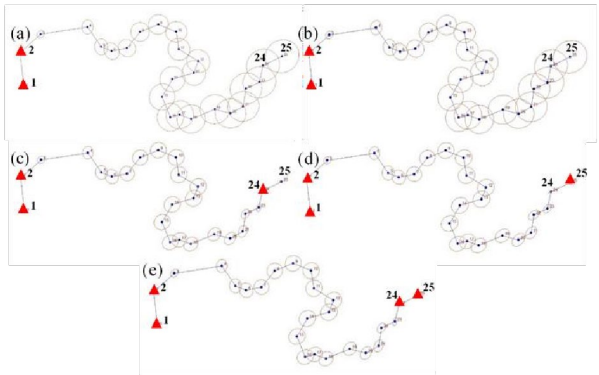

Figure 5: Multi constraints configurations used for link traverse with a single fixed line experiment.

For Figure 5a, due to the non-constrained at the end of the traverse, results from this network represent open traverse. This configuration is very crucial to mathematically evaluate the tendency of adjusted data obtained from single line constraint. To evaluate the reliability of multi constraints configurations, adjusted data acquired from both traverses, which constrained via known points (red triangles as depicted in Figure 4e and Figure 5e) were employed as benchmarks. Other than analysing the significance of independent line constraint, this experiment also intends to identify an appropriate solution for line constraints dilemma. Through the aid of point constraints at the initial (Figure 4c and Figure 5c) and end (Figure 4d and 5d) of line, a robust conclusion could be achieved to utilise line constraint properly.

Perpustakaan Negara Malaysia eISBN 987-967-17889-6-7

Multi-Lines Constraints

Inherit Cadastral legacy datasets that utilising Bowditch adjustment for traverse network, there is a situation where azimuth (yielded through solar observation) have been exploited multiple times. For instance, the first azimuth was used to fix the traverse direction, and the others constrained the network as illustrated in Figure 6, and Figure 7 for polygon and link traverses, respectively. This second experiment is very crucial to visual the effect of multi independent lines constraints in a traverse or cadastral block adjustment. In contrast with the previous experiment, five types of constraints were employed at two (2) lines for both traverses (as demonstrated in Figure 6 and Figure 7 for polygon and links traverses, respectively).

i. No lines and points constraints except for the initial control point (Figure 6a and Figure 7a);
ii. Independent lines constraints (Figure 6b and Figure 7b);
iii. Constraints using both lines and initial points (Figure 6c and Figure 7c);
iv. Constraints using both lines and endpoints (Figure 6d and Figure 7d); and
v. Constraints using points for both lines (benchmark as illustrated in Figure 6e and Figure 7e).

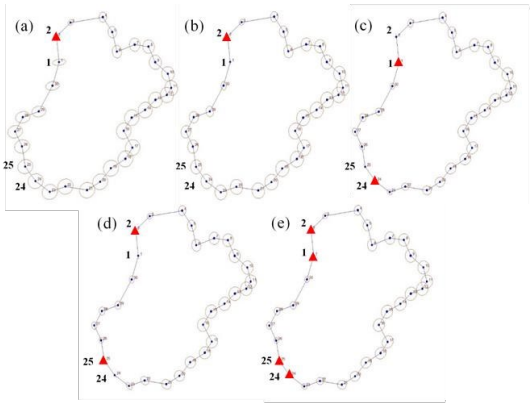

Figure 6: Multi-lines constraints experiments for polygon traverse.

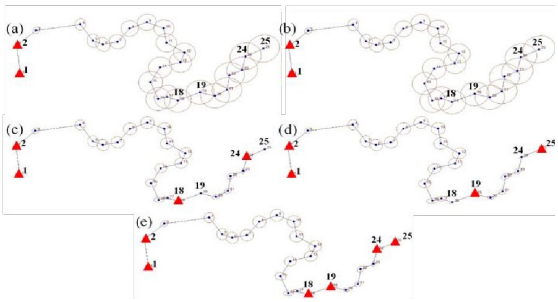

Figure 7: Multi-lines constraints experiments for link traverse.

To measure the propensity of adjusted data yielded from independent lines constraints (Figure 6b and Figure 7b) to adjusted data with less constrained, this study has utilised single point constraints for polygon traverse (Figure 6a) and no constrained at the end of link traverse (Figure 7a). For assessment purpose, benchmark networks that constrained by known points (red triangles in Figure 6 and Figure 7) were exploited for both polygon (Figure 6e) and link (Figure 7e) traverses. This is to quantify the damage that has been suffered from using multi independent lines constraints. With the aid of adjusted data derived from open traverse (Figure 7a), tendency analysis can be performed to identify the most applicable approach to carry out constraint adjustment. Similar as single line experiment, fixed points at initial (Figure 6c and Figure 7c) and end (Figure 6d and Figure 7d) of lines to strengthen the lines constraints solution were implemented to quantify the best practice in fixing multiline for traverse network.

Sub-Network Line Constraint

Whether to control the direction or constrained the traverse, there is a circumstance where solar observation cannot be carried out through the network. To resolve this situation, the subnetwork line, as shown in Figure 8 (polygon traverse) and Figure 9 (link traverse) was adopted. For line-based adjustment (i.e. Bowditch method), line constraint has proven the reliability to hold the direction and network. However, using parametric linear regression that embarks positional accuracy, independent line constraint might demonstrate contradict solution. To verify this hypothesis, using both types of closed traverses (Figure 8 and Figure 9 for polygon and links traverses, respectively), five types of constraints were utilised:

i. No line constraint (Figure 8a and Figure 9a);
ii. Independent line constraint using azimuth at line 4-10 (Figure 8b) and 12-26 (Figure 9b);
iii. iii. Constraints using line and initial point (Figure 8c and Figure 9c);
iv. Constraints using initial point (Figure 8d and Figure 9d); and
v. Constraints using points (benchmark as visualised in Figure 8e and Figure 9e).

Perpustakaan Negara Malaysia eISBN 987-967-17889-6-7

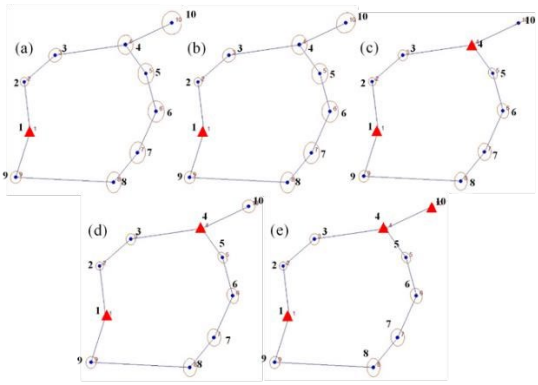

Figure 8: Multi sub-network constraints experiments for polygon traverse.

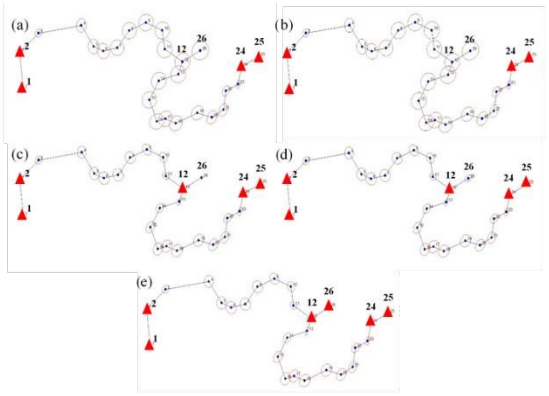

Figure 9: Multi sub-network constraints experiments for link traverse.

In contrast with the previous two experiments, as presented in Figure 9a, less constrained configuration for link traverse has been fixed using two control points at the end of the network. Since the examination is focused on the sub-network effect, thus, unbiased solution for both less and independent line (Figure 9b) constraints with respect to benchmark traverse (Figure 9e) become the main priority. To evaluate this final experiment, adjusted data from traverse networks in Figure 8e (polygon traverse) and Figure 9e (link traverse) were established as a reference to other configurations. Any discrepancies obtained will graphically and mathematically indicate the significant of azimuth to be independently employed as traverse constraint in parametric LR adjustment. In this experiment, the investigation also has been carried out to measure the significance of line constraint at sub-network. These two configurations were designed two scrutinise this issue, the first configuration utilizes point (at the initial line) and line constraints (Figure 8c and Figure 9c for polygon and link traverse, respectively), while later configuration only exploit point constraint at the initial line (Figure 8d and Figure 9d for polygon and link traverse, respectively).

Results and Analyses

There are multi configurations designed for both polygon and link traverses to investigate the reliability and identifying the appropriate procedure to employed constrained adjustment by holding the lines (i.e. azimuth or direction). Results obtained (adjusted data) from the multi configurations have been analysed using errors trend analysis.
As discussed in Section 3.0, the analysis used to visually and numerically clarify the limitation of independent lines constraints and advice the suitable approach to utilise it.

Errors Trend

As illustrated in Figure 10a, single line constraint experiment for polygon traverse has demonstrated the uncertain outcomes for parametric LR adjustment. Due to force direction and polygon geometry condition, adjusted data for independent line constraint has drastically deviated from reference values (i.e. benchmark configuration). As expected, similar errors trend was yielded for link traverse (Figure 10b). Moreover, worsen the situation is the independent constrained adjustment for link traverse have produced similar adjusted values as open traverse except for point 25, due to the direction constraint. Through visual (errors trend in Figure 10) and numerical (Table 1) results, pre-conclusion has indicated disagreement with independent line constraint. Nevertheless, the assistance of control point at the initial or end of line able to increase the positional accuracy of the network. For optimise data quality, RMSEs in Table 1, have obviously advice that for both closed traverse types, the best option to aid direction constraint is control point at the initial line.

Table 1: Root mean square errors for single line constraint experiment.

Constrained Configuration	RMSE for Polygon Traverse (m)	RMSE for Link Traverse (m)
No Line Constraint	0.01174	0.00525
Independent Line Constraint	0.01111	0.00109
Line & Initial Point Constraints	0.00056	0.00005
Line & End Point Constraints	0.00245	0.00016

Perpustakaan Negara Malaysia eISBN 987-967-17889-6-7

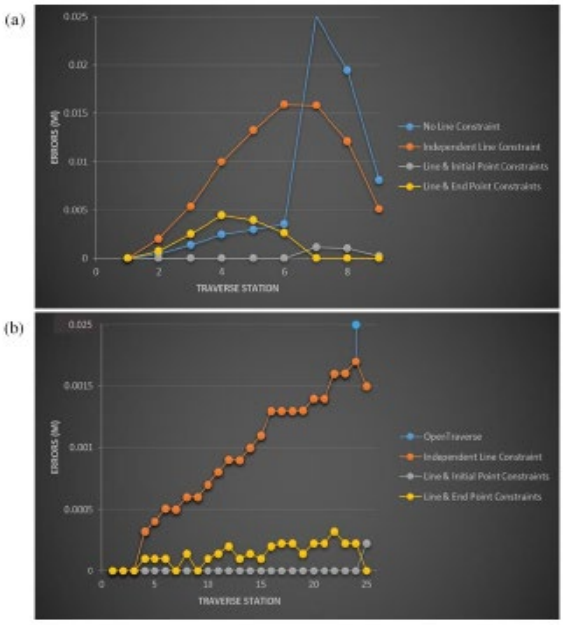

Figure 10: Errors trend of single line constraint experiment for the polygon (a) and link (b) traverses.

Similar to previous constrained configuration, multi-lines constraints experiment has exhibit the significant uncertainties fluctuation of adjusted data from exploiting independent lines constraints (as shown in Figure 11). This circumstance could jeopardise the geodetic network that consists of multi-direction constraints. Depicted in Figure 11a and Figure 11b, maximum error yielded from the constraints of the independent line is 0.027m and 0.019m for polygon and link traverses, respectively. Furthermore, for link traverse network, the significant similarity of errors trend (Figure 10b and Figure 11b) have been demonstrated between adjusted data derived from an independent constrained and open traverse. These findings have mathematically verified the irrelevant and hazardous uncertainties caused by independent direction constraints. Computed RMSEs (Table 2) and errors trend have once again verified the necessity of control points to assist the constrained adjustment with favourable data quality go-to points at the initial line.

Table 2: Root mean square errors for multilines constraints experiment.

Constrained Configuration	RMSE for Polygon Traverse (m)	RMSE for Link Traverse (m)
No Line Constraint	0.01737	0.00898
Independent Lines Constraints	0.01629	0.00731
Lines & Initial Points Constraints	0.00031	0.00023
Lines & End Points Constraints	0.00093	0.00022

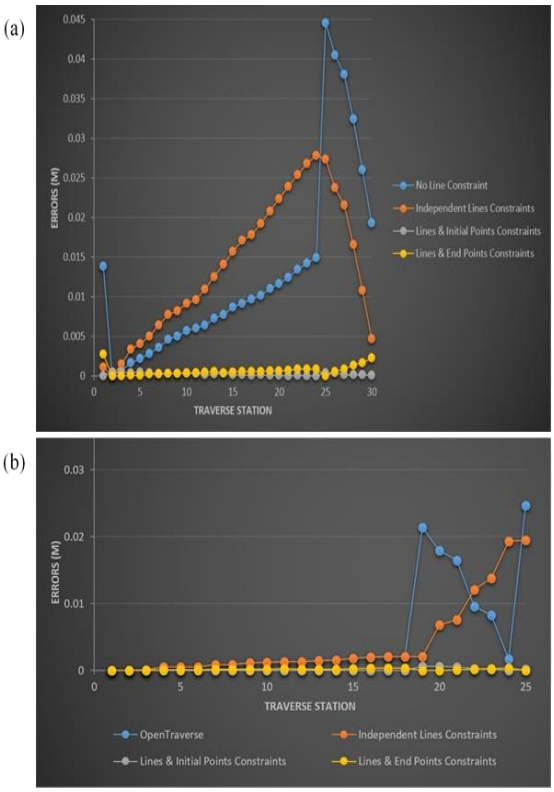

Figure 11: Errors trend of multi-lines constraints experiment for the polygon (a), and link (b) traverses.

The tendency of similar errors trend between fewer constraints configuration (No-line constraint in Figure 12) and independent line constraint has again demonstrated in the final experiment. The outcomes from the previous two experiments have been concretely proved with homogenous trends presented in plotted errors trend and computed RMSEs. Table 3 has shown an agreement with the mandatory requirement of control points to strengthen the parametric constrained adjustment. From Figure 12a and Figure 12b, both traverses types have illustrated an interesting trend for initial point constraint configuration. Errors of 0.034m and 0.019m have been yielded for polygon and link traverses, respectively. Conversely, zero errors were obtained for other points except for sub-network point. This situation might be occurred due to weak geometry condition caused by radial measurement.

Perpustakaan Negara Malaysia eISBN 987-967-17889-6-7

Table 3: Root mean square errors for subnetwork line constraint experiment.

Constrained Configuration	RMSE for Polygon Traverse (m)	RMSE for Link Traverse (m)
No Line Constraint	0.01116	0.04618
Independent Line Constraint	0.00123	0.04494
Line & Initial Point Constraints	0.00013	0.00008
Initial Point Constraints	0.01074	0.00353

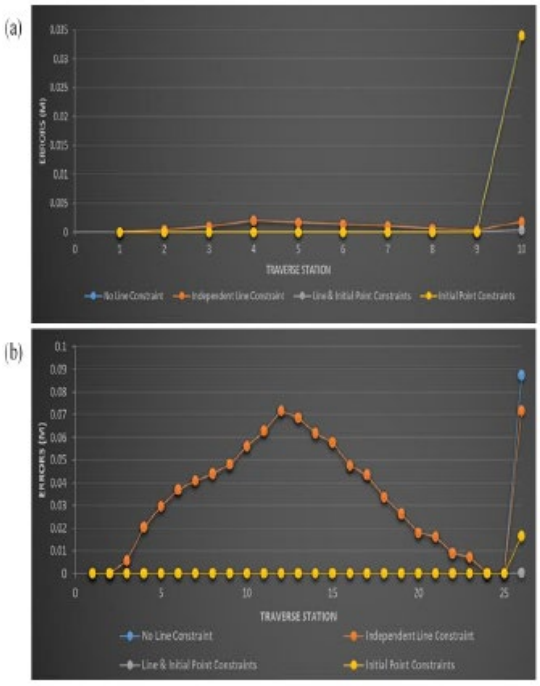

Figure 12: Errors trend of sub-network line constraint experiment for the polygon (a) and link (b) traverses.

From plotted errors and computed root mean square errors, these three experiments have exemplified an agreement regarding the insignificant of independent lines constraints as well as the crucial prerequisite of control points to (especially at initial of the line) ensure the quality of parametric linear regression results.

Conclusions

With the current requirement for positional accuracy and involvement of multi-sensors in mapping jargon, changing of adjustment approach from traditional (i.e. Bowditch and Transit) into more rigorous technique (i.e. parametric linear regression) is inevitable. However, legacy datasets are quite challenging to reprocess especially when involving with azimuths constraints which derived from solar observation. This kind of constraints have shown significant reliability for traditional adjustment approach, but it remains questionable for parametric LR. This study has thoroughly scrutinised this issue using multi constraints for polygon and link traverses. Through errors trend analysis, single line, multi-lines and sub-network line constraints configurations have exemplified that constrained adjustment via independent lines; constraints are inapplicable. To ensure the quality solution from using lines constraints, support from other control points, whether at initial (recommended) or end of lines are essential. Another interesting finding from this research is regarding radial measurement. Significant uncertainties have been demonstrated due to weak geometry condition. Further investigation is compulsory to examine the effect of radial data in traverse network adjustment.

REFERENCES

Sisman, Y. (2014). Coordinate Transformation of Cadastral Maps Using Different Adjustment Methods. Journal of the Chinese Institute of Engineers, 37(7), 869-882.

Haanen, A., Bevin, T., and Sutherland, N. (2002). e-Cadastre – Automation of the New Zealand Survey System. FIG XXII International Congress Washington, D.C. USA, April 19-26 2002.

Hope, S., Gordini, C., & Kealy, A. (2008). Positional Accuracy Improvement: Lessons Learned From Regional Victoria, Australia. Survey Review, 40(307), 29-42.

Mohd Yusoff, M. Y., Jamil,H., Abdul Halim, N. Z., Mohamed Yusof, N. A. and Mohd Zain, M. A. (2013). Ekadaster: A Learning Experience for Malaysia. FIG Pacific Small Island Developing States Symposium Policies and Practices for Responsible Governance Suva, Fiji, 18 – 20 September 2013.

Ceh, M., Gielsdorf, F., Trobec, B., Krivic, M. and Lisec, A. (2019). Improving the Positional Accuracy of Traditional Cadastral Index Maps with Membrane Adjustment in Slovenia. ISPRS International Journal Geo-Information 2019, 8, 338.

Perpustakaan Negara Malaysia eISBN 987-967-17889-6-7

Ghilani, C. D. and Wolf, P. R. (2015). Elementary Surveying: An Introduction to Geomatics, 14th Edition. Pearson Education, Inc., Upper Saddle River, New Jersey.

Halim, S. (1995). S-Transformations: A Practical Computational Tool for Deformation Monitoring. 3rd Symposium on Surveillance and Monitoring Surveys, Melbourne, Australia, pp. 154-164, 1-2 November 1995.

Woodgate, P., Coppa, I., Choy, S., Phinn, S., Arnold, L. and Duckham, M. (2017). The Australian Approach to Geospatial Capabilities; Positioning, Earth Observation, Infrastructure and Analytics: Issues, Trends and Perspectives. Geo-spatial Information Science, 20:2, 109-125.

Ghilani, C. D. (2017). *Adjustment Computations: Spatial Data Analysis*, Sixth Edition. New York: John Wiley & Sons, Inc.

Hashim, N. M., Omar, A. H., Omar, K. M., Abbas, M. A., Mustafar, M. A. and Sulaiman, S. A. (2019). Cadastral Positioning Accuracy Improvement (PAI): A Case Study of Pre-Requisite Data Quality Assurance. The International Archives of the Photogrammetry, Remote Sensing and Spatial Information Sciences, Volume XLII-4/W16, 2019. 6th International Conference on Geomatics and Geospatial Technology (GGT 2019), 1–3 October 2019, Kuala Lumpur, Malaysia.

Felus, Y. A. (2007). On the Positional Enhancement of Digital Cadastral Maps. Survey Review, 39(306), 268-281.

Perpustakaan Negara Malaysia eISBN 987-967-17889-6-7

Numerical Simulation of Ground Penetrating Radar (GPR) Signal for Laterite Soil Using Finite Difference Time Domain (FDTD)

Muhammad Aiman Safi'n[1], Mimi Diana Ghazali[2]

[1] Faculty of Architecture, Planning & Surveying, Universiti Teknologi MARA, Perlis Branch, Arau Campus, 02600 Arau, Perlis, Malaysia

e-mail: aimansafin@gmail.com

Abstract

Numerical simulation of the ground-penetrating radar (GPR) signal was a calculation that runs on a computer which implemented a mathematical model and physical system. The simulation can be approximately accurate by considering some element which is dielectric constant and soil conductivity. The aim and objectives of this study are to investigate the electrical parameter and to construct the numerical simulation of GPR signal related to laterite soil using Finite Difference Time Domain (FDTD). This study was carried out at UiTM campus Arau, Perlis, which nearby to Star Complex. The selection of the site location depends on some factors, such as soil material. There is some difference soil material in this area, such as laterite soil, sand, and others. Thus, for this study, the Finite Difference Time Domain (FDTD) method has been selected as a simulation method to build the radargram simulation. This method constructs a model response to the behaviour of the ground-penetrating radar signal, and the selection of this method was decided after considering all factors, especially related to complex calculation through to laterite soil. As a result, the two-dimensional numerical models were produced and make a comparison with the actual radargram as a validation.

Keywords: GPR, gprMax, FDTD, Laterite Soil.

Introduction

Ground-penetrating radar (GPR) is a geophysical technique based on the wave of electromagnetic, which is one of the non-destructive methods currently popular used to investigate the buried material without damage to any part of the original material (Shokri & Mat Amin, 2016). GPR has been created over the past three decades for the high-resolution examination of the underground of land. GPR is a time-dependent geophysical method which can produce a 3-D pseudo image of the subsurface of the earth, including the four dimensions of colour, and can also give an accurate estimation of depth for subsurface objects.

GPR uses the concept of electromagnetic waves scattering to identify the objects under the surface. The basic principles and theory of application for GPR have expanded through the concept of electrical engineering, seismic expedition, and practitioners of GPR should have some knowledge either in geophysical or electrical engineering to perform it. GPR is one technique that is usually used for the study of environmental, engineering work, archaeological investigation, and other shallow determination. The basic fundamental concept of GPR application is the same as that was applied to detect aircraft overhead. Still, GPR antennas are shifted across the surface instead of rotating around a fixed point. For getting an accurate estimation of subsurface, the soil properties should examine especially relate to physical properties such as density, magnetic susceptibility, and permeability, dielectric permittivity, electrical conductivity.

The electrical properties, such as relative permittivity, have a preeminent role in affecting the depth investigation. The relative permittivity is one factor of electromagnetic reflection signal, while the conductivity parameter is weakening to an electromagnetic signal. The higher permittivity in the electrical medium gives an effect to reflected amplitude (Alsharahi et al., 2016). Furthermore, the permittivity for every type of soil structure was the difference.

However, soil structure such as granular, blocky can give a massive effect on GPR signal performance (Miller et al., 2002) and make difficulty to practitioners to the interpretation of GPR radargram. The variation distribution of grain size and grain form in a particular area is one of the causes

Perpustakaan Negara Malaysia eISBN 987-967-17889-6-7

that influence the electric permittivity of GPR (Guillemoteau et al., 2012). The incorrect electrical permittivity value will contribute to erroneous signal penetration and usually occurs in contaminated soils.

The contamination soil by petroleum often contains an abundant number in carbon. It consists of a small value of nitrogen compound that changes in this structure, and organic soil composition will have some impact on the conductivity of soil and others(Wang et al., 2017). Furthermore, petroleum also has small density, higher viscosity, and lower emulsification capability make it easy to be absorbed into the subsurface and also give some impact to the permeability and porosity of soil (Wang et al., 2017). As a result, the contaminated soil gives others results compare to uncontaminated soil. Thus, for interpretation differences of GPR radargram between contaminated soil and uncontaminated soil needs, some method that can provide more accessible the interpretation of radargram. Currently, there are many researchers have done using FDTD method to investigate and simulate GPR signal radargram such as (Giannakis et al., 2016), (Li et al., 2019), (Lambot et al., 2006) and (Mapoka et al., 2016).

Finite-Difference Time-Domain (FDTD) is an excellent simulation tool method that used to solve electromagnetic problems which introduce by Yee in 1966 (Lei et al., 2019) and it has stability and convergence. The system of Finite-Difference TimeDomain (FDTD) provides direct integration of the time-dependent equations of Maxwell. Nowadays, the FDTD approaches are rapidly developed and have been used in GPR work to simulate the GPR wave. The time-domain nature of FDTD based program is capable of visualising the complex electromagnetic phenomena such as electromagnetic wave propagation in different media (Howlader & Sattar, 2015). Besides, the most popular tool that using FDTD is gprMax. To used gprMax for simple 2D modelling, some input file needs to calculate such as permittivity value, permeability, conductivity, time window, waveform, and other (Warren et al., 2016).

However, the study that using FDTD through to laterite soil is not yet because not everywhere have laterite soil. For example, (Mapoka et al., 2016) have done a study in clay soil and sand soil by using FDTD. Thus, to overcome this problem, this research is conducting as a solution to this problem. The objective of this study is to investigate the electrical parameter on laterite soil, generate the numerical model, and evaluate the model. The final output for this study is 2D of radargram simulation for GPR signal through the laterite soil.

Material and Method

Material

The site simulation is an estimation imitation of the operation of a process, and it usually used for simulation of technology for performance optimization. The simulation site was constructed with a concrete block and filled by soil. The polyvinyl chloride (PVC) with a diameter of 4.5 cm was located 0.5m depth in the simulation site. In the middle of the PVC pipe, the random point for diesel leak (3cm diameter) has been perforated. The simulation of diesel leak has been made in selected soil. The simulation of the site has been shown below.

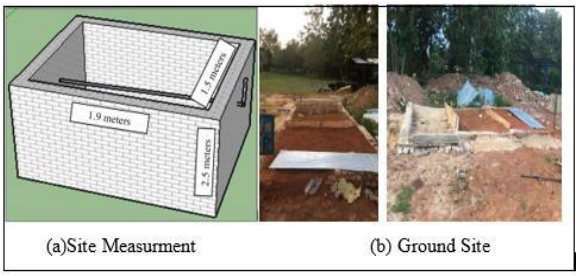

Figure 1: (a) Site Measurement and (b) Ground Site

Soil selection in this research study is laterite soil. The laterite soil is a combination of soil and rock that rich in iron and aluminium. Almost all the laterites soil is rusty red colouration, and it commonly can find in hot and wet tropical areas such as Malaysia. For this study, laterite soil that was filled into testbed is taking from outside the area from Unit Ladang of UiTM Perlis, which is 6°27'11" N and 100°16'45" E. The laterite soil was selected because not many researchers have done this soil, such as Mapoka et al. (2016) have done a study in clay soil and sand soil. Another example is research by Abdelgwad & Said (2016), which is used the sandy soil. Figure 2 shown the sample of laterite soil that has at the testbed site location.

Figure 2: Sample of laterite soil

The location of the site study is located at UiTM campus Arau, Perlis, which is located at the top North of Peninsular Malaysia that shown by Figure 3 below. The coordinate of location is 6°27'11" N and 100°16'45" E. Consideration of the

Perpustakaan Negara Malaysia eISBN 987-967-17889-6-7

site location was depending on far from the water source, crop, and type of existing soil. In this site, the dimension of the simulation test was designed as 2.5 meters for depth,
1.9 meters length, and 1.5 meters width for the dimension. Furthermore, the site location was created by using three types of soil, which are laterite soil, sandy soil, and clay soil and laterite soil. However, in this study was focus on laterite soil.

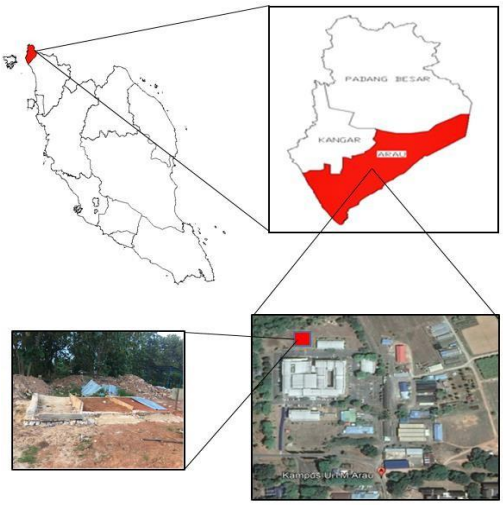

Figure 3: Simulation Site Located at University Technology MARA, Perlis

Data Collection

The frequency of GPR antenna that usually used in the industries sector is typically ranged from 25 MHz to 1 GHz. However, the selection of antenna frequency needs to be suitable for investigation purposes. The relationship between the resolution and depth of penetration needs to be considered because, for the high frequency, it more suitable use in shallow target and small material. Meanwhile, the low frequency of the antenna is suitable to use in a deeper target and usually for the detection of a large object. Before selecting of GPR frequency antenna in this study, some criteria were considered, such as material size, depth, type of subsurface, and resolution.

The data collection has been performed purposefully for model verification. Related to this study, the antenna used is 800Mhz, which the most suitable and sufficient frequency to fulfil the testbed site of the simulation. Other than that, selection of this frequency is influenced by the investigation purpose, such as in this study, the scanning of subsurface through laterite soil. This equipment has been prepared at the Geomatic equipment store.

Data Processing

There are two software selected for this study, which are gprMax and ReflexW. Both software has different functionalities in this study. The selection was decided based on some criteria that required for this study.

ReflexW is a Windows software that commonly used for the data processing and interpretation of transmission and reflection data from ground-penetrating radar (GPR), reflection and refraction seismic, and ultrasound). This software was designed exclusively used for data processing and was recommended to use in 16-bit high colour resolution. This program capable of reading many different formats of data such as SEGY, SEG2, GSSI, MALA RD3, PULSE-EKKO, and others.

GprMax software was used in this research study to the developed simulation of the electromagnetic wave propagations from the GPR signal. This program is designed to solve Maxwell's 3D equations using the Finite-Difference Time-Domain (FDTD) process, which was also created to demonstrate ground penetration radar (GPR) but can also be used for prototypical propagation of electromagnetic waves for many other uses. This software released under General Public License v3 (GNU), and it is mainly written in phyton with important performance parts written in cython to build the numerical simulation.

Finite Difference Time Domain

Finite-Difference Time-Domain (FDTD) is an excellent simulation tool method that used to solve electromagnetic problems which introduce by Yee in 1966 (Lei et al., 2019) and it has stability and convergence. The system of Finite-Difference TimeDomain (FDTD) provides direct integration of the timedependent equations of Maxwell. Nowadays, the FDTD approaches are rapidly developed and have been used in GPR work to simulate the GPR wave. The time domain nature of FDTD based program is capable of visualising the complex electromagnetic phenomena such as electromagnetic wave propagation in different media (Howlader & Sattar, 2015). Besides, the most popular tool that using FDTD is gprMax. To used gprMax for simple 2D modelling, some input file needs to calculate such as permittivity value, permeability, conductivity, time window, waveform, and other (Warren et al., 2016).

FDTD Based Framework for Modelling

The electromagnetic equations of Maxwell, which is mathematically express the relationship between the electromagnetic field concept of

Perpustakaan Negara Malaysia eISBN 987-967-17889-6-7

quantities and depending on the sources that have been used to describe all electromagnetic phenomena. The common concept of these equations for modelling using FDTD are:

$$\nabla \times E = -\frac{\mu_r}{C_0}\frac{\partial H}{\partial t} \quad (1)$$

$$\nabla \times H = -\frac{\varepsilon_r}{C_0}\frac{\partial E}{\partial t} \quad (2)$$

Where t is time in seconds, E is the electrical field, H is the magnetic field, and εr, μr are the values of the relative permittivity and the magnetic permeability of the medium, respectively. Such parameters are the position, distance, field strength, and time functions of the field applied, integrating the amount of flux with the intensities of the electrical and magnetic field. From Equations 3 until Equation 8, three-dimensional partial differential equations of Maxwell's equations will be written as:

$$\frac{\partial E_z}{\partial y}-\frac{\partial E_y}{\partial z}=-\frac{1}{C_o}\left(\mu_{xx}\frac{\partial H_x}{\partial t}+\mu_{xy}\frac{\partial H_y}{\partial t}+\mu_{xz}\frac{\partial H_z}{\partial t}\right) \quad (3)$$

$$\frac{\partial E_x}{\partial z}-\frac{\partial E_z}{\partial x}=-\frac{1}{C_o}\left(\mu_{yx}\frac{\partial H_x}{\partial t}+\mu_{yy}\frac{\partial H_y}{\partial t}+\mu_{yz}\frac{\partial H_z}{\partial t}\right) \quad (4)$$

$$\frac{\partial E_y}{\partial x}-\frac{\partial E_x}{\partial y}=-\frac{1}{C_o}\left(\mu_{zx}\frac{\partial H_x}{\partial t}+\mu_{zy}\frac{\partial H_y}{\partial t}+\mu_{zz}\frac{\partial H_z}{\partial t}\right) \quad (5)$$

$$\frac{\partial H_z}{\partial y}-\frac{\partial H_y}{\partial z}=-\frac{1}{C_o}\left(\varepsilon_{xx}\frac{\partial E_x}{\partial t}+\varepsilon_{xy}\frac{\partial E_y}{\partial t}+\varepsilon_{xz}\frac{\partial E_z}{\partial t}\right) \quad (6)$$

$$\frac{\partial H_x}{\partial z}-\frac{\partial H_z}{\partial x}=-\frac{1}{C_o}\left(\varepsilon_{yx}\frac{\partial E_x}{\partial t}+\varepsilon_{yy}\frac{\partial E_y}{\partial t}+\varepsilon_{yz}\frac{\partial E_z}{\partial t}\right) \quad (7)$$

$$\frac{\partial H_y}{\partial x}-\frac{\partial H_x}{\partial y}=-\frac{1}{C_o}\left(\varepsilon_{zx}\frac{\partial E_x}{\partial t}+\varepsilon_{zy}\frac{\partial E_y}{\partial t}+\varepsilon_{zz}\frac{\partial E_z}{\partial t}\right) \quad (8)$$

Parameter Calculation

Several parameters need to be calculated to simulate the GPR radargram. All necessary parameters were calculated before running as an input command to gprMax. All parameters connected with simulated space must be specified in meters, all parameters related to time should be in second, and the denoting frequency must in Hertz. Most of the commands in FDTD are alternative. Still, there are some essential commands which are necessary to building any model like none of the media, and object commands are essential to run a model. However, without setting any material in the gprMax model, free space (air) is simulated, and if it a single is not particularly useful for GPR modelling. Suppose the practitioner has not specified a command that is necessary to run a model, such as the size of the model. In that case, gprMax will terminate completion and issue an acceptable error message.

Discretisation of Space

Dx_Dy_Dz is the discretisation of space in the x, y, and z directions separately (Δx, Δy, Δz). The syntax command that used is "#dx_dy_dz: f1 f2 f3" which are f1 is the spatial step in the x-direction (Δx), f2 is the spatial step in the y-direction (Δy), and f3 is the spatial step in the z-direction (Δz). The spatial discretisation controls the maximum permissible time step Δt with which the solution is advancing in time to reach the simulated time window required. The relation between Δt and Δx, Δy, Δz, which shown in Equation 9 below was shown the example.

1

$$\Delta t \leq \frac{1}{\sqrt{\frac{1}{(\Delta x)\text{^}2}+\frac{1}{(\Delta y)\text{^}2}+\frac{1}{(\Delta z)\text{^}2}}} \quad (9)$$

Where c value is the speed of light, the equality is used to define Δt from Δx,Δy,Δz. The small value of Δx,Δy,Δz will give a small value of Δt that means more iterations to reach a given simulated time.

Time Window

The time window is the required time of the simulation program to generate one (1) A-Scan (Okonkwo et al., 2020). The command to complete the program for the time window is "#time_window: f1. Equation 10 below shown the formula used.

$$tw = \Delta t(N) \quad (10)$$

Material

The material is an essential component that needs to be declared in the input data, and it can be more than one (1) depending on the material used. This study was used three (3) types of material, which are contaminated soil, PVC, and laterite soil. The syntax of the command of material being used in gprMax as "#material: f1 f2 f3 f4 str1". Where f1 is relative permittivity, f2 is conductivity, f3 is permeability, and f4 is magnetic loss (Ohms/meter). The relative permittivity and electrical conductivity will be calculated by using Equation 11 and Equation 12 as below.

$$\mathrm{k} = \left(\frac{c}{v}\right)^2 \quad (11)$$

$$\sigma = \frac{\alpha\sqrt{k}}{1.69} \quad (12)$$

Perpustakaan Negara Malaysia eISBN 987-967-17889-6-7

Simulation Radargram Output

Simulation radargram of GPR signal is the data processing stage which is in this study. The gprMax was selected as the method which has two option to run this simulation. The two option is by using Matlab software and python. The written command in python for this study was involved in two parts, which are in A-scan and B-scan. To run the A-scan model, the data need to be calculated and saved in the input format. The wrong value of the parameter will give an error of simulation radargram, and sometimes it cannot be processed by python. After that, B-scan was followed by the process. The B-scan radargram is a radargram that produced by multiple traces of A-scan data. The command and input data used for processing is the same as for A-scan, which is "python -m gprMax" but there is some additional command need to clarify which is iteration number such as "python -m gprMax user_models/cylinder_Bscan_2D.in -n 80". The command of "-n" represents the value of the integer of iteration needs, and every iteration calculated is influenced by the time window value. Figure 4 below showed the input data for A-scan and B.

```
#title: Laterite Soi 2D
#domain: 0.38 0.5 0.003
#dx_dy_dz: 0.002 0.002 0.002
#time_window: 10e-9

#material: 6.636 0 1 0 Laterite_soil
#material: 8 0 1 0 my_pvc
#material: 8 0.08 1 0 my_contamination

#waveform: ricker 1 8e8 my_ricker
#hertzian_dipole: z 0.07 0.45 0.0 my_ricker
#rx: 0.14 0.45 0.0
#src_steps: 0.002 0 0
#rx_steps: 0.002 0 0

#box: 0 0 0 0.38 0.45 0.002 Laterite_soil
#cylinder: 0.17 0.25 0 0.17 0.25 0.002 0.005 my_pvc
#triangle: 0.08 0.16 0 0.12 0.16 0 0.10 0.20 0 0.3 my_contamination
#triangle: 0.22 0.16 0 0.26 0.16 0 0.24 0.20 0 0.3 my_contamination
```

Figure 4: Input data for A-scan and B-scan

Cross-Validation

Cross-validation, sometimes called rotation estimation, is a model verification procedure for evaluating exactly how the results of statistical analysis, which regression analysis and root mean square error (RMSE) conclusion. There are two sources of cross-validation, which are from GPR Scanning and gprMax simulation. GPR scanning is the stage of data collection for verification, interpretation, and analysis of the actual data. The process was included in data filtering and image enhancement. The purpose of data filtering (12) is to obtain true velocity, right depth, and dielectric constants by using REFLEXW and following module 3D data analysis. The second process is image enhancement. This process is a crucial part in data processing due to removing the noise for getting a clear
image

Root Mean Square Error (RMSE)

Root Mean Square Error measures the error between the set of data. In other words, it compares the prediction data and the actual data. The smaller RMSE is nearest to zero is the best result. The equation below shows the formula of RMSE calculation (Arthur et al., 2019). The value of prediction is getting from the data analysis processing, and the value of prediction in this study is taken from gprMax values.

$$RMSE = \sqrt{\sum \frac{(Predict - actual)^2}{N}} \quad (13)$$

The relationship of two values will be defined as good when the correlation coefficient is nearest to one (1), and the RMSE will be nearest to zero (0). Based on this study, the sample of data was taken from Ascii output data, and the total sample that has been used for applied this formula is fifteen (15).

Regression Analysis

Regression analysis is a gathering of statistical methods that attend as a root for illustration corollaries about relationships among connected variables (Humpage, 2014). In this study, regression analysis was defined as a connection of the result between GPR simulation radargram and GPR scanning radargram. The primary purpose of regression analysis is to analyse the relationship of the variable, which simulated amplitude and actual amplitude. From this comparison, a relationship statistical will be calculated.

The regression analysis is determined by using excel software by used data analysis tools that attached in excel. The relationship of results for both software was established, and the R-square is the benchmark for both relationships. The positive values of the R-square represent the uphill and vice versa. Other than that, the analysis also to identify by referred to the line graph and point. All of the points lie on the regression line, and therefore, there are no errors. Lastly, the regression analysis also takes into consideration for p-values, which is the limitation for the best is less than 0.05.

The correlation coefficient also is known as the Pearson correlation, which purpose of measuring the strength of the relationship between two variables, which is the x-axis and y-axis. The range values acceptable for the correlation coefficient is -1 until 1.

Perpustakaan Negara Malaysia eISBN 987-967-17889-6-7

The positive number represents the positive uphill relationship, and the negative values represent the downhill linear relationship.

3.0 Results and Analysis

Input Parameter of Numerical Simulation Radargram

The input parameter of numerical is calculated parameter based on the actual size of the site to suit with radargram simulation. All equation that has been used in this calculation was discussed in methodology. The performance of the radargram model simulation was depended on the input parameters that were entered. The calculated parameter, as shown in Table 1, totally contributes to the achievement of the output radargram simulation model. There was consisted of thirteen (13) parameters that have been calculated. The Input data is the main component that needs to run the gprMax simulation software.

Table 1: Input Parameter for Simulation of Radargram Model

No	Parameter	Description		
		Position (X,Y,Z)	Radius	Dielectric Properties
1	Title	Laterite Soil		
2	Domain	0.38 0.5 0.003	-	-
3	Time_Window	0.003 0.003 0.003	-	
4	Material (Laterite)	-	-	6.363 0.07 1 0
5	Material (PVC)	-	-	8 0.08 1 0
6	Material (Contamination)	-	-	8 0.08 1 0
7	Waveform: Ricker	ricker 1 8e8 my_ricker		
8	Hertzian_Dipole	z 0.07 0.45 0.0	-	-
9	Rx	0.14 0.45 0.0	-	-
10	Src_Steps	0.003 0 0	-	-
11	Rx_Steps	0.003 0 0	-	-
12	Box	0 0 0 0.38 0.45 0.002	-	-
13	Cylinder	0.17 0.25 0 0.17 0.25 0.002	0.005	-
14	Contamination	0.08 0.16 0 0.12 0.16 0 0.10 0.20 0 0.3	-	-
15	Contamination	0.22 0.16 0 0.26 0.16 0 0.24 0.20 0 0.3	-	-

The domain was represented the original size of the site, which is 1.9 meters for the x-axis, 1.5 meters for the y-axis, and 2.5 meters for the z-axis. However, table 1 were shown the difference values because of the scaling factor that has been done. Then, for the discretisation of space in the x, y, and z-direction was calculated by the following formula that has been discussed in 2.5. As a result, the actual value that has been computed for discretization is 0.00375. However, in this case, the study was used at 0.003, which is smaller than the actual. This finding was supported by Warren et al. (2016), which is the small values of the discretization, will give better accuracy.

Furthermore, three materials were used in this study, which is laterite soil using for the box medium, polyvinyl chloride (PVC), and diesel contamination. The dielectric values of each material are different, and it was determined based on the calculation which is taken from ReflexW radargram. For the box medium, the laterite soil permittivity was determined based on the velocity from radargram in ReflexW process, and the value was calculated is 6.363 for the dielectric constant. Compared to a study by Takahashi et al. (2014) on the influence of heterogeneous soils and clutter on the performance of ground penetrating radar for landmine detection, the laterite soil is 14.9. However, in this study was used less than 14.9 because the soil was contaminated by diesel.

Furthermore, the PVC permittivity was taken of the prior research, which is 3 - 8 mentioned by (Li et al., 2019). The third material classified as contaminated soil by diesel. The value that was used for the diesel contamination was 8.

Moreover, the waveform that was used in this study is ricker with 800 MHz. The value of the waveform has been determined from a selection of GPR frequency for actual radargram data. This value was written as 8e8 into the command, which represents the 800 MHz frequency. Lastly, the rest parameter was designed in x,y, and z position was based on the actual location of the materials.

Radargram Simulation using FDTD

The design for the site simulation is the most critical part that was considered. In this study, contaminated areas, PVC pipe, and laterite soil were located at the actual position. The site simulation designed as Figure 5 below.

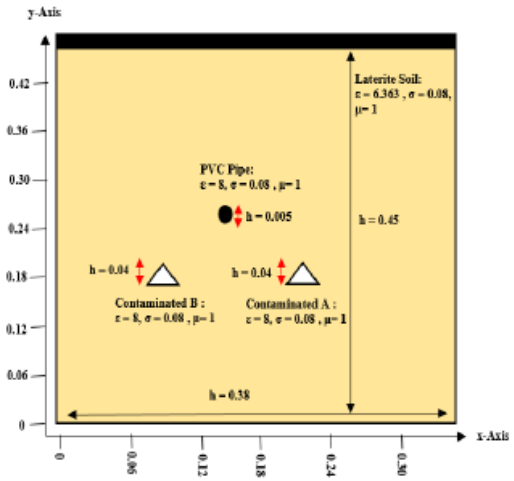

Figure 5: Simulation Site Design

The simulation site was designed in 0.38 for the xaxis and 0.45 for the y-axis. The properties of

Perpustakaan Negara Malaysia eISBN 987-967-17889-6-7

laterite soil were designed is 6.363 for relative permittivity, 0.08 for conductivity, and the permeability was assumed as 1. Other than that, the contaminated for both areas were assumed as same, which is 8 for the relative permittivity, 0.08 for the conductivity, and 1 for the permeability. Last but not least, the properties for the PVC pipe is 8 for the relative permittivity, 0.08 for the conductivity, and 1 for the permeability. All values were calculated as discussed in 3.1.

The simulation of radargram is an imaginary radargram that has been built as a prediction result for GPR scanning. This radargram was generated by using the concept of physic, which is made by Maxwell called Maxwell's equation. The simulation of radargram was designed such an actual site, which is consists of the pipeline, contamination area with the laterite material. Figure 6 shows the B-scan radargram simulation that has been represented 2D model in gprMax, while Figure 7 shows B-scan actual radargram that has been taken from ReflexW software.

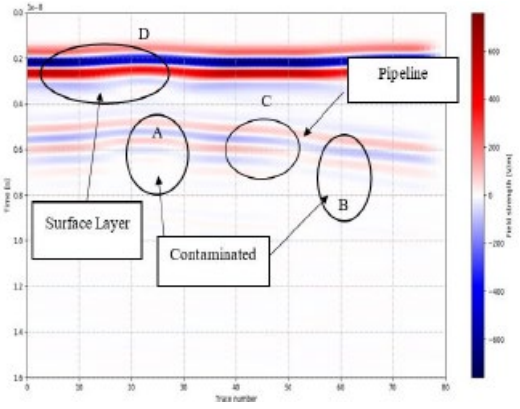

Figure 6: B-scan Radargram Model from gprMax

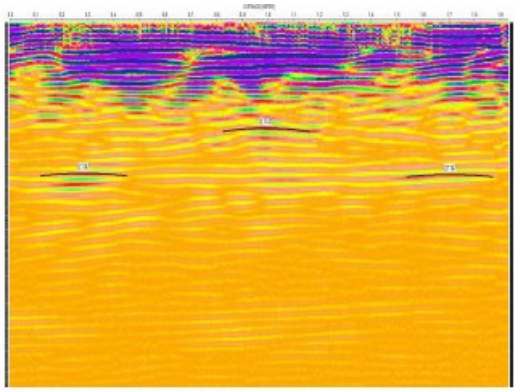

Figure 7: B-scan Radargram Model from ReflexW

The interpretation of this radargram was divided into three (3) part, which is the surface layer, soil contaminated, and hyperbolic. Firstly, the top radargram D is representing the surface layer. The red colour represents the surface of the laterite soil, and the blue colour is air space. The amplitude at the top layer is high than below is influenced by sources of the electromagnetic and dielectric properties of the laterite soil.

Besides, based on Figure 6 above, two areas have been labelled as A and B was contaminated areas due to leakage. Next affects the clarity of the radargram, and it happened caused by the reflected signal is low (Srigutomo et al., 2016). Next, the centre of the radargram was showing the hyperbolic area labelled as C, which is representing the PVC pipe. Clarity on hyperbola was affected due to the presence of contamination on soil both sides on the PVC pipe. However, the hyperbolic for the PVC pipe is easy to be identified, which is by referring to the amplitude values and shape of hyperbolic.

Figure 7 shows the actual radargram, which is generated from ReflexW software and the comparison between simulation and original radargram have a small difference in term of the position of pipe and contamination. The dissimilarity of both radargrams occurs because of space limitation in gprMax software and weakness that have due to the laptop processor. Moreover, the clarity of the original radargram is better than the simulation. However, the performance of the simulation model for radargram was evaluated based on RMSE and regression analysis.

Root Mean Square Error for Hyperbolic (PVC)

This error was performed based on the value taken from the GPR radargram through ReflexW and gprMax. There are (fifteen) 15 samples from the hyperbolic amplitude that were selected, and it was taken from the Ascii. The gprMax amplitude was taken from the trace 40 and for the ReflexW was taken from trace 230.
Table 2 presented the data of the hyperbolic result.

Table 2: Accuracy Assessment for PVC

Data	**ReflexW (Actual)**	**gprMax (Predicted)**
Maximum Amplitude	764	602.630
Minimum Amplitude	356	544.098
RMSE	0.056548139	

Table 2 shows the values of amplitude for the hyperbolic area. The amplitude from the ReflexW software was determined as actual values, and from the gprMax is predicted values. The highest value for the amplitude was recorded is 764, which is from the actual value. Meanwhile, the lowest is 356. Moreover, based on the calculation that has been

Perpustakaan Negara Malaysia eISBN 987-967-17889-6-7

done, the RMSE for the amplitude in hyperbolic is 0.056. Based on the previous study by Szerement et al. (2019) on measurements of soil water content in a well-defined sample volume was obtained the RMSE between 0.012 to 0.042 for all samples which are from the simulation and experiment.

Root Mean Square Error for Contaminated

The RMSE of the contaminated area was divided into two, which are A and B. As displayed in Figure 6, where A is located at the left side and B on the right side. Besides, both sides were designed with the same value of permittivity but with a different position. Table 3 below shows the result of RMSE in the contaminated area.

Table 3: Accuracy Assessment for Contaminated Area Compared Between ReflexW (as actual data) and gprMax (as simulation data)

Data		ReflexW (Actual)	gprMax (Predicted)
A	Maximum Amplitude	491	387.913
	Minimum Amplitude	290	349.735
B	Maximum Amplitude	734	569.93384
	Minimum Amplitude	400	522.0856
RMSE A		0.039068074	
RMSE B		0.037611832	

Table 3 shows the data of amplitude related to the contaminated area compared with the simulation model generated from gprMax and actual data from ReflexW through real site measurement. The highest amplitude for the contaminated A was recorded is 491 while the lowest is 290. Next, the highest amplitude for the contaminated area B is 734, and the lowest is 400. Furthermore, based on the calculation that has been done, the RMSE value was acceptable for the contaminated area A is 0.039, and for the contaminated area, B is 0.037.

Cross-Validation of GPR

Correlation Coefficient for The PVC Pipe

The variable correlation coefficient that involves in PVC pipe relation is two, which are amplitude data from the ReflexW for the x-axis and amplitude data from the gprMax for the y-axis. Figure 8 below shows the regression correlation coefficient result of PVC pipe.

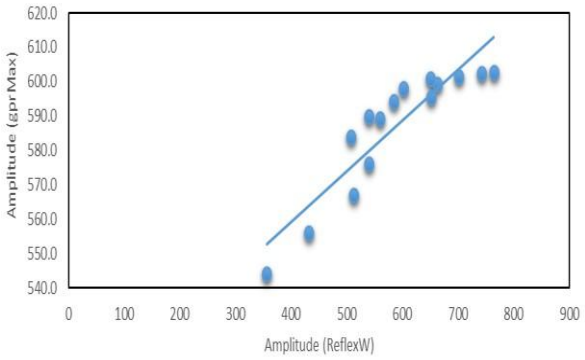

Figure 8: Correlation Coefficient Result of PVC Pipe

As illustrated in Figure 8, the regression analysis was done by using linear regression, which involves the two variables. As a result, the R-squared value was evaluated on 0.8298. Thus, the result shows the positive, strong uphill relationship between both variables and with a positive linear equation, which is y = 0.1473x + 500.34. Other than that, the P-value of the regression between the two variables is 2.36062510809708E-06. Thus, this result represents the good as long as the P-value of less than 0.05. Similar approached by Galagedara et al., (2005), that was, get the solid linear relationship, in the study on sandy soil to determine the direct ground wave sampling depth.

Correlation Coefficient for the Contaminated A

The correlation coefficient has been involving in contaminated area A is the amplitude of data from ReflexW for the x-axis and amplitude of data from gprMax for the y-axis. Figure 9 below shows the regression correlation coefficient result of contaminated area A.

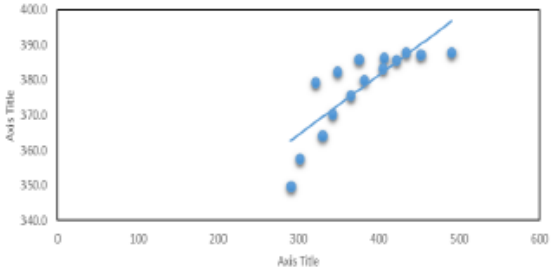

Figure 9: Relationship of simulation GPR signal and actual signal for contamination Plame A

According to Figure 9 above, the regression analysis has been used to build the correlation of two variables. The type of correlation coefficient that was used is a linear regression that is involved in the actual and simulation values of the amplitude. The

Perpustakaan Negara Malaysia eISBN 987-967-17889-6-7

verification show, the model, was moderate, predicts the experiment of the contaminated area. As a result, the r-square value was calculated is 0.6713, and the equation of the regression is y = 0.1697x + 313.45. Since the result of the r regression is positive, it shows the positive uphill. Thus, 0.6713 for the R-square represents the moderate uphill relationship, and the P-value for this regression is 0.0001. The method of verification study was approved by Sulaymon & Gzar, (2011) in the study on developed GPR radargram for light nonaqueous phase liquid dissolution and transport in a saturated zone of the soil. However, Sulaymon & Gzar (2011), was obtained on validation GPR radargram model predicted correlation coefficient is ranging between 0.8485 to 0.9986.

Correlation Coefficient for the Contaminated B

The correlation coefficient of the contaminated area B was involved with two parameters, which is the amplitude data from the ReflexW for the x-axis and amplitude data from the gprMax for the y-axis. Figure 10 below shows the regression correlation coefficient result of contaminated area B.

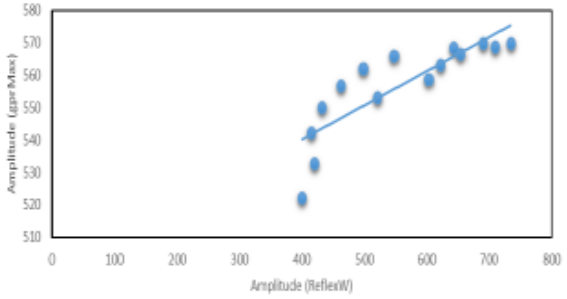

Figure 10: Correlation Coefficient Result of Contaminated Area B

According to Figure 10 above, this regression analysis has been used to create the correlation of two variables. The linear correlation coefficient has been selected, and it involved the actual and simulated values of the amplitude. As a result, the r-square value was calculated is 0.7073, and the equation of the regression is y = 0.1048x + 498.36. Since the result of the regression is positive values, it means the positive uphill relation. Thus, 0.7073 for the R-square signified the strong uphill relationship, and for the P-value in this regression is 0.0001. As approved by Wijewardana et al. (2017), the developed GPR radargram model also has been tested using regression analysis in a study on sub-surface salt contamination and solid waste. The study was obtained, the predicted correlation coefficient study is 0.85, and the P-value that has been obtained is 0.0043 to 0.132.

Conclusion

Generally, the all objective of this research has met the goal. Based on the finding that has been discussed in the previous chapter, all parameter that needs to be calculated was done entirely, and simulation of radargram was finished build. Based on the result, the numerical simulation method was founded as the most suitable method to develop the radargram simulation, and the accuracy of the data predicted was nearest to the real value.

Furthermore, the accuracy that was achieved between the simulation radargram and actual radargram very close. Other than that, the method used in gprMax software to predict is one of the most suitable for build the simulation radargram. Besides, from the result, the presence of diesel contamination was effect by the dielectric constant and affected the clarity of the radargram. The highest value of dielectric constant on the medium was produced the highest amounts of amplitude.

The relationship between gprMax software and actual data process by ReflexW software has RSME below than zero, which is 0.03 for the contaminated area, and 0.05 for the un-contaminated area has significantly proven in correlation coefficient relationship.

REFERENCES

Abdelgwad, A. H., & Said, T. M. (2016). Measured dielectric permittivity of contaminated sandy soil at microwave frequency. *Journal of Microwaves, Optoelectronics and Electromagnetic Applications*. https://doi.org/10.1590/2179-10742016v15i2591

Alsharahi, G., Driouach, A., & Faize, A. (2016). Performance of GPR Influenced by Electrical Conductivity and Dielectric Constant. *Procedia Technology*. https://doi.org/10.1016/j.protcy.2016.01.118

Arthur, C. K., Temeng, V. A., & Ziggah, Y. Y. (2019). Novel approach to predicting blast-induced ground vibration using Gaussian process regression. *Engineering with Computers*, 0(0), 0. https://doi.org/10.1007/s00366-018-0686-3

Perpustakaan Negara Malaysia eISBN 987-967-17889-6-7

Galagedara, L. W., Redman, J. D., Parkin, G. W., Annan, A. P., & Endres, A. L. (2005). Numerical modeling of GPR to determine the direct ground wave sampling depth. *Vadose Zone Journal*. https://doi.org/10.2136/vzj2004.0143

Giannakis, I., Giannopoulos, A., & Warren, C. (2016). A Realistic FDTD Numerical Modeling Framework of Ground Penetrating Radar for Landmine Detection. *IEEE Journal of Selected Topics in Applied Earth Observations and Remote Sensing*, 9(1), 37–51. https://doi.org/10.1109/JSTARS.2015.2468597

Guillemoteau, J., Bano, M., & Dujardin, J. (2012). *Influence of grain size , shape and compaction on georadar waves : examples of aeolian dunes*. 1455–1463. https://doi.org/10.1111/j.1365-246X.2012.05577.x

Howlader, M. O. F., & Sattar, T. P. (2015). FDTD based numerical framework for ground penetrating radar simulation. *Progress In Electromagnetics Research M*, 44(September), 127–138. https://doi.org/10.2528/PIERM15090304

Humpage, S. (2014). An introduction to regression analysis. *Sensors (Peterborough, NH)*, 17(9), 68–74.

Lambot, S., Antoine, M., Vanclooster, M., & Slob, E. C. (2006). Effect of soil roughness on the inversion of off-ground monostatic GPR signal for noninvasive quantification of soil properties. *Water Resources Research*, 42(3), 1–10. https://doi.org/10.1029/2005WR004416

Lei, J., Wang, Z., Fang, H., Ding, X., Zhang, X., Yang, M., & Wang, H. (2019). Analysis of GPR Wave Propagation in Complex Underground Structures Using CUDA-Implemented Conformal FDTD Method. *International Journal of Antennas and Propagation*, 2019, 1–11. https://doi.org/10.1155/2019/5043028

Mapoka, K. O. M., Birrell, S. J., & Mehari, T. (2016). Modeling ground penetrating radar (GPR) technology for seed planting depth detection using numerical scheme based on finite difference time domain (FDTD) method. *2016 American Society of Agricultural and Biological Engineers Annual International Meeting, ASABE 2016*. https://doi.org/10.13031/aim.20162460299

Miller, T. W., Borchers, B., Hendrickx, J. M. H., Hong, S. H., Dekker, L. W., & Ritsema, C. J. (2002). Effects of soil physical properties on GPR for landmine detection. *Fifth International Symposium on Technology and the Mine Problem.*

Shokri, N. H., & Mat Amin, Z. (2016). Ground Penetrating Radar (GPR) Application in Archaeology: A Case Study. International Graduate Conference on Engineering, Science and Humanities 2016, August, 1–8.

Srigutomo, W., Trimadona, & Agustine, E. (2016). Investigation of Underground Hydrocarbon Leakage using Ground Penetrating Radar. *Journal of Physics: Conference Series*, 739(1). https://doi.org/10.1088/1742-6596/739/1/012137

Sulaymon, A. H., & Gzar, H. A. (2011). Experimental investigation and numerical modeling of light nonaqueous phase liquid dissolution and transport in a saturated zone of the soil. *Journal of Hazardous Materials*, 186(2–3), 1601–1614. https://doi.org/10.1016/j.jhazmat.2010.12.035

Szerement, J., Woszczyk, A., Szypłowska, A., Kafarski, M., Lewandowski, A., Wilczek, A., & Skierucha, W. (2019). A seven-rod dielectric sensor for determination of soil moisture in well-defined sample volumes. *Sensors (Switzerland)*, 19(7), 1–12. https://doi.org/10.3390/s19071646

Takahashi, K., Igel, J., Preetz, H., & Sato, M. (2014). Influence of heterogeneous soils and clutter on the performance of ground-penetrating radar for landmine detection. *IEEE Transactions on Geoscience and Remote Sensing*, 52(6), 3464–3472. https://doi.org/10.1109/TGRS.2013.2273082

Wang, S., Xu, Y., Lin, Z., Zhang, J., Norbu, N., & Liu, W. (2017). *The Harm of Petroleum-Polluted Soil and its Remediation Research*. 020222. https://doi.org/10.1063/1.4993039

Wijewardana, Y. N. S., Shilpadi, A. T., Mowjood, M. I. M., Kawamoto, K., & Galagedara, L. W. (2017). Ground-penetrating radar (GPR) responses for subsurface salt contamination

Perpustakaan Negara Malaysia eISBN 987-967-17889-6-7

and solid waste: modeling and controlled lysimeter studies. *Environmental Monitoring and Assessment*, 189(2). https://doi.org/10.1007/s10661-017-5770-4

Warren, C., Giannopoulos, A., & Giannakis, I. (2016). gprMax: Open source software to simulate electromagnetic wave propagation for Ground Penetrating Radar. *Computer Physics Communications*. https://doi.org/10.1016/j.cpc.2016.08.020

Perpustakaan Negara Malaysia eISBN 987-967-17889-6-7

Assessment of Automated Road Features Extraction Algorithm from UAV Images

Amirul Ahmad1, Sharifah Norashikin Bohari1

[1] *Faculty of Architecture, Planning & Surveying, Universiti Teknologi MARA, Perlis Branch, Arau Campus, 02600 Arau, Perlis, Malaysia*

e-mail: amirulahmad@zoho.com

Abstract

In these days, thorough documentation of the road network is vital. It is especially true for many applications such as managing transportation and automation of navigation. Therefore, the extraction of road network such as from Unmanned Aerial Vehicle (UAV) imagery is needed so that it can be made use for these applications. The road network extraction can be done manually; however, it is costly and time-consuming to update and utilize the spatial information compared to automatic extraction. The aim of this study is to analyze the capabilities of automatic road extraction from UAV images using Trainable Weka Segmentation (TWS), Level Set (LS) and Seeded Region Growing (SRG) method. To achieve this, the objectives of this study are to 1) extract road automatically using TWS, LS and SRG method and 2) examine the capabilities of automatic road extraction from UAV images. The study area was carried out at UiTM Arau, Perlis, Malaysia. To ensure the completion of all objectives, several Ground Control Points (GCPs) had been established at UiTM Arau. Lastly, Agisoft PhotoScan had been used to build the orthophoto, which then the road network in the orthophoto had been segmented and extracted using these ImageJ Fiji. The automatically extracted road network had then been compared to manually extracted road network. It was found that the SRG method is slightly better in extracting road features compared to the LS method. This study can help to reduce the cost and time consumed in extracting features, especially the road network, by using automatic extraction instead of manual extraction.

Keywords: Automatic Road Extraction, Unmanned Aerial Vehicle, Trainable Weka Segmentation, Level Set, Seeded Region Growing

Introduction

The contribution of spatial features such as roads is huge since it is important for economic development and its growth followed by benefitting people's life. Furthermore, roads provide ways for people to fight poverty since it grants access to many things that can improve their lives, such as employment and education services. Roads lead to enhancement of urban facilities and inadvertently will increase the economy of state or country and at the same time will increase the social development. Therefore, road infrastructure is important and the information regarding it must be updated consistently and efficiently. Apart from that, the use of UAV for photogrammetry is increasing rapidly. It is not surprising since it is more cost-effective to use GPS enabled UAVs for aerial surveying compared to buy thousand Ringgit worth of equipment followed by the use of an aerial vehicle which will definitely increase the cost. Because of this, most organizations purchased UAV or drone, for the purpose of surveying. Nowadays UAV equipped with powerful computers and digital cameras has an accuracy right down to 1 centimetre.

Many GIS purposes require the uses of geospatial databases. Therefore, it needed to be created and updated. This can be accomplished by extracting spatial features such as roads and buildings (Rizeei & Pradhan, 2018). Therefore, road features should be carefully and accurately extracted. However, it is expensive and requires more time to manually bring up-to-date and utilize spatial information (Kahraman, Turan, & Karas, 2015). Furthermore, the many types of drones and a plethora of high-resolution imagery with diverse purposes have made automatic feature extraction, especially for roads, difficult compared to manually extracting features (Hormese & Saravanan, 2016). Automatic road features extraction has been studied many years

Perpustakaan Negara Malaysia eISBN 987-967-17889-6-7

before, but most of the studies use different methods than the others. Li, Hu, Guan, & Liu (2016) uses mean shift algorithm, principal component analysis and least square fitting to detect and extract the road centerlines in urban areas. Their method achieved good performance result with less computational cost compared to their old method, which was MTH method. Abdollahi et al. (2019) uses TWS method and LS method to segment and extract road features from two UAV images. The result verified that both methods are very effective for road extraction from UAV images. The reliability of road detection and extraction can also be improved by integrating imagery such as from UAV with LiDAR data or existing geo-database, but the need of accuracy and precision in rectification and registration of many different data sources prove that it is hard and expensive. There were also several past works regarding the automatic road features extraction. Singh and Garg (2013) manage to produce the road features from an image using morphological operations and adaptive global thresholding, but there are problems in the section of other than the road.

Study Area

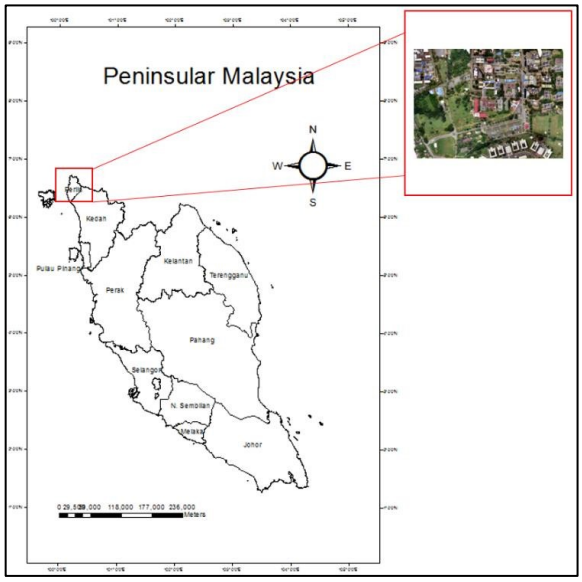

Figure 1 Map of UiTM Arau located in Perlis, Malaysia

Based on Figure 1, the location of the study is UiTM Arau, Perlis, Malaysia. It is approximately 10KM west of Kangar. For this study, the road network of UiTM Arau had been used to segment and extract the road features from the non-road features.

Research Methodology

The methodology of this study consists of four phases, as shown in Figure 2. The four phases are planning, data acquisition, data processing and result and analysis. The first phases are focusing on literature reading was done regarding today's technology of automatic road extraction. The study by Abdollahi et al. (2019) is used as the basis for this research study. Furthermore, phase one primarily used to learn and explore the software that has been used in this research. The software consists of Agisoft PhotoScan, ImageJ Fiji and ArcGIS. Also, the instrument that had been used in this study is Trimble R6 which is a GNSS instrument that is crucial to collect ground control points (GCPs). The second phase is known as data acquisition. This phase consists of acquiring more than 200 UAV images. Then, the images had been processed to build unregistered orthophoto so that the distribution of GCPs can be determined before proceed with going to the field. After the GCPs has been determined and its distribution has been considered good, fieldwork can be done to gather data on each GCPs. Trimble R6 was used for GPS observation using the RTK method for every GCPs. The correction was obtained from Virtual Reference Station (VRS). The setting that was used was two initializations, ten epochs with a 1-second interval for each GCPs. The GCPs value had been used to proceed with the orthophoto generation. Next, the third phase is data processing. It focuses on using the data gathered on each GCPs to build orthophoto. The UAV images had been added in Agisoft PhotoScan. Then, the GCPs data had been added to the software so that the process of building registered orthophoto can be done. The registered orthophoto had then be divided into five samples and be used as input for TWS to segment the road features. The same five samples of orthophoto had also been used as references by manually digitizing the road features using ArcGIS. The output of TWS had then be used to extract the road features using LS and SRG method. The process of segmenting and extracting road features was done by using ImageJ Fiji. The last phase is the results and analysis. The results of TWS, LS method and SRG method, which are the extracted road network had been analysed by comparing it to manually digitized road features. Both the LS method and SRG method had also be compared to each other for accuracy assessment. Furthermore, equations completeness, correctness and quality percentage had been used to assess the accuracy of the road extracted by using the basic parameters of True Negative (TN), False Positive (FP), False Negative (FN) and True Positive (TP):

Perpustakaan Negara Malaysia eISBN 987-967-17889-6-7

$$\text{Quality Percentage} = \left(\frac{TP}{TP+FP+FN}\right) * 100$$

$$\text{Correctness} = \left(\frac{TP}{TP+FP}\right) * 100$$

$$\text{Completeness} = \left(\frac{TP}{TP+FN}\right) * 100$$

TN is the number of which pixels is identified as non-road sections. FN is the number of road sections extracted as the non-road sections, FP is the number of non-road sections identified as the road sections, and TP is the number of road section that is accurately extracted.

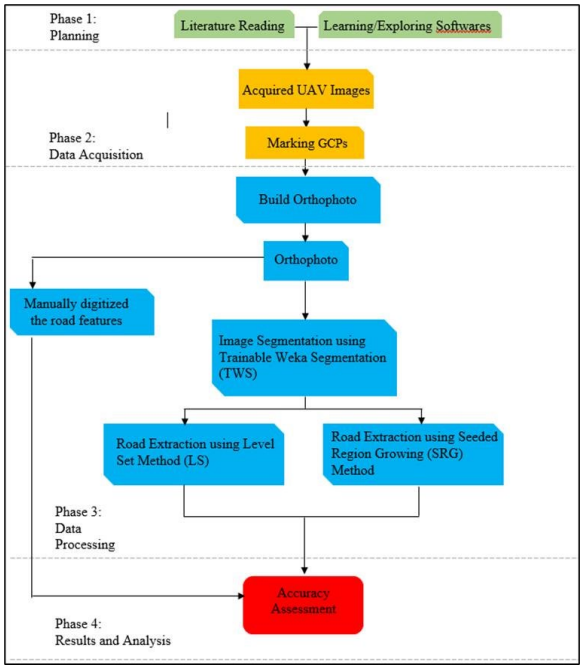

Figure 2: The methodology phases of this project

Orthophoto Generation

The images were loaded in Agisoft PhotoScan so that the camera positions can be determined. Since the images already have coordinates, align photos had been done to finds matching points between overlapping images which estimates the camera position for each photo. Then, the coordinates of the marker had been inputted. The markers had been placed to optimize the camera position and orientation data. 13 GCPs has been marked and distributed evenly within the area of interest based on this purpose. Then, the camera alignment had been optimized to achieve higher accuracy in calculating camera external and internal parameters. Based on the estimated camera positions, dense point cloud had been built by calculating the depth information for each camera. After that, the polygonal mesh had been generated based on the dense cloud data. Then, orthophoto had been built so that it can be used as input to manually digitized road features and road segmentation using TWS. Since TWS requires heavy computing power, the orthophoto had been cropped into five different samples. Based on Figure 3, sample 1 is the road at the roundabout near Gate B of UiTM Perlis. Sample 2 is the road at Beringin and near to Apple Cafeteria. Sample 3 is the road at the library. Sample 4 is the road at the parking lots and Pusat Islam. Sample 5 is the road at Blok C and Bangunan Al-Farabi 1.

Figure 3 Orthophoto divided into five samples to compensate for TWS heavy computing power

Segmentation and Extraction of Road Features

The five samples of orthophoto had been used as input for TWS to segment the road features. Besides that, the road network in the five samples of orthophoto had been digitized manually on ArcGIS with reference from points data that has been taken from road lines and road curves. The same orthophoto had also been loaded on ImageJ Fiji so that the process of automatic extraction can be done using TWS. TWS change the segmentation problem into a pixel classification problem by categorizing each pixel to specific features or section. Furthermore, the classifier had been trained by applying a specified collection of input pixels. The training features in TWS that had been used include Different of Gaussians, Sobel filter and Gaussian blur.

Different of Gaussian is a filter that identifies edges. By performing Gaussian blur on a picture at a specified standard deviation, the Different of Gaussian performs edge detection. The image that

Perpustakaan Negara Malaysia eISBN 987-967-17889-6-7

appears is a blurred version of the source picture. Then, the filter conducts yet another blur with a sharper theta that blurs the picture less than before. Afterwards, the final image is determined by replacing each pixel with the difference between the two blurred images and detecting when the zero values overlap. The resulting zero crossings had concentrated on edges or pixel areas with some variance in their surrounding neighbourhood. Sobel filter is also used for edge detection by creating images emphasising edges. The Sobel filter is based on converting the image in horizontal and vertical directions with a low, separable, and integer-evaluated filter. All of these parameters had been utilized by the Random Forest (RF) algorithm, which is an ensemble classifier that had been used to generate several decision trees by selecting samples and a subset of training variables. This technique is chosen because of its efficiency. Moreover, it is a machine learning technique that is usually applied in the classification of image and connected objects creation such as road network. Compared to other machine learning techniques such as artificial neural network, this technique does not need many parameters for it to be run.

After segmentation has been done, the LS method had been used by extracting the segmented road. LS method also utilized seed points before proceeding with active contours to grow and extract the road features. The key to adapting the LS method is by formulating F. F is a vector field which tells the direction and magnitude of surface movement at every point. Deriving F from the segmented image is needed so that the road extraction can be done. LS method is influenced by using a speed function. Speed function needs to be more than zero so that it can spread. So, outer energy needs to be specified so that the zero-speed curvature can move towards the object borders. Using ImageJ Fiji, the region of interest had been selected before starting the process of growing the region into full road features.

The same outputs of TWS had also been used to extract the road features using SRG method. Several regions had been selected as seeds points such as non-road features and road features. By selecting those seed points, it will be used as initial seed points to start growing the regions based on the user criteria.

Results and Analysis

This study consists of building orthophoto, which then is divided into 5 different samples of orthophoto located in UiTM Arau, Perlis. The road features of 5 samples of orthophoto had been digitized manually so that it can be used as a reference for accuracy assessment. The same orthophotos had also been used as input for TWS to segment the road features. Then, the output of TWS had been used to extract the road features using LS and SRG method.

Overlaying Results of LS Method and SRG Method with Reference Data

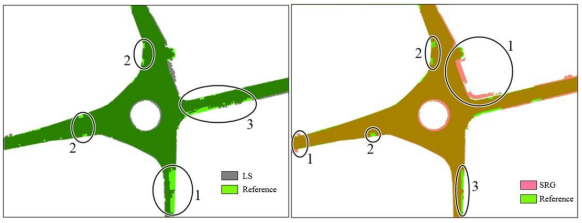

Figure 4 Sample 1 of LS & SRG overlaying with reference

Based on Figure 4 it shows that the LS method manages to extract the shape of the road features correctly. However, some parts of the road features cannot be extracted. At the bottom of the road (circle 1), several trees are obstructing the aerial view, which makes it difficult for the algorithm to extract the road features. At the top and left of the road (circle 2), several tiny features were also failed to be extracted as roads since it is road surface markings which do not have the same characteristics as a typical road. At the right side of the road (circle 3), LS failed to extract several pixels as road features because there are trees' shadows obstructing the aerial view. Apart from that, it also highlighted that SRG method succeeded to extract the overall shape of the road features. However, there are some problems in a certain area. At the right side near the centre of the road features (circle 1), it detected the sidewalk as road features. This is because the sidewalk shares the same characteristics with road features. This is also the same at the most left side of the road and the rightest side of the road. Plus, at the top of the road features (circle 2), SRG fails to detect a tiny bit of features as road features because of the presence of road markings. This is also the same on the left side of the road. Some of the bottom road features (circle 3) also failed to be extracted as road features because of the presents of trees and its shadows.

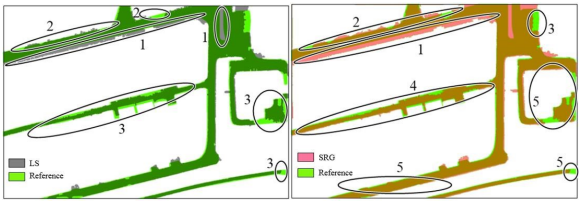

Figure 5 Sample 2 of LS & SRG overlaying with reference

Perpustakaan Negara Malaysia eISBN 987-967-17889-6-7

Based on Figure 5 it highlighted how the LS method extracts the road features from sample 2. The algorithm manages to get the right shape of the road features, although that are some features that were extracted incorrectly. The road features at the top from left all the way to the right (circle 1), LS incorrectly extracted other features as road, especially at the bottom. This is due to that area is a sidewalk which shares the same characteristics with road features. There are also trees that obstructing the aerial view (circle 2). This is also the same at the top right of the road features. At the middle section of the road (circle 3), there are several features that were failed to be extracted as road features. This is because the road is covered with laterite which does not share the same characteristics with road features. This is also the same at the rightest side and bottom right of the road features. Besides that, the SRG method also manages to extract the overall shape of the road features. However, the area at the top from left all the way to the right side of the road features (circle 1) is worse because of the presents of the sidewalk. This is because the sidewalk shares the same characteristics as the road features. Plus, there are also several trees obstructing the aerial view (circle 2), which makes the extracted road features is a lot worse. At the top rightest side of the road features (circle 3), there are several cars obstructing the aerial views which make the algorithm fails to detect it as a road. At the middle of the road (circle 4), laterite is present, which make the algorithm fails to detect some of the road features. Apart from that, there are also shadows obstructing the aerial view (circle 5) at the bottom left, bottom right and also at the rightest side of the road which makes it difficult for the algorithm to detect it as road features.

Figure 6 Sample 3 of LS & SRG overlaying with reference

Based on Figure 6 it shows that the LS method manages to extract the overall shape of the road features. However, there are several parts of the road features that were wrongly extracted. At the right side of the road features (circle 1), the road was covered with laterite and trees, which makes it difficult for LS to extract the road features. Also, the road at the top area (circle 2) also has several holes in them because of the presence of car and shadows. At the bottom area of the roads (circle 3), it was heavily obstructed by dark shadows produced by nearby buildings which makes the algorithm fails to detect it as road features. Apart from that, the SRG method also manages to extract the overall look and shape of the road features. But there are several parts of road features that the algorithm fails to extract. At the right side near the centre (circle 1) of the road features, there are trees and laterite present at the road features which makes the algorithm fails to extract several pixels of the road features as road features. In addition, the obstruction of trees at the rightest side of the road features (circle 2) makes it more difficult for the algorithm to detect the road features. At the bottom part of the road features (circle 3), there are dark shadows produced by nearer buildings which makes the process of extracting road features worse.

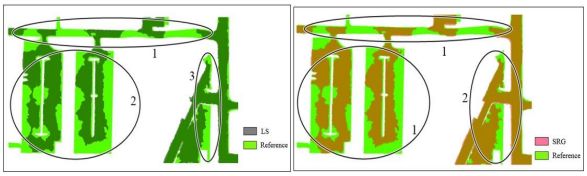

Figure 7 Sample 4 of LS & SRG overlaying with reference

Based on Figure 7 it highlighted how the LS method extracted the road features presents in the output of TWS. Sample 4 is one of the worst road features extracted by the LS method because the road features located at the area has more trees than any other samples. This can be seen by the way the features were extracted. The road features at the top from left all the way to the right (circle 1) has big trees that are obstructing the aerial views. This makes the extracted road features looks like dotted lines. The road features on the left and near the centre (circle 2) also suffer the same problem, which makes the extracted road features does not look well. There also several shadows that were obstructing the aerial views near the road features at the right (circle 3), which makes it worse. Apart from that, while the extracted road features of SRG greatly mimic the overall location of the road features, this is one of the worse samples produced by the SRG method. This is because the area of sample 4 is greatly presented with many trees and obstruction. At the top of the left side all the way to the right side (circle 1), there are trees presents and obstructing the aerial view. This significantly makes the algorithm fails to detect several road features and extracted it. This is also the same at the centre all the way to the left side of the road features. Apart from that, the presents of laterite and cars also make the algorithm fails to extract several road features at the bottom right side (circle 2).

Perpustakaan Negara Malaysia eISBN 987-967-17889-6-7

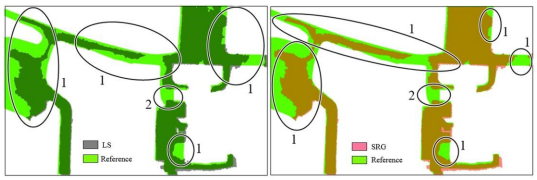

Figure 8 Sample 5 of LS & SRG overlaying with reference

Based on Figure 8 it shows that the result is the second-worst one apart from sample 4. LS method fails to accurately extract a big portion of the road features. This is because there are countless trees obstructing the aerial view, especially at the left side of the road all the way to the centre of the road (circle 1). This is also the same at the bottom of the road and also the top and right side of the road. Furthermore, there is also a sidewalk roof blocking the aerial view (circle 2), which makes the algorithm fail to detect it as road features. Besides that, this is also the second worse road features extracted by SRG method apart from sample 4 because of the same issues, many trees obstructing the aerial view. This is especially true on the left side all the way to the centre of the road features (circle 1). It is also the same at the right side, top right side and bottom centre of the road features. Plus, the present of sidewalk rooftop at the centre of the road features (circle 2) also makes it more difficult for the algorithm to detect the road features since it is obstructing the aerial view.

Comparison between LS and SRG Method

Table 1 Road extraction accuracy of the LS method

LS	TN	FN	FP	TP
Sample 1	4,126,222	16,820	17,304	838,958
Sample 2	4,013,546	29,580	27,422	1,061,124
Sample 3	4,150,100	58,244	46,277	997,458
Sample 4	2,512,841	612,472	266,142	1,276,751
Sample 5	1,739,139	254,744	123,489	531,196

Table 2 Road extraction accuracy of the SRG method

SRG	TN	FN	FP	TP
Sample 1	4,120,936	14,496	12,432	851,440
Sample 2	4,014,774	25,968	22,780	1,068,150
Sample 3	4,047,145	41,221	39,271	1,124,442
Sample 4	2,476,654	582,166	248,230	1,361,156
Sample 5	1,751,165	232,930	120,277	544,196

Table 3 Performance measures based on equations completeness, correctness and quality of LS

LS	Completeness (%)	Correctness (%)	Quality (%)
Sample 1	98.03	97.98	96.09
Sample 2	97.29	97.48	94.90
Sample 3	94.48	95.57	90.52
Sample 4	67.58	82.75	59.24
Sample 5	67.59	81.14	58.41

Table 4 Performance measures based on equations completeness, correctness and quality of SRG

SRG	Completeness (%)	Correctness (%)	Quality (%)
Sample 1	98.33	98.56	96.93
Sample 2	97.63	97.91	95.64
Sample 3	96.46	96.63	93.32
Sample 4	70.04	84.58	62.11
Sample 5	70.03	81.90	60.64

Based on Table 1 and Table 2, the number of pixels for each sample of both methods which is based on TN, FN, FP and TP was used to assess the performance measures by using equations completeness, correctness and quality. The equations derive the percentages on how well the algorithm extracted the road features. The completeness percentages determined the percentage of how the algorithm exploited the source data precisely. The correctness percentages determined the percentage of correctly extracted road pixels as road pixels. The quality percentages determined the overall accuracy of the extracted road pixels.

For the LS method, sample 1 has the most percentages for the performance measures based on equations completeness, correctness and quality, which makes up to 98.03%, 97.98% and 96.09%. Sample 2 is the second-highest percentages which make up to 97.29%, 97.48% and 94.90%. While sample 1 and sample 2 are very close to each other, sample 3 is slightly further, which makes up to 94.48%, 95.57% and 90.52%. Sample 4 and 5 are worse because many things that are obstructing the aerial view of the road features such as trees, cars, shadows and road markings. The percentages of sample 4 make up to 67.58%, 82.75% and 59.24%, while the percentages of sample 5 make up to 67.59%, 81.14% and 58.41%. Both sample 4 and 5 are very close to each other.

For the SRG method, sample 1 has the most percentages, which makes up to 98.33%, 98.56% and 96.93%. Sample 2 is the second-highest percentages which make up to 97.63%, 97.91% and 95.64%. Sample 3 is the third-highest percentages which make up to 96.46%, 96.63% and 93.32%. While these three samples are the highest in terms of completeness, correctness and quality, sample 4 and 5 is worse. Just like the LS method, this is because of the presence of obstructions such as trees, cars, shadows and car markings. The percentages of sample 4 make up to 70.04%, 84.58% and 62.11% while the percentages of sample 5 make up to 70.03%, 81.90% and 60.64%. This shows that the SRG method is slightly better in extracting road features than the LS method.

Perpustakaan Negara Malaysia eISBN 987-967-17889-6-7

Conclusion

This study illustrates the capabilities of automatic road extraction from UAV photogrammetry using TWS, LS and SRG method. The 5 samples of the road feature segmented using TWS were used as inputs for the road extraction using LS and SRG method. Based on the equation's completeness, correctness and quality percentages for sample 1 of LS method, it makes up to 98.03%, 97.98% and 96.09%. For sample 2 of the LS method, 97.29%, 97.48% and 94.90%. For sample 3 of the LS method, 94.48%, 95.57%, and 90.52%. For sample 4 of the LS method, 67.58%, 82.75%, and 59.24%. For sample 5 of the LS method, 67.59%, 81.14% and 58.41%. Meanwhile, the equations completeness, correctness, and quality percentages for sample 1 of SRG method makes up to 98.33%, 98.56% and 96.93%. For sample 2 of SRG method, 97.63%, 97.91% and 95.64%. For sample 3 of SRG method, 96.46%, 96.63% and 93.32%. For sample 4 of SRG method, 70.04%, 84.58% and 62.11%. For sample 5 of SRG method, 70.03%, 81.90% and 60.64%.

While both methods were capable of extracting the road features of UiTM Perlis, the obstructions of cars, shadows, trees greatly affected the extracted road features negatively. This was especially true for sample 4 and 5 for both methods since those two samples were greatly obstructed with trees and shadows. This significantly affects the equations completeness, correctness and quality percentages which determine the accuracy of the extracted road features. However, both methods achieved more than 90% accuracy for sample 1, 2, 3, which proved that both methods were more than capable of extracting some of the road features located at UiTM Perlis. Based on the performance measures, the SRG method was slightly better in extracting the road features from all samples compared to the LS method. The percentages only differ from 1% to 2% only.

REFERENCES

Abdollahi, A., Pradhan, B., & Shukla, N. (2019). Extraction of road features from UAV images using a novel level set segmentation approach. *International Journal of Urban Sciences*, 23(3), 391–405. https://doi.org/10.1080/12265934.2019.1596040

Hormese, J., & Saravanan, C. (2016). Automated Road Extraction From High-Resolution Satellite Images. Procedia Technology. 24, 1460–1467. https://doi.org/10.1016/j.protcy.2016.05.180

Kahraman, I., Turan, M. K., & Karas, I. R. (2015). Road Detection from High Satellite Images Using Neural Networks. *International Journal of Modeling and Optimization*, 5(4), 304–307. https://doi.org/10.7763/ijmo.2015.v5.479

Li, Y., Hu, X., Guan, H., & Liu, P. (2016). An Efficient Method for Automatic Road Extraction Based on Multiple Features from LiDAR Data. *International Archives of the Photogrammetry, Remote Sensing and Spatial Information Sciences*, 41(July), 289–293. https://doi.org/10.5194/isprsarchives-XLI-B3-289-2016

Rizeei, H. M., & Pradhan, B. (2018). Extraction and accuracy assessment of DTMs derived from remotely sensed and field surveying approaches in a GIS framework. *IOP Conference Series: Earth and Environmental Science*, 169(1). https://doi.org/ 10.1088/1755-1315/169/1/012009

Singh, P. P., & Garg, R. D. (2013). Automatic Road Extraction from High Resolution Satellite using Adaptive Global Thresholding and Morphological Operations. *Journal of the Indian Society of Remote Sensing*. 41(3), 631–640. https://doi.org/10.1007/s12524-012-0241-4

Perpustakaan Negara Malaysia eISBN 987-967-17889-6-7

Seamless Vertical Datum Model over Sarawak Region using KTH Method

Nurfarhah Razali[1], Muhammad Faiz Pa'suya[1], Ami Hassan Md Din[2]

[1] *Faculty of Architecture, Planning & Surveying, Universiti Teknologi MARA, Perlis Branch, Arau Campus, 02600 Arau, Perlis, Malaysia*
[2]*Geoscience and Digital Earth Centre (INSTEG), Faculty of Built Environment and Surveying, Universiti Teknologi Malaysia, 81310 Johor Bahru, Johor, Malaysia*

e-mail: [1]nurfarhahrazali@gmail.com
[2]mhmdfaiz86@gmail.com
[3]amihassan@utm.my

Abstract

Sarawak had known as a rugged topographic area because it had many mountains, dense rainforest and much of it protected parkland. Because of that, the traditional levelling network in Sarawak was difficult to carry out. When the levelling network can't be carried out because of that situation, it was had several vertical datum networks that refer differences tide gauge, and from that, it will provide the inconsistencies in height at Sarawak. The research aims of this research are to establish a seamless model of vertical datum over Sarawak region by using KTH method. To achieve the aim for this research, firstly, it will be validated GGM that refers to the inner region and outer region of the research area. After that, the two GGM that had been selected based on validation at the inner region and outer region will be combined with DEM data and gravity data to produce a gravimetric geoid model by using KTH method. From that, it will identify the effect of Global Geopotential Model (GGM) onto gravimetric geoid modelling. In the next step, the gravimetric geoid model will integrate with local datum to produce hybrid geoid model. Lastly, hybrid geoid model will compare with existing hybrid geoid model to see the differences. The significant that will be provided by this research is it be provided seamless vertical datum model which is new gravimetric geoid modelling that using KTH method for Sarawak region and identify the effect of GGM toward generating gravimetric geoid modelling.

Keywords: KTH method, gravimetric geoid, Sarawak.

Introduction

In surveying, one of the basic components to measure is heighting. In measuring the height for each positioning point, it must refer to a vertical datum which is a reference for heighting component. In 1912 the British Admiralty established the first national levelling datum for Peninsular Malaysia with the first line levelled between Port Klang and Kuala Lumpur using levelling method. (Jamil, 2011). This vertical datum was established with 8 months tidal observations and known as Land Survey Datum 1912 (LSD1912). Due to the growth in the development of infrastructures that require an accurate height control, Department of Survey and Mapping Malaysia had a study of existing height control in Peninsular in 1979 intending to redefine a new National Geodetic Vertical Datum (Ses & Gilliland, 2013). Lastly, Department of Survey and Mapping Malaysia had replaced the older datum (Land Survey Datum) with Peninsular Malaysia Geodetic Vertical Datum (PMGVD1994) based on Mean Sea Level at Port Klang with adjustment (Ses & Gilliland, 2013).

The Topographic Section of the Department of Survey and Mapping Sarawak was established in 1989, and its early tasks were to look after the levelling network of Sarawak, and it was handled by Jabatan Tanah & Survei Sarawak (JTS) (Som et al., 2016). Levelling network in Sarawak was referred to various datum. It happened due to the vast size of Sarawak and limited accessibility for the height network during that early period, and it causes the created three zones that using separate datum point (Som et al., 2016). Azhari Mohamed said it is abnormal to have multiple vertical datum that propagated from separate tide gauge (Othman et al., 2014). According to Mustafar (2005), geoid modelling is one of an alternative to creating vertical datum. The geoid is the surface along which gravity is equal, and the direction of gravity is always

Perpustakaan Negara Malaysia eISBN 987-967-17889-6-7

perpendicular. In heighting component, it needed the orthometric height, and GNSS receiver can provide the ellipsoidal height. To transform the ellipsoidal height that getting from the GNSS receiver, the precise geoid needs to be used to obtain orthometric height easily, faster and at a lower cost (Othman et al., 2014). One of geoid model is gravimetric geoid modelling and for getting this model is was the combination of airborne gravity data, terrestrial gravity data and marine gravity data.

In determining gravimetric geoid, there are have several methods to the generated gravimetric geoid. The methods that can be used are Remove-Compute-Restore (RCR), Least Square Modification of Stokes (LSMS) or known as KTH method and lastly is Stokes-Helmert's formula. In Malaysia, it had generated gravimetric geoid by using Remove-Compute-Restore method that had known as MyGeoid. The accuracy of gravimetric geoid in Malaysia, which is MyGeoid indicates about 5 cm has been adopted in GNSS levelling application (Jamil, Kadir, Forsberg, et al., 2017). The accuracy of the gravimetric geoid was estimated to be less than 5 cm across most of East Malaysia (Jamil, Kadir, Forsberg, et al., 2017). One the other method to generate gravimetric geoid modelling is using KTH Method. KTH method had proven successful put forward by New Zealand (Abdalla & Tenzer, 2011), Turkey (Abbak et al., 2012), Iran (Kiamehr, 2006), Tanzania (Ulotu, 2009) and Sweden (Ågren, 2004). In Peninsular Malaysia, it is shown that the KTH method gave a better result which is RMSE ±0.268 compared to geoid model that computed using RCR method with RMSE ±1.1656 (Pa'suya et al., 2018).

In the computation of the gravimetric geoid model, several data will be involved in that computation. One of that data is Global Geopotential Model (GGM). In the recent development, in satellite technique and computation of algorithms improve in the determination of global gravity field model where was led to the computation of a number GGM and improvement in the long and medium wavelength of gravity field spectrum have been achieved (Erol et al., 2009). From that improvement, it was anticipated for regional geoid model. This is because the GGM model will represent as underlying geopotential in the determination of precise geoid model. In order to determine the suitable GGM model that suited to as a base model in the research area, comparison and validation of GGM model will be done with references data. In this research, it will use the KTH method in generating gravimetric geoid modelling for Sarawak region and investigate the effect of GGM model toward the computation of precise geoid model.

Problem statement

In heighting component, ideally, it must refer to single vertical datum to increase the consistency in height system. In Sarawak, it has rugged topography feature in its region because it has many mountains, dense of rainforest, wide river and much-protected parkland. From that, it was very difficult to carry traditional method which is direct levelling method in transferring benchmark from one vertical datum because limited access to track. Traditional levelling method is simple, an operation is effective, the method has remained unchanged, and it can achieve a remarkable accuracy, but it has longer observation time and make it slow, labour-attentive and has costly operation (Jamil, 2011). Besides that, the line operation must be connected to form the series of levelling line (Jamil, 2011).

Because of that issue, the Sarawak region was referred to various vertical datum. Sarawak had established three vertical datum at Kuching, Bintulu and Miri. From that, it was formed three different levelling network that is not connected that come from three different tide gauges because of the limited access track to connect that three tide gauges. It is uncommon to have multiple vertical datum that propagated from separate tide gauge (Othman et al., 2014). In the present circumstances, Global Navigation Satellite System (GNSS) had been used as height determination, and it can provide heighting in ellipsoidal height which is the geometrical height (Othman et al., 2014). The heighting that given by this technology is the height that cannot be used straightway with traditional orthometric height datum, and it needs geoid-ellipsoid separation to respect to a vertical datum (Jamil, 2011). One alternative that can be done to generate vertical datum is using geoid modelling (Othman et al., 2014).

In generating geoid modelling, there are has several methods. The methods that commonly used are the Least Square Modification of Stokes (LSMS) or known as KTH method, Remove-Compute-Restore (RCR) and lastly Stokes-Helmert's formula. There are several countries that used geoid modelling as vertical datum such as New Zealand and Canada, and that proved geoid model had been universal choices as a vertical datum in current or future (Othman et al., 2014).

In Malaysia, whether in Peninsular Malaysia and East Malaysia, it had used the geoid model as a vertical datum and that model is known as MyGeoid. MyGeoid is gravimetric geoid modelling that had to establish using Remove-Compute-Restore (RCR) method. Based on the study that had been done, there are has several limitations in Remove-Compute-Restore method and one of them is it determine that method had provided the accuracy around 10cm in

Perpustakaan Negara Malaysia eISBN 987-967-17889-6-7

geoid model and it was improved by Bjerhammar and Moritz for better accuracy but it still not put into effect in RCR method to achieve the objective of centimetre geoid model (Ulotu, 2009). One alternative method that can be done is Lease Square Modification of Stokes with Additive Correction (LSMSA) or known as KTH method (Sjoberg et al., 2015). This method had minimizes the expected global mean square error of the estimated geoid height and reducing the truncation error (Sjoberg et al., 2015). KTH method had proven successful put forward by New Zealand (Abdalla & Tenzer, 2011), Turkey (Abbak et al., 2012), Iran (Kiamehr, 2006), Tanzania (Ulotu, 2009) and Sweden (Ågren, 2004).

Besides that, in generating gravimetric geoid modelling, several data is used in the processing and the most important data in generating gravimetric geoid modelling are Global Geopotential Model (GGM) and Digital Elevation Model (DEM). It is because, in geoid modelling technique it needs the use of Global Geopotential Model (GGM) to represent the global variation or long wavelength of the earth gravitational field and Digital Elevation Model is used to describe the topography of the local area (Al-Krargy et al., 2015). Therefore, the precise of Global Geopotential Model (GGM) and Digital Elevation Model (DEM) was influences to obtain precise geoid modelling. Lastly, the new gravimetric geoid modelling needs to fitting to the local vertical datum that can be used as a vertical datum. The new gravimetric geoid modelling cannot straightly be fitted to benchmarks because it will phase down the accuracy of the model and that fitting process should be avoided because of various aspect such as benchmark that can lead to error come from land subsidence and uplift, and damaged by widened road construction. (Othman et al., 2014). Therefore, this research has been proposed a generating gravimetric geoid modelling by using KTH method.

Significant of Study

This research which is produced gravimetric geoid modelling, will have significant or benefit in several purposes that involved in geomatics field. Firstly, the new gravimetric geoid modelling will produce by using two different types of Global Geopotential Model (GGM). From this, the effect of the GGM toward the computation of gravimetric geoid modelling can be assessed in the investigation of GGM used. Based on the statistical analysis of gravimetric geoid modelling, it can be used to illustrate how far the GGM will affect the computation of gravimetric geoid modelling and whether it can give the impact toward the accuracy of geoid modelling.

Besides that, new gravimetric geoid modelling will pluses with offset, which is the difference between the gravimetric geoid and geometrical geoid at each tide gauge and it will be resulting in three hybrid geoids. The significant from that, the user can be used that three models of hybrid geoid in height measurement using GNSS Levelling. The heighting, which is the orthometric height, can be calculated by extracting from this geoid model at any point on the topography surface based on the area of observation. For example, the user wanted to refer at Kuching tide gauge, so his or she can use the hybrid geoid that applies the offset at Kuching.

Other than that, this research will produce seamless vertical datum over Sarawak region, which is gravimetric geoid modelling. The significant from that, that model can be for any point of height measurement using GNSS on topography survey. It means the observation of heighting over Sarawak region can only refer that this gravimetric geoid model. This can save the time and cost of observation, especially for the project that involves large area coverage. Lastly, from this research, it can identify the differences between RCR method and KTH method that adopted in geoid computation.

Methodology

In the accomplishment of the aim and objective of this research, there are have several phases of research methodology that had been done. In this section, it was contenting the information of research methodology for this research. The phase of methodology was divided into four phases which are planning, data preprocessing, data processing and lastly result and analysis. The first phases are focusing on the selected study area, selection software used, preliminary study and research problem identification and data acquisition. The second phase is known as pre-data processing. This phase is reviewing the validation of data that divided into two-part, which are cross-validation for gravity data and validation for GGM and DEM data. These data that had done the validation process then undergo data processing phase where geoid height computation using KTH Geolab Software to produce gravimetric geoid modelling. Lastly, it will continue to result and analysis phase. In this phase, the data is processed based on the aim and objectives of the study. An analysis is a closure to the study where all result is explained into details for the readers understanding throughout the process.

Perpustakaan Negara Malaysia eISBN 987-967-17889-6-7

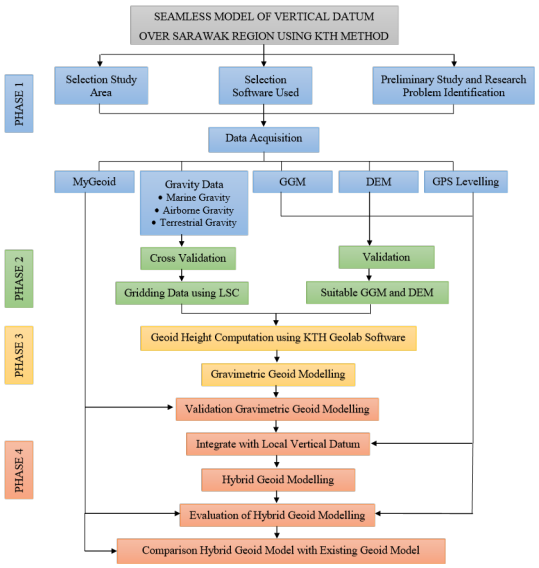

Figure 4.1 The flow of methodology of this research

Modification Coefficient Parameter

Modification coefficient parameter must determine accurately and this parameter is dominance by a set of condition, namely choice of capsizing, correlation length and standard deviation of terrestrial gravity (Pa'suya et al., 2018). By using different standard error for the terrestrial gravity data, the behaviour of the modification parameter is numerically tested (Ssengendo, 2015). In determining the foremost modification coefficient parameter, evaluation of the spherical harmonic degree of Global Geopotential Model, upper bound of the Stokes function, integration cap, correlation length, and terrestrial error need to be determined.

Table 4.1 Modification coefficient parameter

The upper limit of GGM = Upper bound of Stokes's function (M=L)	GOCO SPW R2 = 240 0 GOCO TIM R6 = 300 0
Integration Cap ($\boldsymbol{\psi 0/0}$)	3.0 0
Correlation Length ($\boldsymbol{\psi 1/2/0}$)	0.2 0
Terrestrial Error ($\boldsymbol{\sigma \Delta g}$)/$\boldsymbol{mGal}$	2.0

Approximate Gravimetric Geoid

The approximate gravimetric geoid is the result or output from the signal and error degree variance, choice of the capsize and modification coefficient parameter. This gravimetric geoid is resulting from the combination of gravity anomaly of terrestrial gravity, marine gravity and airborne gravity and lastly the selected Global Geopotential Model. The computation of approximate gravimetric geoid modelling as the following formula:

$$\tilde{N} = c\sum_{n=2}^{\infty}\left(\frac{2}{n-1} - Q_n^L - s_n^*\right)(\Delta g_n + \varepsilon_n^T) + c\sum_{n=2}^{N}(Q_n^L + s_n^*)(\Delta g_n + \varepsilon_n^T) \quad (4.1)$$

Additive Correction and Final Gravimetric Geoid

In the additive correction, it involved five processing which is the combined topographic, the downward continuation (DWC), the total topographic effect, the total atmospheric and lastly is the ellipsoidal correction. In the combination of topographic correction, the computation involved the topographic height of point, the mean radius of the earth, constant gravitational time the constant standard topographic density and normal gravity of the computation point. The processing of topographic correction will reduce in combine topographic effect on the geoid (Kiamehr, 2006). The DWC correction is computed using DEM and GGM data. The observed surface gravity anomalies must be downward continued to the geoid and this correction applies to surface gravity anomalies (Kiamehr, 2006). In the total topographic effect, its determination can be obtained from a combination of topographic correction and DWC correction. The next correction is the total atmospheric correction. For atmospheric correction, it used the GGM. This error can provide the error of 0.3% in the estimated of geoid model (Kiamehr, 2006). Lastly, the final correction is ellipsoidal correction. In the ellipsoidal correction, it involved the GGM and its computed based on the Mean Earth Ellipsoid instead of the Mean Earth Sphere (Ssengendo, 2015). By using a combination of this correction, it will attach with approximate gravimetric geoid to produce final gravimetric geoid modelling. This computation through the following formula:

$$N = N' + \delta N_{TOPO} + \delta N_{DWC} + \delta N_{ATMO} + \delta N_{ELL} \quad (4.2)$$

Gravimetric Geoid Model Accuracy Evaluation

In the processing of the gravimetric geoid model accuracy evaluation, the gravimetric geoid model will compare with the MyGeoid. The orthometric height from the gravimetric geoid modelling will compare with orthometric height of Mygeoid at every benchmark. In this processing, it will prepare the coordinate of each benchmark that will be used to extract the height from the gravimetric geoid model. The extract of heighting will be done using Geocom Software, where it will use the interpolation method to extract the heighting. One the extraction heighting is done from the gravimetric geoid model, it will compare with heighting from the MyGeoid. The analysis can be done using the Root

Perpustakaan Negara Malaysia eISBN 987-967-17889-6-7

Mean Square computation and the computation through the following formula:

$$\bar{x} = \frac{1}{n}\sum_{i=1}^{N} x_i \quad (4.3)$$

$$\sigma = \sqrt{\frac{1}{(n-1)}\sum_{i=1}^{N}(x_i - \bar{x})^2} \quad (4.4)$$

$$RMSE = \sqrt{\frac{1}{(n-1)}\sum_{i=1}^{N}\left(\frac{x_i - x_{true}}{x_{true}}\right)^2} \quad (4.5)$$

Development of Hybrid Geoid Model

In the development of hybrid geoid model, the gravimetric geoid modelling will be fitted to local vertical datum. In practical, the geoid model is compensated by u to 1 – 2 meters from the actual GNSS Levelling geoid height. To make sure it consistent with existing levelling, there are need to fit gravimetric geoid modelling surface to the local vertical datum. The fitting process will be computed using several methods which are root mean square error, linear form, polynomial with various order and 4parameter Helmert Model. For this research, in the development of hybrid geoid model, the difference between the gravimetric geoid and geometric geoid will be computed using the following formula:

$$\varepsilon = N_{GNSS} + N_{grav} \quad (4.6)$$

N_{GNSS} is obtained from GNSS levelling method and N_{grav} is obtained from gravimetric geoid model. The final hybrid model will be computed using the following formula:

$$N_{Hybrid} = N_{grav} + \varepsilon \quad (4.7)$$

Lastly, the hybrid geoid modelling will compare with existing geoid modelling and GNSS Levelling. Geoid modelling from new hybrid geoid model and existing hybrid geoid model will compare with GNSS levelling for evaluation of hybrid geoid model.

Result and Analysis

Validation of Global Geopotential Model (GGM)

Refer to Figure 5.1 and Figure 5.2; it showed the result of Global Geopotential Model (GGM) validation. The purpose of this process was carried out is to validate the GGM that are suitable or providing minimum accuracy assessment for been used in the further processing of gravimetric geoid modelling. As was mention before, GGM will represent the global variation or long wavelength of the gravitational earth field. From that, it can be stated that the precise GGM will give the influences in generating gravimetric geoid modelling. In this research, GGM will be validated with GNSS Levelling data which is the estimation of geoid height from GGM will compare with geoid height that computes from GNSS Levelling data and lastly compute the root mean square error for each type of GGM. Besides that, in this research, it had using 12 types of GGM for validation.

In the processing of gravimetric geoid modelling using KTH method, it was divided into two sized of the research areas, which is called as the inner region and outer region. The outer region is the extended area from the inner region with a selected degree of capsize and for this research, it had used 3 degrees of capsizing. The function of capsizing is to reduce the effect of undetected systematic or gross error that contain in gravity data from the measurement, and this capsizes also used to provided uniform gravity data. Refer back to Figure 5.1, it shown the result of validation for GGM using inner region of the research area and Figure 5.2 is shown the result validation for GGM using outer region. The meaning of validation using inner and outer region is the GNSS Levelling point that will be used for this validation was filtered based on the region or sized of research area had been used. For example, if the validation is doing an inner region, the GNSS Levelling point will be filtered and only used the point that is located in the area of the inner region and this is the same concept with validation in the outer region.

As a result, that state in Figure 5.1, it is shown that the type of GGM for model number 1 consist of the minimum accuracy assessment compare to other types of GGM for the inner region. The value of RMSE for type number 1 of GGM is 0.451, and number 1 is a model of GO_CONS_GCF_2_SPW_R2 which is one type of GGM. In Figure 5.2, it was shown that model number 6 consist of minimum accuracy assessment for the outer region, which RMSE value is 0.614. The type of model number 6 is GO_CONS_GCF_2_TIM_R6 model which is one type of GGM. Based on the result, it can be assuming that GOCO SPW R2 is suitable to be used for the inner region and GOCO TM R6 is suitable to be used for the outer region. Besides that, refer to these two types of validation result, it shown that validation of the inner region and outer region provided a different type of GGM that consist minimum accuracy assessment. From this result, it can be concluded that the different sizes of the research area will be provided with a different type of GGM. For this research, it will use these two types of GGM that had minimum accuracy assessment in the inner region and

Perpustakaan Negara Malaysia eISBN 987-967-17889-6-7

outer region for generation gravimetric geoid modelling and the effect of these selected GGM will be discussed in the next subsection.

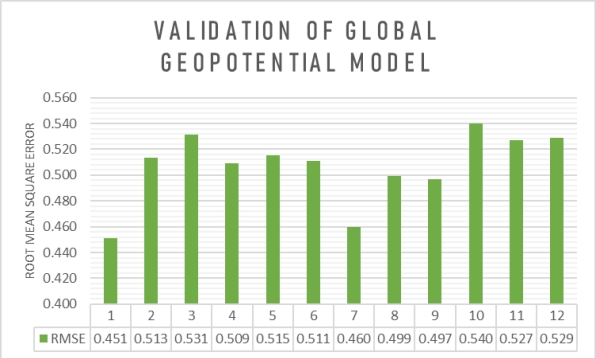

Figure 5.1 Validation of GGM using the inner region of the research area

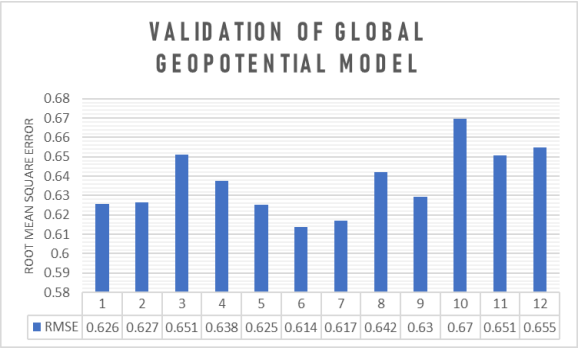

Figure 5.2 Validation of GGM using the outer region of the research area

Final Gravimetric Geoid Model of Sarawak

In this research, it was provided two final gravimetric geoid model that based on two types of GGM that had been chosen based on validation process that refer to different sizes of the research area which is called as the inner region and outer region. The outer region is the extended area from the inner region with a selected degree of capsize and the function of capsizing is to reduce the effect of undetected systematic or gross error that contain in gravity data from the measurement and to provided uniform gravity data. As illustrated in Figure 5.3 and Figure 5.4, it was the final gravimetric geoid modelling for both models, which are GOCO SPW R2 and GOCO TIM R6. Final gravimetric geoid modelling is a combination of approximate geoid height and additive correction. Based on both result of final gravimetric geoid model, the range of geoid height is from 15 meters to 56 meters. As illustrated in Figure 5.3 and 5.4, the geoid height is had the same pattern, which is declining from southeast to northwest for both results. Besides that, in Figure 5.5, it showed the differences in geoid height between two geoid model that was generated by using different of GGM. From the result, it can see that over research area had the height of differences geoid height between these two types of model. The range of differences value for geoid height between two types of model is 0.6 meters to -0.7 meters. Based on the statistical analysis on table 5.1, it is shown that the mean and standard deviation for differences geoid height are -0.0439 and 0.2327. Respectively the result that was presented above, it can be seen that there are have much different, which is have 70 cm of differences between geoid height that are generated by using a different type of GGM. In the table of statistical analysis is shown that GOCO SPW R2 model has the lowest standard deviation compared to another model. However, these two types of the model will be evaluated the accuracy by using 53 points of GNSS levelling that are provided by the Department of Survey and Mapping Malaysia. (DSMM) and this evaluation will discuss in the next subsection.

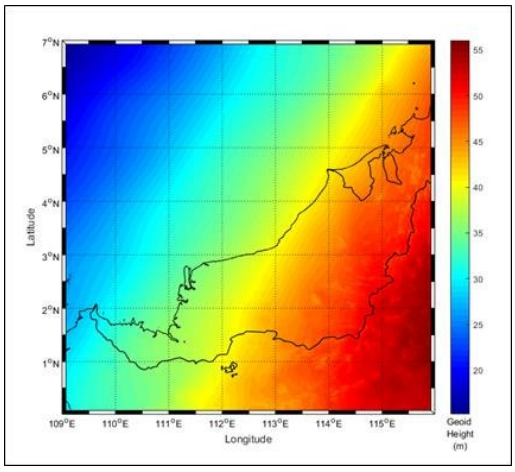

Figure 5.3 Final gravimetric geoid model from GOCO SPW R2

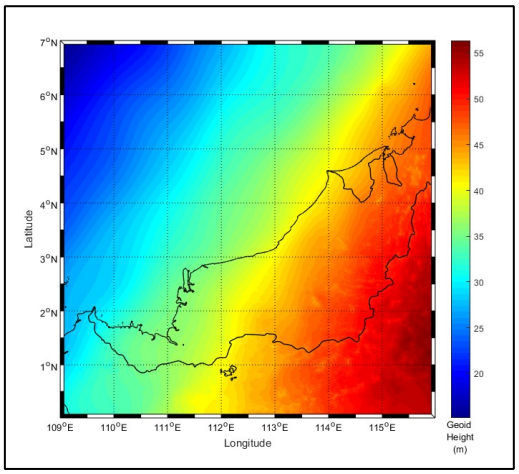

Figure 5.4 Final gravimetric geoid model from GOCO TIM R6

Perpustakaan Negara Malaysia eISBN 987-967-17889-6-7

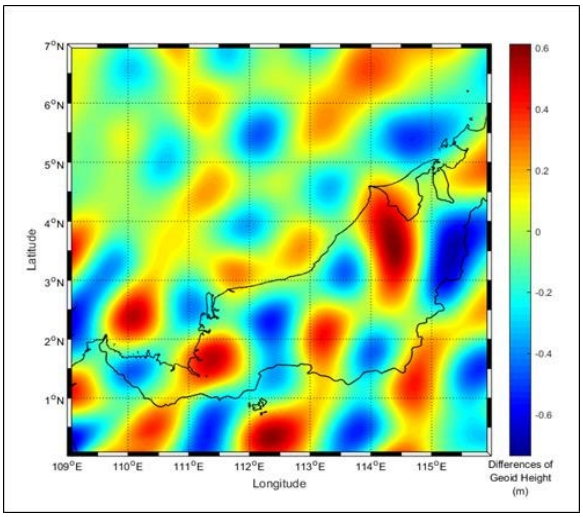

Figure 5.5 Differences of geoid height from two GGM

Table 5.1 Statistical analysis of final gravimetric geoid

GGM	Max Degree (0)	Mean	Std Dev
GOCO SPW R2	240	-0.1331	0.3598
GOCO TIM R6	300	-0.1336	0.3610
Differences Geoid Height		-0.0439	0.2327

Evaluation of Final Gravimetric Geoid Model using Official Geoid Model

To evaluate the accuracy assessment of the generated gravimetric geoid model, there are have two methods which are internal accuracy assessment and external accuracy assessment. For this research, it will use the external accuracy assessment method. According to Ssengend (2015), for the one hand, internal accuracy assessment is founded on error propagation and it can't find alone to use to express how good gravimetric geoid model that had been generated while, for another hand, external accuracy assessment is founded on independent data set and this is a good pointer of accuracy for the gravimetric geoid model.

In this research, it will use new official gravimetric geoid data and fitted the geoid model as independent data to do a comparison with new gravimetric geoid modelling. For the first one, it had to validate with the new official gravimetric geoid model. New official gravimetric geoid model is the gravimetric geoid model that had been produced using remove-compute-restore (RCR) technique. This gravimetric geoid model is using the mixed spherical harmonic model EGM08/GOCO to the spherical harmonic degree with 7200, SRTM digital elevation model, DTU15 satellite altimeter and 107 000 km flight line of airborne gravity data. The comparison of between new official gravimetric geoid data and new gravimetric geoid had been done on 35 GNSS levelling which using the bicubically interpolated method to interpolated geoid heighting from new official gravimetric geoid and new gravimetric geoids model. GNSS levelling point is used to represent as a verified point to doing a comparison between both data. Based on Figure of graph 5.6, it showed the residual on 35 GNSS levelling data.

Refer to the result in Figure 5.6, is shown that the RMSE of comparison for GOCO SPW R2 model is 0.7730 and for GOCO TIM R6 model is 0.7683. From that, it can be seen that the GOCO TIM R6 model had the lowest value of RMSE compare to another model. To make it more clearly or confirming that result of validation, the validation had been continued with the second validation with fitted or hybrid geoid model. In the second validation, it had applied the same concept, such as the first validation which is a direct comparison between new gravimetric geoid modelling. Based on Figure 5.7, it is shown that RMSE of GOCO SPW R2 before fitting is 0.3720 and for GOCO TIM R6 is 0.4245. However, the direct comparison will lead to the systematic biases that produce from reference data and new gravimetric geoid. In order to solve the problem, these differences are fitted using a 4-parameter model as a function to absorption of the systematic geoid. By using 4-parameter to remove the biases or error for reference data and new gravimetric geoid model, both types of gravimetric geoid model were fitted to reference. This is because to fairly standardized in comparison of residual at the verified point. As refer back to Figure 5.7, the RMSE of GOCO SPW R2 after fitting is 0.2163 and RMSE of GOCO TIM R6 is 0.2645.

From these results, it can conclude that the new gravimetric geoid modelling that used GGM model from GOCO SPW R2 is the best suitable model that fits Sarawak region by providing the lowest RMSE compare to another model. Other than that, based on this result, it is shown that the selected GGM model will bring effect to the development of gravimetric geoid modelling. As mention before, GOCO SPW R2 is the selected model from validation on the inner region of the research area and the GOCO TIM R6 is model from validation on outer region. From that, it is seen that the GGM that nearly focus on the Sarawak region provided the lowest RMSE compare to another model.

Perpustakaan Negara Malaysia eISBN 987-967-17889-6-7

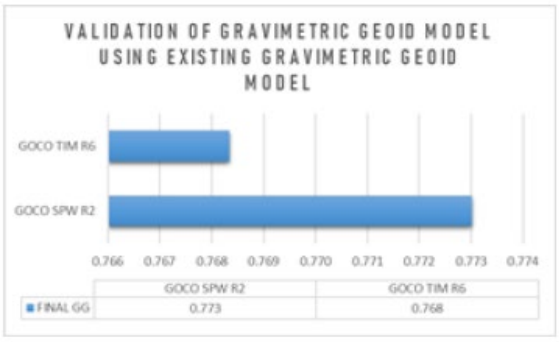

Figure 5.6 Evaluation of gravimetric geoid using existing gravimetric geoid model

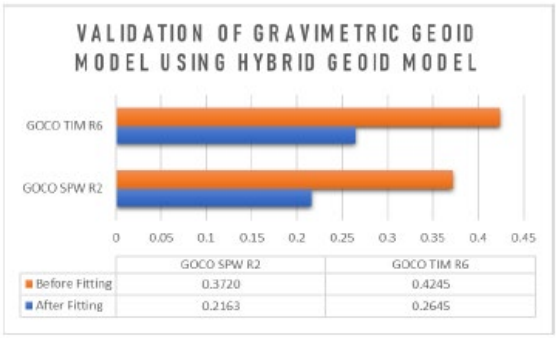

Figure 5.7 Evaluation of gravimetric geoid using hybrid geoid model

Hybrid Geoid Model

In theory, geoid can be assumed coincide with mean sea level (MSL). Nevertheless, in practice, there are has differences between the geoid and the mean sea level (MSL). This difference is known as vertical datum bias. Besides that, the levelling is referred to as the mean sea level. In the situation of survey work that using GNSS instrument, the value of heighting that getting from the instrument is ellipsoidal height and if apply with geoid height from gravimetric geoid, the orthometric height that generating is not same with the height that refers to levelling datum. To overcome this problem, the fitting process is needed. The fitting process is the process of fit gravimetric geoid modelling to mean sea level. This process will be resulting in the new geoid model known as hybrid geoid model. The process of fitting has several methods. In this research, it will use a direct method for fitting a gravimetric geoid model to local vertical datum. Firstly, for the fitting processing using the direct method, it will calculate the comparison between gravimetric geoid height with mean sea level at GNSS levelling point. For getting the value of geoid height from gravimetric geoid model, the gridded gravimetric geoid will be using bicubically interpolated methods to the location of GNSS levelling for getting geoid height, and this heighting will compare with mean sea level value.

As refer back to the result of the evaluation of gravimetric geoid model by using a different type of GGM, it is shown that gravimetric geoid model using GOCO SPW R2 model is provided lowest standard deviation compare to another. In this subsection, it will use gravimetric geoid modelling from GOCO SPW R2 for proceeding with the fitting process. Based on table 5.2, it showed the result of the comparison. The offset column if the value of comparison between geoid height and mean sea level at three tide gauge in Sarawak which is Miri, Bintulu and Kuching. Refer to the result of the comparison, the offset at Miri, Bintulu and Kuching are 0.2073, 0.6545 and -0.1567. This each of offset value will be added to gravimetric geoid modelling to produce hybrid geoid model that based on mean sea level.

Table 5.2 GNSS levelling at three tide gauge location in Sarawak

Station ID	Tide Gauge Station	GPS Ellipsoidal Height h^{GPS} (m)	MSL H (m)	Geoid Height N^{True} (m)	Geoid Height N^{Grav} (m)	Offset (m)
133	Miri	44.399	2.6637	41.7353	41.528	0.2073
T002	Bintulu	46.176	5.4275	40.7485	40.094	0.6545
K013	Kuching	37.366	3.3817	33.9843	34.141	-0.1567

Evaluation of Hybrid Geoid Model with GNSS Levelling

As mention before, the evaluation of the geoid model must be determining for checking the accuracy of that geoid model. In this subsection, it will evaluation the 3-hybrid geoid model that fitting using offset from 3 tide gauge. This evaluation process had using 35 GNSS levelling as independent data. The geoid height from 3 hybrid geoids had using the bicubically interpolated method to interpolated geoid height at references point. Besides that, the existing hybrid geoid model had also evaluated with independent data. For the existing hybrid geoid model, it had applied the same method with the new hybrid geoid model for evaluation. Refer to Figure 5.8 and Figure 5.9, it showed the result of RMSE that using the direct fitting and apply 4-parameter in the fitting. In Figure 5.8, it showed the RMSE result of evaluation hybrid geoid model with GNSS levelling by using direct fitting. Based on the result, RMSE for new hybrid geoid model that using offset Miri, Bintulu and Kuching are 0.4045, 0.4646 0.6397. For the existing hybrid geoid model, it showed the result of RMSE 0.2517.

In another hand, as refer to Figure 5.9, it showed the result of an evaluation that apply 4-parameter in the fitting process. It present that the new hybrid geoid model had RMSE with 0.2581 and existing hybrid geoid model with 0.186. Based on both result of the evaluation, the existing geoid model has had the lowest value of RMSE compare to new hybrid geoid model with have 0.0721 meters which

Perpustakaan Negara Malaysia eISBN 987-967-17889-6-7

are 7 cm. One main factor that contributes to the different value of RMSE is due to the different sources of data that had been used in the computation of gravimetric geoid modelling. In the computation of existing geoid model, it had used the additional data with is marine gravity data that had survey using airborne that was done under MAGIC Project which is the development of marine geodetic infrastructures in east Malaysia waters.

According to H. Jamil et al. (2017), with the advantage that has airborne scalar gravity which is the production system with its detailed error models, it will make it possible to use airborne gravimetry as a relatively standard technique in geodesy to achieve the best accuracy around 1-2 mGal. With the combination of gravity data on land and marine area using airborne survey, it can provide more accurate compare to this research study that only used limited gravity data using airborne on land area. From that situation, it can see that the selected data for generating the geoid model will affect the accuracy of the geoid model. Besides that, in this research, it only used 3 degrees for capsizing and 240 degrees for the spherical harmonic degree. The selected of this degree is important to reduce systematic error and gross error in gravity data and to provide the uniform gravity data. However, there is no optimum degree for numerical integrate by KTH method and it needs to be tested and evaluated to find the best suitable suited in the research area and for this research, it only using 3 degrees and 240 degrees in capsizing and spherical harmonic degree. From that this can be assumed as one factor that contributed to differences with existing hybrid geoid model. However, as refer to Figure 5.8, it is shown that the result of RMSE that using offset Miri for new hybrid geoid give the minimum accuracy assessment compare to another tide gauge. From that, it can be assuming that offset Miri can be the best fitting for the Sarawak region.

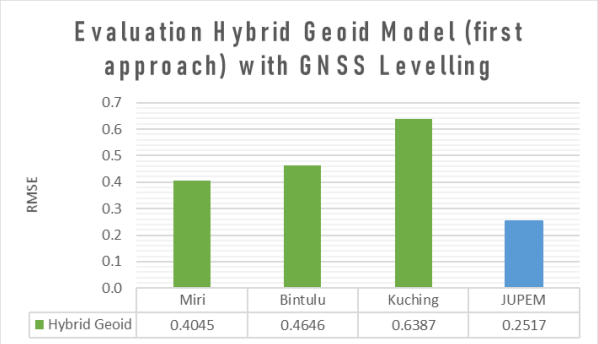

Figure 5.8 Evaluation hybrid geoid model with GNSS levelling (Direct fitting)

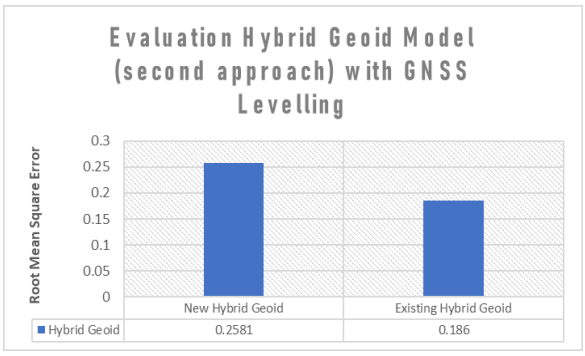

Figure 5.9 Evaluation hybrid geoid model with GNSS levelling apply 4-parameter fitting

Conclusion

Nutshell, all objectives of this research is successfully achieved. All of the results obtained is answering the objectives of the research. In the first objective is to identify the effect of GGM toward generating gravimetric geoid modelling. To satisfy the first objective, the validation of suitable GGM needs to perform. As refer to validation result, the GGM model of GOCO SPW R2 and COGO TIM R6 has been chosen in the main of processing to produce two different gravimetric geoid modelling. Based on the result, it showed the final gravimetric geoid model for the GOCO SPW R2 model give the lowest RMSE compare to GOCO TIM R6 model which 6 cm differences. From that, it can be concluded that the selected of GGM will give the effect in generation accurate gravimetric geoid modelling. Other than that, the mean sea level and geoid is had differences and not coincides. Besides that, the levelling is referred to mean sea level and if heighting of a survey that using GNSS instrument and apply geoid height, the orthometric height that was produced is not same with the height refer to levelling datum. To overcome that problem and produce workable geoid model, the final gravimetric geoid model that has been generated were fitted to the local vertical datum. From that, it will produce a new geoid model known as hybrid geoid model, and this will satisfy the second objective of this research. The final gravimetric geoid that had been selected had fitting to three vertical datum of Sarawak and resulted in three hybrid geoids which are fitted at Miri, Bintulu and Kuching at the end. However, to prove the accuracy of hybrid geoid model that had been developed, validation had been done by using references data which is GNSS levelling point. The new hybrid geoid model and existing geoid model had to validate with GNSS levelling point and the result shown the existing geoid model had the lowest RMSE compare to new hybrid geoid due to the different sources of data that had been used which is existing hybrid geoid model was using additional data which is marine gravity data

Perpustakaan Negara Malaysia eISBN 987-967-17889-6-7

using the airborne survey. As it is known, airborne gravity data can provide accuracy better than 2.0 mGal. Lastly, it can be seen that the type of input data will be given the effect of generating precise gravimetric geoid modelling. Other than that, the spreading of gravity data that covering the all study area will reduce the possible error that might be happened during processing. This is because, when doing the interpolation data, it will be computed based on the accurate value and minimize the error that can be produced.

Recommendation

The development of seamless vertical datum over Sarawak region using KTH method for this research had been achieved but not able to achieve the recommended level of accuracy compared with existing hybrid geoid model. These are because of several issues that need to be considered for resulting in the more precise geoid model in future development. The recommendation and suggestion are as following:

i. The distribution of terrestrial gravity data needs to cover the research area. to achieve a consistent and accurate enough of gravimetric geoid modelling, it necessitates the assorted distribution of terrestrial gravity data
ii. For the future development of gravimetric geoid modelling, the using airborne gravity data for land and marine area need to be fulfilled. This research can be evidence with the lack of airborne gravity data; it is impossible to reach high-quality gravimetric geoid modelling. The airborne gravimetry is recommended to increase the quantity and quality of gravity data inland and marine area because this was proved that can provide 2 mGal accuracies by the previous study.
iii. One of another recommendation is the distribution of GNSS levelling point. The distribution of GNSS levelling point is to use in validation and refinement the gravimetric geoid modelling. Besides that, the GNSS levelling point was distributed to cover the region area; it can improve in the fitting process between gravimetric geoid modelling and GNSS and improved the new height datum.
iv. The selected of DEM and GGM data in processing for generating gravimetric geoid modelling. This is because these types of data were also important in generating gravimetric geoid modelling. It is important because the GGM model represents the global variation or long wavelength of the earth gravity field, and DEM is to describe the topography of the local area.
v. The last recommendation is the selected capsize and spherical harmonic degree. The chosen of capsizing and spherical harmonic degree is important in generating gravimetric geoid modelling because every area will be provided different capsize and spherical harmonic degree that suitable for that area. It is important to use to reduce the effect of undetected systematic of gross error that consists of gravity data and provided uniform gravity data. For future development, the capsize and spherical harmonic degree need to be evaluated.

Acknowledgement

Special thanks to the Department of Survey and Mapping Malaysia (DSMM) for providing several data that had been used for this final year project. The data that had been providing are terrestrial gravity data and GNSS levelling data over Sarawak region. Without this data, this project can't be carried out with success and the authors feeling so appreciated for their commitment.

REFERENCES

Abbak, R. A., Sjöberg, L. E., Ellmann, A., & Ustun, A. (2012). A precise gravimetric geoid model in a mountainous area with scarce gravity data: A case study in central Turkey. *Studia Geophysica et Geodaetica*, 56(4), 909–927. https://doi.org/10.1007/s11200-011-9001-0

Abdalla, A., & Tenzer, R. (2011). The evaluation of the New Zealand's geoid model using the KTH method. *Geodesy and Cartography*, 37(1), 5–14. https://doi.org/10.3846/13921541.2011.558326

Ågren, J. (2004). *Regional geoid model determination methods for the era of satellite gravimetry (Numerical investigations using synthetic earth gravity models*) (Issue October).

Al-Krargy, E., Hosny, M., & Dawod, G. (2015). Investigating the Precision of Recent Global Geoid Models and Global Digital Elevation Models for Geoid Modelling in Egypt. *Regional Conference on Surveying & Development*, December, 3–6.

Perpustakaan Negara Malaysia eISBN 987-967-17889-6-7

Erol, B., Sideris, M. G., & Çelik, R. N. (2009). Comparison of Global Geopotential Models from the Champ and Grace Missions for Regional Geoid Modelling in Turkey. *Studia Geophysica et Geodaetica*, 53(4), 419–441. https://doi.org/10.1007/s11200-009-0032-8

Jamil, H., Kadir, M., Forsberg, R., Olesen, A., Isa, M. N., Rasidi, S., Mohamed, A., Chihat, Z., Nielsen, E., Majid, F., Talib, K., & Aman, S. (2017). Airborne Geoid Mapping of Land and Sea Areas of East Malaysia. *Journal of Geodetic Science*, 7(1), 84–93. https://doi.org/10.1515/jogs-2017-0010

Jamil, H, Kadir, M., Forsberg, R., Olesen, A., Isa, M.N., Rasidi, S., Mohamed, A., Chihat, Z., Nielsen, E., F.Majid, K.Talib, & S.Aman. (2017). *Airborne geoid mapping of land and sea areas of East Malaysia*. 84–93. https://doi.org/10.1515/jogs-2017-0010

Jamil, Hasan. (2011). GNSS Heighting and Its Potential Use in Malaysia. FIG Working Week 2011, *Bridging the Gap between Cultures, Marrakech Morocco*, 18-22 May 2011, 5410, 1–19.

Kiamehr, R. (2006). Precise Gravimetric Geoid Model for Iran Based on GRACE and SRTM Data and the Least-Squares Modification of Stokes ' Formula with Some Geodynamic Interpretations. In *Royal Institute of Technology (KTH)* (Issue October). https://doi.org/http://urn.kb.se/resolve?urn=urn :nb n:se:kth:diva-4125

Othman, A. H., Omar, K., Othman, R., Som, M., Z, A., & Opaluwa, Y. . (2014). Unification of Vertical Datum in Sabah and Sarawak. *Jurnal Teknologi*, 4, 21–22.

Pa'suya, M. F., Yusof, N. N. M., Din, A. H. M., Othman, A. H., Som, Z. A. A., Amin, Z. M., Aziz, M. A. C., & Samad, M. A. A. (2018). *Gravimetric geoid modeling in the northern region of Peninsular Malaysia (NGM17) using KTH method*. https://doi.org/10.1088/17551315/169/1/012089

Ses, S., & Gilliland, J. R. (2013). A New Height Control for Peninsular Malaysia. *Survey Review*, 34(265), 151–158. https://doi.org/10.1179/sre.1997.34.265.151

Sjoberg, L. E., Gidudu, A., & Ssengendo, R. (2015). *The Uganda Gravimetric Geoid Model 2014 Computed by The KTH Method*. 35–46. https://doi.org/10.1515/jogs-2015-0007

Som, Z. A. A., Yazid, A. M., Ming, T. K., & Yazid, N. M. (2016). *The Unified Levelling Network of Sarawak and Its Adjustment*. XLII(October), 3–5. https://doi.org/10.5194/isprs-archives-XLII-4-W1-271-2016

Ssengendo, R. (2015). *A HEIGHT DATUM FOR UGANDA BASED ON A GRAVIMETRIC QUASIGEOID MODEL AND GNSS / LEVELLING.*

Ulotu, P. E. (2009). *Geoid Model of Tanzania from Sparse and Varying Gravity Data Density by the KTH Method*.

Perpustakaan Negara Malaysia eISBN 987-967-17889-6-7

Integration of Sirah and Geography Elements in Teaching and Learning using Multimedia Approach

Erna Nurfazana Nurizan[1], Ernieza Suhana Mokhtar[1], Siti Zulaiha Ahmad[2], Nur Hazwani Kasban[1]*

[1] Faculty of Architecture, Planning & Surveying, Universiti Teknologi MARA, Perlis Branch, Arau Campus, 02600 Arau, Perlis, Malaysia
[2]Faculty of Computer & Mathematical Sciences, Universiti Teknologi MARA, Perlis Branch, Arau Campus, 02600 Arau, Perlis, Malaysia

**e-mail: ernieza@uitm.edu.my*

Abstract

Teaching and learning in *Sirah* are connected to spatial information such as locations, direction, distance, area, and journey. However, students encountered difficulties in memorizing a critical event related to Islamic history using traditional teaching methods, whiteboard explanations with the absence of the geography element. Therefore, the teaching approach can be enhanced by integrating three elements; *Sirah*, Geography, and Multimedia through storytelling video in an application. This study investigates the teacher, parents, and student perception on teaching and learning of *Sirah* subject with/without geography elements and constructing an application prototype with a storytelling video of the *Sirah* subject which covers the year five subtopic of the Islamic education syllabus. A questionnaire was distributed, and 148 respondents gave feedback on the proposed idea in new teaching and learning platform. The *Sirah* video prototype was designed based on the geography elements (e.g., location, direction, and journey) which integrated with *Sirah* using a multimedia platform. The feedback was responded.

Keywords: *Sirah*, geography elements, multimedia, storytelling, teaching and learning

Introduction

Nowadays, teaching and learning mostly used the conventional method such as face to face (F2F) methods and it might affect student understanding and resulting to slow learning in the passive environment (Li, Antonenko, and Wang, 2019; Sellers et al., 2007). Mohd Sharif et al. (2017) stated that teaching and learning *Sirah* using a passive method is the easiest way to apply, which results in the lack of active methods in

Islamic education. It can lead to declining in students' performance because of flaws created by the teaching and learning process (Fadzilah, 2017). Therefore, a new approach should be taken into consideration to encounter student learning outcomes using the conventional method.

Multimedia platform able to impress the student for better Islamic learning such as *Sirah* games in the form of computer science (Tularam and Machisella, 2018; Mohd Sharif et al., 2017; Park et al., 2019). Students used YouTube as one of the tools for teaching and learning is believed can help improve learning because of visual rendering that can be easily understood (Moghavvemi et al., 2018). However, watching YouTube provides less two-way interaction, and Mohd Sharif et al. (2017) stated that by just listening in the class, the student might not be able to understand the whole flow of the *Sirah*. In another way, teaching and learning can be blended, for example, face to face and online medium.

Therefore, it is approved that traditional classroom learning is less effective nowadays, and a new approach needs to be carried out to improve the understanding of students in the class. This study will contribute to the integration of *Sirah* and geography with the use of the multimedia approach. This study will contribute to testing the effectiveness of multimedia usage in teaching and learning nowadays. This study will enhance the two ways of interaction while learning using the multimedia approach in teaching and learning and expected can employ the need of students in education through elements of geography and *Sirah*.

Problem Statement

Students should be exposed to different learning and learning styles, that needs to change over time (Lambri and Mahamod, 2014). The student interest will lack if the teachers unable providing

Perpustakaan Negara Malaysia eISBN 987-967-17889-6-7

creative teaching and learning styles (Tamrin, Azkiya, and Sari, 2017), which can influence the students' cognitive level (Kassim, 2013). So, to encounter the deficiencies of conventional teaching and learning, the use of text and pictures as the two-way approach has been implemented to enhance learning and resulting in better outcomes rather than verbal method (Li, Antonenko, and Wang, 2019). Combination of various media likely to show information and enhance people's understanding and memory of information and by using multimedia technology, students' interest in learning can be enhanced and using helpful teaching tools and also resulting from simplifying teachers' teaching tasks (Guan, Song, and Li, 2018).

The solution to the problem

Sirah and geography elements are related to each other and using multimedia; it can be used as an enhancement of teaching aid during teaching and learning sessions. Teacher and parents' perception of *Sirah* learning using multimedia platform has been analyzed in this study. This study found most of the respondents agreed on integrating geography and multimedia elements in *Sirah* as this can be an additional teaching aid for a student to understand and memorize the flow and important event of *Sirah*. Thus, in order to improvise the current teaching and learning, a prototype has been built which integrated between *Sirah* and geography using a multimedia approach through storytelling video in an application platform to merge all the video in one. The prototype consists of storytelling video, mind test, and two-way interaction as the student can access the image of specific places such as the journey from Mecca to Madinah.

i) Teacher and parents' perception

The interview conducted to get teacher perception shows current teaching and learning in *Sirah* subject still using the textbook as the primary material. Thus, improvement of teaching and learning using an integration of *Sirah* and geography elements as a new method can help in enhancing the learning quality of student at once help to minimize teacher theory explanation by the usage of teaching aids.
Figure 1 shows a summary of the percentage of geography knowledge in *Sirah*. Majority of respondents have an interest in geography while knowing that geography is essential in daily life and *Sirah* and agreed to integrate between *Sirah* and geography

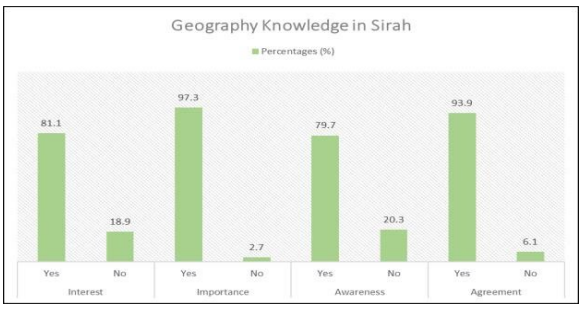

Figure 1: Geography knowledge in *Sirah* summary in percentages

Figure 2 shows the summary of percentage in *Sirah* and technology. Some of the respondents still encounter difficulties in learning *Sirah* and most of the respondent agreed on integrating *Sirah* and multimedia in the context of multimedia effectiveness. Additionally, respondent still has less interest in two-way learning; however, a study by Beth, Wallace, and Nixon (2013) stated that interaction, the student can enhance critical thinking and problem-solving skills through social interaction during learning.

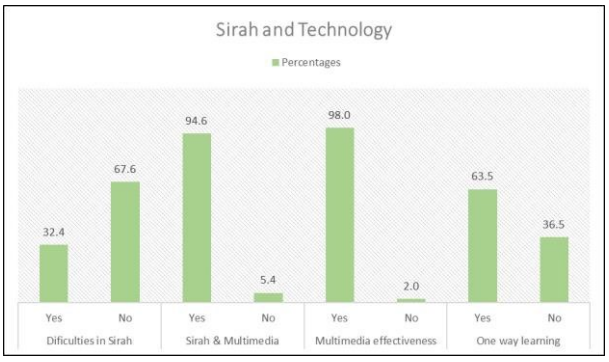

Figure 2: *Sirah* and technology responses in percentages

Figure 3 shows the summary of percentage in the medium used for teaching and learning *Sirah* subject in the classroom. In conclusion, textbook, reading material and storytelling practically still be used as the medium for teaching and learning.

Perpustakaan Negara Malaysia eISBN 987-967-17889-6-7

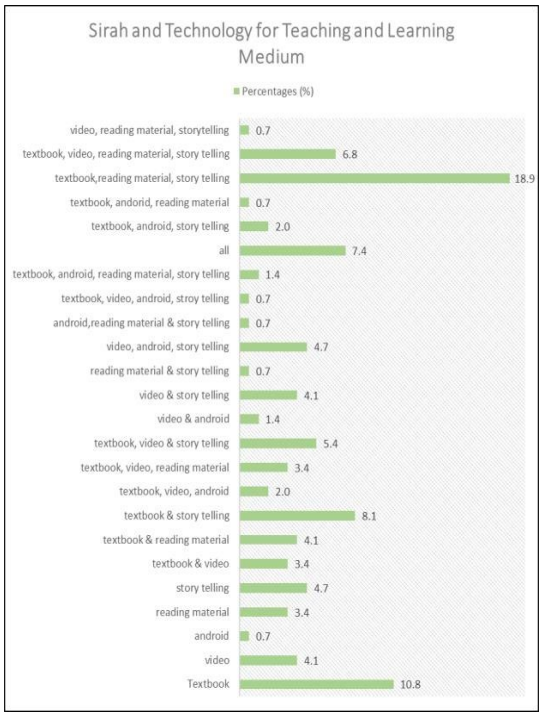

Figure 3: *Sirah* and technology for teaching and learning medium responses in percentage

In building the prototype, it consists of two product which are the storytelling videos and the *Israk* and integration of some geography elements through multimedia. Application platform prototype. Storytelling videos are the extraction for Islamic education of Year 5 primary school students syllabus. Figure 4 below shows the cut scene from Israk dan *Mikraj* video, where it consists of the journey of *Israk* and integration of some geography elements through multimedia

Figure 4: Cut scene from *Israk & Mikraj* storytelling video

Figure 6(a-e) shows the interface for the application starting from the main page throughout the apps. The colour integrated for the whole apps is between blue, mauve to pink with additional black colour. The colour

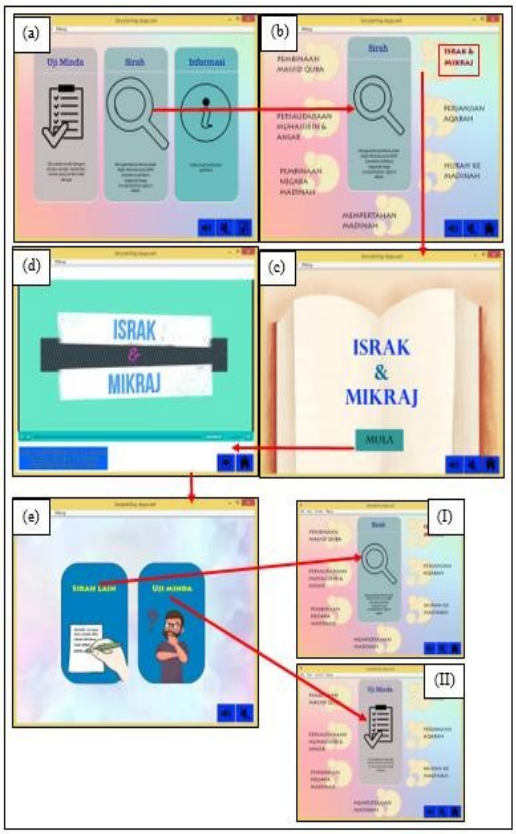

.Figure 1 (a-e): Application prototype

Planning structure

The methodology consists of four stages which are i) data acquisition, ii) data processing, iii) system design, and iv) system development. A questionnaire was distributed, and about 148 respondents have answered through Google Form media. The questionnaire consists of four sections; demographic, learning style, geography knowledge in *Sirah*, and technology which is designated to define the teacher and parents' perception towards *Sirah* learning with or without geography elements.

The second stage is data processing consist of software used for statistic calculation of questionnaire and spatial data for geography elements. Statistical Package for the Social Sciences (SPSS) was used to calculate the frequency and statistic information (e.g., mean and standard deviation) for the questionnaire distributed. Additionally, spatial data such as distance, area, coordinate, journey, and direction retrieved from various open-source platforms such as ArcGIS to create an interactive map of Saudi Arabia, Google Earth, and Google Map.

The system design is divided into two, which are for storytelling video and build application prototype. Storytelling video consists of *Sirah* subtopic for year five students and each storyboard for storytelling developed based on integrated *Sirah*, geography, storytelling, and multimedia elements.

Perpustakaan Negara Malaysia eISBN 987-967-17889-6-7

The system then developed using various software such as for animation, Animaker software was used. Wondershare Filmora 9 used for editing and merging the video content, and NCH Voxal Voice Changer used for changing the frequency of narration to change the gender of the voice. Also, the prototype platform was constructed using Adobe Flash Professional CS6.

Knowledge impact

Practically, teaching and learning nowadays in *Sirah* are still using textbooks, and there is little improvement has been made. *Sirah* integrated with geography using a multimedia approach is believe can help students to be active learners during learning. The prototype can increase the student critical thinking starting from low knowledge such as student able to distinguish and know where certain places of Sirah event happen (e.g., Mecca and Madinah) to more complex analysis and high level thinking such as determination of exact location and event happen on that particular location, distance from one place to another, the direction and also journey of movement in Sirah are. Thus, this approach can help both teacher and student as the teacher be able to show and teach *Sirah* in a much simpler method, and students can increase the visualization and memorization ability towards watching the video and answer the questions based on the video. In addition, through this platform, teaching and learning can achieve IR Vision 4.0.

Contribution to society and country

The *Sirah* integrated with geography using a multimedia approach contribute to help teachers and students in teaching and learning as it can improve Islamic education specifically in *Sirah*. The contribution varied from various aspects, such as teachers can have more comfortable teaching aid for teaching. In contrast, students have a new approach in learning that may compatible with individual learning style and resulting in a better understanding of *Sirah* education. Moreover, it can employ the need of the students in education through elements of geography and *Sirah* as this approach of geography connected to teacher and student daily life to develop higher critical thinking. Also, this approach also contributes to enhancing the way of teaching and learning using more fun and attractive method that could increase the interest of students in learning *Sirah.* Through this platform, students able to create a comfortable learning situation as the video can be accessed through any platform and anywhere. Finally, through multimedia elements, students able to feel more motivated in the learning process as it is more interesting in contrast to the reading textbook as previously.

Cost impact

This study involved indirect time and cost development. The prototype has been developed for about a month. However, no-cost implication on software is used because it is in the trial version.

Commercialization potential

The multimedia approach has brought about a significant paradigm change in education that can have a very positive effect on our educational system and the way of study for teachers and students. Trends clearly show that interactive teaching and learning can gain ground in higher learning and multimedia institutions in Malaysia as an essential forum for teaching and learning in the classroom. In this context, Sirah integrated with geography using a multimedia approach can be used as a strategic training medium for teaching and learning in our education system. By incorporating multimedia in education, we can create a workforce that suits the demands of IR 4.0.

REFERENCES

Beth, H., Wallace, R., & Nixon, S. (2013). The Impact of Social Interaction on Student Learning. A *Journal of Literacy and Language Arts Article*, 52(4), 375–397. https://doi.org/10.1080/15534510601154413

Fadzilah, A. H. (2017). *Pelaksanaan Pengajaran dan Pembelajaran Koperatif Berasaskan Abad ke-21: Satu Tinjauan di Sekolah Menengah Kebangsaan Pekan Nenas.*

Guan, N., Song, J., & Li, D. (2018). On the Advantages of Computer Multimedia-aided English Teaching. *Procedia Computer Science*, 131, 727–732. https://doi.org/10.1016/j.procs.2018.04.317

Kassim, H. (2013). The Relationship between Learning Styles, Creative Thinking Performance and Multimedia Learning Materials. *Procedia - Social and Behavioral Sciences*, 97, 229–237. https://doi.org/10.1016/j.sbspro.2013.10.227

Lambri, A., & Mahamod, Z. (2014). Pelaksanaan Aktiviti Pembelajaran Berasaskan Masalah dalam Proses Pengajaran dan Pembelajaran

Perpustakaan Negara Malaysia eISBN 987-967-17889-6-7

Bahasa Melayu. *Jurnal Bahasa Dan Sastera Melayu*, (May), 98–117.

Li, J., Antonenko, P. D., & Wang, J. (2019). Trends and issues in multimedia learning research in 1996– 2016: A bibliometric analysis. *Educational Research Review*, 28(June), 100282. https://doi.org/10.1016/j.edurev.2019.100282

Moghavvemi, S., Sulaiman, A., Jaafar, N. I., & Kasem, N. (2018). Social Media as a Complementary Learning Tool for Teaching and Learning: The Case of Youtube. *The International Journal of Management Education*, 16(November 2017), 37–42. https://doi.org/10.1016/j.ijme.2017.12.001

Mohd Sharif, M. S. A., Kamarudin, M. F., Kamarulzaman, M. H., Muhd Saali, M. M. S. N., & Esrati, M. Z. (2017). The Teaching and Learning of Sirah using the Game Method Among Gifted Students. *The 3rd International Conference On Education In Muslim Society (ICEMS)*, (October 2017), 1–5.

Park, C. W., Kim, D. gook, Cho, S., & Han, H. J. (2019). Adoption of multimedia technology for learning and gender difference. *Computers in Human Behavior*, 92(November 2018), 288–296. https://doi.org/10.1016/j.chb.2018.11.029

Tamrin, M., Azkiya, H., & Sari, S. G. (2017). Problems Faced by the Teacher in Maximizing the Use of Learning Media in Padang. *Al-Ta Lim Journal*, 24(1), 60–66. https://doi.org/10.15548/jt.v24i1.262

Tularam, G. A., & Machisella, P. (2018). Traditional vs Non-Traditional Teaching and Learning Strategies -- The Case of E-Learning. *International Journal for Mathematics Teaching and Learning*, 19(1), 129–158.

Perpustakaan Negara Malaysia eISBN 987-967-17889-6-7

Effect of Partially Fix in the least Squares Adjustment

Mohamad Amirul Bin Rozali[1], Norshahrizan bin Mohd Hashim[1]

[1]Faculty of Architecture, Planning & Surveying, Universiti Teknologi MARA, Perlis Branch, Arau Campus, 02600 Arau, Perlis, Malaysia

E-mail: amirulrozali735@gmail.com

Abstract

The Department of Survey and Mapping Malaysia (DSMM) having issues regarding adjustment primarily related to least square adjustment (LSA). The way of adjusting the data using LSA is still can be improved by DSMM. Hence, this research aims to study is to investigate the impact of partially fix in cadastral adjustment. To achieve this aim, the objectives of this study identify the impact weight to the observation precision and to investigate the impact of partially fix to the adjusted coordinate. Thus, the most suitable adjustment method is obtained according to the results of the application.

Keywords: partially fix, least-square adjustment.

Introduction

In the cadastral survey, three good boundary marks are being used as a control in starting an orientation job. After the observation had been done, the data will be adjusted using the Least Squares. In adjusting the data, three good boundary marks had been used as a control point to adjust the observation. The control point from a good boundary mark will be "held fix" in the adjustment. However, if the boundary marks out of position had been held fixed, it would interrupt the related observation. So, the control point that moved within the tolerance, it needs to "partially fix" in the adjustment. The suitable weight in partially fix is significant produces the best quality of the data. Nonetheless, the best weightage in adjusting data is still undefined. After the data finish adjusted, it will be applied in the NDCDB block adjustment. During the process, the control point of good boundary marks from the data observation not anymore being used but replace with the existing control from the block adjustment. The impact is there is a difference in position for the three good boundary marks after applying in block adjustment. Other than that, there is no standard operating procedure as a guideline to produce the best quality of the data.

Research Methodology

For the methodology, this research was done by applying an adjustment to the many set of data. The data are obtained from JUPEM and also Licensed Land Surveyor. Each of them consists of three sets of data. All these set of data had been tested the different weightage on it. This data will consist of bearing, distance, and also the control point of the observation. In the stage of data processing, both data from JUPEM and Licensed Land Surveyor will be used. From the existing data provided, the difference in weightage will be applied to the data to test its suitability. The weightage that applied in every set of data is 1cm, 2cm, and 3cm for the coordinate adjustment. Then, the position of the boundary marks will be observed whether it stay at its position or will be shifted after the adjustment. The parameter that will be measure is bearing, distance, and coordinate. The software that involved in this research is notepad software. This Notepad software is significant in this research to key in the observation data with the correct format by saved as ".DAT". Then, the data can be run in the MicroSurvey STAR*Net software to adjust the data.

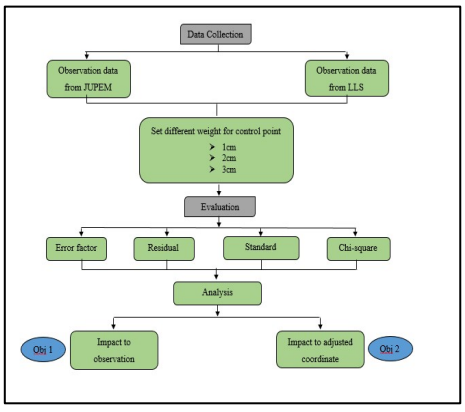

Figure 1: Flowchart Methodology

Perpustakaan Negara Malaysia eISBN 987-967-17889-6-7

Results and Analysis

Impact weight to the Observation Precision

In investigating the impact weight of the observation precision, six sets of data were involved in this research, which are PUBLPS90_2015, PUBLPS68_2018, PUBLPS127_2018, PUPS6_2018, PUPS7_2018, and PUBLPS377_2018. All these jobs were being adjusted using a different weight of each. The weight that used was 3cm, 2cm, and 1cm on the control coordinate while one coordinate was being held to fix its coordinate.

PUBLPS90_2015

3CM

Table 1: Statistical test of bearing and distance in 3cm weight of job PUBLPS90_2015

Mean	0.0000097776	0.0000846154
Minimum	-0.00207778	-0.00070000
Maximum	0.00111111	0.00150000
Range	0.00318889	0.00220000
Standard deviation	0.00080060031	0.00047471449

2CM

Table 2: Statistical test of bearing and distance in 2cm weight of job PUBLPS90_2015

Mean	0.0000724444	0.0001230769
Minimum	-0.00203333	-0.00060000
Maximum	0.00111111	0.00160000
Range	0.00314444	0.00220000
Standard deviation	0.00080060031	0.00051092676

1CM

Table 3: Statistical test of bearing and distance in 1cm weight of job PUBLPS90_2015

Mean	0.0000340000	0.0002153846
Minimum	-0.00193611	-0.00060000
Maximum	0.00113889	0.00190000
Range	0.00307500	0.00250000
Standard deviation	0.00080010689	0.00064850123

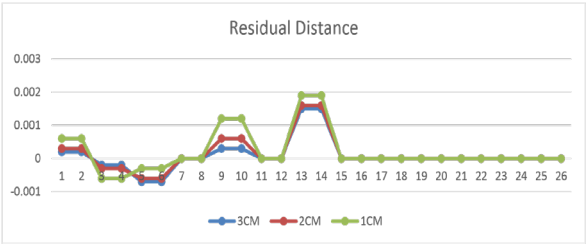

Figure 2: Residual Distance for PUBLPS90_2015

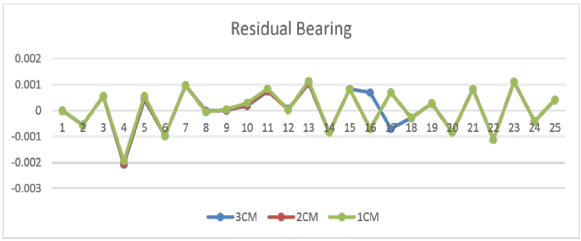

Figure 3: Residual Bearing for PUBLPS90_2015

PUBLPS68_2018

3CM

Table 4: Statistical test of bearing and distance in 2cm weight of job PUBLPS90_2015

Mean	0.0000104445	-0.0002230769
Minimum	-0.00149722	-0.00240000
Maximum	0.00138889	0.00200000
Range	0.00288611	0.00440000
Standard deviation	0.00092369452	0.00097828736

2CM

Table 5: Statistical test of bearing and distance in 2cm weight of job PUBLPS90_2015

Mean	0.0003497778	-0.0003923077
Minimum	-0.00138889	-0.00280000
Maximum	0.00160000	0.00180000
Range	0.00298889	0.00460000
Standard deviation	0.00086387516	0.00112104347

1CM

Table 6: Statistical test of bearing and distance in 1cm weight of job PUBLPS68_2018

Mean	-0.0001646666	-0.0009384615
Minimum	-0.00192778	-0.00410000
Maximum	0.00138889	0.00090000
Range	0.00331667	0.00331667
Standard deviation	0.00098670584	0.00183892945

Perpustakaan Negara Malaysia eISBN 987-967-17889-6-7

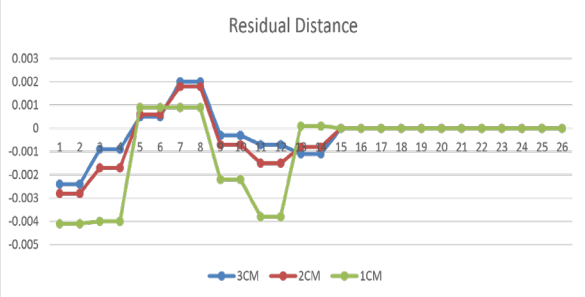

Figure 4: Residual Distance for PUBLPS68_2018

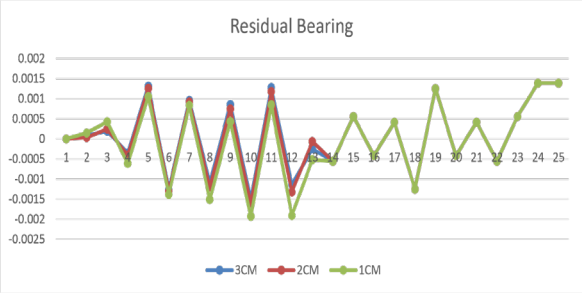

Figure 5: Residual Bearing for PUBLPS68_2018

PUBLPS127_2018

3CM

Table 7: Statistical test of bearing and distance in 3cm weight of job PUBLPS127_2018

Mean	-0.0000250751	-0.0001210526
Minimum	-0.00138889	-0.00120000
Maximum	0.00140278	0.00060000
Range	0.00279167	0.0018
Standard deviation	0.00085248049	0.00047485867

2CM

Table 8: Statistical test of bearing and distance in 2cm weight of job PUBLPS127_2018

Mean	-0.0000346847	-0.0002157895
Minimum	-0.00138889	-0.00130000
Maximum	0.00138889	0.00070000
Range	0.00277778	0.002
Standard deviation	0.00085410846	0.00057446865

1CM

Table 9: Statistical test of bearing and distance in 1cm weight of job PUBLPS127_2018

Mean	-0.0001646666	-0.0003894737
Minimum	-0.00192778	-0.00220000
Maximum	0.00138889	0.00150000
Range	0.00331667	0.0037
Standard deviation	0.00098670584	0.00091112923

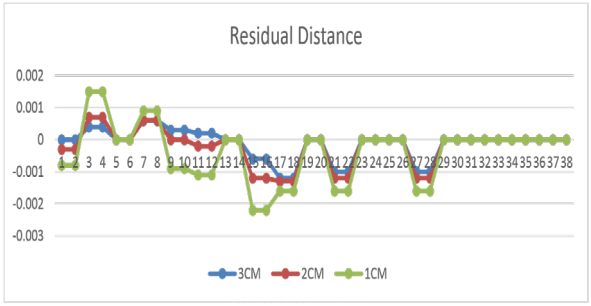

Figure 6: Residual Distance for PUBLPS127_2018

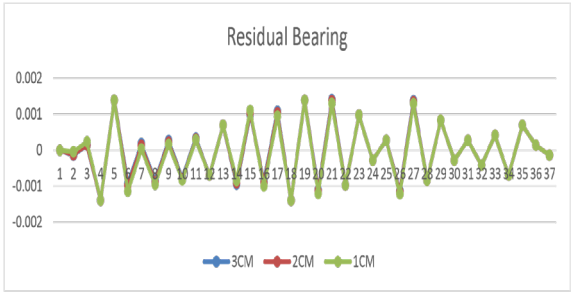

Figure 7: Residual Bearing for PUBLPS127_2018

PUPS6_2018

3CM

Table 10: Statistical test of bearing and distance in 3cm weight of job PUPS6_2018

3cm	Residual Bearing	Residual Distance
Mean	0.0000279462	0.0004352941
Minimum	-0.00172778	-0.00490000
Maximum	0.00179444	0.00570000
Range	0.00352222	0.01060000
Standard deviation	0.00069720424	0.00240023766

2CM

Table 11: Statistical test of bearing and distance in 2cm weight of job PUPS_2018

Mean	0.0000296296	0.0009235294
Minimum	-0.00180278	-0.00470000
Maximum	0.00217778	0.00710000
Range	0.00398056	0.01180000
Standard deviation	0.00077412827	0.00285732009

Perpustakaan Negara Malaysia eISBN 987-967-17889-6-7

1CM

Table 12: Statistical test of bearing and distance in 1cm weight of job PUPS6_2018

1cm	Residual Bearing	Residual Distance
Mean	-0.0000348484	0.0024058824
Minimum	-0.00220000	-0.00440000
Maximum	0.00404444	0.01350000
Range	0.00624444	0.01790000
Standard deviation	0.00122412490	0.00480762911

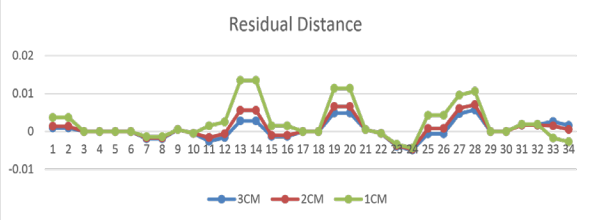

Figure 8: Residual Distance for PUPS6_2018

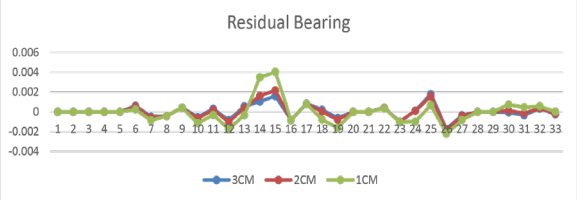

Figure 9: Residual Bearing for PUPS6_2018

PUPS7_2018

3CM

Table 13: Statistical test of bearing and distance in 3cm weight of job PUPS7_2018

Mean	-0.0003580556	0.0011700000
Minimum	-0.00217778	-0.00370000
Maximum	0.00198056	0.00930000
Range	0.00415833	0.01300000
Standard deviation	0.00116289013	0.00391274570

2CM

Table 14: Statistical test of bearing and distance in 2cm weight of job PUPS7_2018

Mean	-0.0008111111	0.0018900000
Minimum	-0.00298889	-0.00510000
Maximum	0.00132222	0.01380000
Range	0.00431111	0.01890000
Standard deviation	0.00149875357	0.00607643420

1CM

Table 15: Statistical test of bearing and distance in 1cm weight of job PUPS7_2018

Mean	-0.0008961113	0.0029300000
Minimum	-0.00380556	-0.01320000
Maximum	0.00299722	0.02080000
Range	0.00680278	0.03400000
Standard deviation	0.00217600873	0.01061211324

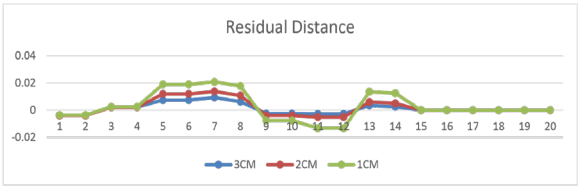

Figure 10: Residual Distance for PUPS7_2018

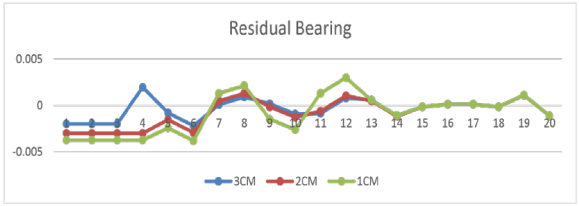

Figure 11: Residual Bearing for PUPS7_2018

PUPS377_2018

3CM

Table 16: Statistical test of bearing and distance in 3cm weight of job PUPS377_2018

Mean	0.0000721537	-0.0000146341
Minimum	-0.00158333	-0.00310000
Maximum	0.00148611	0.00260000
Range	0.00306944	0.00570000
Standard deviation	0.00055452841	0.00108116557

2CM

Table 17: Statistical test of bearing and distance in 2cm weight of job PUPS377_2018

Mean	0.0000827847	-0.0001146341
Minimum	-0.00158333	-0.00530000
Maximum	0.00192778	0.00260000
Range	0.00351111	0.00790000
Standard deviation	0.00067160521	0.00139859912

Perpustakaan Negara Malaysia eISBN 987-967-17889-6-7

1CM

Table 18: Statistical test of bearing and distance in 1cm weight of job PUPS377_2018

Mean	0.0003311385	-0.0005707317
Minimum	-0.00378056	-0.01470000
Maximum	0.00641389	0.00260000
Range	0.01019445	0.01730000
Standard deviation	0.00151096259	0.00291820543

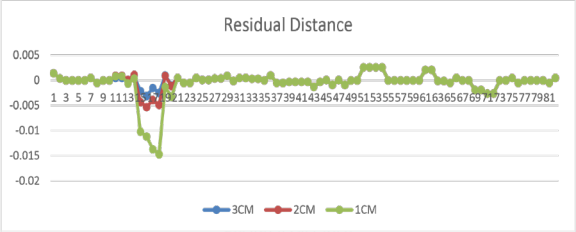

Figure 12: Residual Distance for PUPS377_2018

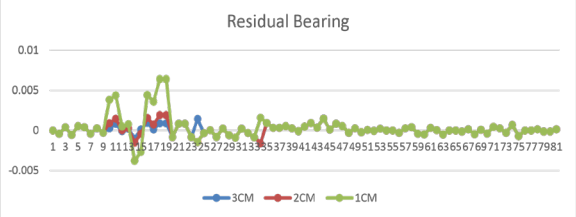

Figure 13: Residual Bearing for PUPS377_2018

In the least-squares adjustment, the standard deviation is being used as a benchmark in describing the precision observation—the lower value of the standard deviation, the higher precision of the data. The weightage needs to be set higher if observation passed with a high standard deviation. The most file passed the chi-square test when setting 1cm weight so that the weightage can be set lower. By set different weightage, we can know how precise the data could be. In the Department Survey and Mapping Malaysia, they prefer to use the constant value for the weight, which 3cm for the coordinate. Otherwise, the way of practising weightage can still be improved to get the best quality of the data.

Impact of Partially Fix to the Adjusted Coordinate

In investigating the impact of partially fix to the adjusted coordinate, all the files from JUPEM and Licensed Land Surveyor had been applied partially fix with the weight 3cm, 2cm and 1cm.

PUBLPS127_2018

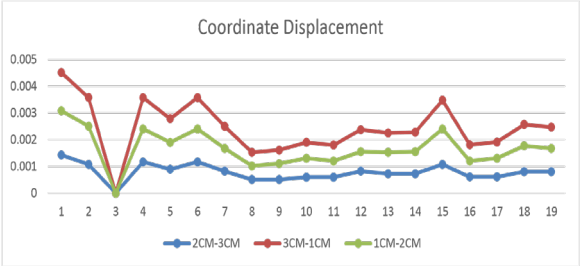

Figure 14: Coordinate Displacement for PUBLPS127_2018

PUBLPS68_2018

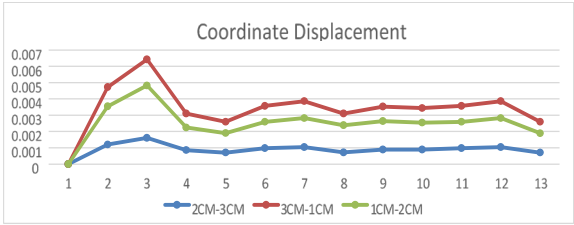

Figure 15: Coordinate Displacement of PUBLPS68_2018

PUBLPS90_2015

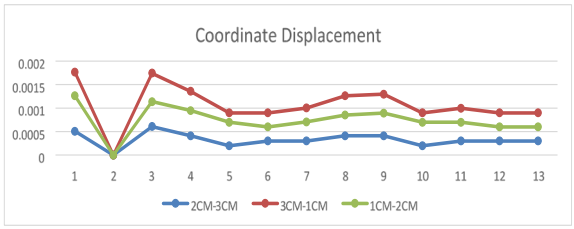

Figure 16: Coordinate Displacement for PUBLPS90_2015

PUPS6_2018

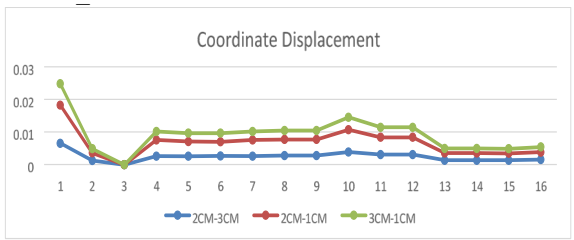

Figure 17: Coordinate Displacement for PUPS6_2018

PUPS7_2018

Perpustakaan Negara Malaysia eISBN 987-967-17889-6-7

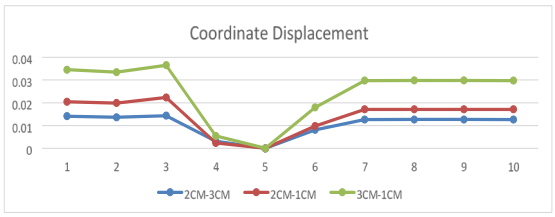

Figure 18: Coordinate Displacement for PUPS7_2018

PUPS377_2018

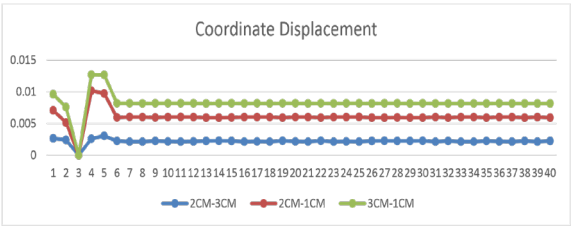

Figure 19: Coordinate Displacement for PUPS377_2018

For the analysis, when set a different weight to the observation, the coordinate of the observation will change its position. The weight that set in 1cm is more compatible compare to 3cm. For the case of the observation that passed the test with one or two cm observation, the data are had been losing its quality and are not the best quality of its data. The wrong weightage used in adjustment will occur the displacement on the coordinate. For the comparison of the differences between 1cm to 3cm weightage, the displacement can occur until 2cm and 3cm. These clearly show that the difference in weight set in the partially fixes impacted the adjusted coordinate.

Conclusion

As a result, all statistical tests performed in this analysis indicate that the residual adjustment provided by the bearings, distances, and coordinates of the adjusted data using different weightage. Referring to the overall chi-squares test, most of the data were passed with the 1cm weight. However, when evaluating the residual for the weight of 3 cm, 2 cm, and 1 cm, the result shows that the adjusted bearing value, distance, and coordinate have a different value. Differences in the value of these residuals affect the location of observation, especially for the coordinates. Even the weight that set is from 3cm to 1cm is small, but it gave the different coordinates for the observation point. When applying 3cm weight, not produce the same value with the 1cm, which up to 2cm displacement. It means that it had a significant impact on the observation. The result proved that there is an impact of the partially fix in cadastral adjustment on the precision observation and to the adjusted coordinate. If the data that passed the test with a first standard deviation, the data needs to be set with the higher weight to achieve the best quality of the data. The weight needs to choose wisely because the unsuitable of weight can impact the position of the boundary mark.

References

C. Ghilani (2016). What Is a Least Squares Adjustment Anyway Retrieved from https://www.xyht.com/surveying/least-squares-adjustment-anyway/

W. Kenton (2019). Least Squares Criterion. Retrieved from https://www.investopedia.com/terms/l/least-squares.asp

N. M. Hashim, A. H. Omar, K.M. Omar, N. M. Abdullah, M. H. M. Yatim (2016). Cadastral Positioning Accuracy Improvement: A Case Study In Malaysia. Retrieved from https://www.int-archphotogramm-remote-sens-spatial-inf- sci.net/XLII- 4W1/265/2016/isprs-archives-XLII-4W1-265-2016.pdf

R. A. Frank (1996). Starplus Software's Star*Net GPS. Retrieved from https://www.johnsonfrank.com/pdf/StarNet%20ProSuveyor%2010-96.pdf

B. Way, Oakland (2002). STAR*NET-PRO V6 Least Squares Survey Adjustment Program. Retrieved from http://people.dicea.unifi.it/fausto.sacerdote/materiale_studenti/starnet_did/StarNet -V6PRO-Manual.pdf

Halim, Nur Zurairah Abdul, Sulaiman, S. A. H., Talib, K. H., Yusof, O. M., Wazir, M. A. M., & Adimin, H. M. K. (2017). Legal significance of National Digital Cadastral Database (NDCDB) in Malaysia cadastral system. 2017 IEEE 8th Control

Perpustakaan Negara Malaysia eISBN 987-967-17889-6-7

Development of Android Application for Peninsular Malaysia Geoid Height Calculator

Mohamad Nazir Md Nazri[1], Muhammad Faiz Pa'suya[1]

[1]Faculty of Architecture, Planning & Surveying, Universiti Teknologi MARA, Perlis Branch, Arau Campus, 02600 Arau, Perlis, Malaysia

Email: 2017800198@isiswa.uitm.edu.my

Abstract

There are several mobile applications available for providing geoid height. Unfortunately, this software has many weaknesses, lack some features, and most importantly, it does not provide a geoid model specialized for Malaysia. This study aims to produce an android application for Peninsular Malaysia geoid height calculator. The research begins with the collection of data which is geoid model WMGEOID04, PMGG2020 and PMSGM2014. There is four interpolation method implement in this study which is Bilinear Interpolation, Bicubic Interpolation, Inverse Distance Weighted Interpolation (IDW) and Simple Kriging. The development of an android application is done and provided with the calculation, which is an absolute method, relative method and finding suitable geoid model method. There is also an analysis that been done which is the verification of the algorithm in the developed application and the comparison between a different interpolation method. This analysis is done to verify the algorithm of interpolation method and to find the best interpolation method for implement in the developed android application. Verification of algorithm of interpolation method had verified that only two interpolation methods are useable for producing results which are Bilinear Interpolation and IDW. In the comparison between different interpolation methods, the IDW show the best result and suitability to be implemented in the android application. Based on the result and analysis, the developed android application had been rebuilt and implement the IDW method to generate results. As a result, it can be concluded that this geoid height interpolation android application was successfully developed.

Keywords: geoid height, interpolation, Malaysia, android application.

Introduction

Nowadays, there is much mobile application for providing geoid height to survey application such as Trimble, EOS Positioning Systems, Mapit GIS, EGM96 High Precision Geoid Undulation, EGM2008 High Precision Geoid Undulation and many more (Osedok, 2017; Moazezi & Zomorrodian, 2012). Furthermore, smartphone and tablet also act as an efficient miniature computer that equipped with a various application such as GPS module, electronic compass, digital camera, gyroscope and many more to support user (Bednarczyk & Janowski, 2014).

The geoid height, N is described as the ellipsoidal height from an ellipsoidal datum to a geoid surface which is an equipotential surface of the Earth's gravity nearest to the Mean Sea Level (Jalal et al., 2019). This geoid height can be obtained from geoid model by using interpolation method to extract the data for providing data on any position of earth's surface (Arana et al., 2018; Radanović & Bašić, 2018; Barthelmes, 2009). In this day, many interpolation techniques been developed to provide accurate data (Abd-Elmotaal & Kühtreiber, 2019).

Thus, this study aim is to develop an android application for Peninsular Malaysia geoid height calculator. The android application had been chosen because it is the most device that been used, thus can make many people get benefit from it. This android application can help the user by providing the geoid height in a way that they can decide the calculation method to be used.

Problem statement

Nowadays, there is much mobile application for providing geoid height to survey application such as Trimble, EOS Positioning Systems, Mapit GIS, EGM96 High Precision Geoid Undulation, EGM2008 High Precision Geoid Undulation and many more (Osedok, 2017; Moazezi & Zomorrodian, 2012). Unfortunately, this software has many weaknesses,

Perpustakaan Negara Malaysia eISBN 987-967-17889-6-7

lack some features and most importantly, it does not provide a geoid model specialized for Malaysia (Osedok, 2017; Moazezi & Zomorrodian, 2012). However, in the development of this mobile application, the important aspect is to make sure that the coding been developed is written correctly the algorithm and formula of mathematic and verify by comparing the result from this mobile application with the result from existing software been used in survey application (Oliveira Júnior et al., 2019; Osedok, 2017; Moazezi & Zomorrodian, 2012). It also to mention that there is yet any discussion of the suitable interpolation method to be used in the Malaysia country (AbdElmotaal & Kühtreiber, 2019; Arana et al., 2018; Radanović & Bašić, 2018; De & Murillo, 2014; Richard H. Rapp & Sansb, 1991).

The solution to the problem

The solution for this problem is to develop an android application for Peninsular Malaysia geoid height calculator. This android application can help the user by providing the geoid height in a way that they can decide the calculation method to be used. The study aim is to produce an android application for Peninsular Malaysia geoid height calculator. There are two objectives in this study which is to identify the optimum interpolation methods for geoid height calculation and to produce an android application for Peninsular Malaysia geoid height calculator using Android Studio.

Planning structure

The methodology of this study consists of five phases, as shown in Figure 2. The five phases are project planning, data acquisition, development, analysis and result. The first phase of this study is project planning. This phase involved the selection of study area, selection of software used and preliminary study of the research. After the project planning phase is data acquisition, the data that needs to be collected is the geoid model of Peninsular Malaysia. There are four types of geoid model been collected. The next phase is the development of an android application which is the android application for Peninsular Malaysia geoid height calculator. It is developed by using Android Studio software and provided with three types of geoid models. Then, the analysis phase is an analysis of the data from the developed android application. The analysis is done to verify the developed android application and to find the best interpolation method to be implemented in the developed android application.

The final phase is the result phase which is the result of development android application. This result is the rebuilt of android application with a decided interpolation method to be used.

Project Planning was the first phase involved in this research study. This process includes planning for the study area, software, data acquisition and data processing. Preliminary studies were the first phase involved in this research study. This process includes reviewing as much as possible any scholarly article, reference journal, report, and any other sources to get more understanding. In this phase, a review was done specifically on any research about the method to provide geoid height from the geoid model. The study area for this study is the whole of Peninsular Malaysia or known as West Malaysia. Suitable software is very important to apply the calculation to generate geoid height. There is software used in this study which is Android Studio software.

The data for this research are MyGEOID which is WMGEOID04, PMGG2020 and PMSGM2014. MyGEOID is a fitted geoid that is created for application in Malaysia. In this study, the WMGEOID04 was chosen. This geoid model was computed by fitting the gravimetric geoid and GPSlevelling, which fits the local Mean Sea Level. In Malaysia, the geoid is calculated based on the available gravimetry, which is soil, airborne and satellite altimetry, which is continued down to the topography surface after a spherical harmonic expansion of the reference field (Ismail et al., 2018).

After data acquisition, data processing is an important part of this study. The data processing is divide into three phases which is begin with the development phase, analysis phase and result phase.

The first phase is the development phase which is consists of five main tasks to build an application for interpolating geoid height by using the Android Studio IDE. The first task is the API and activity configuration. In this study, the minimum level for Android version that used is API19 that stand for KitKat platform operating system. The second task is the interface design. The developed application was designed to consist of six main activities or navigation pages which are Home Page, Selection Page, Module 1 for suitable hybrid geoid, Module 2 for absolute method and Module 3 for relative method. The third task is the algorithm programming used in this research is four interpolation method which is Bilinear Interpolation, Bicubic Interpolation, Inverse Distance Weighted and Simple Kriging formula. Refer to (Iyengar & Jain, 2009), the interpolation for the Lagrange method is defined as: The fourth task is the application testing. It is necessary to carry out to ensure the geoid height interpolation calculation application is free from errors or bugs that exist in the written codes. The last task is the building of the Android Package Kit (APK) file. Once the error and bugs in the program

Perpustakaan Negara Malaysia eISBN 987-967-17889-6-7

have been fixed during testing activity, then generate the final output must be done so that the application can be published.

The second phase is the analysis phase. It consists of two parts which are the verification of the algorithm used and analysis of the result of different interpolation method. The first part is the verification of an algorithm which has two sections which are the verification of calculation formula and verification of algorithm in the developed android application. This verification of the calculation formula is done by comparing the result from the manual calculation with the result from the developed android application. The verification of calculation formula in the developed android application by verifying the result from the manual calculation is done by only comparing the result from one observation point which is at 5.97659° latitude and 100.39858° longitude. The verification of algorithm in the developed android application is by verifying the algorithm used in the developed android application by compare result with the Geocom. The verification of the algorithm in the developed android application is done by comparing the result from 10 observation points. The interpolation method used in the developed android application verifies if the result from the interpolation method is not more than 0.010 meters difference. The second part is the analysis result from a developed application by using different interpolation method which is Bilinear Interpolation method, Bicubic Interpolation method, Simple Kriging method and IDW is to find the suitable interpolation method to be used in the developed android application. There is one analysis done which is by comparing the result from the developed android application with the result from Geocom. The best interpolation method is chosen from the result produced by the interpolation method that nearly similar to the result of Geocom. There are 173 observation points used in this analysis.

In the result phase, it is about providing the result, which is an android application of geoid interpolation for Peninsular Malaysia. Based on the analysis in the third phase, the android application will be rebuilt and improved.

Knowledge impact

This chapter divide into two sections which is the analysis of the interpolation formula suitability for generating geoid height in android application and the final product of the development of an android application. The verification of the algorithm is to verify the algorithm used to be approval usage to generate geoid height. The analysis result of the different interpolation method is to find the accurate interpolation method to be used to generate geoid height.

There will be two types of analysis which are the verification of algorithm and the analysis of different interpolation method. The verification of the algorithm for interpolation calculation has two sections which are the verification of calculation formula and verification of algorithm in the developed android application. The verification of the calculation formula is done by comparing the result from the manual calculation with the result from the developed android application on one observation points. Table 1 shows the comparison result from the manual calculation and developed android application.

Table 1: Comparison Result from Manual Calculation and Android Application

Method	Bicubic	Bilinear	IDW	Kriging
Difference (m)	0.017	0.009	0.001	0.005

Based on table 1, all of the interpolation methods have result less than 0.010 meters difference for a result from the manual calculation and developed android application except for Bicubic Interpolation. Based on the result, there is two interpolation method that produces the minimum difference, which is IDW which have 0.001 meters difference. There is one interpolation method produce the highest difference, which is Bicubic Interpolation which has 0.017 meters difference.

The verification of algorithm in the developed android application is by verifying the algorithm used in the developed android application by compare result with the Geocom. The verification of the algorithm used in the developed android application by compare result with Geocom is done for 10 observation points. Figure 4.1 and Table 4.2 show the residual of result for verification algorithm used in the developed android application by compare result with the Geocom.

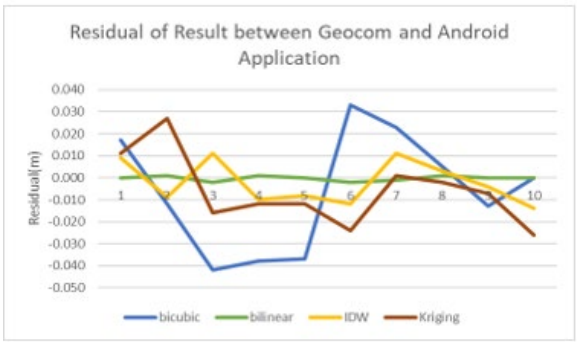

Figure 1: Residual of Result between Geocom and Developed Android Application

Perpustakaan Negara Malaysia eISBN 987-967-17889-6-7

Table 2: Descriptive Statistical of Geocom with Developed Android Application

indicator	Bicubic	Bilinear	IDW	Kriging
Ɛ min(m)	-0.042	-0.002	-0.014	-0.026
Ɛ max(m)	0.033	0.001	0.011	0.027
Ɛ span(m)	0.075	0.003	0.025	0.053
Ɛ median(m)	-0.006	0.000	-0.006	-0.0100
Ɛ mean (m)	-0.006	-0.001	-0.002	-0.006
RMSE(m)	0.022	0.0008	0.0091	0.0138

Based on figure 1 and table 2, the minimum residual was produced by Bicubic Interpolation, which is -0.1 meters while the maximum residual was also produced by Bicubic Interpolation, which is 0.078 meters. The longest span of residual was produced by Bicubic Interpolation, which is 0.178 meters while the shortest span of residual was produced by Bilinear Interpolation, which is 0.003 meters. Based on the result, the highest RMSE was produced by Bicubic Interpolation, which is 0.028 meters, while the smallest RMSE was produced by Bilinear Interpolation, which is 0.0008 meters.

The analysis of different interpolation method done to find the suitable interpolation method to be used for developed android application. This analysis is done by comparing the result from the developed android application with the Geocom's result on 173 observation points. Figure 2 and Table 3 show the residual of result for this analysis.

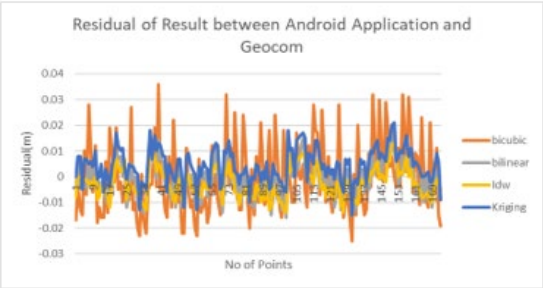

Figure 2: Residual of Result between Developed Android Application and Geocom

Table 3: Descriptive Statistical of Developed Android Application with Geocom

Indicator	Bicubic	Bilinear	IDW	Kriging
Ɛ min(m)	-0.0250	-0.0160	-0.0140	-0.0150
Ɛ max(m)	0.0360	0.0180	0.0130	0.0210
Ɛ span(m)	0.0610	0.0340	0.0270	0.0360
Ɛ median(m)	-0.0040	-0.0020	-0.0030	0.0050
Ɛ mean(m)	-0.0002	-0.0016	-0.0024	0.0044
RMSE(m)	0.0118	0.0060	0.0052	0.0065

Based on figure 2 and table 3, the minimum residual was produced by Bicubic Interpolation, which is -0.025 meters, and the maximum residual was also produced by Bicubic Interpolation, which is 0.036 meters. The longest residual span was produced by Bicubic Interpolation, which is 0.061 meters and the shortest residual span was produced by IDW, which is 0.027 meters. Based on the result, the highest RMSE was produced by Bicubic Interpolation, which is 0.0118 meters, while the smallest RMSE was produced by IDW, which is 0.0052 meters.

Overall, a result from the analysis of interpolation formula for geoid height can be used for this study. Based on the result of analysis of different interpolation method, the IDW method shows the best result for generating geoid height because it produces the smallest RMSE, which is 0.0052 meters. Thus, the developed android application is rebuilt and implement the IDW method in providing geoid height.

This android application has five main activities or navigation pages, which are Home Page, Selection Page, Module 1 for suitable hybrid geoid, Module 2 for absolute method and Module 3 for relative method. This android application provides three functions which are represented in three modules which is module 1, module 2 and module 3.

The Home Page is the first page that appears when open this android application. This page provides information about this android application. The title, developer and organization's contribution are described in this page. Figure 5 shows the Home Page of this android application. This page also shows the figure of Peninsular Malaysia in the grid

Perpustakaan Negara Malaysia eISBN 987-967-17889-6-7

model. Figure 3 shows the Home Page of this android application.

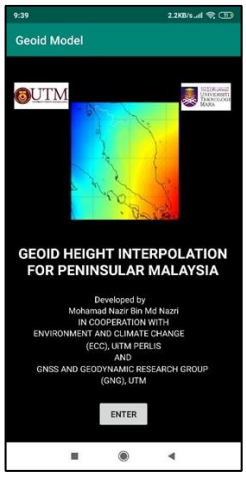

Figure 3: Home Page

The Selection Page is the next page that appears after the enter button was touched. This page was designed for the user to pick any module that provided which is Module 1, Module 2 and Module 3. This page shows the three-button that have been assigned, which are each of them served a specific purpose for the user. The first button is the suitable hybrid geoid button which assigned for guide the user to Module 1, which is suitable hybrid geoid. The second button is the absolute method button which assigned for guide the user to Module 2, which is an absolute method. The last button is the relative method button which assigned for guide the user to Module 3, which is a relative method. It is advised for the new usage of this android application to pick the first button for finding the suitable geoid model to be used in the survey application. It also advised picking the first button for the survey application in the new and unfamiliar district or region. Figure 4 shows the Selection Page.

Figure 4: Selection Page

Module 1, which is the suitable hybrid geoid, was designed for providing the user with the usage of finding the suitable hybrid geoid model to be used in the survey application. This module provides the user with the ability to check the accuracy of the geoid in a certain place to give better accuracy of the result. This method can be done when the GPS observation is done on the benchmark, subbenchmark or any mark that have known orthometric height that transfer from mean sea level. This module was provided with two-button, which is a select button for the selection of state to be used and the calculate button for starting the calculation and produce a result. There is four input in this module which is latitude, longitude, ellipsoidal height and benchmark(H_MSL) which is the height of mean sea level. All of these inputs need to be filled in by the user to calculate the result. The result produced after the calculate button was clicked is the difference of orthometric height from this calculation with the H_MSL inserted by the user. This result will help the user for deciding the suitable geoid to be used. In this module, the calculation formula is the calculation of the difference of orthometric height(H) from the android application with the mean sea level's height(H_MSL) given by the user. Figure 5 shows the Module1.

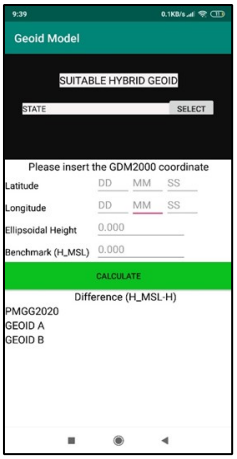

Figure 5: Module 1

Module 2, which is the absolute method, designed for providing the user with the absolute method of generating height. This method of calculation is the same as the absolute method used in the levelling. This module was provided with three-button, which is two select buttons for selecting the state and geoid model to be used and one calculates button for starting the calculation and produces a result. There is three input in this module which is latitude, longitude and ellipsoidal height. All of these inputs also need to be filled in by the user to calculate the result. The result produced after the calculate button was clicked is the geoid height and orthometric height which is produced by using the

Perpustakaan Negara Malaysia eISBN 987-967-17889-6-7

absolute method. In this module, the calculation formula is the calculation of orthometric height(H) by using the absolute method. Figure 6 shows the Module 2.

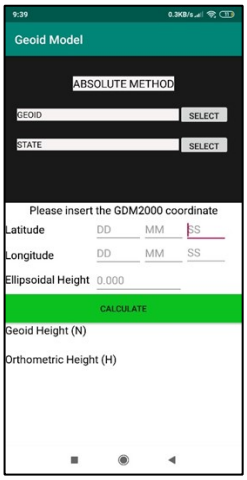

Figure 6: Module 2

Module 3, which is the relative method, was designed for providing the user with the relative method to generate geoid height. This method of calculation is the same as the relative method used in the levelling. This module was provided with three buttons which are two select buttons for selecting the state and geoid model to be used, and one calculates button for starting the calculation and produces the result. There is seven input in this module. These inputs are divided into two sections which are input for known station and input for the unknown station. The input for the known station has 4 input which is latitude, longitude, ellipsoidal height and H_MSL. This known station is for the station's information that had known its height of mean sea level. The input for the unknown station has 3 input which is latitude, longitude and ellipsoidal height. All of these inputs also need to be filled in by the user to calculate the result. The result produced after the calculate button was clicked is the orthometric height which is produced by using a relative method. In this module, the calculation formula is the calculation of orthometric height(H) by using the relative method. Figure 7 shows the Module 3.

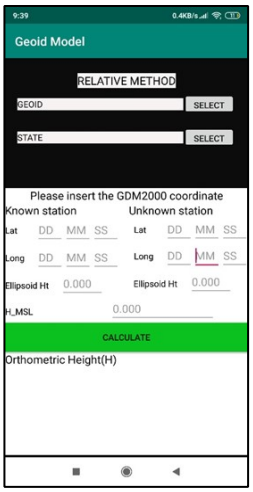

Figure 7: Module 3

Nutshell, all objectives of this study is successfully achieved. All of the results obtained is answering the objectives of the study. In the first objective is to identify the optimum interpolation methods for geoid height calculation. Based on the verification of the algorithm of the interpolation method and the analysis of different interpolation method, it can be defined that the IDW method is the most suitable method to be implemented in this application because it was approved to be useable by the verification of the algorithm and it produces the smallest RMSE within the four interpolation method. It should be noted that methods were tested using default interpolation parameters, so the possibility of obtaining different results by tweaking them exist. Lastly, the developed android application was rebuilt to implement the IDW method based on the result of previous analysis. It can be concluded that this android application is well functioning and successfully designed to provide geoid height for the people in Peninsular Malaysia with three functions that are currently not existed in any mobile application.

Contribution to society and country

This study can provide people with the geoid height interpolation android application. This application could provide a user with an accurate and fast calculation for interpolate geoid height and geoid model specialized for the area of Peninsular Malaysia. This application is provided with three geoid models as a choice for the user to pick the method that they want. This study can provide with the almost suitable interpolation method for the Peninsular Malaysia region.

Perpustakaan Negara Malaysia eISBN 987-967-17889-6-7

Cost impact

This project does not expand any cost in the development of the android application for Peninsular Malaysia geoid height calculator.

Commercialization potential

This study produces an android application that can be used for finding the geoid height based on the coordinate, and it is very useful in the land survey section. It is affordable to be bought and accessible by only using a mobile phone. This product target the user from the land surveyors, engineers and any persons that are working in the section of building and survey.

REFERENCES

Abd-Elmotaal, H. A., & Kühtreiber, N. (2019). Suitable gravity interpolation technique for large data gaps in Africa. *Studia Geophysica et Geodaetica*, 63(3), 418–435. https://doi.org/10.1007/s11200-017-0545-5

Arana, D., Prol, F. dos S., Camargo, P. de O., & Guimarães, G. do N. (2018). Errors measurement of interpolation methods for geoid models: A study case in the Brazilian region. *Boletim de Ciencias Geodesicas*, 24(1), 44–57. https://doi.org/10.1590/S1982-21702018000100004

Barthelmes, F. (2009). *Definition of Functionals of the Geopotential and Their Calculation from Spherical Harmonic Models*. https://doi.org/http://doi.org/10.2312/GFZ.b103-09026

Bednarczyk, M., & Janowski, A. (2014). Mobile application technology in levelling. Acta *Geodynamica et Geomaterialia*, 11(2), 153–157. https://doi.org/10.13168/AGG.2014.0004

De, A., & Murillo, M. (2014). Geoid Determination. In *Springer*. https://doi.org/10.1007/978-3-642-32408-6

Ismail, M. K., Din, A. H. M., Uti, M. N., & Omar, A. H. (2018). ESTABLISHMENT OF NEW FITTED GEOID MODEL IN UNIVERSITI TEKNOLOGI MALAYSIA. In The *International Archives of the Photogrammetry, Remote Sensing and Spatial Information Sciences*. https://doi.org/10.5194/isprs-archives-XLII-4-W9-27-2018

Iyengar, S. R. K., & Jain, R. K. (2009). NUMERICAL METHODS. Retrieved from http://www.ghbook.ir/index.php?name=فرهنگ و رسانه های نوین&option=com_dbook&task=readonline&book_id=13650&page=73&chkhashk=ED9C9491B4&Itemid=218&lang=fa&tmpl=component

Jalal, S. J., Musa, T. A., Md Din, A. H., Wan Aris, W. A., Shen, W., & Pa'suya, M. F. (2019). Influencing factors on the accuracy of local geoid model. *Geodesy and Geodynamics*, 10. https://doi.org/10.1016/j.geog.2019.07.003

Moazezi, S., & Zomorrodian, H. (2012). GGMCalc a software for calculation of the geoid undulation and the height anomaly using the iteration method, and classical gravity anomaly. *Earth Science Informatics*, 5(2), 123–136. https://doi.org/10.1007/s12145-012-0102-2

Oliveira Júnior, A. J. de, Souza, S. R. L. de, Dal Pai, E., Rodrigues, B. T., & Souza, V. C. de. (2019). Aurora: Mobile application for analysis of spatial variability of thermal comfort indexes of animals and people, using IDW interpolation. *Computers and Electronics in Agriculture*, 157(December 2018), 98–101. https://doi.org/10.1016/j.compag.2018.12.029

Osedok. (2017). mapitGIS - Spatial Asset Collection, GPS Surveys and Data Management for Android. Retrieved from Mapit GIS LTD website: ttps://mapitgis.com/category/articles/

Radanović, M., & Bašić, T. (2018). ACCURACY ASSESSMENT AND COMPARISON OF INTERPOLATION METHOD ON GEOID MODEL. In *GEODETSKI VESTNIK* (Vol. 62).

Rapp, R. H., & Sansb, F. (1991). Determination of the Geoid Present and Future. In *Springer-Verlag* (Vol. 106). https://doi.org/10.1007/1345_2015_205

Perpustakaan Negara Malaysia eISBN 987-967-17889-6-7

Reliability of Angular Adjustment Approach to Reduce Error In Cadastral Databased

M A H Kamaruzzaman[a,1], M A Abbas [a], and N M Hashim[a]

[a]*Faculty of Architecture, Planning & Surveying, Universiti Teknologi MARA, Perlis Branch, Arau Campus, 02600 Arau, Perlis, Malaysia*

[1]*E-mail: aliffsk70@gmail.com*

Abstract

A cadastral survey in Malaysia has implemented the bearing as main data for cadastral adjustment; the bearing has been produced by the mathematical calculation based on the angle in the survey equipment. However, the mathematical calculation for producing the bearing having an issue on systematic error due to indirect measurement. This will approach to error propagation in the data acquisition and will issue low positional accuracy in cadastral databased. To reduce systematic error in the calculation, angle measurement is an option for direct measurement in data acquisition implement to cadastral survey and cadastral adjustment. Therefore, the purpose of this research is to study of angular adjustment approach to improve the accuracy of cadastral databased. The method that been use for this study is converting bearing to angular. The angular adjustment results will be analysed based on statistical analysis such as residuals (i.e. observations and adjusted parameters) and standard deviations. This study focuses on positional improvement accuracy (PAI) in cadastral databased by using the angular constraints in the least square adjustment. As the result of conversion bearing to angle able to reduce the propagation of errors in cadastral in adjustment, which eventually increase the accuracy of positional in the cadastral databased

Keywords: cadastral databased, angular constrain, bearing constrains, positional accuracy, uncertainties

Introduction

A cadastral survey can be described as a survey work that has been carried out for land title registration. It shows the boundary limit of the land lot with the accepted accuracy according to the survey rules and regulation which related to registration of land. There are several methods that have been used for the data acquisition such as traverse, radiation, intersection, resection and global navigation satellite system. The main data that been collected in the cadastral survey is bearing and distance. The bearing has been issued by a mathematical calculation based on the angle measure (Charles D & Paul R, 2012). All the data will be processed in cadastral adjustment for verification; the adjustment is an angular adjustment, linear adjustment, Bowditch adjustment or transit adjustment. The Bowditch adjustment or transit adjustment not been used nowadays after the establishment of cadastral databased. The importance of information technologies has the influence to every discipline, geomatic one of the disciplines that involve in technologies development. In geomatic information technologies as known as geographical information system is an efficient application that manages the data accordingly. The updating process will be more efficient, terms of minimizing the time update, minimize error in updating legacy dataset and minimize the mismatch in databased.

Principally, the issues to achieve efficient and accurate dataset are the error in field data observation. As a result, the database can be classified as low positional accuracy, this cause of error in measurement. (Sisman, 2014). The error in field data observation occurred of indirect measurement by using the bearing method. The bearing has been produced by a mathematical calculation based on the angular. The bearing will consist of systematic error and occurred the error propagation in the raw data observation (Ogundare, 2018). Thus, the accuracy of the data will decrease due to the error that occurred.

The potential issues can solve by the several methods, such as geometrical alignment adjustment, least-square adjustment based on area and resurvey every lot. For the geometrical alignment, adjustment is based on the geometrical structure that identifies as homogenous to each structure (Dalyot, Dahinden,

Perpustakaan Negara Malaysia eISBN 987-967-17889-6-7

Schulze, Boljen, & Sester, 2012). However, this method is suitable for inconsistency spatial and for local topological spatial. The least-square adjustment based on area method approach to the shape of an area such as rectangular, polygon and parcel of a polygon with arcs (Tong, Shi, & Liu, 2005). Thus, this method only focusing on the area of the parcel. Resurvey is a conventional method that will give high accuracy data, but this method is tedious due to complete all the task.

Considering the limitation of bearing measurement that expose to various error sources, thus, it is beneficial to investigate the reliability of angular based measurement to increase data quality in cadastral data acquisition. The focus of this paper is to propose of angular implementation in the cadastral adjustment using least square adjustment.

Problem statement

Nowadays, the importance of information technologies has an influence on every discipline, geomatic one of the disciplines that involve in technologies development. In geomatic information technologies as known as geographical information system is an efficient application that manages the data accordingly. The updating process will become more efficient, terms of minimizing the time update, minimize error in updating legacy dataset and minimize the mismatch in databased. Besides that, it can enhance the accuracy of large scale map and delineating all cadastral parcel consists of cadastral overlay in one database (Shatnawi, Maan, & Khaldoun, 2017).

The issues to achieve efficient and accurate dataset are the error in field data observation. As a result, the database can be classified as low positional accuracy, this cause of error in measurement. (Sisman, 2014). The error in field data observation occurred of indirect measurement by using the bearing method. The bearing has been produced by a mathematical calculation based on the angular. The bearing will consist of systematic error and occurred the error propagation in the raw data observation (Ogundare, 2018). Thus, the accuracy of the data will decrease due to the error that occurred.

This issue needs to be solved because of involving the whole database that been used nowadays. There are several methods that can be applied, such as geometrical alignment adjustment, least-square adjustment based on area and resurvey every lot. For the geometrical alignment, adjustment is based on the geometrical structure that identifies as homogenous to each structure (Dalyot et al., 2012). However, this method is suitable for inconsistency spatial and for local topological spatial. The least-square adjustment based on area method approach to the shape of an area such as rectangular, polygon and parcel of a polygon with arcs (Tong et al., 2005). Thus, this method only focusing on the area of the parcel. Resurvey is a conventional method that will give high accuracy data, but this method is tedious due to complete all the task

Considering the limitation of bearing measurement that expose to various error sources, thus, it is beneficial to investigate the reliability of angular based measurement to increase data quality in cadastral data acquisition.

Least Square Adjustment (LSA)

The least-squares are appropriate for adjusting any of the basic types of survey measurements and are relevant to all currently used survey procedures. The method enforces the condition of reducing the sum of observation weights times their corresponding square residuals. This basic condition, which for the normal error distribution curve is developed from the equation, provides the most likely values for the adjusted quantities. Therefore, it also helps the estimation of the accuracy of the adjusted results, shows the existence of errors so that steps can be taken to eradicate them, and allows for the optimal layout of the office survey procedures before proceeding to the field to make observations.

The basic assumptions behind the principle of the least-squares are the mistakes and systematic errors have been removed so that only random errors remain. The amount of observations being modified is large and the probability distribution of errors is standard. Although these premises are not always satisfied, the approach of adjustment of the least-squares always offers the most comprehensive error treatment available and hence in modern surveying. It has become very popular and important.

In this study, the parameter adjustment of the functional model is applied. Horizontal angle, azimuth and distance have been used in the adjustment process as three mathematical models of observation. The mathematical model of horizontal angle, bearing and distance observation are like equation (1), (2), and (3) respectively (Hashim, Omar, Ramli, Omar, & Din, 2017).

$$\theta_1 = \tan^{-1}\left(\frac{X_B - X_A}{Y_B - Y_A}\right) \quad (1)$$

$$\theta_1 = F(X_{AO}Y_{AO}X_{BO}Y_{BO}) + \left(\frac{X_{BO} - Y_{AO}}{L_{ABO}^2}\right)\partial X_A + \left(\frac{Y_{AO} - Y_{BO}}{L_{ABO}^2}\right)\partial X_B + \left(\frac{X_{BO} - X_{AO}}{L_{ABO}{}^2}\right)\partial Y_A + \left(\frac{X_{AO} - X_{BO}}{L_{ABO}{}^2}\right)\partial Y_B$$

Where $\theta_1 = bearing$
$X_{AO}Y_{AO}$ = point A estimated coordinate

Perpustakaan Negara Malaysia eISBN 987-967-17889-6-7

$X_{BO}\,Y_{BO}$ = point B estimated coordiante
L_{ABO} = Estimated horizontal distance $A-B$

$$\Delta\theta = \tan^{-1}\left(\frac{X_D - X_A}{Y_D - Y_A}\right) - \tan^{-1}\left(\frac{X_B - X_A}{Y_B - Y_A}\right)$$

$$\Delta\theta = F(X_{AO}Y_{AO}X_{BO}Y_{BO}X_{DO}Y_{DO}) + \left(\frac{Y_{AO}-Y_{DO}}{{L_{ABO}}^2} + \frac{Y_{BO}-Y_{AO}}{{L_{ABO}}^2}\right)\partial X_A \quad (2)$$

$$+\left(\frac{Y_{AO}-Y_{BO}}{{L_{ABO}}^2}\right)\partial X_B + \left(\frac{Y_{DO}-Y_{AO}}{{L_{ABO}}^2}\right)\partial X_D$$

$$+\left(\frac{X_{AO}-X_{DO}}{L_{ADO}^2} + \frac{X_{BO}-X_{AO}}{L_{ABO}^2}\right)\partial Y_A$$

$$+\left(\frac{X_{AO}-X_{BO}}{{L_{ABO}}^2}\right)\partial Y_B + \left(\frac{X_{DO}-X_{AO}}{{L_{ADO}}^2}\right)\partial Y_D$$

Where $\Delta\theta$ = Horizontal angle
$X_{AO}\,Y_{AO}$ = point A estimated coordinate
$X_{BO}\,Y_{BO}$ = point B estimated coordiante
$X_{DO}\,Y_{DO}$ = point D estimated coordinate
L_{ABO} = Estimated horizontal distance $A-B$
L_{ADO} = Estimated horizontal distance $A-D$

$$L_{AB} = \sqrt{(X_B - X_A)^2 + (Y_B - Y_A)^2} \quad (3)$$

$$L_{AB1} = F(X_{AO}Y_{AO}X_{BO}Y_{BO}) + \left(\frac{X_{BO}-Y_{AO}}{L_{ABO}}\right)\partial X_A + \left(\frac{Y_{AO}-Y_{BO}}{L_{ABO}}\right)\partial X_B$$

$$+\left(\frac{X_{BO}-X_{AO}}{L_{ABO}}\right)\partial Y_A + \left(\frac{X_{AO}-X_{BO}}{L_{ABO}}\right)\partial Y_B$$

Where L_{AB} = distance
$X_{AO}\,Y_{AO}$ = point A estimated coordinate
$X_{BO}\,Y_{BO}$ = point B estimated coordiante
L_{ABO} = Estimated horizontal distance $A-B$

Methodology

The research study area is in Arau, Perlis, as shown in figure 1. The area covers 30 parcels, the raw data for the adjustment process acquired from the DSSM Perlis in the form of bearing and distance. In this paper, the method that been applied by the bearing is declared as the old method. Meanwhile, the method proposed to produce the new accurate data is a new method to identify and clarify the ideal solutions to the identified problem (Moshe Benhamu, 2002). The first phase involves calculating the cadastral parcel's interior angle. The current raw data used by DSMM in the LSA are bearing and distance. In this study, the proposed method is based on the LSA angular and distance. The primary justification used by the angle approach is that raw data, which included minimal gross and systematic errors, are independent of or observed directly. The bearing value is a very reliant data where it is largely based on the origins of the original bearing. DSMM's common practice in previous work is based on three strong boundary points on solar observations and internal angles. The quality of the reference bearing used in the previous work is therefore extremely difficult to check. In this analysis, the interior angle of these data is separate data measured from the bearings of two boundary lines. Although the control of the bearing includes gross and systems errors, these aspects do not influence the interior angle between the two boundary lines.

For the adjustment purposes, the Star*net software was used. Star*net is the most comprehensive platform for the study of 2D and 3D networks. The output is a file with adjusted station co-ordinates and statistical adaptation analysis. Furthermore, the graphics are provided so that the user can trace the network, including the adjusted point error ellipses and the relative error ellipses between stations. Star*net can individually and by category weights all input data, which implies that it can be categorized as FREE, FIXED, respectively. Star*net will monitor the weighting of the input data when values are correctly considered to be less precise than those proven to be.

The detailed step of the processing in Star*net is shown in Figure 1. A new project is created which have two input files, bearing- distance and angle-distance. The bearing-distance input data is the current technique; meanwhile, the angle- distance input data is the new approach which is proposed in this study.

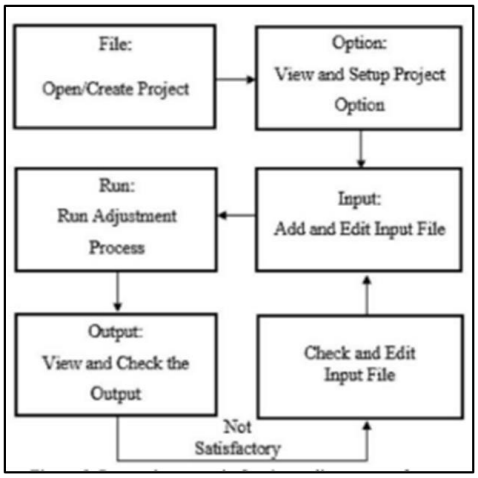

Figure 1: processing data

Result

In this stage, the result of the bearing implementation has been compared with the result of angle implementation. The result has been compared based on three factors, global test (chi-square test), the standard deviation of single observation data and coordinate.

Perpustakaan Negara Malaysia eISBN 987-967-17889-6-7

Table 1: Chi-Square Test for Bearing

Observation	Count	Sum Squares of StdRes	Error Factor
Distances	3025	3232.518	1.426
Az/Bearings	3025	35705.212	4.74
Total	6050	38937.73	3.5
Warning: The Chi-Square Test at 5.00% Level Exceeded Upper Bound Lower/Upper Bounds (0.975/1.025)			

Table 2: Chi-Square Test for Angle

Observation	Count	Sum Squares of StdRes	Error Factor
Angles	3024	28999.551	4.28
Distances	3024	2519.793	1.262
Total	6051	31519.632	3.155
Warning: the chi-square test at5.00% level exceed upper bound lower/up bounds (0.975/1.025)			

(refer to Table 1, Table 2) show the result of a global test between the bearing and angle implementation; both results are exceeded lower bound. However, the error factor for the result is a difference. There are 3.5 for the bearing implementation and for the angle, the error factor is 3.155

Table 3: Residual t for Angle

RESIDUAL	RSME	MIN	MEDIAN	MAX
Angle	0.01287	0	0.001	0.22371
Distance	0.00912343	0	0.0041	0.08

Table 4: Residual for Bearing

RESIDUAL	RSME	MIN	MEDIAN	MAX
Bearing	0.01431	0	0.001	0.27808
Distance	0.01033846	0	0.0053	0.08

Throughout the (table 4 and table 5) show the result of residual for angular constraints and bearing constraints. This show the RSME for bearing constraints a the largest, but the data on the angle constraints produced lowest RSME. Thus, based on the RSME have shown the angle constraints is the best application for implement into cadastral databased to achieve high accuracy databased.

Table 4: Differential Coordinate for Angle

Stone Id	verification Station		Angle Constraints		Angle Displacement
6381062450	-46380.507	56249.45	46380.516	56249.703	0.2531
5661765570	-45660.232	56559.968	45660.319	56559.864	0.1358

Table 4: Differential Coordinate for Bearing

Stone Id	verification Station		Bearing Constraints		Bearing Displacement
6381062450	-46380.507	56249.45	46380.474	56249.765	0.3162
5661765570	-45660.232	56559.968	45660.402	56559.869	0.1961

The coordinate differential has been calculated based on the reference point (verification station). The result of bearing displacement is the higher between the angle displacement this proved the angle able to reduce the error in the cadastral databased

Conclusion

In a nutshell, to accomplish the objective aim, which is to evaluate the angular adjustment in improving the cadastral data quality. The angular constraints that been converted from bearing and bearing constraints data have taken in the same block, and the same lots need to evaluate the precision of the data. Both data have been run on least square adjustment. The data will be evaluated based on the chi-square test, residual of data, and differential coordinate between the known point. Based on section 4.3 result have proven the angular reliability adjustment able to improve the accuracy of cadastral data based. Therefore, angular constraints able to apply in the block adjustment to improve accuracy.

REFERENCES

Charles D, G., & Paul R, W. (2012). *Elementary surveying-An Introduction to Geomatics.*

Dalyot, S., Dahinden, T., Schulze, M. J., Boljen, J., & Sester, M. (2012). Geometrical Adjustment Towards the Alignment of Vector Databases. *ISPRS Annals of the Photogrammetry, Remote Sensing and Spatial Information Sciences*, 1(February 2015), 13–18. https://doi.org/10.5194/isprsannals-I-4-13-2012

Hashim, N. M., Omar, A. H., Ramli, S. N. M., Omar, K. M., & Din, N. (2017). Cadastral database positional accuracy improvement. *International Archives of the Photogrammetry, Remote Sensing and Spatial Information Sciences* - ISPRS Archives, 42(4W5), 91–96. https://doi.org/10.5194/isprs-archives-XLII-4W5-91-2017

Perpustakaan Negara Malaysia eISBN 987-967-17889-6-7

Ogundare, J. O. (2018). Analysis and Error Propagation of Survey Observations. *Understanding Least Squares Estimation and Geomatics Data Analysis*, 39–79. https://doi.org/10.1002/9781119501459.ch2

Shatnawi, N., Maan, H., & Khaldoun, Q. (2017). *Development of Cadastral Spatial Data Infrasture in Syria*. (January 2017).

Shoshani, U., Benhamu, M., Goshen, E., Denekamp, S., & Bar, R. (2004). Registration of Cadastral Spatial Rights in Israel a Research and Development Project. *Appropriate Technologies for Good Land Administration – 3D Cadastre, FIG Working Week 2004* Athens, Greece, (May 22-27), 1–17.

Sisman, Y. (2014). Coordinate transformation of cadastral maps using different adjustment methods. *Journal of the Chinese Institute of Engineers, Transactions of the Chinese Institute of Engineers,Series A/Chung-Kuo Kung Ch'eng Hsuch K'an*, 37(7), 869–882. https://doi.org/10.1080/02533839.2014.888800

Tong, X., Shi, W., & Liu, D. (2005). A least squares-based method for adjusting the boundaries of area objects. *Photogrammetric Engineering and Remote Sensing*, 71(2), 189–195. https://doi.org/10.14358/PERS.71.2.189

Perpustakaan Negara Malaysia eISBN 987-967-17889-6-7

Identifying Factor of Forest Fire Risk in Selangor using Analytical Hierarchy Process (AHP)

Nur Amirah Mohammad Noor Azam[1], Nursyahani Nasron[1], Noorazwani Mohd Razi[1], Azlizan Adila Mohammad[2], Sazwan Ahmad Pugi[2]

[1] Faculty of Architecture, Planning & Surveying, Universiti Teknologi MARA, Perlis Branch, Arau Campus, 02600 Arau, Perlis, Malaysia
[2]Faculty of Architecture, Planning & Surveying, Universiti Teknologi MARA, Perak Branch, Seri Iskandar Campus, 32610 Seri Iskandar, Perak, Malaysia.

E-mail: amierazm@gmail.com.my

Abstract

Forest fire is one of the major environmental issues, that can damage the environment and human lives as well. Forest fire usually caused by natural or man-made reasons and can cause haze pollution, which will give bad effects on human health such as asthma and skin infection. Forest fire is becoming an issue in Selangor because of its high frequency occurs over the year. To solve this problem, a map of forest fire risk zone is produced. The aim of this research is to identify the factor of forest fire risk in Selangor using Analytical Hierarchy Process (AHP). To achieve the aim of the study, there are three objectives that will be done which is to identify parameters that influence forest fire, to determine weightage factor of each parameters using AHP technique, and lastly to classify forest fire risk zone. The data used in this research are Landsat 8 OLI and Digital Elevation Model (DEM) data, which is Shuttle Radar Topography Mission (SRTM). Meanwhile, the software used in this research is Erdas Imagine, Excel and ArcGIS. At the end of the result, the forest fire risk zone can be determined.

Keywords: Fire Risk Zone Mapping, Forest Fire, GIS, Analytical Hierarchy Process (AHP).

Introduction

Nowadays, a forest fire is still one of the major environmental issues that can damage the environment and human lives. Natural forces or human activities usually are the causes of a forest fire to happen. According to Qadri (2001), a forest fire can contribute to haze, and gave a bad impact on the natural environment, and had threatened the sustainable development and management of the natural resource. Therefore, the forest fire risk zone must be identified to get a detailed assessment of forest fire problems in order to solve the problem (Jaiswal et al.,2002).

Therefore, the Analytical Hierarchy Process (AHP) technique is used in this research. This method is used by assigning subjective weights to each parameter according to their sensitivity to fire. In order to understand the behaviour of forest fire, the factors that influence fire behaviour also need to be considered when producing a map of forest fire risk zone.

According to Suliman and Mahmud (2013), forest fire frequently happened in Selangor. There are some of the areas that have been identified most frequently are burning such as Bestari Jaya, Ulu Tinggi, Kuala Kubu Baru, Kuala Langat, Banting, Dengkil, and Sepang. For example, there are few cases of the forest fire that happened in 2017 where 95 hectares of the forest in Selangor are burned, and the most recent cases happened in March 2020 where 110 hectares of the forest in Selangor are burned down. This is the most important reason why forest fire risk zone mapping must be done in Selangor.

Nevertheless, this research is done to make use of the competencies of AHP and GIS techniques by suggesting the correct process for forest fire risk zone mapping so that it will be useful for further research. Last but not least, the use of GIS also can give many benefits to people.

Problem statement

There are many cases of forest fire happened in Selangor during the past year until now. Due to that, the city in Selangor is always exposed to bad air quality, which is harmful to human health. The previous study said that Selangor is a highly

Perpustakaan Negara Malaysia eISBN 987-967-17889-6-7

populated region and is exposed to hazardous air quality conditions related to the increased of pollutant concentrations from wildfire (Mead et al., 2018).

Moreover, according to Astro Awani (2019), Selangor is reported among the highest cases of forest fire in 2019 with 226 cases recorded, and the Deputy Minister of Housing and Local Government himself verified it. For example, during the year 2017 Hutan Simpan Kuala Langat Utara in Selangor where 95 hectares out of 958 hectares of the forest are burned. According to Berita Harian (2020), the most recent cases of forest fire happened in March 2020, where 110 hectares of forest were burned down.

The solution to the problem

There are many fire outbreak cases happen in Selangor's forest, although the situation is not severe as Indonesia. But, to overcome the problem, the map of the forest fire risk zone will be produced so that other parties can take early precautions to avoid the forest fire in the future. The problem will be solved by identifying forest fire risk zone in Selangor by integrating the factors that influence forest fire using Analytical Hierarchy Process (AHP) technique.

Planning structure

This section will explain the methodology used to solve the problem. There are five phases altogether, which is planning, data acquisition, data pre-processing, data processing and result and analysis. Moreover, the study area chosen is Selangor and the software used in this research are Erdas Imagine and ArcGIS software. Figure 1 below shows the flow chart of the methodology.

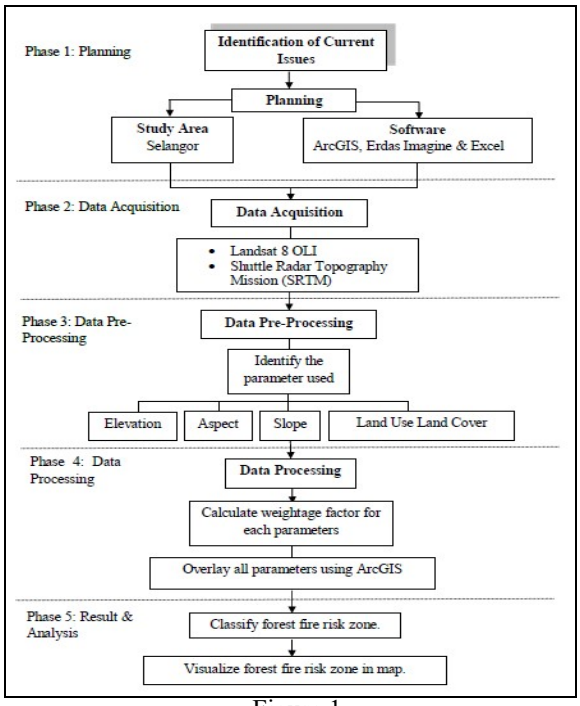

Figure 1

Identify Parameters

The selection of the parameters depends on the availability of the data in the study area. The final parameters used for this study are land use land cover, slope, aspect and elevation. The parameters are decided by the availability of data where Landsat 8 OLI and Shuttle Radar Topography Mission (SRTM) are acquired in an open-source website.

The parameters are derived from the data acquired. Data of Landsat 8 OLI are used to produce a map of land use land cover using Erdas Imagine software. Meanwhile, data of SRTM are to produce a map of slope, elevation and aspect using ArcGIS software. Table 1 below shows the list of data acquired to produce a map for each parameter.

Table 1

Data	Data Type	Source
Shuttle Radar Topography Mission (SRTM) • Slope • Aspect • Elevation	Tiff	Open Topography Website
Landsat 8 OLI • Land Use • Land Cover	Tiff	United States Geological Survey (USGS) Website

Perpustakaan Negara Malaysia eISBN 987-967-17889-6-7

Apply Analytical Hierarchy Process (AHP)

The AHP is one of the first methods developed in an environment of discrete multicriteria decision. The AHP method divides the problem into hierarchic levels, which makes its comprehension and evaluation easier and clearly for decision-makers, prioritizing or classifying them after finalizing the method. The AHP decomposes a large problem into smaller sub-problems in hierarchical levels and assigns weights to the decision-making criteria.

Firstly, perform a pairwise comparison matrix for several criteria, let Pij reveal the preference score of criteria I to criteria j using the nine-integer value scale (Saaty, 2008). The scale is shown in Table 2 below. Pij denotes the entry in i row and j column of matrix m. The entries of preference score Pij and Pji must satisfy the following constraint in Eq. (1):

$$Pij.\ Pji = 1 \quad (1)$$

Table 2

The score of criteria *i* to criteria *j* (P*ij*)	Definition
1	Criteria *i* and *j* are of equal importance
3	Criteria *i* is slightly more important than *j*
5	Criteria *i* is moderately more important than *j*
7	Criteria *i* is strongly more important than *i*
9	Criteria *i* is extremely more important than *j*
2, 4, 6, 8	Intermediate values

Then, establish a normalized pairwise comparison matrix; the sum of each column must equal to 1. This can be obtained using Eq. (2) to calculate Pij for each entry of the matrix. Table 3 below shows the normalized comparison matrices that had done by assigning score level in Table 2 based on personal judgment.

$$P_{ij} = \frac{P_{ij}}{\sum_{i=1}^{n} P_{ij}} \quad (2)$$

Table 3

Criteria	C1	C2	C3	C4
(C1) Land Use Land Cover	1	2	5	7
(C2) Slope	1/2	1	2	4
(C3) Aspect	1/5	1/2	1	2
(C4) Elevation	1/7	1/4	1/2	1

Next, the average across rows is computed to obtain the relative weights using Eq.(3). For each element, the relative weight is within the range of 0–1; a higher weight shows a greater influence of the element to the forest fire risk zone. Table 4 below show the value of the criteria weight.

$$w_i = \frac{\sum_{i=1}^{n} P_{ij}}{n} \quad (3)$$

Table 4

Criteria	Criteria Weight
(C1) Land Use Land Cover	0.54
(C2) Slope	0.26
(C3) Aspect	0.13
(C4) Elevation	0.07

Finally, check the consistency by finding the weighted sum value. The weighted sum value is determined by multiplying the criteria weight with each of the criteria in pairwise comparison matrices. Then, all the criteria will be sum up, and the total given is the weighted sum value that is shown in Table 5.

Table 5

Criteria	Criteria Weight	Weighted Sum Value
(C1) Land Use Land Cover	0.54	2.2
(C2) Slope	0.26	1.07
(C3) Aspect	0.13	0.51
(C4) Elevation	0.07	0.29

After that, determine maximum lambda by calculating the lambda value for each parameter. The lambda value for each parameter is determined and shown in Table 6. Then, the maximum lambda is determined by dividing the total value of lambda of each parameter by the number of criteria, which is 4.

Table 6

Criteria	λ
(C1) Land Use Land Cover	4.07
(C2) Slope	4.12
(C3) Aspect	3.92
(C4) Elevation	4.14

Moreover, CR is determined by dividing CI with RI, where RI is the random consistency index that varies according to the number of criteria in a comparison (n) as shown in Table 7. The consistency index (CI) is calculated using Eq. (4).

Perpustakaan Negara Malaysia eISBN 987-967-17889-6-7

$$CI = \frac{(\lambda_{max} - n)}{n-1} \quad (4)$$

Table 7

n	RI
2	0
3	0.58
4	0.90
5	1.12
6	1.24
7	1.32
8	1.41
9	1.45
10	1.49
11	1.51
12	1.48

So, if CR ⩽ 0.15, the degree of consistency is considered satisfactory; otherwise, there are serious inconsistencies in the pairwise comparison. Therefore, the AHP may not return meaningful results.

Overlay Parameter

Overlay all the parameters using ArcGIS software to identify the relationships between all the parameters by combining the raster data and the attribute table of the data input. The percentage influence used is the percentage of criteria weight, and the sum of influence must be 100%. This is needed to generate which parameter dominates most of the criteria. The final output will show which parameters contribute the most in spreading the fire or influence forest fire.

Map of Forest Fire Risk Zone

The final product for this research is the map of the forest fire risk zone. Figure 2 below shows the zone of the forest fire that is represented by the colours. The very high-risk area is more at the hilly forestry area. Although, the high-risk area located at a low and high slope and elevation, it can still spread the fire because the area surrounding has a lot of trees that can help the fire to spread faster. This shows that the AHP technique is accurate to state that land use land cover is highly important in the spreading of fire.

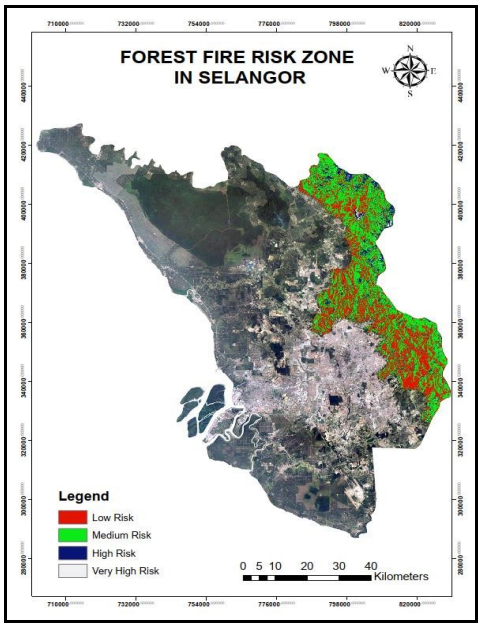

Figure 2

Knowledge impact

This research focuses on identifying factor of forest fire risk using Analytical Hierarchy Process (AHP). Based on this research, people can improve the uses of Geographic Information System (GIS) and AHP for other applications such as agriculture, social science and many else. By integrating GIS and AHP can help the exploration for the future development of GIS application.

Contribution to society and country

The finding of this study will give benefits toward societies considering that it also plays an important role in the environment and human health. The research's goal of this study is to give benefit towards government and any agencies to use the map to monitor forest fire and determine the risky places of the forest fire. It will also help to clarify which factor is the most influential for the spreading of fire. Thus, the government and agencies that use this study will be able to prevent and minimize forest fire activities in the future. For example, the Department of Forestry Management can use this study to monitor forest fire, minimize forest fire activities, and so on. Lastly, this study can be used as a reference for any researchers to enhance or apply it for future research.

Cost impact

There is no cost involved in this research because all the data acquired are free and can be downloaded from the open-source website.

Perpustakaan Negara Malaysia eISBN 987-967-17889-6-7

Commercialization potential

This research is very useful for monitoring forest to avoid any forest fire cases that can harm the environment and human health. By doing this research, we can locate which area is risky and we can take measure precaution on the issues. Although this research is not very popular in Malaysia like other foreign countries, this research has full potential to become popular and useful for government, forest department or any agencies that are involved with the forest.

REFERENCES

Ghobadi, G. J., Gholizadeh, B., & Dashliburun, O. M. (2012). Forest Fire Risk Zone Mapping From Geographic Information System in Northern Forests of Iran (Case study, Golestan province). *International Journal of Agricultured and Crop Sciences*, 4(12), 818–824.

Kou, G., Ergu, D., Lin, C., Chen, Y., & Group, F. (2017). *Pairwise comparison matrix in multiple criteria decision making*. 4913. https://doi.org/10.3846/20294913.2016.1210694

Mead, M. I., Castruccio, S., Latif, M. T., Nadzir, M. S. M., Dominick, D., Thota, A., & Crippa, P. (2018). Impact of the 2015 wildfires on Malaysian air quality and exposure: A comparative study of observed and modeled data. *Environmental Research Letters*, 13(4). https://doi.org/10.1088/1748-9326/aab325

Pandey, K., & Ghosh, S. K. (2018). Modeling of parameters for forest fire risk zone mapping. *International Archives of the Photogrammetry, Remote Sensing and Spatial Information Sciences - ISPRS Archives*, 42(5), 299–304. https://doi.org/10.5194/isprs-archives-XLII-5-299-2018

Podvezko, V. (2009). Application of AHP technique. *Journal of Business Economics and Management*, 10(2), 181–189. https://doi.org/10.3846/1611-1699.2009.10.181-189

Yakubu, I., Mireku Gyimah, D., & Duker A, A. (2015). Review of methods for modelling forest fire risk and hazard. *African Journal of Environmental Science and Technology*, 9(3), 155–165. https://doi.org/10.5897/ajest2014.1820

U. S. Geological Survey (n.d.). USGS EROS Archive - Digital Elevation - Shuttle Radar Topography Mission (SRTM) 1 Arc-Second Global. Retrieved from https://www.usgs.gov/centers/eros/science/usgs-eros-archive-digital-elevation-shuttle-radartopography-mission-srtm-1-arc?qt science_ center_objects=0#qt-science_center_objects

Suliman, M. D. H., & Mahmud, M. (2013). Analisis Potensi Kebakaran Hutan Menggunakan Teknik Georuang. *Sains Malaysiana*, 42(5), 579–586.

Jaiswal, R. K., Mukherjee, S., Raju, K. D., & Saxena, R. (2002). Forest fire risk zone mapping from satellite imagery and GIS. *International Journal of Applied Earth Observation and Geoinformation*, 4(1), 1–10. https://doi.org/10.1016/S0303-2434(02)00006-5

Kamaruddin, H., Md Khalid, R., Supaat, D. I., Abdul Shukor, S., & Hashim, N. (2016). *Deforestation and Haze in Malaysia: Status of Corporate Responsibility and Law Governance*. (November), 374–383. https://doi.org/10.15405/ epsbs. 2016.11.02.34

Qadri, S. T. (2001). Fire, smoke, and haze: the ASEAN response strategy. In Asean (Vol.10).Retrieved from http://scholar.google.com/scholar?hl=en&btnG=Search&q=intitle:Fire,+Smoke+and+Haze:+The+ASEAN+Respnse+Strategy#0

Kou, G., Ergu, D., Lin, C., Chen, Y., & Group, F. (2017). *Pairwise comparison matrix in multiple criteria decisions making*. 4913. https://doi.org/10.3846/20294913. 2016.1210694

Perpustakaan Negara Malaysia eISBN 987-967-17889-6-7

Affected Area Estimation using Calibrated Discharge at Ungauged Catchment

Mohamad Nur Syafiq Mohamad Faisa[1], Ernieza Suhana Mokhtar[1], Farah Hanani Amran[1]

[1]Faculty of Architecture, Planning & Surveying, Universiti Teknologi MARA, Perlis Branch, Arau Campus, 02600 Arau, Perlis, Malaysia

E-mail:ernieza@.uitm.edu.my

Abstract

Flood event that occurred at Kepala Batas in November 2010 has greatly damaged the surrounding area along Kedah River where majority land-use is developed area. However, the river discharge is not available in this area, and it is difficult to determine the flood-prone areas during flooding in 2010. Accuracy of flood mapping at the ungauged station still in debating issue due to unavailability discharge value. Therefore, this study is carried out to i) identify the calibrated discharge value by comparing the flood depth of HEC-RAS model with water level station that suitable for ungauged area station and ii) determine affected area during flooding in 2010 at MADA administration area. Monte Carlo simulation is used to estimate discharge at the ungauged station. The calibrated discharge is tested by comparing the water depth delineated by HEC-RAS model and in-situ data from telemetry station using RMSE method. The flood inundation mapping was produced, and the affected area was determined using the integration of geospatial technologies and hydraulic modelling. Finally, the contribution of this study can help the determination of water availability at ungauged catchment. With the availability of water value in the ungauged catchment, the flood estimated of that area can be provided precisely in the future.

Keywords: Discharge, Flood inundation, GIS, Monte Carlo simulation

Introduction

Floods are among the most devastated of water-related hazards and are the main responsible for the loss of human lives, damage of properties and economic losses (Tsakiris, 2014). Discharge is one of the essential hydrological elements in flood inundation modelling (Mokhtar et al., 2017). The data of discharge is required to stimulate flood characteristics such as flood inundation extent and water depth. But, most of the previous studies (Ahmad et al., 2016; Marimin et al., 2018; Papaioannou et al., 2017), have been carried out at gauged watersheds using information from hydrometric stations with discharge data. The use of gauged data, for calibration and validation of the hydraulic-hydrodynamic models, is the most common approach in floodplain modelling and mapping process (Bates et al., 2006).

However, model calibration and validation based on water level and flow observations for uncertain data is a necessary step to determine any model's ability to reproduce reality (Matte, Secretan and Morin, 2017). The most commonly used parameter for calibrating river models is the Manning roughness coefficient (Baldassarre et al., 2010; Barthelemy et al., 2017).

This study presents the use of Monte Carlo simulation to generates random variables for modelling uncertainty analysis, which is used to estimate discharge by Bjerklie's equation at ungauged catchment. Then, the affected area during the flooding in 2010 can be estimated especially at the ungauged area using the calibrated discharge value.

Problem statement

Existing uncertainties of the hydraulic variables used in the empirical equation to estimate river discharge at the data-scarce area for flood inundation mapping still require further exploration (Mokhtar et al., 2018). Furthermore, the researches sometimes deprived to have an accurate forecast of flood magnitude as a crucial factor for a credible flood inundation mapping due to lack of data for ungauged rivers (El-Naqa & Jaber, 2018). Hydraulichydrodynamic model is required to simulate flood characteristics such as flood inundation extent and water depth accurately (Papaioannou et al., 2017).

Perpustakaan Negara Malaysia eISBN 987-967-17889-6-7

Lastly, the areas that affected by flash floods are small and medium-sized ungauged catchments, and appropriate flood data are not available because of the nature of the extreme event (Papaioannou et al., 2016). This is why floodplain modelling and mapping was always used the gauged data in previous studies due to unavailability discharge at the ungauged river.

The solution to the problem

The comparison between estimated discharge value using Bjerklie equation was compared to the water level station observed during flooding in 2010 at MADA administration area. The sensitivity analysis performed by Monte Carlo simulation method to determine estimated discharge using min-Q, mean-Q and Max-Q that comprised of two set combination of main river and tributary have been applied in the hydraulic model. Therefore, the problem of unavailability discharge data is overcome using the calibrated discharge computed from the equation to estimate the flood hazard area.

Planning structure

Study Area

Kepala Batas is a small town located in Kubang Pasu District, Kedah. It was located in the northern part of Peninsular Malaysia. The study area consists of the main river, Kedah River that is flowing from Kepala Batas to Alor Setar, Malaysia. The area is selected due to the flood event happened in Kedah in the year 2010. Also, the availability of the spatial data of the study area.

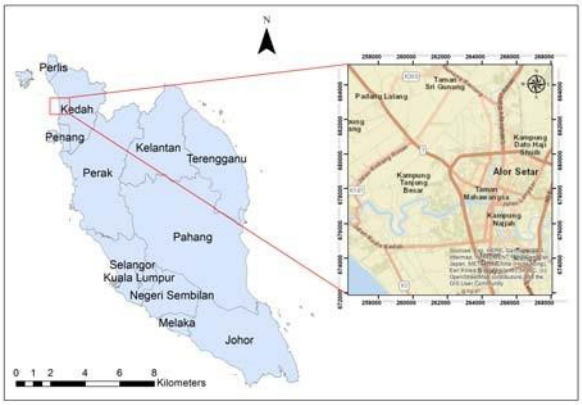

Figure 1: Location Map

Data

Topographic data such as IFSAR DEM, land-use data, google map and water level are listed in Table 1. IFSAR DEM data is used as input to quantify the characteristics of the land surface with 5 meters ground resolution. Then, land-use data is used to extract Manning's n provided by MADA in a vector-based format. It is classified into five classes that comprised of the waterbody, bare land, cultivated and brush, forest and developed area that represents the land-use of the study area. Water level data is acquired from the Department of Irrigation of Drainage (DID) for date 3th November 2010. The data consist of station names, water depth and coordinates. This study needs to calculate the discharge value to be used in the HEC-RAS model.

Table 1: Details of different data used in the study.

Type of Data	Description
DEM data	Quantify land surface
Land use data	Manning's n extraction
Google Map	Digitize spatial data
Water level	Calculate discharge

Methods

Calculate discharge

The discharge was calculated using Bjerklie's equation. Channel slope, the river width and water depth are needed to calculate the discharge value, The discharge has been calculated using Equation (1), and it was used as model input for data processing to generate a hydraulic model.

$$Q = 7.22W^{1.02}Y^{1.74}S^{0.3} \quad (1)$$

Where Q is water discharge value in m3/s, W is the width of the river (m), Y is water depth, and S is channel slope. The value of channel slope is calculated using Equation (2)

$$S = \frac{\text{Upper Elevation} - \text{Lower Elevation}}{\text{Length River}} \quad (2)$$

In addition to that, two estimated discharge have been calculated for the main river and its tributary. The estimation has been made using Monte Carlo simulation, which performs multiple simulations with randomly selected model inputs for defined parameters. It has been divided into three performances which are Min-Q, Mean-Q and Max-Q. Those values can be referred to in Table 2.

Perpustakaan Negara Malaysia eISBN 987-967-17889-6-7

Table 2: Estimated discharge for each reach of the river using MC simulation.

	Min-Q	Mean-Q	Max-Q
Main River	218.295	432.249	749.757
Tributary	12.176	24.237	41.934

Manning's n

Manning's n values were applied for cross-sections using land-use data. The Manning's n values represent the roughness of the channel surface, which can influence the overall flow rates and velocities in the channel. A Manning's roughness values were assigned to each land cover category as Table 3.

Table 3: Manning's n for each land cover category.

No.	Class	n Values
1	Bare Land	0.03
2	Cultivated and Brush	0.03
3	Developed Area	0.01
4	Forest	0.15
5	Water	0.04

Result and Analysis

Comparison of flood depth estimated and water level station

Discharge (Min-Q, Mean-Q and Max-Q) value were tested by delineating the flood inundation and flood depth simulated by HEC-RAS (Table 4). The flood depth of the inundated area was compared to the water level station.

Table 4: The hydraulic variables of discharge estimated.

		Width (W)	Water Depth (Y)	Channel Slope (S)	Discharge (Q)
Main River	Min	21.198	7.77	0.00009	218.295
	Mean	26.357	9.682	0.00011	432.249
	Max	31.509	11.552	0.00013	749.757
Tributary	Min	42.818	0.972	0.00009	12.176
	Mean	53.356	1.215	0.00011	24.237
	Max	63.756	1.447	0.00013	41.934

Table 5 shows, the observed water level for station Titi Baru K. Batas, Pantai Johor, Sg. Anak Bukit and Sg. Kedah was recorded at 5.50 m, 2.90 m, 2.19 m and 2.06 m, respectively. Only station Titi Baru K. Batas and Sg. Kedah has the smallest difference between predicted and the observed value of flood depth which are -1.58 m, -0.45 m and 1.00 m for Titi Baru K. Batas station and -0.22 m, 1.23 m and 0.27 m for Sg. Kedah station. The result of flood depth from HEC-RAS using Min-Q and Mean-Q at station Titi Baru K. Batas were predicted lower than observed water level station, which is 3.90 m and 5.05 m, respectively. Also, the predicted flood depth using Min-Q at station Sg. Kedah was also recorded lower than observed water level station, which is 1.84 m.

Table 5: Predicted flood depth, observed water level station, their difference and RMSE.

Stn Name		Predict (m)	Observed (m)	Difference (m)	RMSE
Titi Baru K.Batas	Min-Q	3.92	5.50	-1.58	0.01766
	Mean-Q	5.05	5.50	-0.45	0.00503
	MaxQ	6.50	5.50	1.00	0.01118
Pantai Johor	Min-Q	6.38	2.90	3.48	0.03891
	MeanQ	7.46	2.90	4.56	0.05098
	MaxQ	8.54	2.90	5.64	0.06306
Sg. Anak Bkt	Min-Q	5.88	2.19	3.69	0.04126
	MeanQ	8.17	2.19	5.98	0.06686
	MaxQ	7.33	2.19	5.14	0.05747
Sg. Kedah	Min-Q	1.84	2.06	-0.22	0.00246
	MeanQ	3.29	2.06	1.23	0.01375
	MaxQ	2.33	2.06	0.27	0.00302

*Note: Negative (-) symbol means the predicted value is smaller than observed value and positive (+) symbol means the predicted value is more extensive than the observed value.

The result indicates that Pantai Johor station has a huge difference between predicted and observed, which are 3.48 m for Min-Q, 4.56 m for Mean-Q and 5.64 m for Max-Q. Supposedly, that station must be obtained around 2.90 m, but those performances have been predicted 6.38 m, 7.46 m and 8.54 m of flood depth using Min-Q, Mean-Q and Max-Q, respectively. At station Sg. Anak Bkt, the flood depth was predicted to 5.88 m (Min-Q), 8.17 m (Mean-Q) and 7.33 m (Max-Q) rather than 2.19 m as an observed value from water level station. The difference between those performances is 3.69 m, 5.98 m and 5.14 m for Min-Q, Mean-Q and Max-Q, respectively. The differences might influence due to lack of data at other sub-tributaries river.

Perpustakaan Negara Malaysia eISBN 987-967-17889-6-7

In terms of RMSE, the Min-Q for Sg. Kedah station has produced the smallest RMSE which is 0.00246m compared to other stations. Meanwhile, the Mean-Q for Sg. Anak Bkt has produced the highest RMSE value with 0.06686m because of high difference that obtained between predicted and observed value due to inappropriate of the estimated discharge used. Another reason is the lack of data for uncertainty river leads to the low accuracy of calibrated performances (Ha, Kim and Bae, 2020). Therefore, this study concludes that using Min-Q to calculate estimated discharge is suitable because it gives a better result. At the same time, the worst is Max-Q due to the highest difference obtained between predicted and observed value compared to other performance.

Affected area during flooding in 2010 at MADA administration area

A comparison was made for this type of land-use and presented in Table 6. The developed area is the most affected area during the flood event in November 2010. All type of estimated discharge shows that developed area has the highest total area affected compared to other land-use with 10.97%, 12.40% and 11.43% for Min-Q, Mean-Q and Max-Q respectively. This is because most of the developed area such as residential area, commercial area and others were constructed nearby to Kedah River. Then followed by bare land with the total area affected was 576.715hectare using Min-Q, 592.804-hectare using Mean-Q and 584.222-hectare using Max-Q.

The determination of the affected area for the residential area along the Kedah River was also performed. Figure 3 shows that the flood inundation map was affected by about 19 residential areas in the study area. The flood inundation mapping was generated using Min-Q due to this performance has produced the best-estimated discharge compared to Mean-Q and Max-Q after calibration have been made. Table 7 shows the total area for the residential area affected by river inundation during the flood event 2010.

Table 6: Affected area by land use during the flood event.

Land-use	Affected Area in November 2010					
	Min-Q		Mean-Q		Max-Q	
	(ha)	(%)	(ha)	(%)	(ha)	(%)
Water	335.935	2.17	338.289	2.19	337.595	2.18
Bare Land	576.715	3.73	592.804	3.83	584.222	3.77
Developed Area	1698.708	10.97	1918.961	12.40	1769.854	11.43
Cultivated and Brush	288.082	1.86	288.13	1.86	288.196	1.86

.

Table 7: The affected area in the residential area during the flood event.

Residential Name	Affected Area Hectare (ha)	Percentage (%)
Kampung Bukit Pinang	56.650	3.33
Kampung Titi Besi	56.980	3.35
Taman Desa Mutiara	34.570	2.04
Kampung Alor Senjaya	86.680	5.10
Taman Aman	35.800	2.11
Taman Berlian	47.430	2.79
Taman Sri Pantai	23.520	1.38
Taman Sri Negeri	60.550	3.56
Taman Pandan	18.160	1.07
Kampung Pumpong	8.230	0.48
Taman Seri Menanti	17.210	1.01
Kampung Lubok Peringgi	64.580	3.80
Taman Mahawangsa	18.950	1.12
Taman Sri Belimbing	20.190	1.19
Taman Air Putih	111.510	6.56
Taman Seri Impian	47.600	2.80
Taman Cemara	36.540	2.15
Kampung Tengah	106.250	6.25
Taman Baru Kuala Kedah	145.700	8.58

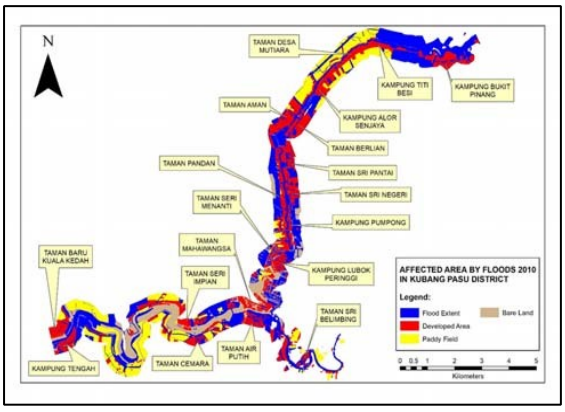

Figure 2: Affected area mapping.

The result indicated that Taman Baru Kuala Kedah has the highest percentage among the other residential area, with 8.58% of the flood inundation. Next, the second and third highest of the affected area by flood inundation are Taman Air Putih and Kampung Tengah with 6.56% and 6.25%,

Perpustakaan Negara Malaysia eISBN 987-967-17889-6-7

respectively. It is due to the location situated at the lowest elevation of 0 - 3.086m, and near to the river bank. Three (3) residential areas that located in an upstream area which are Kampung Bukit Pinang, Kampung Titi Besi and Taman Desa Mutiara were recorded the affected area as 56.650 hectares (3.33%), 56.980 hectares (3.35%) and 34.570 (2.04%), respectively. The elevation of those residential areas is from 6.791-12.347 m. The downstream area was highest affected compared to the upstream area because the flooding often occurs in that area and the high-speed water flows from high elevation to low elevation during a flood event can easily form floods (Wu et al., 2014).

Knowledge impact

Usually, the in-situ gauged discharge was used to predict the accurate flood modelling compare to ungauged discharge due to lack of data. The estimation of discharge using various models, for example, by Bjerklie's equation using Monte Carlo simulation can be used to predict flood inundation since the value of flood depth that produced almost same to the measured value of water level station. Therefore, the estimated discharge can be used in ungauged sites for flood inundation modelling.

Contribution to society and country

The contribution of this study can help the determination of water availability at ungauged catchment. With the availability of water value in the ungauged catchment, the flood estimated of that area can be provided precisely in the future. This can help the community in that area take precautions if there is any flood event could happen from now on. Lastly, this study can also help water industries that want to put up a hydropower plant or a reservoir on a specific watershed of that area

Cost impact

No cost impact in this research as all data was provided by government agencies.

Commercialization potential

Many flood inundation maps need to be revised because they are outdated. The automated mapping technique developed for this research saves time and money versus conventional flood inundation delineation on paper maps. Thus, flood inundation maps can be updated more frequently, as changes in hydraulic conditions warrant. By integrating the hydraulic model with GIS to produces flood inundation maps, multiple stakeholders such as urban planners, city managers and emergency responders can use the maps in planning for long term flood risk, mitigation measures and the appropriate actions to be taken in an emergency. However, the verification process needs to be further investigated to has accurate flood inundation mapping.

Acknowledgement

Thank you to Mr Mukhlis Zainol Abidin from Muda Agricultural Development Authority (MADA) for providing the spatial data of research area.

REFERENCES

Ahmad, M. M., Ghumman, A. R., & Ahmad, S. (2009). Estimation of Clark's Instantaneous Unit Hydrograph Parameters and Development of Direct Surface Runoff Hydrograph. Water Resources Management, 23(12), 2417–2435. https://doi.org/10.1007/s11269-008-9388-8

Baldassarre, G. Di, Schumann, G., Bates, P. D., Freer, J. E., & Beven, K. J. (2010). Floodplain Mapping: A Critical Discussion of Deterministic and Probabilistic Approaches. Hydrological Sciences Journal, 55(3), 364–376. https://doi.org/10.1080/02626661003683389

Barthelemy, Ricci, S., Rochoux, M. C., Pape, E. Le, & Thual, O. (2017). Ensemble-Based Data Assimilation for Operational Food Forecasting - On The Merits of State Estimation for 1D Hydrodynamic Forecasting through The Example of The "Adour Maritime" River. Journal of Hydrology.

Bates, P. D., Wilson, M. D., Horritt, M. S., Mason, D.C., Holden, N., & Currie, A. (2006). Reach Scale Floodplain Inundation Dynamics Observed using Airborne Synthetic Aperture Radar Imagery: Data Analysis and Modelling. Journal of Hydrology, 328(1–2), 306–318. https://doi.org/10.1016/j.jhydrol.2005.12.028

El-Naqa, A., & Jaber, M. (2018). Floodplain Analysis using ArcGIS, HEC-GeoRAS and HEC-RAS in Attarat Um Al-Ghudran Oil Shale Concession Area, Jordan. Journal of Civil & Environmental Engineering, 08(05). https://doi.org/10.4172/2165-784x.1000323

Perpustakaan Negara Malaysia eISBN 987-967-17889-6-7

Grimaldi, S., Li, Y., Pauwels, V. R. N., & Walker, J. P. (2016). Remote Sensing-Derived Water Extent and Level to Constrain Hydraulic Flood Forecasting Models: Opportunities and Challenges. Surveys in Geophysics, 37(5), 977–1034. https://doi.org/10.1007/s10712-016-9378-y

Marimin, N. A., Adib, M., Razi, M., Anjang, M., Adnan, M. S., & Rahmat, S. N. (2018). HEC-RAS Hydraulic Model for Floodplain Area in Sembrong River. 10, 151–157.

Matte, P., Secretan, Y., & Morin, J. (2017). Hydrodynamic Modeling of The St. Lawrence Fluvial Estuary. I: Model Setup, Calibration and Validation. Journal of Waterway, Port, Coastal, and Ocean Engineering, 143(5), 1–15. https://doi.org/10.1061/(ASCE)WW.19435460.0000397.

Mokhtar, E. S., Pradhan, B., Ghazali, A. H., & Shafri, H. Z. M. (2017). Comparative assessment of water surface level using different discharge prediction models. Natural Hazards, 87(2), 1125–1146. https://doi.org/10.1007/s11069-017-2812-8

Mokhtar, E. S., Pradhan, B., Ghazali, A. H., & Shafri, H. Z. M. (2018). Assessing flood inundation mapping through estimated discharge using GIS and HEC-RAS model. Arabian Journal of Geosciences, 11(21). https://doi.org/10.1007/s12517-018-4040-2

Papaioannou, G., Loukas, A., Vasiliades, L., & Aronica, G. T. (2016). Flood Inundation Mapping Sensitivity to Riverine Spatial Resolution and Modelling Approach. Natural Hazards, 83, 117–132. https://doi.org/10.1007/s11069-016-2382-1

Papaioannou, George, Vasiliades, L., Loukas, A., & Aronica, G. T. (2017). Probabilistic Flood Inundation Mapping at Ungauged Streams due to Roughness Coefficient Uncertainty in Hydraulic Modelling. Advances in Geosciences, 44, 23–34. https://doi.org/10.5194/adgeo-44-23-2017

Tsakiris, G. (2014). Flood Risk Assessment: Concepts,Modelling, Applications. Natural Hazards and Earth System Sciences, 14(5), 1361–1369. https://doi.org/10.5194/nhess-14-1361-2014

Wu, C., Huang, G., Yu, H., Chen, Z., & Ma, J. (2014). Spatial and Temporal Distributions of Trends in Climate Extremes of The Feilaixia Catchment in The Upstream Area of The Beijiang River Basin, South China. International Journal of Climatology, 34, 3161–3178. https://doi.org/10.1002/joc.3900

Perpustakaan Negara Malaysia eISBN 987-967-17889-6-7

RELIABILITY STUDY OF UAV PHOTOGRAMMETRY FOR SLOPE MAINTENANCE IN NAKA, KEDAH

Mohamad Fadhilah Azri1, Dr Ashraf Abdullah1

[1] *Faculty of Architecture, Planning & Surveying, Universiti Teknologi MARA, Perlis Branch, Arau Campus, 02600 Arau, Perlis, Malaysia.*

e-mail: m.fadhilah96@gmail.com

Abstract

Unmanned aerial vehicles (UAV) applications have been progressed and developed steadily from time to time, particularly for mapping applications. Also, UAV is one of the solutions to manage a project within time constraints and using less worker compare to a method that using the satellites or unmanned aircraft with more flight costs, a long time to conduct and weather-dependent for data collection, restricted in deploy the equipment, limited in flying time and the resolution of the ground is low in the mapping process. Moreover, the 3D model can be created by applying digital image processing using a UAV image. In civilian and industrial applications, there are already using the UAV, and with today's technology, UAV can be used in many various applications. For instance, the UAV has been widely used in forest-fire monitoring, modelling of the building, and slope mapping, road monitoring, vehicle detection, and disaster management. However, its uncertainty about how much accuracy data from UAV compare to the data from the ground method, especially when it comes to estimating the volume in the slope area. For this purpose, this study focuses on to make a comparison of volume using topography data and UAV application for slope maintenance. The study area for this research will be in Naka, Kedah. The data of topography will be collected by using the Global Navigation Satellite System (GNSS) device and for the UAV, aerial images from the drone will undergo processing to get the digital elevation models (DEM) data. Based on this data, the analysis will be made for these two types of data. In the end, this study can help to determine how accurate the volume estimation between topography data and UAV based DEM.

Keywords: Unmanned aerial vehicles, Global Navigation Satellite System, volume estimation

Introduction

In last decade, Unmanned Aerial Vehicles (UAV) has been introduced as a remote-control plane and already managed for a period of more than 75 years and later with the technology served the purposes of recreation, defence, or research (Deangelo & Deangelo, 2016). As time goes on, technology such as computing hardware, electronics, materials, and the efficiency of those techniques has increased. There has been an effort to make the automated flight. When it was first introduced, the price is a little bit expensive, and after a few years, the price is affordable. UAV systems receive high demands in the business, research institutes and industries since UAV is one of the simple and cheapest equipment in image acquisition (Yoo & Oh, 2016).

For the past few years, the commercial UAV produced by a different company in the industry such as surveying and mapping includes the obtainment of large-scale orthophotography. When it comes to slope mapping, UAV can estimate the volume for that particular area based on digital elevation model (DEM) data. However, they are some issues that arise as to know how accurate the data is given compare to the ground method. Therefore, to solve this issue, this study will focus on the comparison between topography and UAV based DEM data and make some analysis based on this.

In this research, the Global Navigation Satellite System (GNSS) device will use a fast static method to create the topography. The drone will be used to mapping and create the DEM data form UAV. Both data will be made in the area which is at Naka, Kedah. The aerial image with high-resolution quality will be captured from the drone. UAV Images are a valuable resource to extract various geospatial data

Perpustakaan Negara Malaysia eISBN 987-967-17889-6-7

like High-Resolution Ortho Photo, DSM, DTM and 3D Spatial Models (J. Leo Stalin & RPC. Gnanaprakasam, 2017a). The use of UAV application will help to calculate the calculation volume for that area.

Study Area

The study area was conducted at Lot 60078 Pekan Naka, Daerah Padang Terap, Kedah. The area in this lot around 1.7km with the perimeter of 525.911m. In this area, there are already have a construction site for the project, which is power supply using paddy husk. The environment in this area has a hill with stranded land area. The hill will be used to get slope data to be used in this research. This area will be used to conduct the research. The study area chosen is shown below.

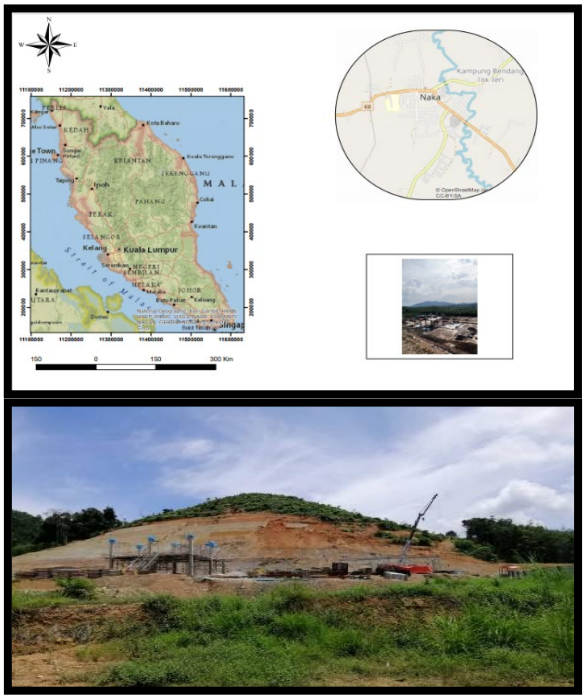

Figure 1: Project area in Naka, Kedah

Research Methodology

In order to achieve the aim and objective, several things must be done to make sure the data is well taken. For this research, there is 5 phase which is Preparation, Data Collection, Data Processing, and Analysis made in the result.

The first step involves the selection in the study area and software. The area selected locations in the Naka, Kedah. This site area already has development and construction to build a power supply using a paddy husk. The software involved in data processing is Agisoft and Pix4D.

The second phase involves data collection. It involves two flow which is a Global Navigation Satellite System (GNSS) device will be using the fast-static method. An unmanned aerial vehicle (UAV), three steps involve which is flight planning, raw image acquisition, and proposed Verification Point (VP) and Ground Control Point (GCP).

The third step of this research is making data processing. The data that have been collected will undergo processing which is data from GNSS will create a topography data and image with GCP and VP will be processed in Agisoft and Pix4D. The final output will compare using the same software, which is Global Mapper to compare the volume in the slope area.

The fourth phase is the result and analysis. The analysis that is made will be present using a table of comparison and graph to show the data more clearly. Based on the analysis, the conclusion, and recommendations are made.

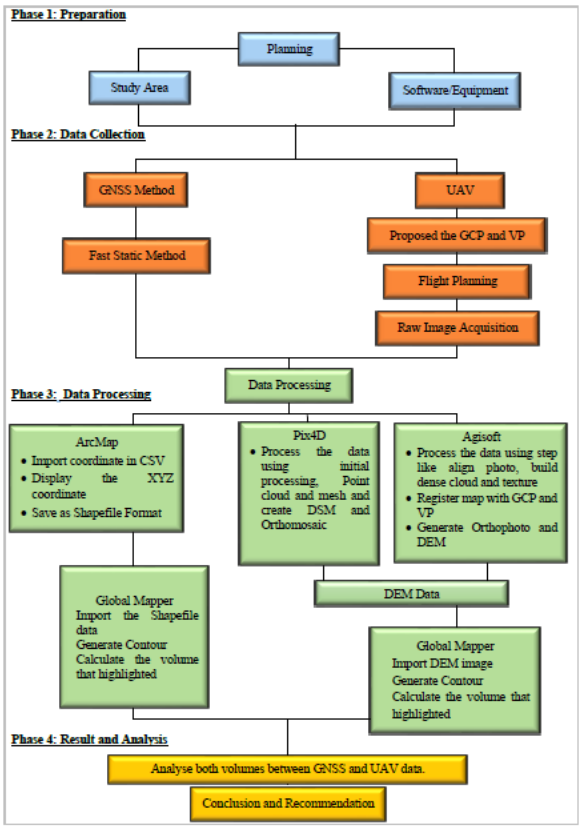

Preparation

Before the flight plan, an operator needs to identify the coverage of the study area in sequence to design a flight plan. The flight plan requires an approximate coordinate as an input to design the flight route. (Yoo & Oh, 2016). This research paper used the aerial photogrammetric technique as a

Perpustakaan Negara Malaysia eISBN 987-967-17889-6-7

method for data acquisition. As a result, the user needs to determine the percentage of the overlap area and side lap area between both the pair of images in the flight plan. Site Preparation involves the development of a layout for control points, checking the accuracy of the camera image used for flight planning, ensuring that there are no obstacles in the way of the UAV, and analysing weather parameters to determine how well a flight can be carried out smoothly. The reconnaissance survey is a comprehensive study of the entire area that could be used for a road or an airfield. Its goal is to eliminate those routes or sites that are unrealistic or unfeasible and to identify more promising routes or sites. At this stage, a site investigation is carried out to ensure that the data acquisition can be obtained without any problems.

Data Acquisition

In this research, it was conducted at Naka, Kedah. The drone will fly and take an aerial image include GCP and VP that are already established. Based on the image, the data will be processed by certain software. The software that will be used is Agisoft to process the image and Pix4D Capture to create flight planning in the study area. To model the topography data, the Global Navigation Satellite System (GNSS) receiver is used to take the topography data in that area. Both data then will undergo processing and lastly will be compared to the volume of the slope using the global mapper.

Data Processing

Agisoft Software

The image that obtained from the drone will take a process in Agisoft Photoscan software. In the figure below, it shows the process involved in the Agisoft software. The quality of output can be set from low until ultra. The higher the setting for the output, the time taken to also become longer as the software needs to use almost the GPU in the laptop to produce the output. Use a high-end laptop or computer with a good graphic card can reduce the time taken for the software to produce the output such as digital orthophoto and DEM map.

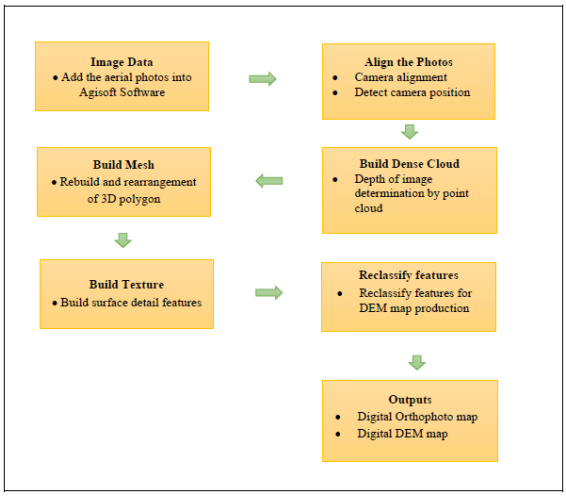

Figure 2 show the step involved in Agisoft

The result from the argisoft is the Orthophoto and DEM map produced from the image captured by the drone in the site project. There are many steps to process the data before the output can be generated. Start the process of importing images into Agisoft software. Align photo would be the first step in finding the camera positions for all photos available with the camera calibration parameter. After the alignment of the photo, the information will undergo a dense cloud phase. Dense cloud is the cloud point building process. The position of the point is determined by calculations of the same point in different images. Multiple images are used; the software can estimate the position of the point cloud. Next step is Build mesh where the process is to rearrange a dense cloud point to produce a 3D shape that represents the features on the surface. After that, the build texture process is a process to create a surface feature in another to generate an orthophoto. After done with the texture, the data will be reclassified. This step is important because it can classify the feature as trees and buildings. After all, DEM maps only provided ground elevation. Finally, export digital orthophoto and DEM maps as a final output.

Pix4D Software

The data that have been collected will undergo the process using Pix4D software. In the figure below, it shows the process involved in the Pix4D software. The time to process depending on how much data that the software needs to process and produce the output such as digital orthophoto and DEM map.

Perpustakaan Negara Malaysia eISBN 987-967-17889-6-7

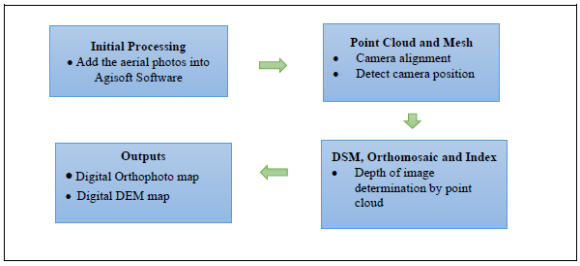

Figure 3 show the step involved in Pix4D

In the first step in Pix4D software is initial processing, the software will compute the key points on the images. It will use the key points to find the match between the photo that acquired. In this step, the software runs an Automatic Aerial Triangulation (AAT) and Bundle Block Adjustment (BBA). The second phase involved in this software is Point Cloud and Mesh. For this phase, the data will be increasing the density of 3D points from the 3d model that has been produced in the step first. This will make the data higher in accuracy for both Orthomosaic and DSM data. This phase contains two sections which are Point Cloud Densification that allows the user to define parameters for the point cloud densification and Point Cloud Classification that allows the user to classify the point cloud. The last step involved in this software is DSM, Orthomosaic, and Index. This step allows the user to change the options of the processing and the output parameter for DSM and Orthomosaic that have been produced in this step. In this phase, it has 4 section, which is resolution, DSM filters, Raster DSM, and Orthomosaic. The researcher can control the data using these 4 sections. The last step is Outputs which is the Digital Orthophoto map, and the Digital DEM map will be produced.

Global Mapper Software

To compute the volume calculation, the software that can be used to make the analysis is Global Mapper. This software can be used to calculate volumes and friendly interface and easier to export the data. The data from argisoft, which is digital orthophoto and DEM map, will be import and overlay the layer with the slope data from GNSS method. The layer shows the highest and lowest ground level, which is the value of volume automatically calculated. By using measure tools in the software, the volume will be shown.

Results and Analysis

Introduction

In this chapter, the analysis will be made based on the result produced from the data processing in chapter three. The data from Agisoft and Pix4d will be compared the accuracy and the data of UAV will be used in the Global Mapper. The result which is from the GNSS method and DEM from UAV image will undergo analysis which is based on its perimeter, area, volume, and the 3D model in the global mapper. Both results would be compared and do some analysis base on their different height and volume.

The Image of Orthophoto

The orthophoto image is the output that produces when using the software, either Agisoft or Pix4D. The result will be compared its accuracy to get the best data from both software. The data are conducted at Pekan Naka, Daerah Padang Terap, Kedah. The software will be used on the same laptop in making the Orthophoto data.

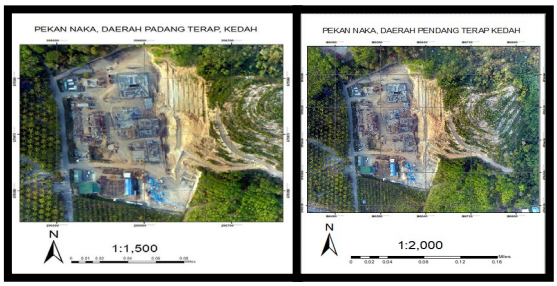

Figure 4 show the Orthophoto Image of Agisoft on the left and Orthophoto Image of Pix4D at the right

Accuracy of UAV Orthophoto Image

The accuracy of the image is measure by the square root value. The average set of squares root value will be computed to make the difference between the benchmark data and the data that will be compared and estimated the position accuracy. In this research, the data of RMSE with the total distribution of 5 GCP and 48VP in both Agisoft and Pix4D software and the result of the orthophoto image will be compared with the actual coordinate of GCP and VP with the coordinate generated by the software. The result is shown in the table below.

Table 1 Accuracy of the ortho-photo of Agisoft

Name	Count	X error (m)	Y error (m)	Z error (m)
GCP	5	0.0510536	0.04585	0.0534612
VP	48	0.50505	0.91482	0.190825

Perpustakaan Negara Malaysia eISBN 987-967-17889-6-7

Table 2 Accuracy of the ortho-photo of Pix4D

Name	Count	X error (m)	Y error (m)	Z error (m)
GCP	5	0.0662938	0.0713010	0.063362
VP	48	0.8485703	0.7185514	0.365653

In the result that has been produced in Table 4.1 and 4.2, it shows there is slightly different the error produced in both software. The Agisoft software shows the error that slightly low compared to the error generated from the Pix4D software. Therefore, the data from orthophoto that generated from the Agisoft are more accurate compared to the Pix4D software.

Volume calculation from GNSS Method

The result of calculates will be based on the grid that is made in the Global Mapper. This is to ensure both data can be compared within the same area. The grid is made with an interval of 10 meters, and the grid size is about 10-meter x 10-meter. The area in 1 grid made is 100m². The figure below shows the volume calculation in the project area, which is at Pekan Naka. Based on the grid that made, the total area is 900m² and the total volume 71063.045 cubic meter. The highest volume of the grid is on Grid 6, which is 8592.4255 cubic meter and the lowest in Grid 1, which is 7219.089 cubic meter.

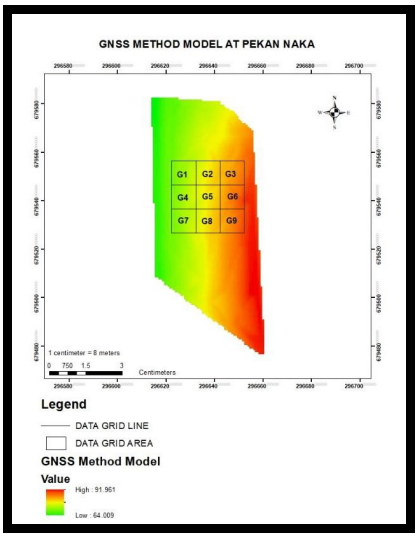

Figure 5 show the GNSS method map

The table below shows the result of every measured grid that is already calculated by the Global Mapper software. The analysis is made using the software and calculates the area and volume ³.

Table 3 show the data in GNSS method

Grid Area	Area (M²)	TOTAL_VOLUME (M³)
G1	100.04 m	7219.089 m
G2	100.04 m	7875.6313 m
G3	100.04 m	8417.7098 m
G4	100.04 m	7269.6641 m
G5	100.04 m	7897.8373 m
G6	100.04 m	8592.4255 m
G7	100.04 m	7251.3749 m
G8	100.04 m	7950.1554 m
G9	100.04 m	8589.1579 m

Global Mapper can be used to see the data in a 3D view. It generates the view to make the output become more realistic and can be used for visual analysis. The table below shows the 3D view data of the GNSS method. The green colour shows the lowest height, and the yellow one shows the point at the higher place.

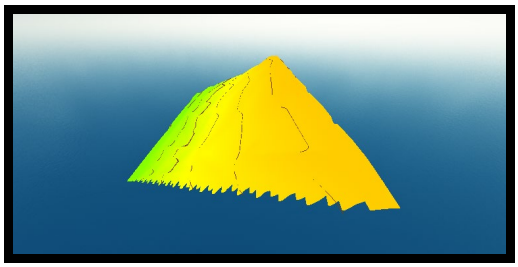

Figure 6 show the 3D view in Global Mapper

Volume calculation from Digital Model Surface from Agisoft Metashape.

The result is obtained from the field survey by using a UAV. The data will undergo processing in Agisoft Metashape. The figure below shows the volume calculation using the DEM in Pekan Naka. The grid is the same with the GNSS method with the interval of 10 meters and the grid size is about 10-meter x 10-meter. The area in 1 grid made is 100m². Based on the grid that made, the total area is 900m² and the total volume 69024.217 cubic meter. The highest volume of the grid is on Grid 9, which is 8341.8459 cubic meter and the lowest in Grid 7, which is 7037.4925 cubic meter.

Perpustakaan Negara Malaysia eISBN 987-967-17889-6-7

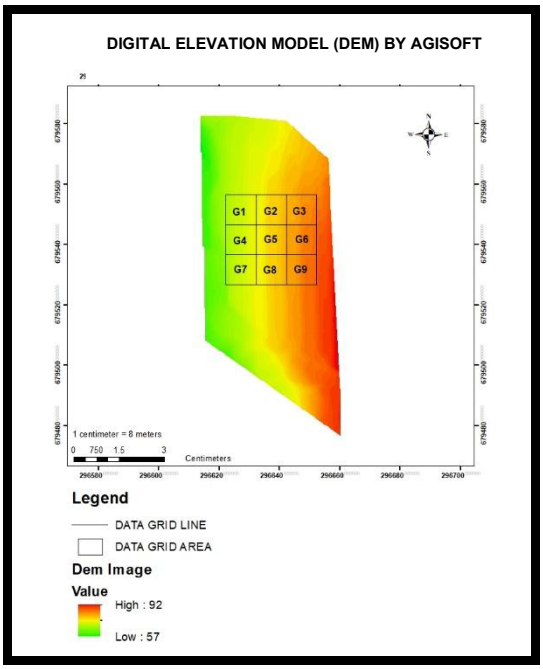

Figure 7 show a DEM map generated by Agisoft

The table below shows the result of every measured grid that is already calculated by the Global Mapper software. The analysis is made using the software and calculates the area and volume for the grid area.

Table 4 show the data in the DEM model generated using Agisoft

Grid Area	Area (M^2)	TOTAL_VOLUME (M^3)
G1	100.04 m	7067.7483 m
G2	100.04 m	7654.3074 m
G3	100.04 m	8197.4381 m
G4	100.04 m	7061.9892 m
G5	100.04 m	7681.4124 m
G6	100.04 m	8298.0427 m
G7	100.04 m	7037.4925 m
G8	100.04 m	7683.9406 m
G9	100.04 m	8341.8459 m

Global Mapper can be used to see the data in a 3D view. It generates the view to make the output become more realistic and can be used for visual analysis. The table below shows the 3D view data of the DEM. The green colour shows the lowest height and the yellow one shows the point at the higher place.

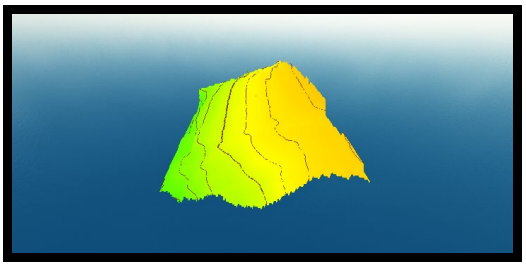

Figure 8 show the 3D view in Global Mapper

Volume calculation from Digital Model Surface from Pix4D.

The result for this section, the data was collected from field survey using a UAV and undergoing three processes, which is Initial processing, Point cloud and mesh and DSM, orthomosaic and index in Pix4D. The figure below shows the volume calculation using the DEM produce by this software. The grid is still the same with the GNSS method and Agisoft data with an interval of 10 meters, and the grid size is about 10-meter x 10-meter. The area in 1 grid made is $100m^2$. Based on the grid that made, the total area is $900m^2$ and the total volume 68473.735 cubic meter. The highest volume of the grid is on Grid 9, which is 8282.4993 cubic meter and the lowest in Grid 7, which is 6894.1402 cubic meter.

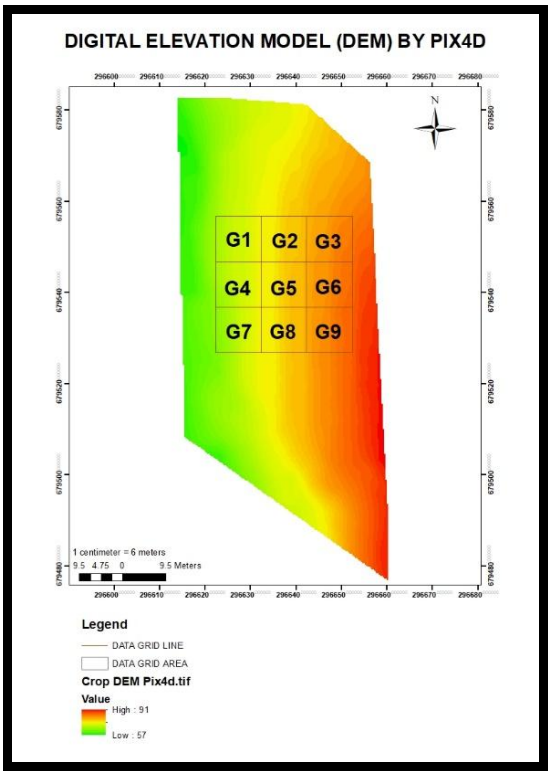

Figure 9 show the DEM map generated by Pix4D

Perpustakaan Negara Malaysia eISBN 987-967-17889-6-7

The table below shows the result of every measured grid that is already calculated by the Global Mapper software. The analysis is made using the software and calculates the area and volume for the grid area.

Table 5 show the data in the DEM model generated using Pix4D.

Grid Area	Area (M²)	TOTAL_VOLUME (M³)
G1	100.04 m	7014.6259 m
G2	100.04 m	7612.4650 m
G3	100.04 m	8165.2923 m
G4	100.04 m	6982.2092 m
G5	100.04 m	7642.8507 m
G6	100.04 m	8238.7974 m
G7	100.04 m	6894.1402 m
G8	100.04 m	7640.8549 m
G9	100.04 m	8282.4993 m

One of the features that exist in the Global Mapper is that it can render a 3D image based on the data given. The app can create a view to make it more practical and can be used for visual analysis. The table below displays the DEM 3D view data using Pix4D software. The green colour indicates the lowest height and the yellow one indicates the point at a higher level.

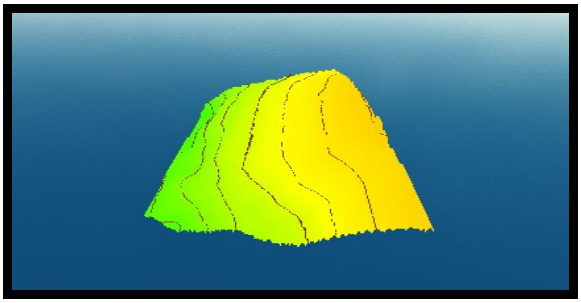

Figure 10 show the 3D view in Global Mapper

Analysis of different volume from DEM and GNSS method.

Based on the result, the volume is different between the two models. There are several analyses made, such as analyse the difference area and volume, land profile, and 3D view.

Comparison of area and volume

Table 6 show the comparison of area and volume between two model data

Grid	Area (M²)			Volume(M³)		
	GNSS Method	Agisoft	Pix4D	GNSS Method	Agisoft	Pix4D
G1	100.04 m	100.04 m	100.04 m	7219.089	7067.7483	7014.6259
G2	100.04 m	100.04 m	100.04 m	7875.6313	7654.3074	7612.465
G3	100.04 m	100.04 m	100.04 m	8417.7098	8197.4381	8165.2923
G4	100.04 m	100.04 m	100.04 m	7269.6641	7061.9892	6982.2092
G5	100.04 m	100.04 m	100.04 m	7897.8373	7681.4124	7642.8507
G6	100.04 m	100.04 m	100.04 m	8592.4255	8298.0427	8238.7974
G7	100.04 m	100.04 m	100.04 m	7251.3749	7037.4925	6894.1402
G8	100.04 m	100.04 m	100.04 m	7950.1554	7683.9406	7640.8549
G9	100.04 m	100.04 m	100.04 m	8589.1579	8341.8459	8282.4993
Total	900.36	900.36	900.36	71063.045	69024.217	68473.735
Different	0.00	0.00	0.00		2.8690%	3.6437%

Based on the comparison table, the data for the region does not vary because the grid region is made using the Global Mapper. The same grid is used for both details. For the measurement of volume, the overall volume indicates a difference. The total volume produced by Agisoft software is 69024.217 M³, and Pix4d data is 68473.735 M³. The data will then be compared to the GNSS method, which will display a difference of around 2.8690 percentage for Agisoft data and 3.6437 percentage for Pix4D data.

Comparison of path profile

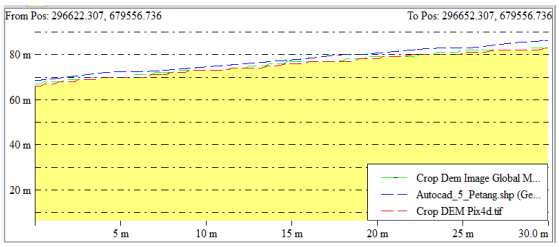

Figure 11 show the Path profile in line 1

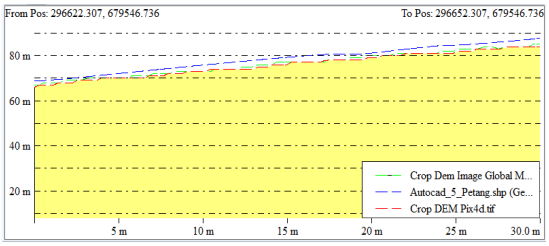

Figure 12 show Path profile in line 2

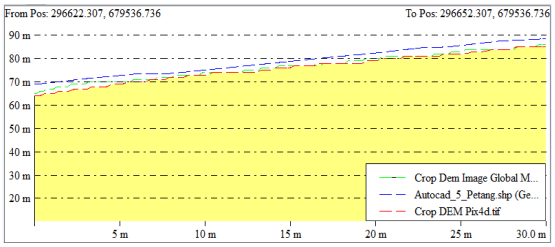

Figure 13 show Path profile in line 3

Perpustakaan Negara Malaysia eISBN 987-967-17889-6-7

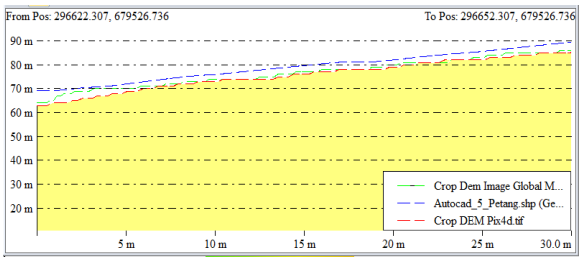

Figure 14 show Path profile in line 4

In the path profile, it shows that in line 1 until line 4, the blue line shows the height from the GNSS method, the green colour is DEM data process by Argisoft software and the red line is DEM data process by Pix4D software. Based on the result, it can be concluded that the data from the GNSS method are a little bit higher compared to both DEM data. The DEM data from Argisoft show a little bit higher compare to the DEM data from Pix4D. This shows that the agisoft makes a DEM more accurate comparison to the Pix4D software because the difference from GNSS method data is small compare to the different DEM generated by Pix4D.

Comparison in 3D view.

Based on the result, the 3D view from both the GNSS method and DEM image is slightly the same. It has a smooth surface in the 3D model, but the GNSS method model is a little bit smoother compared to the DEM image. DEM image has more texture and if the output is generated in the high setting output, more texture can be seen in the DEM data model. For both DEM data, the 3D view image shows that it almost identical with the same view and slightly different in texture because the error is given by the software that may be affecting the 3D view in Global Mapper.

Conclusion

In conclusion, the reliability of UAV photogrammetry for slope calculation shows the data difference between the GNSS method and DEM data for both software. The difference between both data is 2.8690% based on the volume for the DEM data generated by Agisoft and 3.6437% for DEM generated by Pix4D software. The cause of the difference in the result of the volume between the two data generated is the elevation difference. From the result, the Agisoft much better in data elevation compare to the data from Pix4D because the difference of total volume area is small in different compare to the total volume in Pix4D data. It shows that Agisoft is better to produce accurate data compare to the Pix4D software. In the big scale project or construction, the use of UAV in a measure of the earthwork volume can be calculated in a short amount of time compared to the other method. However, UAV has limited use in volume calculation depend on condition like in the closed area or have a lot of disturbance in the air. In short, the UAV method is proved can provide a volume calculation, but inaccuracy can be improved with the more accurate method in established the GCP and VP. The data can be used to give a clear picture of the slope measuring and volume calculation when wanting to do a project. Witl DEM IMAGE GNSS DATA DEM IMAGE PIX4D od, the surveyor will be more confi me measurement using UAV in a future project.

REFERENCES

Israelsen, J., Beall, M., Bareiss, D., Stuart, D., Keeney, E., & Van Den Berg, J. (2014). Automatic collision avoidance for manually tele-operated unmanned aerial vehicles. Proceedings - IEEE International Conference on Robotics and Automation, (August), 6638–6643. https://doi.org/10.1109/ICRA.2014.6907839

J. Leo Stalin, & RPC. Gnanaprakasam. (2017a). Volume Calculation from UAV based DEM. International Journal of Engineering Research And. https://doi.org/10.17577/ijertv6is060076

J. Leo Stalin, & RPC. Gnanaprakasam. (2017b). Volume Calculation from UAV based DEM. International Journal of Engineering Research And, V6(06), 126–128. https://doi.org/10.17577/ijertv6is060076

McAree, O. (2013). Autonomous terminal area operations for unmanned aerial systems. Retrieved from https://dspace.lboro.ac.uk/2134/12535

Seyyedhasani, H. (2018). INTELLIGENT UAV SCOUTING FOR FIELD.

Yoo, C. I., & Oh, T. S. (2016). Beach volume change using UAV photogrammetry Songjung beach, Korea. International Archives of the Photogrammetry, Remote Sensing and Spatial Information Sciences - ISPRS Archives, 41(July), 1201–1205. https://doi.org/10.5194/isprsarchives-XLI-B8-1201-2016

Zahawi, R. A., Dandois, J. P., Holl, K. D., Nadwodny, D., Reid, J. L., & Ellis, E. C. (2015). Using lightweight unmanned aerial vehicles to monitor tropical forest recovery. Biological

Perpustakaan Negara Malaysia eISBN 987-967-17889-6-7

Conservation, 186, 287–295. https://doi.org/10.1016/j.biocon.2015.03.031

Ghilani, C. D., & Wolf, P. R. (2012). Elementary surveying an introduction to geomatics.PhD Proposal. https://doi.org/10.1017/CBO9781107415324.004

Hugenholtz, C. H., Walker, J., Brown, O., & Myshak, S. (2015). Earthwork volumetrics with an unmanned aerial vehicle and softcopy photogrammetry. Journal of Surveying.

Perpustakaan Negara Malaysia eISBN 987-967-17889-6-7

Drone Applications for Sandy Beach Changes in Monsoon Environment

Adina Roslee[1], Effi Helmy Ariffin[1,2] & Azam Yaakob[2]

[1]School of Marine Science and Environment, Universiti Malaysia Terengganu, 21030 Kuala Nerus, Terengganu, Malaysia
[2]Institute of Oceanography and Environment, Universiti Malaysia Terengganu, 21030 Kuala Nerus, Terengganu, Malaysia

Email: effihelmy@umt.edu.my

Abstract

The changes in beach morphology associated with storm season and anthropogenic activities can give the highest impact on our society. The purpose of this study is to evaluate topographic changes of beach area at Pengkalan Maras coast in Kuala Nerus, Terengganu using Unmanned Aerial Vehicle (UAV) survey. In further, can be used for various applications including mapping of the coastal area. In this study, a low coast of drone (DJI Mavic 2 Pro) was used to remotely sense the beach morphology over large spatial scales within a short time (less than 30 minutes of flight) and manage to obtain digital elevation models (DEM) and orthophotos of the coast. For the accurate generation of results, interior and exterior orientation are corrected using the camera calibration. Furthermore, the intensive of Ground Control Points (GCP) are being set up by using the Real-Time Kinematic (RTK) instrument in order to correct the position accuracy of UAV. In addition, the aerial survey reveals for two monsoon seasons which are northeast monsoon storm and the southwest monsoon (calm condition) with tend as worse during storm seasons. Thus, this study could serve as an indicator that an accurate aerial survey can be achieved during monsoon seasons with the support of this detailed spatial information.

Keywords: Aerial survey, Unmanned Aerial Vehicle (UAV), digital elevation models (DEM), beach erosion, monsoon

Introduction

Coastal zone is a transition area between the terrestrial and marine environments. It is a very dynamic environment which related to many physical processes, such as sea-level rise, land subsidence, tidal inundation and erosion-deposition (Yaakob et al., 2018). The physical processes play a crucial role in the changes in the shoreline and coastal topography. However, the dynamic equilibrium of the coastal zone does not only depend on natural forces, but also by anthropogenic activities (Ariffin et al., 2019). The coastal zone provides various services and has become an important region for human activities. Human activities that are actively growing in coastal zones have often caused or enhance various development of coastal structure, such as seawalls and breakwaters, and the advancement of artificial shoreline by land reclamation (Ariffin et al., 2019; Yaakob et al., 2018). Unfortunately, these factors are leading us to the environmental problems in our coastal area such as beach erosion, resource depletion, environmental degradation and destruction of natural habitats (Muslim et al., 2007).

Problem Statement

Due to environmental issues, coastal mapping is necessary for coastal monitoring to manage the coast in a sustainable way. According to Darwin et al., (2018), the generated map can provide coastlines information, land condition, coastal terrain, buildings and residential area. In addition, coastal erosion mapping is frequently used as a preference for stakeholders and agencies to assist in decision making. Chen & Chang (2009) had affirmed, traditional methods for coastal mapping can be based on conventional field surveys or on the interpretation of the aerial photograph. Even though the field survey is using Real-Time Kinematic Global Positioning System (RTK GPS), it still factitious and require a lot of time and manpower. For aerial photograph survey, it is involved a big amount of cost to have frequent coastal monitoring. On the other hand, during the

Perpustakaan Negara Malaysia eISBN 987-967-17889-6-7

storm seasons, it also can be a challenge to identify the aerial photography data such as cloud cover. Normally the cloud cover can be scattered in a monsoon dominated coastal, which is the type of hot and humid of country.

The solution to the Problem

In this era, there are many alternatives in producing the map, and recently, unmanned aerial vehicle (UAV) survey is one of the practical methods. It is one of a low-cost technique with time constraints, and few manpower involves rather than using satellites or expensive manned aircraft. In this case, the study area is located at Pengkalan Maras beach, Kuala Nerus, Terengganu, where located on the east coast of Peninsular Malaysia (Figure 1). The objective of this study is to evaluate the coastal mapping by using UAV at a different season of monsoons which are during northeast monsoon and southwest monsoon. This can achieve the different of weather comparison which northeast monsoon as a storm condition and southwest monsoon reveal a calm condition.

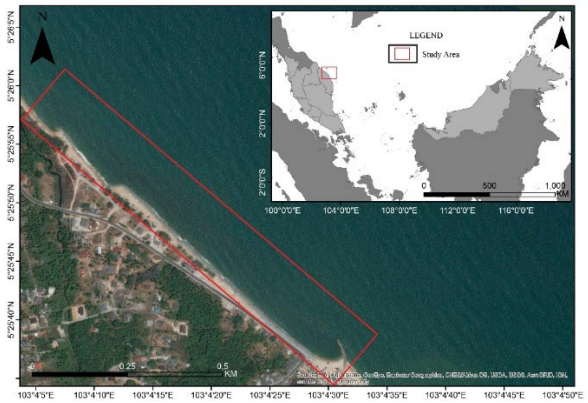

Figure 1: Map of the study area

Coastal Setting

The study area is located on the east coast of Peninsular Malaysia, which the region is in the South China Sea. The South China Sea is the largest semi-enclosed marginal sea in the western North Pacific Ocean, and it is located between 0° – 25° N and 99° – 122° E. The South China Sea experiences strong seasonal variation that area typically associated with the northeast and southwest monsoon system (Kok et al., 2015). Between November and March, there is a northeasterly wind over the South China Sea during the northeast monsoon while between May and September, there is southwesterly wind over the South China Sea during the southwest monsoon. The monsoon transition period is normally in April and October, which the wind is calm and vary in direction (Akhir et al., 2014; Kok et al., 2015).

The east coast of Peninsular Malaysia is located in the southwest region of the southern South China Sea, which in the shallow Sunda Shelf area (Kok et al., 2015). And one of the states that facing the South China Sea is the Kuala Nerus, Terengganu. The coastline of Kuala Nerus is relatively straight for approximately 30km. This region is experiencing wet equatorial climate which high temperature all year and irregular heavy rainfall. The mean annual temperature lies in the range of 25.6 °C – 33.8 °C. Based on Ariffin et al. (2018), the monsoon period has also affected by the rainfall distribution. The high frequency of rainfall in Kuala Nerus is from November to January with an average of 830 mm. In addition, tides in Kuala Nerus are normally semi-diurnal and micro to meso-tidal.

Ariffin et al. (2016) stated during the northeast monsoon season; the coastal area is exposed to strong currents and waves where the surface current is flowing southward along the east coast. The winds are onshore making the strong wave during the northeast monsoon. However, during the southwest monsoon season, the winds are offshore and low energy which resulted in the current moves toward the north and it change with similar strength flowing to the south (Ariffin et al., 2016; Rosnan et al., 2003).

This study is focused on 1.3 km long of the coastal area which located at Pengkalan Maras beach, Kuala Nerus, Terengganu (Figure 1). It is one of the productive areas with recreational activities, tourists spot and residential area. This area is also the fisheries area where the fishermen dock their boats and operate their business here. The aerial survey focuses on the shoreline area where it started from the vegetation line until the lowest tide of water line.

Planning Structure

DJI Mavic 2 Pro is used in this study which gives us better quality and high-resolution images compared to other models of drones. The specifications of the UAV are given in Table 1. The survey lines are planned in LITCHI, a third-party application at an average flight altitude of 160m and acquisition is automatic set on one shot per second. The take-off and landing operations are manually driven by a remote pilot, and the survey has been conducted for northeast monsoon (November 2017 until January 2018) and the southwest monsoon (June 2018 until August 2018) at every fourth week (Casella et al., 2016; Mancini et al., 2013). Then, the original image collection had been processed in the software package called PhotoScan from the Russian

Perpustakaan Negara Malaysia eISBN 987-967-17889-6-7

manufacturer AgiSoft LLC (Mancini et al., 2013) and the steps are according to Figure 2.

Table 1: Specifications system and parameters of UAV

Type	DJI Mavic 2 Pro
Weight	907g
Flight speed	Ascend: 4 m/s, Descend: 3 m/s
Maximum flight speed	72 kph
Maximum flight time	31 kph
Operating temperature range	-10 ºC – 40 ºC
Satellite positioning system	GPS/GLONASS
Hovel accuracy range	Vertical ± 0.1m (when Vision Positioning) ± 0.5m (when GPS Positioning) Horizontal ± 0.3m (when Vision Positioning) ± 1.5m (when GPS Positioning)
Sensor	1 CMOS Effective pixels: 20 million
Lens	FOV about 77o 35mm Shooting range: 1m - ∞ º
Operating environment	Surface with clear pattern, adequate lighting (lux>15) & detects diffuse reflective surfaces (walls, trees, people, etc.)

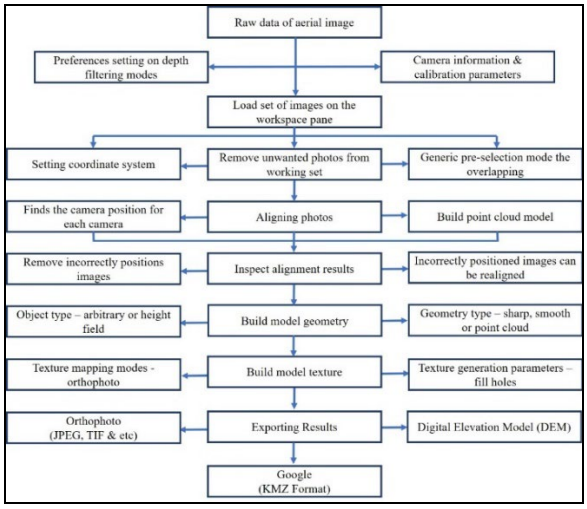

Figure 2: The workflow of aerial image processing in Agisoft Photoscan.

In the first step, the images were performed in the alignment process to detect the image feature points and reconstruct the movement along the sequence of images. Next, a pixel-based dense stereo reconstruction performed starting from the aligned dataset so that the original images could have meshed. Before that, amongst available stereo matching procedures implemented in PhotoScan, the height field was recommended due to the aerial surveys (Mancini et al., 2013). Next, the texturing step have applied to mesh and the point cloud is framed in the UTM 48N coordinates system. Lastly, once the images meshed, the image was exported into orthomosaic in tiff format and georeferencing the image in GIS. For georeferencing, 86 points of Ground Control Point (GCP) are taken by using Real-Time Kinematic Network (RTK-NET) in order to correct the UAV position area (Figure 3). This step is important to a term case which series of the image need to be analysed and the more GCP we take, the better the validation of the image (Kim et al., 2016).

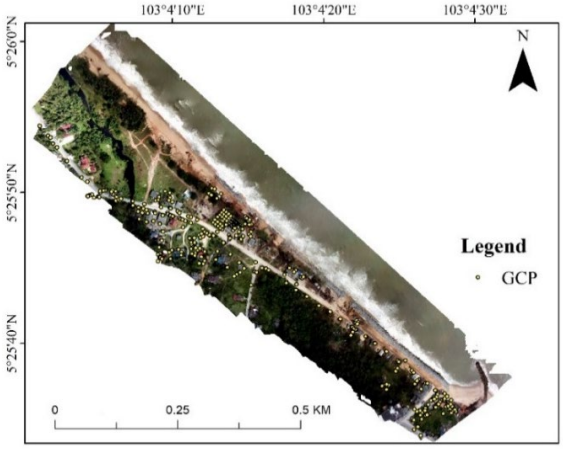

Figure 3: Map of Ground Control Point (GCP) for georeferencing.

Knowledge impact

There are two main results produced from the analysis, which are orthophoto and DEM. In general, orthophoto shows the planimetric position, which is the Easting and Northing, while DEM shows the elevation value (Darwin et al., 2018). The orthophoto accuracy, which includes the planimetric coordinate shall not exceed RMSE value of 1 meter for the scale of 1:40000.

The results of this study will give beneficial to coastal mapping. The quality of the photos releases high degree of detail achieved as it can see clearly not only the coastline but including small height variations such as high-tide water line, small rocks and sediment in the nearshore are visible over the whole extent of the mapped area. Moreover, the DEM shows the elevation of the study area, which erosion

Perpustakaan Negara Malaysia eISBN 987-967-17889-6-7

and accretion are detected in the area during the different monsoon.

Contribution to society and country

High precision and resolution of orthophoto maps and 3D visualisations are hardly achieved from satellite datasets due to the time consuming and resource-intensive (Topouzells et al., 2017; Yoo & Oh, 2016). Even though LIDAR can give high-resolution data products, but it is limit to a certain area. Manned aerial systems and traditional satellite are also can be very challenging due to the deals related to mobilization expenses, cloud cover and resolution (Yang et al., 2019; Yoo & Oh, 2016). Therefore, the UAV-based data gives many valuable opportunities to the scientist and stakeholders in coastal mapping and monitoring such as erosion detection, landscape development and other environmental applications.

Cost-benefit

The benefit of cost using the UAV techniques with a drone as a medium for an aerial photograph survey, it can be indicating less compare using the satellite imagery. Hence, the high resolution without cloud cover interference, it can be more efficient and valuable.

Commercialization potential

In this revolutionary era, technology can make everything possible in this research field. The integration of UAV techniques, photogrammetric software and analysis tools can give new enlightenment into the modification of coastal landscapes by studying the topographic change at advance levels of spatial and temporal detail. Therefore, the results can offer important information to the coastal management and stakeholders in making sustainable development in the coastal area.

REFERENCES

Ariffin, E. H., Sedrati, M., & Daud, N. R. (2019). Shoreline Evolution Under the Influence of Oceanographic and Monsoon Dynamics: The Case of Terengganu, Malaysia. In *Coastal Zone Management*. https://doi.org/10.1016/B978-0-12-814350-6.00005-7

Ariffin, E. H., Sedrati, M., Akhir, M. F., Daud, N. R., Yaacob, R., & Husain, M. L. (2018). Beach morphodynamics and evolution of monsoon-dominated coasts in Kuala Terengganu, Malaysia: Perspectives for integrated management. *Ocean & Coastal Management*, *163*, 498-514.

Ariffin, E. H., Sedrati, M., Akhir, M. F., Yaacob, R., & Husain, M. L. (2016). Open Sandy Beach Morphology and Morphodynamic as Response to Seasonal Monsoon in Kuala Terengganu, Malaysia. Journal of Coastal Research,75(Sp1), 1032-1036. doi:10.2112/si75 207.1

Akhir, M. F., Zakaria, N. Z., & Tangang, F. (2014). Intermonsoon variation of physical characteristics and current circulation along the east coast of Peninsular Malaysia. *International Journal of Oceanography*, *2014*.

Casella, E., Rovere, A., Pedroncini, A., Stark, C. P., Casella, M., Ferrari, M., & Firpo, M. (2016). Drones as tools for monitoring beach topography changes in the Ligurian Sea (NW Mediterranean). *Geo-Marine Letters*, *36*(2), 151-163.

Crowell, M., Edelman, S., Coulton, K., & McAfee, S. (2007). How Many People Live in Coastal Areas? Journal of Coastal Research: Volume 23, Issue 5: pp. ii-vi.

Del Valle, A., Eriksson, M., Ishizawa, E. O. A., & Miranda, J. J. (2019). Mangroves for Coastal Protection: Evidence from Hurricanes in Central America. *World Bank Policy Research Working Paper*, (8795).

Foster, D. S. & Colman, S. M. (1991). Preliminary interpretation of the high-resolution seismic stratigraphy beneath Lake Michigan, U.S.G.S. Open File Report 91-21, 42 pp., 2 plates.

Frihy, O. E. (2001). The necessity of environmental impact assessment (EIA) in implementing coastal projects: lessons learned from the Egyptian Mediterranean Coast. *Ocean & Coastal Management*, *44*(7-8), 489-516.

Perpustakaan Negara Malaysia eISBN 987-967-17889-6-7

Griggs, G. B., & Tait, J. F. (1988). The effects of coastal protection structures on beaches along northern Monterey Bay, California. Journal of Coastal Research, 93-111. Hays, G. C. (2017). marine life. *Current Biology*, *27*(11),R470-R473. https://doi.org/10.1016/j.cub.2017.01.044

Hutchinson, D. R. & Hart, P. E. (2004). Cruise Report for G1-03-GM, USGS Gas Hydrates Cruise, R/V Gyre, 1-14 May 2003, Northern Gulf of Mexico, USGS Open-File Report 03-474, online.

Klein, A. D. F., Silva, G. M. D., Ferreira, O., & Dias, J. A. (2005). Beach sediment distribution for a headland bay coast. *Journal of Coastal Research*, 285-293.Kok, P. H., Akhir, M. F., & Tangang, F. T. (2015). Thermal frontal zone along the east coast of Peninsular Malaysia. *Continental Shelf Research*, *110*, 1-15.

Koraim, A. S., Heikal, E. M., & AboZaid, A. A. (2011). Different Methods Used for Protecting Coasts from Sea Level Rise Caused by Climate Change. *Current Development in Oceanography*, *3*(1), 33–66. Retrieved from http://pphmj.com/journals/cdo.htm

Kulkarni, R. (2013). Numerical Modelling of Coastal Erosion Using MIKE 21. Coastal and Marine Engineering and Management.

Leatherman, S. P., Davison, A. T., & Nicholls, R. J. (1994). Coastal geomorphology. *Environmental Science in the Coastal Zone: Issues for Further Research*, 44-48.

Mancini, F., Dubbini, M., Gattelli, M., Stecchi, F., Fabbri, S., & Gabbianelli, G. (2013). Using unmanned aerial vehicles (UAV) for high-resolution reconstruction of topography: The structure from motion approach on coastal environments. *Remote Sensing*, *5*(12), 6880-6898.

Pranzini, E., Wetzel, L., & Williams, A. T. (2015). Aspects of coastal erosion and protection in Europe. Journal of coastal conservation, 19(4), 445-459.

Rosnan, Y., & Ariffin, E. H. (2010). Effects on sedimentology and beach morphology on tourism at Terengganu Beach, Malaysia. In *International Annual Symposium Universiti Malaysia Terengganu* (pp. 553-557).

Short, A. D. (2012) Coastal Processes and Beaches. *Nature Education Knowledge* 3(10):15

Scheffers, A. M., Scheffers, S. R., & Kelletat, D. H. (2012). Coastal Landforms and Landscapes. In: The Coastlines of the World with Google Earth. Coastal Research Library, Vol 2. Springer, Dordrecht.

Spalding, M. D., Ruffo, S., Lacambra, C., Meliane, I., Hale, L. Z., Shepard, C. C., & Beck, M. W. (2014). The role of ecosystems in coastal protection: adapting to climate change and coastal hazards. Ocean & Coastal Management, 90, 50-57.

Thieler, E. R., Himmelstoss, E. A., Zichichi, J. L., & Ergul, A. (2009). The Digital Shoreline Analysis System (DSAS) version 4.0-an ArcGIS extension for calculating shoreline change (No. 2008-1278). US Geological Survey.

Perpustakaan Negara Malaysia eISBN 987-967-17889-6-7

An Overview on Malay Reserve Enactment between States in Peninsular Malaysia

Siti Maryam Abdul Wahab[1], Nurul Atikah bt Rosli[1]

[1]Faculty of Architecture, Planning & Surveying, Universiti Teknologi MARA, Perlis Branch, Arau Campus, 02600 Arau, Perlis, Malaysia

Email: sitimaryam@uitm.edu.my

Abstract

Malay Reserve Land is interpreted as a unique reservation category of land in Malaysia. According to Federal Constitution, it can only be owned or transacted between Malays. There are a few Malay Reservation Enactments practice among states in Peninsular Malaysia since the determination of Malay status upon individual is given under the power of the state. The lands under the Malay reservation are restricted from sale, lease, transfer of title and mortgage to non - Malays. However, there are many reports and forums discussed on the decreasing of Malay Reserve Land. It is in critical situation and if Malay Reserve Land is not protected, the rights of Malay of the country will eventually disappear. This study is conducted to compare the implementation of Malay Reserve Enactment between states in Malaysia. The objectives of this research are to study on the definition of Malay and its implementation in various state's enactment and the Federal Constitution, to analyse the exchange condition of Malay Reservation land in land conversion, and to map the spatial changes of Malay Reservation Land in Kedah as a sample evident of area. It hoped that, with the identification of the decrease and some of the proposed ways of protecting Malay Reserve Land in this study, it would help the authorities to maintain and enhance the value of Malay Land Rights in the future.

Keyword: Malay Reserve Enactment, land dealing, exchange condition

1.0 Introduction

Malay Reserve Land (MRL) is known as a unique reservation's category of land in Malaysia which is to be allocated with certain portion for each State in Peninsular Malaysia, except Melaka and Pulau Pinang. The land dealings processes and procedures exercised in the stated States are under the power of Sultans and the State Authority. The parties involved in the dealings should be the "Malay" and any dealing with non-Malay can be considered null and void. This special provision is intentionally to protect the Malay rights on the land as stipulated in "Seven Wills of the Malay Rulers". The Wills is then outlined in Federal Constitution to be followed by the Federal and State level.

The specific article mentioned on Malay Reservation is under Art. 89, Federal Constitution, where it outlines on the type of land that can be put under Malay reservation. However, the definition of "Malay" is subject to the Enactment of the Legislature of the State. According to Art 89 (6), "Malay reservation" means land reserved for alienation to Malays or to natives of the State in which it lies; and "Malay" includes any person who, under the law of the State in which he is resident, is treated as a Malay for the purposes of the reservation of land. The statement of "under the law of the State" may contribute the discrepancy and flexibility of Malay definition between the states. Therefore, even they have similarities in the process and procedures for land dealings, the main differentiation can occur in how state defined the person or corporation as "Malay". Due to that, this paper will discuss the differentiation of "Malay" or "Malayan" as define in Malay reservation enactment between the applied States.

The highlighted issue of MRL in media discussion mostly regarding the shortage of total area and lower value than open land market. For instance, as released by MetroTV on 17 September 2020 (*Apa Sudah Jadi dengan Tanah Rizab Melayu*), BHOnline on 16 August 2019 (*Tanah Rizab Melayu Terengganu Kritikal*) and Bernama on 1 November 2018 (*Penyusutan Tanah Rizab Melayu: Tangani Sebelum Parah*). All those articles trigger the

Perpustakaan Negara Malaysia eISBN 987-967-17889-6-7

readers and Malay residents as well in getting the real spatial information on the status of Malay's land disposal. The author believe that a proper spatial information should be shared to the citizen to create Malay's self-awareness in understanding their position and power in land holding.

Thus, the first objective of this study is to give an overview MRL in Enactment of the Legislature of the State. The critical discussion will muchly be focused on the definition of Malay. The comparison will be based on six enactments which are Malay Reservation Enactment (FMS Cap 142), Malay Reservation Enactment Kelantan 1930, Malay Reservation Enactment Kedah 1931, Malay Reservation Enactment Perlis 1935, Malay Reservation Enactment Johor 1936 and Malay Reservation Enactment Terengganu 1941.

The second objective is to provide a sample of geospatial mapping regarding the changes of the Malay land reservation status in an area in Kedah. This sample may help the reader to understand the dynamic of spatial changes in MRL status where it can also happen anywhere else in Peninsular Malaysia due to the development needed in the state.

2.0 Study Area

This study focuses on comparing differences in Malay Reserve Land between states. This study areas are located at the Peninsular Malaysia and there are two states that are excluded from this research which are Melaka and Pulau Pinang. This study areas were chosen according to Federal Constitution and State Malay Reservation Land Enactment. Melaka and Pulau Pinang are exempting from this study due to the absence of Malay Reserve Land Enactment or guideline for both states. The purpose of this study is to identify the discrepancies of those enactment for every state based on the data from PTN. This study covered a total area of 197,927 square kilometers (km^2) that includes nine states which are Selangor, Perak, Negeri Sembilan, Pahang, Johor, Kedah, Terengganu, Kelantan and Perlis. Based on 2018 Peninsular Malaysia data, the reserved land areas in these states covers 4,831,894.86 hectares. It was stated by Deputy Director General of Land and Federal Minerals Departments on Malay Reserve Land Convention on 28th February 2019 in Convention of Malay Land Reservation 2019. For spatial changes, the area is at sub – district Jabi in Kedah. This study area was chosen according to the purpose of this research which is to view any depletion of Malay Reserve Land at Jabi.

3.0 Methodology

This research is conducted to identify the current issues that are related to the depletion of Malay Reserved Land. The information was gathered from many sources such as National Land Code (NLC), newspaper, journal, and Federal Constitution to construct literature review.

The spatial changes Kedah state is selected for this study. At first, the data of MRL was collected from two different PTD offices. Both release two different types of data. It is important to get a good data to produce a good map and an accurate result. PTD provide the data of Malay Reserve Land area, the cancellation and replacement of Malay Reserve Land. Meanwhile, JUPEM provide a sample lot and contains related information of the lot such as file survey number, code type of lot, explanation of the land, legislation, date of the gazette, area, bearing, boundary distance and many more are also included in the database and can be obtained in the map info table file format. The sample of production of Malay Reserve area in only at Jabi, Kedah. The data provided in the table below is the summary of Malay Reserve Land in Kedah.

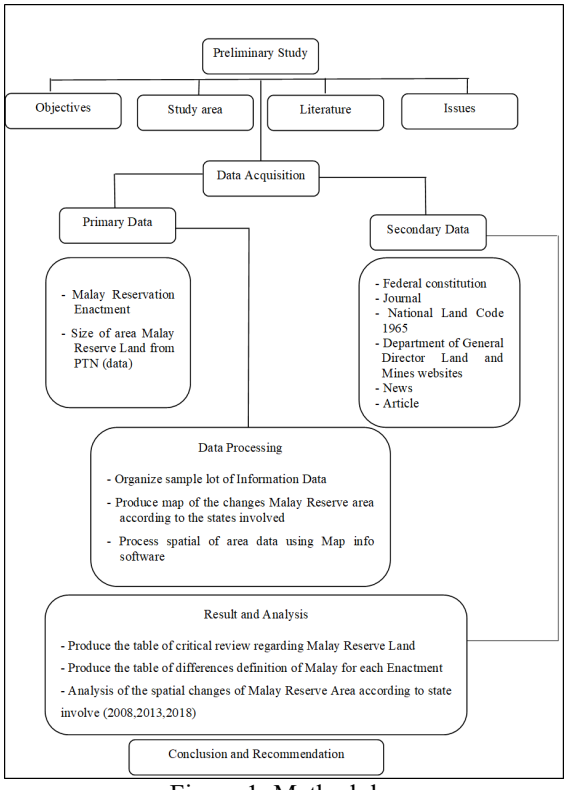

Figure 1: Methodology

Perpustakaan Negara Malaysia eISBN 987-967-17889-6-7

Table 1: Area of Malay Reserve Land in Kedah

Total area of Kedah (Hectare)	Original Area of MRL 1933 (Hectare)	Area of MRL 2008 (Hectare)	Area of MRL 2013 (Hectare)	Area of MRL 2018 (Hectare)
942 700	721 496.949	721 505.67	721 507.48	721 508.28

Table 2: Cancellation and Replacement of Malay Reserve Land in Kedah

No	Year	Area of Cancellation MRL (Hectare)	Area of Replacement MRL (Hectare)
1	2008	100.0002	108.7165
2	2013	21.7689	32.3029
3	2018	247.5261	250.9914

3.1 The Sample size of Malay Reserve Land

The sample size of Malay Reserve Land is used to refer the area of study either it was depleted or not over years. The data of Malay Reserve Land was stated by Deputy Director General of Land and Federal Minerals Departments on Malay Reserve Land Convention on 28th February 2019 in Convention of Malay Land Reservation 2019. The sample size of Malay Reserve Land is the biggest factor on why this research is carried out. The analysis of this sample will be discussed in the result section to complete the third objective. The info data provided by JUPEM can be view in info tools through map info software. It is used to classify the type of data such as the aim of gazette, date of gazette and the updated files.

4.0 Analysis and Result

4.1 The Implementation of Malay Reserve Enactment

The implementation of each Malay Reserve Enactment (MRE) has few similarities in characteristics, although there are separate enactments used in all states in Peninsular Malaysia excluding Pulau Pinang and Melaka. The uniqueness of MRE according to the specific characteristic is used to protect the significant of the enactment itself. Therefore, each enactment provides the restriction according to suitability of the state (Aliasak M.H.H, 2014)

4.2 Restriction against Alienation

State government could only alienate land to Malay and all the Enactment include restriction against alienation. In section 7 MRE of Perlis 1353 emphasis the restriction against alienation which stated that no state Land that are included in a Reservation shall be alienated, sold, leased or otherwise disposed to any person who is not either a Malay or a Siamese. While in MRE Johor 1936, the restriction against alienation is discussed in section 8 which declare that no state land that are included within a Malay Reservation shall be alienated to any person not being a Malay. This implies that if an application for land by a person not being a Malay has been approved prior to the declaration of Malay Reservation, the land that was subjected to such application may be alienated to a person not being a Malay. Section 8 of MRE Terengganu 1941 firm that the restriction on alienation state that no state Land that are included within a Malay Reservation shall be sold, leased or otherwise disposed to any person not being a Malay or in Malay holding company. Section 5 MRE Kedah 1931 stated that all alienated land or state land included within boundaries declared under section 3 or 4 shall be included in a Malay Reservation. It also emphasis that no land shall be declared to be in any Malay reservation which at the time of coming into force with this enactment. The restriction in alienation in MRE Kelantan 1930 stated in section 6, no state land that are included in Malay reservation shall be sold, leased or otherwise disposed to any person not being a Malay, save as provided in this enactment.

4.3 Restriction against Dealings

Any sale or purchase of Malay Reserve Land shall be only between Malays. In section 2 of MRE Perlis 1935 stated that the restriction of dealings in reservation land as follow: “Save as hereinafter provided in this enactment, no reservation land held under a document of title by any Malay shall be mortgaged, charged or leased to any person who is not a Malay and no Reservation land held under a document of title by any Siamese shall be mortgaged, charged or lease to any person who is not either a Malay or Siamese”. Through this section it implies that any dealings in reservation land with non-Malay and Siamese is null and voided. In section 8 of Johor MRE 1936 stated that the restriction as to dealing with the statement every memorandum of transfer, charge or lease of a Malay holding which is executed on behalf of the proprietor thereof by any person not being a Malay who purports to act as attorney of such proprietor shall be void and incapable of registration in any Land Office. While in section 12 of MRE Terengganu 1941 stated that the restriction as to dealings by attorneys; every memorandum of transfer,

Perpustakaan Negara Malaysia eISBN 987-967-17889-6-7

charge or lease of a Malay holding which is executed on behalf of the proprietor thereof by any person who purports to act as attorney of such proprietor shall be void and no such memorandum of transfer, charge or lease shall be capable of registration in any Land Office or Registry of Titles. The restriction against dealing in MRE Kedah is covered by section 11 which present the restriction sale of reservation land to non- Malays. Any reservation land held by a Malay or Siamese under any document of title is subject of a charge created prior to the declaration by which the land was included in Malay Reservation, or where the owner of such land had prior to such declaration entered into an agreement or was under a legal obligation to transfer such land to a person not being a Malay or Siamese, such land may, with the written consent of the Ruler in Council and subject to such condition or limitations as the Ruler in Council may see fit to annex such consent, be sold in the case of a charge to a person of any race upon the application of the charge, and in the case of an agreement or legal obligation to transfer, be transferred, irrespective of race, to the person whom the owner had agreed or was otherwise under a legal obligation to transfer the land or the heirs or assigns of such person. In section 9 of F.M.S Cap 142, there are a restriction as to dealings by attorney which stated that every memorandum of transfer, charge or lease of a Malay holding which is executed on behalf of the proprietor thereof by any person not being a Malay who purports to act as attorney of such proprietor shall be void and no such memorandum of transfer, charge or lease shall be capable of registration in any Land Office or Registry of Titles. In section 8 of MRE Kedah states that no state land included in a Malay Reservation shall be sold, leased or otherwise disposed to any person who is not either a Malay or a Siamese certified by the Director in writing to be a Siamese agriculturist, permanently resident in the state. In section 12(i) of MRE Kelantan, all dealing or disposals of whatsoever and all attempt to deal in or dispose of reservation land contrary to the provisions of this enactment shall be null and void.

4.4 Room for Revocation

In term of size, location and classification, the ruler of the state has the right to alter these things. Section 4 MRE of Perlis declare that the state council may at any time alter the limits or boundaries of any reservation, revoke any declaration under section 3 either as to the whole or any part of the area therein referred to and include in any reservation of any land excludes therefrom. If there such alteration, revocation or exclusion shall take effect on such date as may be fixed by the state council. The Johor MRE also state the alteration and revocation of Malay Reservation under section 4. The commissioner may at any time, with the approval of His Highness, the Sultan in the council, may declare and publish the Gazette after the limit or boundaries of any Malay reservation or revoke any declaration whereby any land has been declared to be a Malay Reservation, either as to the whole or any part of the area therein referred, to or include in any Malay reservation, any excluded therefrom. For MRE Terengganu, the alteration and revocation of Malay reservation is in section 4. The Sultan in the council may at any time by declaration published the Gazette after the limits or boundaries of any Malay reservation or revoke any declaration whereby any land has been declared to be a Malay Reservation, either as to the whole or any part of the area therein referred to or include in any Malay Reservation, any land excluded therefrom. The alteration and revocation of Malay Reservations in F.M.S Cap 142 is discussed in section 4 which it states that the Head of State may at any time, with the approval of the Ruler of the State in Council by declaration published the Gazette and alter the limits or boundaries of any Malay Reservation, revoke any declaration whereby any land has been declared to be a Malay Reservation, either as to the whole or any part of the area therein referred to or include in any Malay Reservation, any land excluded therefrom. Section 4 in MRE Kedah, the Ruler in the Council may at any time either at its own instance or upon the application of any person by declaration gazette and alter the limits or boundaries of any Malay Reservation or revoke any declaration under section 3, either as to the whole or any part of the area therein referred to.

Any laws which contradict to this enactment is automatically be nulled and voided. The MRE has been enacted in several states, and this resulted in the definition of 'Malay' changing as well as the meaning of "anyone defined as Malay" in the MRE. Although the definition of 'Malay' in the MRE of each state varies, it does not contradict the term 'Malay' as defined in the Federal Constitution (Emie Mizura, 2008). However, when in doubt as to either a person is Malay or not, it should be referred to the King who has the right to make the final decision (Section 14, MRE). For the MRE Perlis, it already stated that if any case, any conflict shall arise between the provisions of those enactments, the provisions of this enactment shall prevail. It strengthens this law to be the one that valid in this state for Malay Reserve Land. For Johor MRE, the enactment to prevail against provisions of other laws is in section 21. If in any case, any conflict shall arise between the provisions of this Enactment and the provisions of the Land Enactment, or of the Civil Procedure Code, or of the Powers of Attorney Enactment, the provisions

Perpustakaan Negara Malaysia eISBN 987-967-17889-6-7

of this enactment shall prevail. In section 23 MRE Terengganu firms that this enactment to prevail against provisions of other laws through this statement, if any case, any conflict shall arise between the provisions of this enactment and the provision of the Land Enactment or of the Civil Procedure Code or of The Powers of Attorney Enactment, the provisions of this enactment shall prevail. While in section 21 of F.M.S Cap 142 stated that if in any case any conflict shall arise between the provisions of this Enactment and the provision of the Land Code or of the Civil Procedure Code, or of The Power Attorney enactment, the provisions of this enactment are prevailed. In section 10(iii) of MRE Kelantan, the sanction of His Highness, the Sultan under the provisos to sub section shall only be valid if prior to the date of the sale. The land officer who has ordered the sale has received a certificated signed by the state secretary in the form schedule B and such certificate shall upon registration of the transfer of the land to attach the document together.

4.5 The Interpretation Definition of in Malay Reserve Enactment

Table 3: Interpretation Definition of MRL

References Law	Definition	Addition
MRE Johor	A person from the Malay race or any Malaysian nation who speak Malayan and professes to Islam. State Authority, Board, Society, Association and Companies specified in the Second Schedule to the enactment are included in this enactment.	Must have Malaysia Citizenship and rejecting any person who does not have an identity card. This enactment also does not recognise Syed although it is recognised as Malay in the Federal Constitution
MRE Perlis	A person from any Malay quarter or Arab nation, speak Malay or Malayan language and the religion Islam.	Add Siamese certified by the commissioner in writing to be a Siamese agriculturist permanently resident in the state of Perlis.
MRE Kedah	A person who holds fast to Islam, generally speaks Malay and one of his parents is a Malays or an Arab tribe	Add Siamese who have been confirmed by the Director of State Land and Mines as a resident which permanently resident in the state of Kedah also served as a Malay. This enactment stated that Sanitary Board or city area cannot be declared as MRL
MRE Kelantan	Person from any Malay or Malayan ethnic, speaks any Malayan Language, have any Malay quarter, professes the religion of Islam and include the Islamic Religious Council, Official Assignee as the administrator of the property of the deceased Malays.	Included the term Kelantan native as a condition of owning a land.
MRE Terengganu	A person from any Malayan race who usually speaks Malay or any Malayan language and religion to Islam.	Only town or village land can be declared as a Malay Reservation
MRE F. M. S	Individual who is belong to any Malayan race who speaks the Malay language any Malay language and professes to Islam	Included state of Pahang, Perak, Negeri Sembilan and Selangor

Perpustakaan Negara Malaysia eISBN 987-967-17889-6-7

4.6 Current Issue of Malay Reserve Land

4.6.1 Market Value of Malay Reserve Land

There are issues on MRL in the country with special reference to the land constraint that create limited transferability and low marketability in the market. The fact that the land is held under Reservation title with limited marketability caused a relatively low market value. This fact is supported by Phin Keong Voon in 1977. This limitation on the Malay Reserved Land rights resulted in a lower value than the open market, credit limitation, lack of financing, lower compensation in land acquisition that distort the initiatives of land development. Ismail Omar (2010) implied that the land value constraint emerges when the landowner and the buyer or the developer have different estimation in the price of the land. In general, the aim of any developer is to buy a site for less than it worth and then speculated that they may hold the land as inventory for the purposes of reducing housing supply, as it evident from the sizes of their land banks (Lai and Wang, 1999). Actors in the land market are diverse and have diverge objectives, expectations, and strategies where in some cases, only a few buyers and sellers may participate in particular land markets, and an individual land seller or buyer can greatly influence the market outcomes (Dowall, 1995). According to the amendments of Land Acquisition Act 1960, the government has insisted that the valuation of Malay Reserves cannot be impaired due to its status as a Malay Reserve. In general, most of Malay Reserve Land are sold at lower price as people believe that the value of the land is lower than the other land. As a result, the gap between the Malay reserve land and the other land seems to be increased over years.

Hafizah Aziz (2010), the assistant of development department at Pontian Land and the District Office stated that the attitude of landowners who do not value their own property by making sure it is used productively leads to the abandoned of the land. This cause the landowners to think of selling their land to others for more value. There are also landowners who sell their land to non-Malays for a higher price offer. Besides, there are landlords who rent out their land to another person within a certain period. The attitude of the landowners who want to make profit had become the biggest threat to keep the Malay Reserves Land in the hand of Malays people.

On the other hand, Malay Reserve landowners also find it difficult to obtain economic help from financial institutions to develop their own property. Therefore, the Malay Reserves has low value. Malay Resident landowners are unable to operate their property with productive operations as it requires capital. One of the factors that influence the market value of MRL to be lowered than the other land is because of the replacement of MRL is usually located in rural areas. This statement was supported by one of the staffs, Rizawati Mohamad in 2019. To sum up, this is the time to propose a Master Plan of Transforming Malay Reserved Land to be studied and presented to the government. The proposal plan is presented to take care of all issues and problems in developing Malay Reserved Land. The plan will address the issues and creating ways of developing Malay Reserved Land with reference to the successful development of Malacca Customary Land in Melaka, Native Customary Land rights in Sarawak and Pepateh lands in Negeri Sembilan.

4.6.2 The Condition of Malay Reserve Land

According to the recent studies conducted, it has been found that the size of the Malay Residential Area is decreasing after the relocation for rapid and irreversible development as required by the Federal Constitution. According to the 2013 Auditor General's report, a lot of Malay reserve land status has been changed for the purposes of development, without replacing or taking too long to be replaced. There have also been cases where the State Authority has turned the Reserves into independent holdings to give foreigners the opportunity to own land in the country. This is contradicting to the intention of the Malay Reserve Enactment which was introduced in 1914 to ensure the land owned by the Malays continued to be dominated by the Malays throughout ages (Azhar Abu Samah, 2014).

From a statistical study conducted by Mohd Hasrol Haffiz Aliasak reported by the Sinar Online newspaper on October 26, 2014; the Malay Reserves currently shows a fall of 12 percent or a decrease of 1.57 million hectares in 2009, in which the total size of the Malay Reserves in 1913 was originally 23.92 percent or 3.1 million hectares (Siti Nursyahidah, 2014). There are many factors that lead to the declining of the size and number of Malay Reserves that includes some landowners who have leased or sold their land to non-Malays due to economic factors, lack of infrastructure, transportation problems to exploit, poor management skills and other problems related to the Malays (Abdul Halim, 2014).

Other factors that lead to the declining in the size or number of Malay Reserves was the government's acquisition of land for the public benefit without being replaced or was not replace with the same value as the Malay Reserves. For example, the government took 100 acres of the Malay Reserves but replaced it with only 80 acres. By law, Malay Residential Land Reserves should be replaced immediately (Siti Nursyahidah, 2014). In addition, many Malay Reserves have been forfeited and have not been

Perpustakaan Negara Malaysia eISBN 987-967-17889-6-7

replaced as required by the Malay Reserves Enactment especially for Malay Residential Lands located in major cities in Peninsular Malaysia. For example, the protest from villagers affected by land acquisition that has become the site for the Broken Village Residential Development Project and the Second Road Project to Singapore; the landowners claim that the amount of compensation offered is insufficient and far less than the value of the land taken (Aliasak M.H.H, 2008).

The physical conditions of the land, for example, the type of the soil, its drainage, steepness of the slope are all important factors that influence how difficult it is to determine its potential use, and to extent the redevelopment is extremely costly, local scarcity of develop land imposes a binding long-term supply constraint on a local land market. To make MRL more attractive, the government need to increase the price by injecting infrastructure therein (Ismail Omar, 2019). The Malay Reserves Land which has been taken for public benefit without being gazette and not be replaced is also one of the factors contributing to the reduction in the size or number of Malay Reserves. The size of the Malay Residential Land may be supplemented by the publication of any Government Residential Land. For example, 10, 000 acres of Government Reserves are gazettes as Malay Reserves, while another 10, 000 acres should be opened for public ownership (Siti Nursyahidah, 2014).

This issue has been discussed in depth when there are statements released by Deputy Director General of Land and Federal Minerals Departments explaining the reason for the issue discussed above to occur. According to the existing law, Article 89 (3) of the Federal Constitution stipulates that the revoked and alienated Malay Reserves shall be replaced by the same type of area as the vacated land and if not, it is null and void. The similar characters can be defined by the guidelines which are same economic value relating to the type of cultivation, location such as access to road, potential for development similarity, the same type of soil and the same category of land used. However, there are still PBNs who are unable to carry out these instructions due to the issues and constraints in finding suitable areas for replacement. This issue has caused MRL data to fluctuate when it was reported. The case of V SP Suppiah Chettiar v KS Navaradnanm (1972) for instance, the high Court rule that immediate means allowing reasonable time for doing it.

4.6.3 The Location of Malay Reserve Land

In general, the factors are known as the constrain in land supply that are often resulted in an uneconomical Malay Reserved Land for development purposes. Location of non-strategic MRL and the lack of knowledge about the ways owners can develop the land resulted in unattractiveness and high risks (Ismail Omar, 2019). In addition, the problem that often raised as an obstacle to the development of asset ownership of Malay Reserved Land is the multiple ownerships that lead to indecisiveness. Despite the high demand for the use of land development, the land under the category of Malay Reserved were still left behind in this development even though it has the potential to develop in line with the lands of others non-Malay Reserved.

Typically, the Malay Reserved Land is in the rural areas. This is due to the most extensive and fertile land was owned by the farm operators and livestock since colonial times (Ahmad Nazri Abdullah, 1985). Most of the Malay Reserves are in the hinterland with limited access and poor infrastructure. Most of the Malay Reserves declared by the British government were village land or idle land where the value of the land was low. Some of the land are neglected and not worked on by the owners (Ridzuan Awang, 2007). Usually, the Malay Reserves are inland and poor of quality. This is due to most of the vast and high-quality land was owned by the owners of approved estates in colonial times. The Malay Reserves are located only in the valleys and peat areas. This is probably because of the area was once so popular with the Malay community that it was easy to get water and to cultivate the land. While the area is located close to downtown development, it has potential to be taken by the government through the Land Acquisition Act 1960. Many Malay Reserved Land areas located in the rural areas because of British colonial rule. Malay are encouraged to undertake activities such as farming the paddy for food continuity. This was the reason on why most Malay Reserved Land located in remote areas and in rural areas (Bashiran Begum & Nor Asiah Mohamad (2007).

Due to the declaration of a Malay Residential Land by the British government was not based on the suitability of the land but on their own volition, any land for development especially in the vicinity of urban areas has been exempted from the Malay Reserves. The location of Malay Reserved Land in the remote areas has caused the operators and developers of development projects to rethink about the suitability and the risks that will incur. The geological location and the physical ground condition (marsh) had indirectly lower down the value of the land. (Ismail Omar, 2019). A comparison is made between the capital value of the site to be develop with the ground rent to be received while taking account of both capital and rental appreciation. One

Perpustakaan Negara Malaysia eISBN 987-967-17889-6-7

may find a vast difference between the two such as the case of Kampong Baru. The value of the land has tremendously appreciated due to its strategic location (H. Hamzah, 2015).

4.6.4 The Spatial Changes of Malay Reserve Land

The changes of Malay Reserve Land in Kedah can be viewed through the map as below. The changes of Malay Reserve land between three years which in 2008, 2013 and 2019 show the original, cancellation and replacement of Malay Reserve Land. The original land is in year 1933 according to seven wills of Ruler Council. After some years, the exchange happens in Malay Reserve land. The accusation of the depletion in Malay Reserve land can be denied in sub - district in Kedah because the spatial changes prove the vice versa. The detail map of spatial changes has been done at Jabi, Pokok Sena for 3 three years which are 2008, 2013 and 2018 show the changes in replacement and cancellation of Malay Reserve Land in that sub – district. According to JKPTG, the area of Malay Reserve Land in Kedah in 1933 is 942 700 hectares. However, it shows an increment in 2008 and 2013 with 721 505.67 hectare and 721 507.49 hectare respectively and increase in 2018 with 721 508.28 hectare.

The data given by JKPTG shows that the area of cancellation is less than the replacement of Malay Reserve Land. In 2008, the cancellation area of MRL is 100.002 hectare and was replaced by 108.7165 hectare. In 2013 and 2018, 21.7689 hectare and 247.5261 hectare of land was cancelled and replaced by 32. 3029 hectare and 250.9914 hectare. This situation is happening because of the conditions to exchange the place or area of Malay reserve must be increase by 5 %. The data proof that the depletion in Malay Reservation Land is not happening and it was only an accusation by some parties. Based on the map of spatial changes in 2008, the exchange of Malay Reserve Land at Jabi is the least compare to the year of 2013 and 2018. Jabi is one of the subs – district that are suitable for replacement of cancellation area that meet the requirement as the sub – district of Jabi is in the rural area in which the development is least compare to city area. The map of Malay Reserve Land was provided by JUPEM to shows the exchange of the area in Malay Reserve.

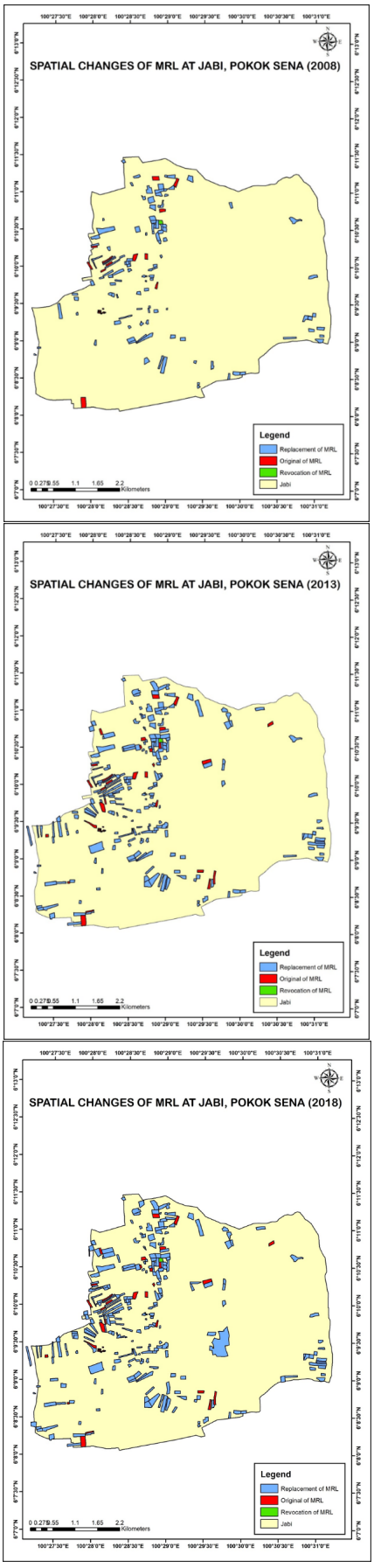

Figure 2: Map of Spatial Changes

Perpustakaan Negara Malaysia eISBN 987-967-17889-6-7

5.0 Conclusion

The result of this research is used to clarify the current issues, to observe the implementation of Malay Reserve enactment and to view the changes of Malay Reserved Land. All of these have been identified in this study. The study has carried three consecutives objectives to fulfil the aim which is to compare the implementation of Article 89 Federal Constitution and its spatial changes of Malay Reserve Land in Kedah.

The issue that have been discussed in the result needs to be refined in the future to maintain and defend the value of Malay Reserved Land. This effort needs to be continued, either wise, the country will face difficulty to defend the privileges of Malays for next generations. The future of Malay Reserved Land is in the hands of the Malays. Malay Reserved Enactment contains many restrictions but does not fully provide the privilege of Malay Reserved Land, especially when the landowner is abused and misappropriated. The trust to protect the Malay Reserved Land depends on the number of different parties, such as the State Authority and the Malaya Rulers Council. The measures need to be taken and may involve amendments to legislation and policy formulation that supposed to not only develop the Malay reserve land alone, but also ensure the retention of ownership in the hands of the Malays so that at some point they can compete with another pay check. This responsibility is only rested on the shoulders of the government, but requires the commitment and support of all parties, especially the Malays.

In conclusion, economy of Malays needs to be improved through education, skills and persistence. Only this way the Malays will succeed in defending their rights and managed to be on par with the other races in the country.

References

[1] Pakhriazad, H. Z., Mohd Zaki, H., Mohd Asmadi, I., Khairil Wahidin A., and Hazandy, H. (2010). Malay Customary Tenure and Conflict on Implementation of Colonial Land Law in Peninsular Malaysia. Journal of Law and Conflict Resolution 4(2).A reference

[2] Resali Muda (2011). Definition of Malay, Policy Malay dan Non - Malay in Malay Reserved Land Enactment: One review, Laws Journal. 2009 (13), hlm. 129-143, 2009..

[3] Siti Nursyahidah, A. B. (2014, October 25). Malay Reserved Land Sold for Immediate Profit. Sinar Harian Online. Taken on October 25, 2014, from http://www.sinar-harian-online.com.

[4] Roslinda Hashim (2018, November 13). Kedah Kekal Dasar Pertukaran Tanah Rizab Melayu. Sinar Harian Online. Taken on November 13, 2018, from http://www.sinar-harian-online.com.

[5] Termizi M, Ismail M (2018). Development Issues on Multiple Ownership Land of Malay Reservation Land. Malaysian Journal of Social Sciences and Humanities

[6] Manaf A, Lyndon N, Selvadurai S, Hussain M, Ramli Z (2015). Factors Preventing the Development of The Malay Reserve Land. Malaysian Journal of Society and Space

[7] Voon, P. K. "Rural Land Ownership and Development in the Malay Reservations of Peninsular Malaysia" dlm. South East Asian Studies 14(4), hlm. 496-512, 1977.

[8] Shahrom Md. Ariffin. "Malay Reservation Land – Unleashing a Century of Trust" International Surveying Research Journal 3(2), hlm. 1-28, 2013..

[9] Nik Haslinda Nik Hussain. "Enakmen Tanah Rizab Melayu Kelantan Dan Pemilikan Tanah, 1930–40" dlm. Jurnal Kemanusiaan 2010 (17), hlm. 37-64, 2010.

[10] Nor Asiah Mohamad & Bashiran Begum Mubarak Ali. "The Prospects and Challenges of Malay Reservation Land in the 21st Century" dlm. Journal of Real Estate. 4 (2), hlm. 1-16, 2009.

[11] Raja Mohar Raja Badiozaman. "Malay Land Reservation & Alienation" dlm. Intisari 1(2), hlm. 19-25, 1964.

[12] Mohd Hasrol Haffiz Aliasak. 2013. Isu penyusutan pemilikan tanah pegangan Melayu Kajian Kes di Daerah Larut, Matang dan Selama, Negeri Perak Darul Ridzuan. Tesis PhD. (tidak diterbitkan). Bangi: Universiti Kebangsaan Malaysia.

[13] Jabatan Pengarah Tanah dan Galian Negeri Perak. 2014. Laporan Tahunan 2014. Malaysia. 2010. Kanun Tanah Negara 1965. Malaysia. 2012. Perlembagaan Persekutuan.

[14] Ahmad Nazri Abdullah (1985) Melayu dan Tanah, Pelanduk Publication

Perpustakaan Negara Malaysia eISBN 987-967-17889-6-7

[15] Ismail Omar et al (2016), Malay Reservation Land – The Way Forward, Lambert Academic Publishing, Germany.

[16] Ismail Omar (2018b), Pindaan Akta Tanah Jamin Keselesaan Rakyat, Berita Harian, 10 November.Keenleyside, C., Baldock, D., Hjerp, P. & Swales, V. (2009) International perspectives on future land use. Land Use Policy. 26S (2009) S14–S29

[17] Lai, N., & Wang, K., (1999), Land Supply Restrictions, Developer Strategies and Housing Policies: The Case in Hong Kong, International Real Estate Review 1999 Vol. 2 No 1: Pp. 143 – 159.

[18] Nik Mohd Zain (1996). Pembangunan Tanah Rizab Melayu dari Perspektif Sejarah, Perundangan dan Pembangunan masa depan. Persidangan Pembangunan Tanah Rizab Melayu, 9 November 1996 di Pusat Perdagangan Dunia Putra (PWTC).

[19] Hafiszah Ismail 2019. Kearah Pembangunan Terancang Tanah Rizab Melayu Utusan Online Taken on Februari 21, 2019 from http://www.utusan.com.my/pendidikan/ke-arah-pembangunan-terancang-tanahrizab-melayu-1.845792

[20] Shahrom Md. Ariffin 2019. Transformasi Tanah Rizab Melayu Utusan Online (26 Februari 2019 9.04 PM) Oleh http://www.utusan.com.my/rencana/utama/transformasi-tanah-rizab-melayu1.849411

[21] Keluasan tanah rizab Melayu kurang kerana tidak diganti. Sinar Harian. Taken on Februari 28, 2019) from https://www.sinarharian.com.my/article/15557/BERITA/Nasional/Keluasantanah-rizab-Melayu-kurang-kerana-tidak-diganti

[22] Ismail Sualman (2019). Menjunjung Wasiat Dan Rizab Melayu. Sinar Harian Taken on March 3, 2019. From https://www.sinarharian.com.my/article/15927/KOLUMNIS/Menjunjungwasiat-dan-rizab-Melayu

Perpustakaan Negara Malaysia eISBN 987-967-17889-6-7

MARINE SPATIAL ALIENATION PERSPECTIVE IN MALAYSIA TOWARDS MARINE CADASTRE IMPLEMENTATION

[1]*Ashraf Abdullah*

[1]*Faculty of Architecture, Planning & Surveying, Universiti Teknologi MARA, Perlis Branch, Arau Campus, 02600 Arau, Perlis, Malaysia*

Email: ashraf@perlis.uitm.edu.my

Abstract

Malaysia covers a land area of 332,556 km' comprising two regions, Peninsular Malaysia and the States of Sarawak and Sabah. The territorial waters of Malaysia totals to about 150,000 km' while the EEZ extends another 450,000 km2 (based on 200 nautical miles or 312 km limit). In Malaysia, marine title does not exist within the marine environment where the government regulates all transactions that occur by defining the boundaries to manage the access and exploitation of various marine resources. The government defines the rights, restrictions and responsibilities attached to such boundaries. It is up to the user to attain knowledge of these rights and to abide them, even if several sets of rights exist within one area. The real need within the marine environment is for the stakeholders to be able to have a clear spatial and legal knowledge to enjoy such rights but not the ability to transfer the rights. This is the fundamental difference between terrestrial cadastre and marine cadastre. This study cover some method involving the focus group discussion and review the all policies from the marine stakeholders established to examines the marine spatial elements in their applications. Finally, many factors must be take for granted to solve the uncertainty about the marine spatial in marine environment and the these solution will contribute the implemented of marine cadastre.

1. Marine Spatial Administration

In Malaysian history, since the ancient times the sea governance is fundamental to the management and control of the economy. This is evident since the Age of Malacca Sultanate which was the establishment of the Law of the Malacca Sea which covered many matters of transportation, management and administrative procedures of ships and operation and tax imposed on ships. This suggests that the sea is a very important trade route for amicable administration. Malaysia is generally known as a maritime nation and has sweeping coastline. The geographical factor of Malaysia see a variety of terrain in the coastal areas. Various conditions indicate that there are some places in Malaysia which have sandy beaches, mangroves, rocky shores and continued to forest areas.

Hence, a specific form of marine administration should be introduced and these resources are managed on an even keel, systematic, sustainable and not detrimental to the natural ecosystem surrounding.

Various issues were raised today where they do not only highlight the rights of land under water but also deal with the rights on the water and in the water column between the water until the water is described as a medium which is vertical (depth). The basic matters in developing the marine alienation policy is need to geared in dynamic issues and does not easy to administer in detail. It should focuses to emphasize the critical issues which can give rise to dispute in the context of a description of the ownership of adjacent or neighborhood.

The dominant power of marine territory is clearly in accordance with the Territorial Bill 2012 which divides the marine boundaries from the lowest water to three nautical miles to the State Government and from three nautical miles to EEZ which are under the control of the Federal Government. However, there are some issues about the marine border where the question on position of marine border is still confusing between the federal and local state and also states and other states. This issue is the basic requirement of large-scale mapping of marine areas for which it becomes the benchmark of the development of a marine cadastre which is more comprehensive than its technical aspects.

Perpustakaan Negara Malaysia eISBN 987-967-17889-6-7

It is a difficult issue, but as a country with regional marine, Malaysia should consider how best to govern the marine natural resources. Malaysia as a maritime country which has many islands that have on the tourism potential has led to a conflict between development priorities and environment imperatives. The study about marine institutional arrangement for reconciling the conflict is one of which is sensitive to federal- state relationship and also facilitates policy and legislation which take into account the need for public participation and which views environment protection and economic development as mutually reinforcing goals. An inter-disciplinary approach which considers, coordinates and integrates the interest of all appropriate economic sectors is required. State can and should play a more active role in marine environment protection and the Federal government can support this by strengthening the State and local authorities in term of technical and financial capacity to manage the environment of islands and their surrounding waters.

Marine governance as a marine parcel management is a tool that brings together multiple users of the ocean – including energy, industry, government, conservation and recreation – to make conversant and coordinated decisions about how to use marine resources sustainably. The marine governance uses maps to create a more inclusive picture of a marine area – identifying where and how an ocean area is being used and what natural resources and habitat exist. That marine governance and parcel supervision is a practical way to create, establish and professionally organize the use of marine space as well as the interactions between its users, in order to equilibrium demands for development with the need to protect marine ecosystems, and to achieve social and economic objectives in an open, designed and managed way (Liu, Wu, Jhan, & Ho, 2011). Therefore, marine administration and parcel organization can be defined as an arrangement of time and space to create and establish rational marine use, which is based on zoning maps, permit systems and other running measures, with which to achieve the social and economic objectives essential for the defense of marine ecosystems (Liu, et al., 2011). Administration and supremacy are the basic of life and community to achieve the capability of human to grab the benefits from the nature and maintain the source of quality continuously. It is also about decision-making and steering, and the distribution of knowledge and power within an organized entity (e.g. a jurisdiction, government department etc.) as that entity pursues its goals and objectives (Paquet, 1994, 1997; Rosell, 1999, Centre on Governance, 2000). Hence, the ocean governance must provide accurate, up-to-date, complete and useful information regarding the resources that currently exist, the nature of the environment within which those resources exist, as well as users' relationships to those resources. Therefore, an effective governance of marine areas is always required. Information on (but not limited to) living and non-living resources, marine contaminants, water quality, shoreline changes, marine bed characteristics, bathymetry, spatial extents, property rights, responsibilities and restrictions, all contribute to the sustainable development and good governance of marine environments (Ng'ang'a, Sutherland, Cockburn, & Nichols, 2004).

The effective implementation on marine parcel management and governance still has no explicit policies on management or utilization of marine and coastal resources. Until now, the spatial data on marine involve much more details and very unique marine features but the implementation of organized marine data still follows the purposes of aims in the department. For the sustainable development in marine, marine spatial data are quite difficult to accurately organize and create. Looking at the sample of marine spatial management like Integrated Coastal Zone Management (ICZM) which is used in many countries as the main subject of tool to manage the marine resource but it only creates a framework for policy- making and decision-making in coastal zones only and it does not cover all the marine spatial and environment. ICZM is also defined as a continuous and dynamic process by which decisions are taken for the sustainable use, development, and protection of coastal and marine areas and resources' (Douven, Buurman, & Kiswara, 2003).

Marine spatial data are more recognized and clear on the concepts of spatial information and they are related to the surface of the earth. Usually, information are related to a location using coordinate x; y; and z-coordinate if height/depth is relevant. Other than that spatial identifiers, like postal codes or regions, can also be used. However, even if postal codes or regions are used, x; y coordinates are always needed to make a representation (a map) of the spatial data. Region boundaries for example consist of x; y-coordinates that are connected by lines. Langkawi Island has many institutions to manage and administer the marine environment. However, the development of institutional area and scope still have some ambiguity, conflict and overlapping marine issues because the organization was established based on

Perpustakaan Negara Malaysia eISBN 987-967-17889-6-7

the act from Parliament resolution. On that physical, especially on marine environments, it is quite difficult to define the delineated and accuracy of the authority area for true governance area. Currently, the administration of Malaysia's marine territory is divided into sections such as enforcement, management, economy, transportation, tourism, fisheries and natural resources and minerals. Specializing in depictions of marine administration related to marine alienation, no independent practice is done and only hinges on legal referral of existing land and acts are share between the Federal and State.

In general, there is no question in terms of conferring the title of which is under the authority of the State under 3 nautical miles while the Federation after 3 nautical miles. The confusion is related in a legal space in which existing marine alienation is debatable in every aspect compared to the alienation of land to be clearer and more precise. Therefore, in order to make the management and administration of the alienation of the related marine space definition, concept and technical should be specified in the existing legislation or issue a new law in support of its application. Besides that, the actions towards endorsing the *1982 United Nations Convention on the Law of the Sea* at the National Level should be given priority if Malaysia is serious about managing its marine environment in a consistent, clear and appropriate manner. Therefore, in the light of Malaysia's recent ratification of the *1982 UN Convention on the Law of the Sea* on October 14, 1996, and especially on the basis of the firm Declaration made by *Wisma Putra,* it is perhaps reasonable to suggest that the following proposals are considered by relevant Government agencies for expeditious implementation in order that the needs and interests of all stakeholders of Malaysia's vast marine environment are adequately met. With regard to, specifically the LOSC such promulgation of national legislation is recommended in giving effect to the LOS Convention. The publication of a chart of a scale or scales adequate for ascertaining the baselines for measuring the breadth of the territorial sea, or alternatively a list of geographical coordinates of those points and the delimitation of internal waters, territorial sea, contiguous zone, EEZ and the continental shelf.

2. Marine Alienation

There is no specific marine title encompasses the marine area. The current practice of marine alienation still follows the same procedure as applied on land. This is clearly seen in reference to the land title. This is because marine alienation is never discussed under the marine perspective. The existing procedure involved in marine alienation indirectly in marine territory has some differences compared to the land procedures. These matters are as follow:

- The technical department in the present of technical comments involved from the marine institutions such as Marine Department, Drainage and Irrigation Department, Fisheries Department, Maritime Enforcement Agency, Department of Environment, District Municipal Council (Coastal and Marine Planning Division), Department of Town and Country Planning (Marine Division).

- The applicant must comply with the conditions imposed by the Land Office where this is compulsory to complete the condition following the marine requirements set.
- This application is given to whom from corporations or organizations with had plans to develop or invest in marine activities and can benefit the state. It is also considered to federal, state and local authority.

Until now, the application of marine title for fish cages, cockle areas, ocean recreation areas, ownership of the island and surrounding waters occur in the form of Temporary Occupation Licence (TOL) which requires a license and needs to be renewed annually. This is because there are no forms of legislative amendments or a new act to enable the marine area to implement a title either permanent or lease. However, there are cases in Malaysia that do not have a clear in legal reference of marine alienation in marine area. It is also because no efforts are put on this matter. The law of marine ownership in general is currently based on the operation and activities on marine coastal. This is to ensure that monitoring in marine activities happens in the best condition. The current issues such marine navigation, the object in navigation, measurement and data collection for marine study and the project development in marine areas have disadvantages in terms of alienation and management of marine space. This is due to the high cost and the ability of management in marine area which make this matter not being taken seriously by the State Authority. In addition, the definition is not strong in the marine cadastre application and the alienation of marine space also becomes a source of awareness among the various parties on this matter. Hence, the need for an amendment of the law and the use of great technology is an important action and must be taken to ensure that implementation of marine

Perpustakaan Negara Malaysia eISBN 987-967-17889-6-7

cadastre can be reality.

3. Marine Cadastre in Malaysia

Around the local states in Malaysia each has marine region and allows business to exploit the marine resources in a more beneficial and profitable way. Development and application of marine living today witness many marine activities conducted in the states and there is also a mega run. Basically, marine cadastre principles are not specifically mentioned and applied in marine environment of Malaysia. Marine cadastre issues are the questions related to space in the marine environment which have the need for a strong definition and this concept can be practiced and included in the law of Malaysia.

However, it has not become a reality until now and the marine administration today is focused only on the orientation of the management and administration of the affairs of marine activities such as shipping, transportation, enforcement, fisheries, marine protection areas and so on. The issue is not the question of marine space for marine administration in Malaysia, but so for marine alienation practice which is not a major issue in Malaysia until now because in practice, it is conducted but the procedures are unclear and prone to conflict. However, it is considered as an isolated issue with the existing powers over the practice of decision-making problem and it occurs in specific needs. Therefore, the specific purpose tools which is also a marine cadastre, is a system of marine title for any party deemed appropriate by the government to dispose of the marine space. However, the legislation has not been officially confirmed in the existing regulations and is exposed to a variety of questions and concerns.

Alienation of marine expresses a big difference compared to with the practice of land ownership. This is because issues are within giving the titles ranging from legal, technical, institutional and procedures. In theory, marine alienation is practiced in Malaysia but in a very poor implementation, with a lot of space that can be disputed and a lot of issues that may conflict with the principles of nature and holding of the world against marine region in general.

According to Grotius (1609), who presented about the Mare Liberum doctrine which stated that the basis of freedom of the seas is the right for human being. It is intended to deny the political stand of Portugal and Spain which prohibits other countries to sail to the Far East, while marine areas should be open to anyone because basically no one owns it. Marine region should be freely used for sailing (freedom of navigation) and are free to take as a result. However, the philosophy today submitted the relevant sea Territorial Sea and the Sea of probes, which in simple understanding is close to the sea called the nation's sovereignty and territorial sea off the coast of the sea is said to be free. It also saw the importance of the sea state government which was first introduced around Law of the Sea of Malacca which served as a law regulating maritime activities such as determining the rules of navigation and trade, maintaining ship officers tasks, setting the security measures on board, regulating the duty crews, the processing of hiring and laying ships and also about the power of the master in sentencing.

Marine cadastre is normally defined for international use as a system to enable the boundaries of marine rights and interests, to be recorded, spatially managed and physically defined in relationship to the boundaries of other neighboring or underlying rights and interests. That definition will be used at international stage but in Malaysia, our own definition must be produced and created based on Malaysia water territories and under factors related to Malaysia culture. Marine cadastre conceptual is about marine administration system and manages the marine spatial definition of marine rights other than those limited to the marine bed only. For example, rights and interests over the water column or air-space above the water surface is needed to be presented as the marine spatial in marine cadastre context. Besides that, the design and implementation of a marine cadastre should seek to maximize the use of legal instrument of state or federal and internationally accepted in spatial referencing systems which are available for use in marine areas and are consistent with those being used in the management of the land cadastre. However, on certain issues about the data acquisition, the marine areas has more complicated data needed to support their characteristics.

Normally, the marine sovereignty for Malaysia is until the Exclusive Economic Zone (EEZ) delimitation and discussion about the spatial extent, the marine ward boundary of the marine cadastre will be the (EEZ) boundary but must go through the legal procedure to define the authority between Federal and State under agreed provisions of both. Note that the design of the automated survey and title system in Malaysia is not inconsistent with potential future requirements to manage a cadastre system covering Malaysia's marine of jurisdiction. It is because the current legal practice is does not specifically state about the marine administration in detailed. The marine cadastre may

Perpustakaan Negara Malaysia eISBN 987-967-17889-6-7

also include marine areas appurtenant to the international neighboring countries for the position of state bordering countries, and this will be returned to the authority of the Federal government especially in Kedah/Thailand matters.

4. Conclusion

As summarises, Malaysian marine cadastral issues in light of the advantages of a marine cadastre referring to practical application of existing, occurring weakness, available opportunities in the foreseeable future as well as some of the risks that may be encountered. This is a number of issues and factors that need to be described in the question of marine cadastre in Malaysia such as the uncertainty in land definition about marine environment and issues, determination of the territorial sea boundary, provisions of law under state and federal and surveying methods and data involved. All the element of marine spatial including the legal perspective and technical approach is the crucial part in order to define the marine spatial clearly under the cadastre principal and technical.

References

[1] Fowler, C., & Treml, E. (2001). Building a marinecadastral information system for the United States-a case study. Computers, Environment and Urban Systems, 25(4-5), 493-507.

[2] Hugo Grotiu(1609)Mare Liberum, sive de jure quod Batavis competit ad Indicana commercia dissertatio Published in English 2004

[3] Liu, W.-H., Wu, C.-C., Jhan, H.-T., & Ho, C.-H. (2011). The role of local Government in marine spatial planning and management in Taiwan. Marine Policy, 35(2), 105-115.

[4] National Oceanography Directorate, Malaysia Ocean Policy 2011-2020.(2011) Ministry of Science, Technology and Innovation, Malaysia

[5] Ng'ang'a, S., Sutherland, M., Cockburn, S., & Nichols, S. (2004). Toward A 3D Marine Cadastre In Support Of Good Ocean Governance: A Review Of The Technical Framework Requirement S. Computers, Environment and Urban Systems, 28(5), 443-470.

Perpustakaan Negara Malaysia eISBN 987-967-17889-6-7

Application of Thailand Realtime CORS GNSS Network for UAVs Photogrammetry

Torlap Kanplumjit[1], Rodjana Koonpoon[1] and Somjai Muenjorn[1]

[1] Survey Engineering branch, Faculty of Engineering, Rajamangala University of Technology Srivijaya, 90000 Songkhla, Thailand

Email: torlap_rmutsv@hotmail.com

Abstract

UAVs Photogrammetry is one of the technologies used to create highly accurate maps, whilst GNSS CORS network has been implemented by several organizations and universities in Thailand in order to serve their mission. The accuracy of maps requires many concrete steps that can take up to an advanced level to suit commercial purposes and cover across industries. It is possible to create maps and 3D models that are accurate enough for even the most advanced projects. The computer vision has driven photogrammetry in recent years which is paralleled with the development of accessible commercial UAVs including GNSS technology. Their solutions allow professionals to integrate these flying robots into existing workflows to generate 3D models. In our last white paper, we showed UAVs and national GNSS CORS networks could deliver accuracy within measurements using Ground Control Points (GCPs) from GNSS CORS network measurements. This paper aims to evaluate the accuracy of spatial data obtained from the consumer-grade UAVs imagery, processed with GCPs obtained from their coordinates based on Thailand GNSS CORS network. The study area is in Bo-yang sub-district, Songkhla Province, covering an area of about 1 square kilometer with a total of 720 images taken at a flying altitude of 100 meters. The averaged GSD is approximately 4 cm. The processed photogrammetry comprises 5 GCPs and 30 CPs using GNSS positioning and three wire leveling determinations. The processed UAVs photogrammetry resulted with their accuracy of horizontal RMSE of 8.83 cm; where the NSSDA standard states the accuracy of CE 95 at 15.28 cm about 3.8 GSD, and vertical RMSE of DSM using 30 checkpoints of 11.71 cm; where the Accuracy by NSSDA standard at CE 95 22.95 cm. The figure is about 4.6 GSD accepted within the TUSE standard.

Keywords: CORS GNSS Network, UAV photogrammetry, Spatial accuracy

1. INTRODUCTION

Currently, UAV and GNSS become means to gather on-demand aerial imageries in various industries such as construction, surveying, insurance and mining. A worldwide Global Navigation Satellite System (GNSS) is widely utilized in most systems that need absolute position. This is because of its accuracy, availability, reliability. GNSS can provide high accuracy positioning results when their error correction techniques are taken into accounts. Thus, the provision of high-accuracy receivers are eventually increased based on applications and markets. Thailand is establishing a national positioning infrastructure to supply the RTK and network-RTK services from the established GNSS CORS network to provide a centimeter-level accuracy throughout the whole country [1]. Real-time GNSS CORS Network in Thailand has been installed and provides service to several government organizations; namely, the Department of Lands, Department of structure and city & Country Planning, Hydro Informatics Institute (Public Organization), and Royal Thai Survey Department whereby in 2019, providing a complete network of 222 GNSS CORSs covering throughout the country. Data obtained from this Real-time CORS GNSS network is extremely accurate and serves spatial data simultaneously; both the horizontal coordinates and heights from datum including the atmosphere's information [2]. It can be widely used in surveys and might be combined with various survey technologies from construction surveys, hydrographic surveys to aerial surveys with UAVs or drones for map making and producing the spatial data. The private UAVs are currently used for leisure, most frequently used for aerial photography, but there's a high potential to be used in mapping. UAVs are now receiving lots of attention for consumer applications since the prices are very affordable and equipped with the GNSS navigation system and Inertial

Perpustakaan Negara Malaysia eISBN 987-967-17889-6-7

Measurement Unit (IMU) which add the essential requirement of an automatic aerial survey [3]. UAV-generated images apply Photogrammetry technique to process a high spatial resolution ortho-imagery, Digital Surface Model (DSM) and Digital Elevation Model (DEM). These require a communication system. Ground Control Points (GCP) is important to provide a centimeter level of accuracy as a photogrammetric output. The use of GCPs in mapping is essential because the outputs obtained from photogrammetry are actual measurements of the model to be mapped. Previously, GNSS static positioning methods were employed to obtain the GCP coordinate, where now the real-time positioning determined from the GNSS CORS network can be used in this coordinate determination. It is expected that the spatial data will become more accurate and meet Thailand UAVs mapping standard.

2. THAILAND GNSS CORS NETWORK

Global Navigation Satellite System (GNSS) technology and a network of Continuously Operating Reference Stations (CORS) with Network Real-Time Kinematic (NRTK) services provide observation data consisting of carrier phase and code range measurements which could be used for 3D positioning, meteorology, space weather, and geophysical applications. They are improved in terms of availability and accuracy by using data from Multi-GNSS that are GPS (USA), GLONASS (Russia), Galileo (EU), BeiDou (China), QZSS (Japan), IRNSS, and NavIC (India) [1]. GNSS applications include the preventions and mitigations of harmful substances, positioning services as of surveying, mapping, urban planning and even are applied to engineering designs for machine control; for example, precision agriculture, and intelligent facilities including smart city managements. Thailand has developed the GNSS CORS network infrastructure and their appliances on data management. This might result in enhancement on the country's competitiveness and preparation to step into the world of a business revolution. Thai industry aims to drive the economy with emerging innovations in-lined with the government's "Thailand 4.0" policy. Surveyors, GIS users, engineers, scientists and thus the general public that collect GNSS data can use these data to improve their positioning's precision. These GNSS CORS provide coordinates which could be enhanced with a post-processing approach with centimeter level of accuracy relative to the National Spatial arrangement, both horizontally and vertically. NRTK technique uses GNSS observation data in conjunction with measurements from ground-based continuously operating networks to improve positioning in real-time to an accuracy of several centimeters [4]. This NRTK method aims to attenuate the influence of the gap-dependent errors on the computed position of a rover within the network boundary. It provides redundancy of reference stations, such that if observations from one reference station are not available, a solution possibly continues to compute since observations are gathered and processed within a common network adjustment. Currently, several solutions to this method are existing; Virtual Reference Station (VRS), Individualized Master-Auxiliary (iMAX) and Area-Parameter Corrections (FKP) [5].

2.1 VRS technique

The Virtual Reference Station (VRS) or Virtual Base Station (VBS) is introduced by Trimble. A base station is artificially created within the vicinity of a rover receiver. All baseline length-dependent errors; such as abnormal troposphere variation, ionospheric disturbances and orbital errors, are reduced for this VRS. The rover receiving VRS information incorporates a lower level of those errors than an overseas base station that is shown in figure 1. The VRS is calculated for an edge, supplied by the rover during communication start-up, with networking software. The VRS position can change if the rover is way aloof from the initial point. The format for sending the rover's position is the standard NMEA format. Most rovers receive VRS data for a calculated base station that's within a pair of metres away [6]. The VRS approach requires bi-directional communication for supplying the rover's position to the networking software.

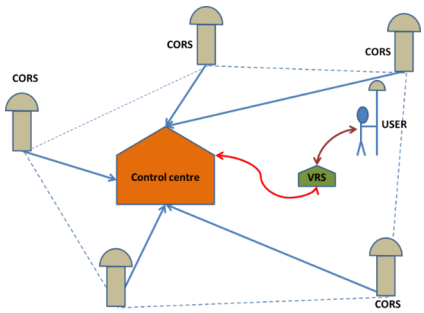

Source: Cina A.(2013)

Figure 1. Virtual Reference Station (VRS) technique

2.2 IMAX technique

The IMAX was introduced by Leica Geosystems. It is a network software correction to determine a rover's position, precisely. It is calculated like VRS. However, rather than calculating the bottom station observations for the provided position, or another position closer to the bottom station, original observation information is corrected

Perpustakaan Negara Malaysia eISBN 987-967-17889-6-7

with the calculated corrections and broadcast. The VRS works that although the rover is unaware of the errors, the VRS takes care of the errors. However, there still could be ionospheric errors remaining within the base station observations. IMAX provides actual base station position information. The rover may assume the bottom station is at a distance and open its settings for estimation of the remaining ionospheric residuals. The IMAX method may trigger the rover to open its settings further than required since the networking software removes a minimum of a part of the ionospheric disturbances. However, compared to VRS above, this approach is safer since it notifies the rover when there may well be baseline length-dependent errors within the observation information. IMAX requires bi-directional communication to the networking software for supplying the bottom station observation information [5].

2.3 FKP technique

With FKP methodology, a model of the gap dependent errors “Flächen-Korrektur-Parameter” FKP is transmitted to the rover. The interpretation of the FKPs and the individualization of the corrections are done at the rover, i.e. the rover can compute its individual corrections within the same way as VRS/PRS or alternatively use its own algorithms, which could be better adjusted to the RTK algorithms of the rovers. Thus the FKP method provides the rover more information than the VRS method, in order that the rover in principle can get more from the received data. FKPs describe the (horizontal) gradients of the corrections. The correction of a (real) reference station is employed together with the FKPs to compute the individualized corrections for the rover position within the simplest case the FKPs describe a linear dependency of the corrections from the position (linear FKP). The FKPs then define an “inclined plane” for the corrections, centred at the (real) reference station. Per satellite and per frequency two parameters are required. FKP models of upper order are possible. Note that the validity of linear FKP is restricted to about 100km radius, thanks to the actual fact that the physical error sources would result in noticeable non-linear effects over longer distances [7].

In Thailand, the VRS technique is currently the most popular and efficient method of transmitting corrections through a data link (internet network) to the users within RTK positioning. The basic theory of the VRS method is to transform measurements obtained at the actual reference stations to the location of the VRS and, therefore, to a different location at the same epoch. The utilization of the CORS station network in Thailand began to develop and establish the network system in 1996 by the Department of Public Works and Town & Country Planning to be used in the survey for mapping and town planning. Later in 2005, the Royal Thai Survey Department (RTSD) has set up a GNSS CORS station the data will later be processed for surveying, and in 2008, the Department of Lands (DOL) has created a GNSS CORS station network, which is the first network that can provide the kinetic survey is conducted immediately (NRTK) based on the principle of VRS for cadastral survey and other survey applications in Thailand, including UAVs photogrammetry [8]. In the near future, the entire Thailand's GNSS CORS networks will serve as a national infrastructure for applying local geoid models via NRTK service and integrate with other GNSS CORS networks from collaborated agencies. GNSS CORS integration includes RTSD 80 CORS, DOL 134 CORS, GISTDA 4 CORS, HII & NIMT 6 CORS, CU 1 CORS, and KMITL 8 CORS as shown in figure 2.

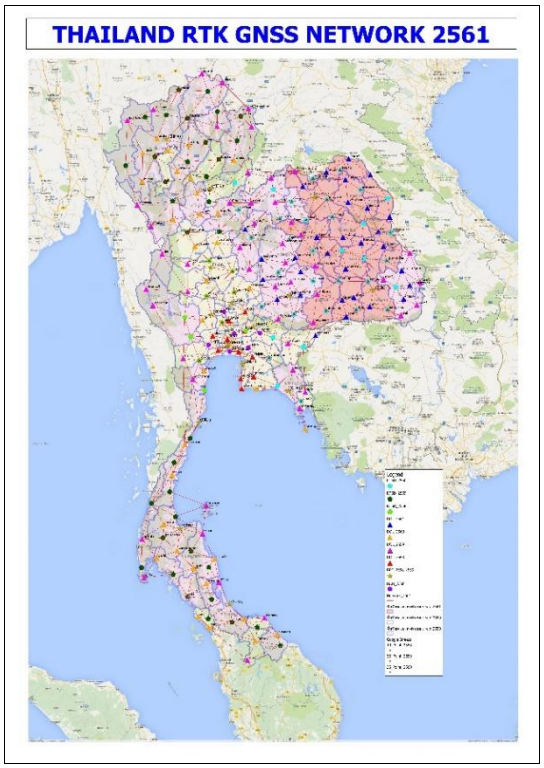

Source: Thailand DOL(2018)

Figure 2. Thailand GNSS CORS Network

3. UAV PHOTOGRAMMETRY

UAVs have become the go-to means for the gathering of on-demand aerial imagery across industries like construction, surveying, insurance, and mining. They quickly capture UAV-generated images and use cloud-based photogrammetry platforms. Solutions allow professionals to integrate these flying robots into existing workflows to map hugged swaths

Perpustakaan Negara Malaysia eISBN 987-967-17889-6-7

of land and may be useful to provide spatial-temporal high-resolution models in competitive period and resources, that providing useful 3D data for several GIS monitoring applications; such as georeferenced information at a large-scale derived from orthoimages and DSM [9]. Ortho-mosaic is usually a photo-map that's geometrically corrected in order that the size is uniform, and is commonly employed in aerial photographic survey measurements, but it's going to be also useful when a close view of the item is required. An ortho-mosaic is directly used for 2D measurements for calculating distances and areas and may be employed in GIS, enables to get high detailed morphological data, and might be processed to come up with a DSM, similar to the Lidar surveying results we will proceed in many cases to update effectively traditional cartography [10]. Accurate determination of the position of the UAVs platform by the GNSS system and its orientation by the IMU is significant for accurate aerial surveying, the payload of professional UAVs is either fixed with a high-resolution camera or it can provide facilities to hold an external instrument, mainly an imaging device [11]. The first goal of this research is to prove and measure spatial accuracy of the results of UAV photogrammetry and GNSS NRTK integration against surveying and leveling methods. employing a GNSS CORS and GNSS rover. The results give insight into the accuracy you'll expect from UAV photogrammetry. The resulting data set also can be wont to determine. The resulting data set may also be wont to determine suitable UAVs mapping missions and for several applications.

3.1 UAV Images processing

Application of technology and software for aerial image processing if the user doesn't understand the essential principles and theory of processing causes spatial error to the end in the processing that is not being of sufficient quality for application in engineering. Therefore, the principle of UAV image processing will give an understanding of basic principles and theories including checking the parameters obtained from the processing to be able to monitor to induce quality results. Principles of UAV image processing, operators must understand the fundamental principles of Photogrammetry. The preliminary processing guidelines as follows.

1) Images matching by tie-point may be a feature that you just can identify in two or more images which you'll select as a point of reference. Tie-points (TPs) do not have known ground coordinates, but it can be used to increase communication systems over areas with no communication system Points (GCPs). employed in rigorous models, aerial photography, optical satellite, and radar satellite math models, TPs identify how the photographs in your project relate to every other. in an exceedingly project using the Rational Functions math model, within which you have got imported the polynomial coefficients distributed with the information, you'll be able to collect TPs and GCPs to compute a metamorphosis to enhance the fit between the pictures [12].

2) Bundle Block Adjustment (BBA) is the problem of refining a visible reconstruction to supply jointly optimal 3D structure and viewing parameter (camera pose and/or calibration) estimates. Optimal implies that the parameter estimates are found by minimizing some cost function that quantifies the model fitting error, and jointly that the answer is simultaneously optimal concerning both structure and camera variations. The name refers to the 'bundles' of light rays leaving each 3D feature and converging on each camera center, which are 'adjusted' optimally for both feature and camera positions. The direct relationship between image and ground coordinates we measure the image coordinates within the images of the block using the collinearity equations, we are able to relate the image coordinates, the corresponding ground coordinates, the IOP, and therefore the EOP [13]. employing a simultaneous least-squares adjustment, we are able to solve for the ground coordinates of the tie points, the EOP, and also the IOP (Camera Calibration Procedure) The image coordinate measurements and therefore the IOP define a bundle of light rays. The EOP defines the position and therefore the attitude of the bundles in space during the adjustment. The bundles are rotated (W, P, K) and shifted (Xo, Yo, Zo) until conjugate light rays intersect yet as possible at the locations of object space tie points.

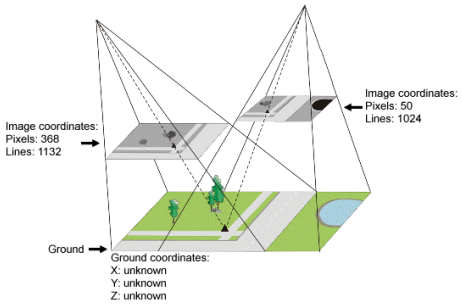

Source: Triggs B. (2000)

Figure 3. Tie point to represent a feature

Perpustakaan Negara Malaysia eISBN 987-967-17889-6-7

3.2 Ground Control Points (GCPs)

Ground Control Points are points on the ground with known coordinates in the spatial coordinate system. GCPs are very important for land survey by aerial photographs. There are coordinates in 3 dimensions. It requires surveying in the field with highly accurate surveying equipment. GNSS receivers are mostly used to collect coordinates for horizontal positioning and leveling for vertical locations. GCPs obtained from the aerial triangulation network are both visible in both the earth's surface and aerial imagery. They are usually used for pre-marking as shown in figure 4 [14]. GCPs for UAVs Photogrammetry surveying can be done in many ways, such as with the total station with the automatic leveling and GNSS receivers. Many methods of satellite surveying are traditionally often used to measure by the fast static and RTK positioning method, which requires the control points whereby surveyed base station coordinates are known [12]. With Thailand GNSS NRTK positioning technology, the GNSS receiver can be used as a rover to collect the coordinate aerial ground control points for UAVs photogrammetry; which the data results are sufficiently accurate in Thailand UAVs Surveying for engineering standard which will be studied in this paper.

Figure 4. The pre-marking GCP.

4. METHODOLOGY

The study area at Samila beach, Songkhla municipality, Thailand, was close to the control points (RTSD) were available for checkpoints (CPs) surveying. The study area is approximately 1 square kilometres as shown in Figure 5. The exact location of the study area is at a latitude of 7.212 degree and longitude of 100.591 degree and is situated in the landmark of Songkhla which has many terrain and land use areas. The area was aerially surveyed with a DJI Phantom 4 consumer-grade UAV with NRTK GNSS compared with CPs surveyed by GNSS fast static method and leveling. To meet the primary objective of this study, the horizontal and vertical accuracy of the results as Ortho imagery and DEM. In this study UAVs used was DJI Phantom4 Advance, quadcopter type, designed and assembled by DJI company ready to work autonomously offering cameras, including the FC6310 with a focal distance 8.8 mm. Rolling shutter and sensor RGB utilized in this aerial survey [15]. GNSS receivers for NRTK process by VRS technique with CORS round the study area as illustrated in figure 6.

Source: Google Map (2019)

Figure 5. The Study area close to Samila beach Songkhla province

The use for five GCPs was the S10 model from Stonex manufacturer, S10 the foremost advanced integrated GNSS Receiver ever appeared on the geomatic scene. Stonex S10 with its 220 channels, provides a superb onboard real-time navigation solution with high accuracy. All GNSS signals GPS, GLONASS, BEIDOU, and GALILEO are included [16]. Photogrammetric processing of images from UAV was done using Pix4DMapper pro. That calculates the position and original image orientation by Automatic Aerial Triangulation (AAT) and Bundle Block Adjustment (BBA), DEM is generated supported 3D cloud point obtained from AAT and BBA, in step with Wolf and Mikhail and Bethel.[17] The ortho-rectification and mosaicking are performed from the projection and combination of original images with DEM.

Perpustakaan Negara Malaysia eISBN 987-967-17889-6-7

Figure 6. The Equipment of the project.

Points of known coordinates within the project area called GCPs. These coordinates are measured with traditional surveying methods or are obtained by other sources like GNSS and during this project, GCPs coordinate are often obtained from RTK CORS GNSS network, required to calculate absolutely the position information of the products for increased accuracy.[14] it's possible to get georeferenced products even without GCPs because the images are geocoded by the GNSS device of the UAVs, but it's highly recommended to possess a significant number of GCPs to get reliable products. to increase absolutely the accuracy of a project, placing the model at the precise position on the earth. GCPs are typically statically placed on the surface edge and several others on the inside of the project area. Checks points (CPs) were used for independent verification of the project accuracy and points are randomly spaced throughout the project.[18]

Figure 7. The location of GCPs and CPs.

A total of 30 CPs were established for this research. Types of pre-marker for GCPs and CPs used which is the pre marker size is 1x1 m. (vinyl) which enclosed the study area. All GCPs and CPs have distributed throughout the study area 35 points as shown in Figure 7 used as control points and a total of 5 points used as a checkpoint for GCPs accuracy checking out of 30 points measured by rapid static technique with the Royal Thai Survey Department (RTSD) control point as GNSS based and three wire leveling for vertical coordinate. In this paper Pix4DMapper as a photogrammetry software manual highly recommended adding more 5 GCPs in the project to make the 3D map more stable and accurate.[19] For example, based on the Thailand UAV mapping standard suggested to 5 GCPs for square block and distance, not more than 500 m. [20] because of good results for the Root Mean Square Error (RMSE) vector of Easting and Northing. To measure the GNSS coordinates of each GCP, we used NRTK by VRS technique to calculate a position, and each CP needs either a rapid static and post-processing as shown in figure 8 (a) (b). The coordinates of all GCPs measured with GNSS Stonex S10 were shown in table 1.

(a)

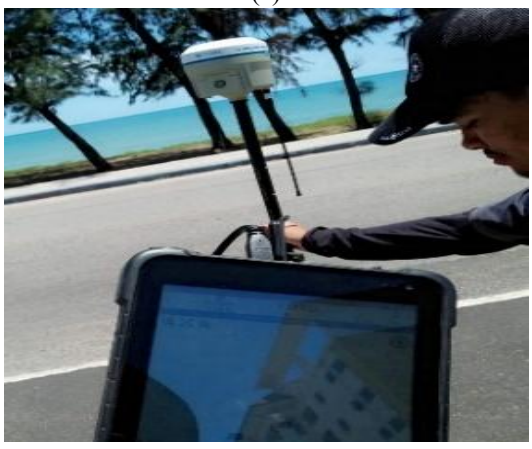

(b)

Figure 8. Rapid static GNSS surveying (a) and NRTK GNSS surveying. (b)

Perpustakaan Negara Malaysia eISBN 987-967-17889-6-7

GCPs (VRS)	Northing (m.)	Easting (m.)	Height (m.)
GCP1	**797210.859**	**676013.4546**	**3.839**
GCP2	**797626.251**	**676116.3076**	**2.414**
GCP3	**797481.518**	**675883.8154**	**36.107**
GCP4	**797197.020**	**675698.7348**	**3.848**
GCP5	**797711.838**	**675405.3659**	**1.585**

The UAVs mission planning generally consists of two items; flight map and specifications, which outline how to take them, including specific requirements such as the camera requirements, scale, flying height, over-lap, side-lap, and Ground Sampling Distance (GSD) [19]. GSD varies with the flying height so it has a direct influence on the achievable accuracy and the amount of detail in the final product. Flight planning was done with the aid of an application called Pix4D Capture for images acquisition with the mission planner many parameters can be adjusted to allow the UAV to capture images to cover the area with good GSD for high-resolution output. The parameters for flight planning are flying height at 100 m, forward overlap 80 %, sidelap 70%, GSD 4 cm, maximum speed 15 m/s, and flight time about 30 minutes, all constant throughout the mission was shown in figure 9.

Source: Pix4D Capture (2019)

Figure 9. Pix4D capture as flight planning application.

From a flying height of UAV planning at 100 m. The average GSD is approximately 4 cm. 80 percent in front and 70 percent inside overlap, receiving 720 images. Aerial triangulation by using Pix4d Mapper software. Import the tie the images by matching tie points (key points) between the overlapping images median 5,104 points per image. Importing and measuring 5 GCPs and 30 CPs on software. To adjust the image to improve the triangular network. The Bundle Block Adjustment (BBA) has the following details; the number of 2D key-point observations for BBA was 1,216,945 points. The number of 3D points for BBA was 332,465 points, and the most important mean Reprojection error 0.101 pixels that are no more than standard at 0.3 pixels, all in the quality report as shown in figure 10.

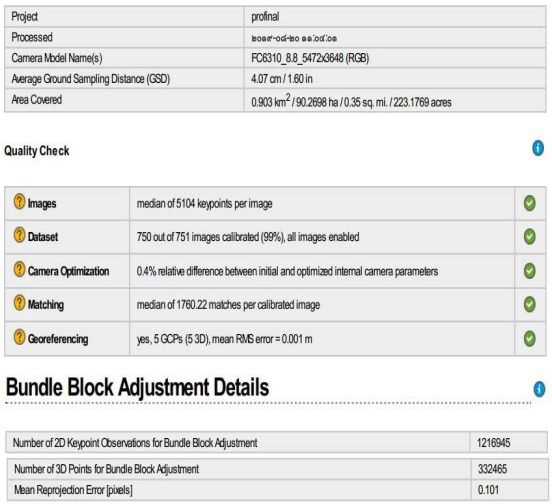

Project	profinal
Processed	[illegible]
Camera Model Name(s)	FC6310_8.8_5472x3648 (RGB)
Average Ground Sampling Distance (GSD)	4.07 cm / 1.60 in
Area Covered	0.903 km^2 / 90.2698 ha / 0.35 sq. mi. / 223.1769 acres

Quality Check

Images	median of 5104 keypoints per image	✓
Dataset	750 out of 751 images calibrated (99%), all images enabled	✓
Camera Optimization	0.4% relative difference between initial and optimized internal camera parameters	✓
Matching	median of 1760.22 matches per calibrated image	✓
Georeferencing	yes, 5 GCPs (5 3D), mean RMS error = 0.001 m	✓

Bundle Block Adjustment Details

Number of 2D Keypoint Observations for Bundle Block Adjustment	1216945
Number of 3D Points for Bundle Block Adjustment	332465
Mean Reprojection Error [pixels]	0.101

Source: Torlap (2019)

Figure 10. Photogrammetric quality report.

Create 3D coordinate points and mesh using the "point cloud and mesh" tool. These points represent coordinates in the earth's surface or in photogrammetry called a triangulated irregular network or "TIN" for use in DSM and Ortho imagery generated. Photogrammetric products like ortho-mosaic and DSM were generated automatically in Pix4D both with GCPs. Surface reconstruction by generating the point cloud and mesh. Starting from the known exterior orientation and camera calibration parameters, a scene can be digitally reconstructed by means of automated dense image matching techniques [17]. A powerful image matching algorithm in the software is able to extract dense 3D point clouds with a sufficient resolution to describe the object's surface. The generated point cloud is then triangulated to create a mesh. A powerful image matching algorithm in the software is able to extract dense 3D point clouds with a sufficient resolution to describe the object's surface. The generated point cloud is then triangulated to form a mesh. Pix4d mapper generating DSM and producing orthophoto of the study area.[19] The GCPs were accustomed to perform the aerial triangulation to provide a 3D model that has project georeferencing by mean RMS error was 0.001 m. GCPs were also accustomed to geo-reference images to the UTM system. This step is sustained by generating DSM and Orthophoto of aerial imagery as shown in figure 11.

Perpustakaan Negara Malaysia eISBN 987-967-17889-6-7

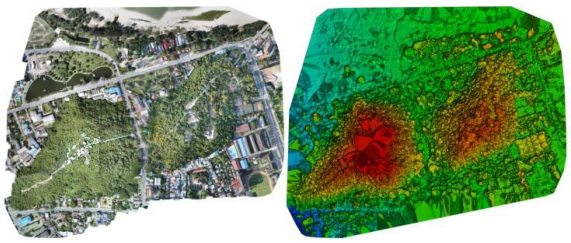

Source: Torlap (2019)

Figure 11. Ortho imagery and DSM as Photogrammetric products.

The generated output from the UAV images is DSM because the photogrammetry techniques take into consideration the surface texture to perform the triangulation process. The generated orthophoto was used for accuracy assessment and visualization. Spatial analysis was done by analyzing the standard of the generated ortho-mosaic map and DSM. Besides, the measuring is finished by using the coordinate of CPs that output data compare with GNSS and leveling survey as shown in table 2 for RMS error and shown the difference between photogrammetric data and field survey of 30 checkpoints in figures 12- 13.

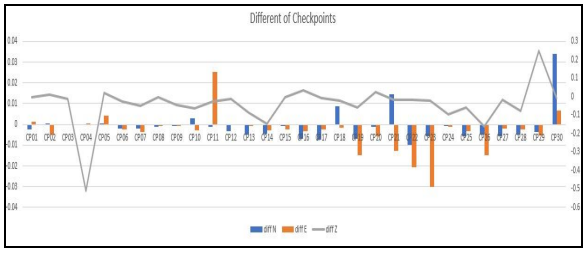

Figure 12. Different of 30 checkpoints

Table 2. CPs coordinate by GNSS & Leveling compared with Ortho & DEM

CP	N GNSS	E GNSS	H MSL	N Ortho	E Ortho	H DEM	Diff N	Diff E	Diff H
CP01	797742.201	676121.455	2.296	797742.203	676121.454	2.298	-0.002	0.001	-0.002
CP02	797674.927	675861.130	2.108	797674.926	675861.135	2.098	0.000	-0.005	0.010
CP03	797598.735	675659.673	1.720	797598.735	675659.673	1.731	0.000	0.000	-0.011
CP04	797568.763	675518.249	1.697	797568.763	675518.248	2.206	0.000	0.001	-0.509
CP05	797537.985	675386.656	1.789	797537.985	675386.652	1.767	0.001	0.004	0.022
CP06	797515.997	675332.808	1.664	797515.999	675332.810	1.690	-0.002	-0.002	-0.026
CP07	797704.239	675462.756	1.518	797704.241	675462.760	1.567	-0.002	-0.003	-0.049
CP08	797766.465	675350.070	1.856	797766.466	675350.070	1.860	-0.001	-0.001	-0.004
CP09	797650.028	675398.262	1.750	797650.028	675398.262	1.794	-0.001	-0.001	-0.044
CP10	797609.204	675349.738	2.267	797609.201	675349.740	2.328	0.003	-0.003	-0.061
CP11	797615.878	675305.294	1.843	797615.879	675305.269	1.869	-0.001	0.025	-0.026
CP12	797173.457	675675.690	3.971	797173.460	675675.690	3.985	-0.003	0.000	-0.014
CP13	797193.803	676023.542	3.951	797193.808	676023.543	4.037	-0.005	-0.001	-0.086
CP14	797262.388	675996.022	3.887	797262.392	675996.025	4.036	-0.005	-0.003	-0.149
CP15	797508.015	676141.055	3.028	797508.016	676141.057	3.032	-0.001	-0.002	-0.004
CP16	797678.172	676096.730	2.583	797678.179	676096.733	2.549	-0.007	-0.003	0.034
CP17	797437.713	675960.960	33.276	797437.720	675960.962	33.282	-0.007	-0.002	-0.006
CP18	797479.080	675872.142	36.958	797479.071	675872.143	36.978	0.009	-0.002	-0.020
CP19	797361.215	675863.842	50.757	797361.222	675863.857	50.815	-0.007	-0.015	-0.058
CP20	797331.640	675715.120	10.982	797331.641	675715.126	10.958	-0.001	-0.006	0.024
CP21	797259.253	675489.768	89.259	797259.239	675489.781	89.276	0.014	-0.013	-0.017
CP22	797234.001	675371.174	62.182	797234.011	675371.195	62.201	-0.010	-0.021	-0.019
CP23	797186.815	675321.457	51.127	797186.820	675321.487	51.147	-0.006	-0.030	-0.020
CP24	797792.051	676067.813	0.910	797792.052	676067.814	1.004	-0.001	-0.001	-0.094
CP25	797774.993	675907.464	0.893	797774.999	675907.468	0.951	-0.006	-0.003	-0.058
CP26	797766.016	675674.834	0.938	797766.020	675674.849	1.098	-0.005	-0.015	-0.160
CP27	797739.984	675598.889	1.482	797739.990	675598.891	1.497	-0.006	-0.002	-0.015
CP28	797653.762	675492.632	2.663	797653.767	675492.634	2.741	-0.005	-0.003	-0.078
CP29	797796.405	675516.570	1.392	797796.409	675516.576	1.144	-0.004	-0.005	0.248
CP30	797722.189	675326.497	1.392	797722.155	675326.490	1.399	0.034	0.007	-0.007
						X	Y	XY	Z
					SUM	0.00193	0.00279		0.41132
					MEAN	0.00006	0.00009		0.01371
					RMSE	0.00803	0.00964	0.00883	0.11713

Source: Torlap (2019)

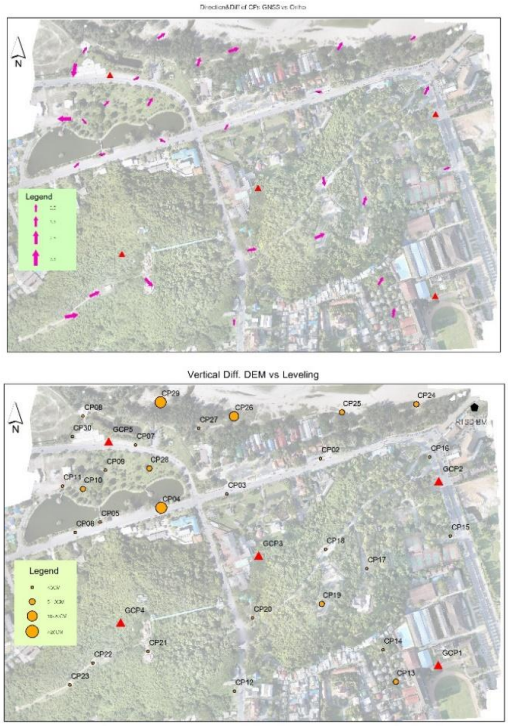

Figure 13. Distribution of horizontal and vertical error

Perpustakaan Negara Malaysia eISBN 987-967-17889-6-7

5. ACCURACY ASSESSMENT

The accuracy of spatial data is reported to be consistent with the National Standard for Spatial Data Accuracy (NSSDA) by the Federal Geographic Data Committee (FGDC) Geospatial Positioning Accuracy Standards. The accuracy of existing or legacy spatial data and maps are also reported, as specified, consistent with the NSSDA or the accuracy standard by which they were evaluated. Describes Root Mean Square Error (RMSE) as applied to individual x-, y-, z components, former the National Map Accuracy Standard (NMAS), and also the American Society for Photogrammetry and Remote Sensing (ASPRS) accuracy standards for large-scale maps. These standards, their relationships to NSSDA, and accuracy labeling are described to make sure that users have some means to assess the positional accuracy of spatial data or maps for their applications. NSSDA standard for spatial data accuracy of horizontal accuracy is 1.7308 x RMSe(xy) and vertical accuracy 1.9600 x RMSe(z).

And with Thailand UAVs Surveying for Engineering standard (TUSE) by The Engineering Institute of Thailand under H.M., The King's Patronage defines accuracy by UAVs camera because cameras have a direct effect on the spatial accuracy of UAVs surveying thus, this standard will classify digital cameras on UAVs consistent with accuracy. The position of the data will be produced with parameters that are divided into a shutter type lens type sensor size. The 3 types of resolution and accurate location of the photo coordinate are Consumer-grade, Professional grade, and Survey grade was shown in Table 3. During this project, a UAV camera with consumer-grade type, the spatial data accuracy for horizontal Ortho imagery was 5 GSD or about 20 cm and vertical accuracy of DEM was 6 GSD or about 24 cm.

UAV Camera Type (Grade)	Shutter Type	Images Coordinate	Horizontal Accuracy	Vert. Acc
Consumer	Rolling	DGPS	5 GSD	6 GSD
Professional	Global	DGPS	2 GSD	3.5 GSD
Survey	Global	PPK / RTK	2 GSD	3 GSD

6. RESULTS

The UAV photogrammetric output data were generated such as DEM and Orthophoto. They were processed using the data obtained from UAV imagery with 5 GCPs surveyed from the RTK network that was the Thailand GNSS CORS network with VRS technique. The results of the 3D mapping from UAV imagery achieved a remarkable centimeter-level accuracy. Accuracy was computed by comparing with the checkpoints coordinate surveyed by GNSS rapid static method and three wire leveling with RTSD control points as the base. The standard deviation of spatial error on horizontal was 0.006 and vertical was 0.133 and the distribution of error of spatial coordinate compared with elevation as shown in figure 13. Standard error at the confidence level of 95 percent (CE95) was 15.28 cm. About 3.8 GSD accepted within the TUSE standard. The quality of products shown by RMSE of 30 checkpoints was checked to show that the output of both data sets in total error as shown in table 4. The coordinate error of CPs on spatial data should be less error compared to field survey CPs to state that the output of photogrammetric products with GCPs is a good in accuracy that shows by the CE95. Based on the analysis, the vertical accuracy by RMSE of DEM with 30 checkpoints was 11.71 cm. The accuracy by NSSDA standard at CE95 was 22.95 cm, about 5.6 GSD accepted based on the TUSE standard. The horizontal RMSE of Ortho imagery from 30 checkpoints was 8.83 cm based on the accuracy by NSSDA

Avg. GSD 4 cm.	Horizontal RMSe (cm.)	Vertical RMSe (cm.)	Horizontal Acc. (CE95)	Vertical Accuracy (CE95)
Results	8.83	11.71	15.28 cm.	22.95cm
TUSE	5 GSD	6 GSD	20.00 cm.	24.00 cm.
Status	3.8 GSD	5.6 GSD	Accepted	Accepted

7. CONCLUSION

The Application of Real Time GNSS CORS network for GCPs of UAVs surveying with the photogrammetry process of the Bo-yang, Songkhla, Thailand confirms the importance of good georeferencing to obtain sufficiently accurate results. The quality of this georeferencing can be verified using enough uniformly distributed checkpoints. This paper presents an overview of using and spatial accuracy of the GNSS CORS network with UAVs imagery for aerial mapping complementary to digital

Perpustakaan Negara Malaysia eISBN 987-967-17889-6-7

photogrammetry. However, a careful analysis of the point cloud is also necessary to obtain high quality and reliability. The geometry of the acquisition of GCPs and images has an impact on the precision of a photogrammetric survey. Regardless of the low cost, consumer-grade UAVs provide a platform and Real Time GNSS service capable enough to be applied for accurate aerial mapping which used to be a costly and time-consuming task a decade ago. The degree of accuracy than would be expected on certain projects is dependent on the intended use of the survey data. In this project, compared with a better surveying method as the GNSS Rapid Static method and three wire leveling, the quality of photogrammetric spatial data products such as Ortho imagery and DEM were obtained with horizontal accuracy by CE95 of 15.28 cm and vertical accuracy by CE95 of 22.95 cm by a Phantom 4, the consumer-grade UAVs images which were geometry adjustment by 5 GCPs from NRTK with VRS technique. The selected study area varies terrain for 30 Cps as beach, mount, and urban, covering most of the study area with more 720 images. DJI Phantom4 as the UAVs combine with the GNSS and IMU devices, the flying operation is automated by Pix4d capture application flight planning application set altitude 100 m with project average GSD about 4 cm. and processing by photogrammetry software as Pix4dMapper pro (Perpetual License). The study proves that inexpensive UAVs photogrammetry can provide highly accurate and high-resolution products, the horizontal accuracy of 3.8 GSD accepted for Thailand UAV Surveying for Engineering standard and vertical accuracy of 5.6 GSD accepted and also within the standard. Shortly, Thailand Real-time GNSS CORS network will be combined into a national CORS which means that it will be easy to access and obtain high precision coordinates with the GNSS receiver, it able to be used in various survey fields especially UAVs photogrammetry surveying.

References

Satirapod C. (2019). Thailand GNSS CORS Infrastructure for Positioning and Timing Applications, Chulalongkorn University, Bangkok, Thailand.

Rizos and Satirapod C. (2011). Contribution of GNSS CORS Infrastructure to the mission of Modern Geodesy and Status of GNSS CORS in Thailand, Engineering Journal (vol.15)

Mulakala J. (2018). Measurement Accuracy of the DJI Phantom 4 RTK & Photogrammetry, DJI Enterprise White Paper.

Charoenkalunyuta T. Satirapod C. Hung-Kyu L. and Yoon-Soo C. (2012). Performance of Network-Based RTK GPS in Low-Latitude Region: A Case Study in Thailand, Engineering Journal (vol.12)

Hitarget M. (2017). Concept and Comparison of VRS MAX IMAX FGK in GPS networks Hitarget Content Educational.

Cina A., Dabove P., Ambrogio M. and Piras M. (2015). Satellite Positioning - Methods, Models and Applications INTECH p 23

Pehlivan, H., Bezcioglu M. and Yilmaz M. (2019). Performance of Network RTK Correction techniques (FKP, MAC and VRS) Under limited Sky view condition, International Journal of Engineering and Geosciences.

Nich T. (2019). Analysis and implementation of Thai GNSS CORS data application development project, CHC Navteq Thailand.

Bendea H., Chiabrando F., Tonolo F. and Marenchino D. (2007). Mapping of archaeological areas using a low-cost UAV., International CIPA Symposium, Athens, Greece.

Giulia S. and Antonia S. (2016). DEM Generation based on UAV Photogrammetry Data in Critical Areas., 2nd International Conference on Geographical Information Systems Theory, Applications and Management, P 92-98.

Segales A., Gregor R., Rodas J., Gregor D. and Toledo S. (2016) Implementation of a low cost UAV for photogrammetry measurement applications., International Conference on Unmanned Aircraft Systems (ICUAS), Arlington VA USA. P 926 - 932.

Triggs B., McLauchlan P., Hartley R. and Fitzgibbon A. (2000). Bundle Adjustment A Modern Synthesis Seminar in Computer Graphics., P 298 – 371

Wolf P. R. and Dewitt B.A. (2000). Ground Control Points Elements of Photogrammetry with Applications in GIS.

ASPRS (2014). Positional Accuracy Standards for Digital Geospatial Data., 1st Ed, V.1, American Society for Photogrammetry and Remote Sensing.

Perpustakaan Negara Malaysia eISBN 987-967-17889-6-7

The Engineering Institute of Thailand under H.M. The King's Patronage (2018). GCPS for UAVs Mapping Thailand UAV surveying for Engineering standard.

FGDC (1998). Spatial assessment method Geospatial Positioning Accuracy Standards Federal Geographic Data Committee USA

Uysal M., Toprak A. and Polat N. (2015). DEM generation with UAV Photogrammetry and accuracy analysis in Sahitler hill., Measurement (vol.73)

Perpustakaan Negara Malaysia eISBN 987-967-17889-6-7

eISBN 978-967-17889-6-7

Perpustakaan Negara Malaysia
eISBN 987-967-17889-6-7